TECHNISCHE UNIVERSITÄT MÜNCHEN
DEPARTMENT CHEMIE
LEHRSTUHL FÜR ORGANISCHE CHEMIE I

Bioinspired Site- and Enantioselective Hydroxylation Reactions Enabled by Molecular Recognition

Finn Marten Burg

Vollständiger Abdruck der von der Fakultät für Chemie der Technischen Universität München zur Erlangung des akademischen Grades eines Doktors der Naturwissenschaften genehmigten Dissertation.

Vorsitzender:		Prof. Dr. Klaus Köhler
Prüfer der Dissertation:	1.	Prof. Dr. Thorsten Bach
	2.	apl. Prof. Dr. Wolfgang Eisenreich
	3.	Prof. Dr. Mathias Senge Trinity College Dublin

Die Dissertation wurde am 20.05.2020 bei der Technischen Universität München eingereicht und durch die Fakultät für Chemie am 30.06.2020 angenommen.

The presented Ph.D. work was carried out at the Lehrstuhl für Organische Chemie I at the Technische Universität München between May 2017 and May 2020 and supervised by Prof. Dr. Thorsten Bach.

Part of this work has been published:

F. Burg, M. Gicquel, S. Breitenlechner, A. Pöthig, T. Bach, *Angew. Chem. Int. Ed.* **2018**, *57*, 2953-2957.; *Angew. Chem.* **2018**, *130*, 3003-3007.

F. Burg, T. Bach, *J. Org. Chem.* **2019**, *84*, 8815-8836.

F. Burg, S. Breitenlechner, C. Jandl, T. Bach, *Chem. Sci.* **2020**, *11*, 2121-2129.

In this thesis, the relative configuration of racemates is represented by straight lines (bold or hashed). The absolute configuration of enantiomerically pure or enriched compounds is represented by wedge-shaped lines (bold or hashed).

racemate 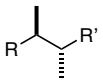

enantiomerically pure
or enantiomerically enriched 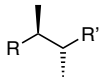

Acknowledgements (German)

Mein größter Dank gilt meinem Doktorvater Thorsten Bach für die bedingungslose Unterstützung während meiner gesamten Zeit am Lehrstuhl. Insbesondere die ausgiebige Freiheit im Rahmen meines Forschungsvorhabens habe ich sehr genossen, sowie die zahlreichen zukunftsweisenden Gespräche, sei es fachlicher oder persönlicher Natur.

Ich möchte Frau Voigt danken, die mir stets geholfen hat einen kühlen Kopf zu bewahren, wenn es um bürokratische Angelegenheiten ging und dafür gesorgt hat, dass ich niemals eine Frist verpasst habe. Bei Andreas Bauer und Stefan Breitenlechner möchte ich mich für ihre Hilfe bei allerlei organisatorischer und wissenschaftlicher Probleme bedanken. Besonderer Dank gilt dabei Stefan für sein unermüdliches Engagement bei mechanistischen Fragestellungen.

Olaf Ackermann, Jürgen Kudermann, Alexander Pöthig, Christian Jandl, sowie dem ESI-HRMS Team der *Sieber* Gruppe möchte ich ausdrücklich für einen reibungslosen Ablauf bei allen analytischen Methoden danken.

Weiterhin bedanke ich mich herzlich für die tatkräftige Unterstützung meiner Forschungspraktikanten Hussayn Ahmed, Maximilian Iglhaut, Wolfgang Büchele, Maximilian Stierle und Christoph Buchelt.

Den aktuellen und ehemaligen Mitgliedern der *Bach* Gruppe sei an dieser Stelle aufrichtig für das angenehme Arbeitsklima und die spannende Zusammenarbeit gedankt – vor allem Maxime, der den Grundstein für die in dieser Arbeit behandelten Projekte legte.

Table of Contents

Small Molecule Drug Discovery – A Historical Perspective

More than 200 years ago the 21-year-old pharmacists' apprentice Friedrich Sertürner was the first ever to isolate a pharmacologically active pure compound from a plant.[1] Named after Morpheus, the Greek god of dreams, morphine (**1**) eventually became one of the most recognized pain killers of the opiate family.[2] Its exact structure and pharmacological properties were elucidated many years later[3-4] and it has remained a historically important example how a plant-derived drug can be used for therapeutic treatments. Although opium was a common analgesic for many centuries, it was a substantial progress to be able to isolate one of its main active ingredients in a pure form thus enabling the administration in precise dosages without any deviation caused by the source or age of the material.

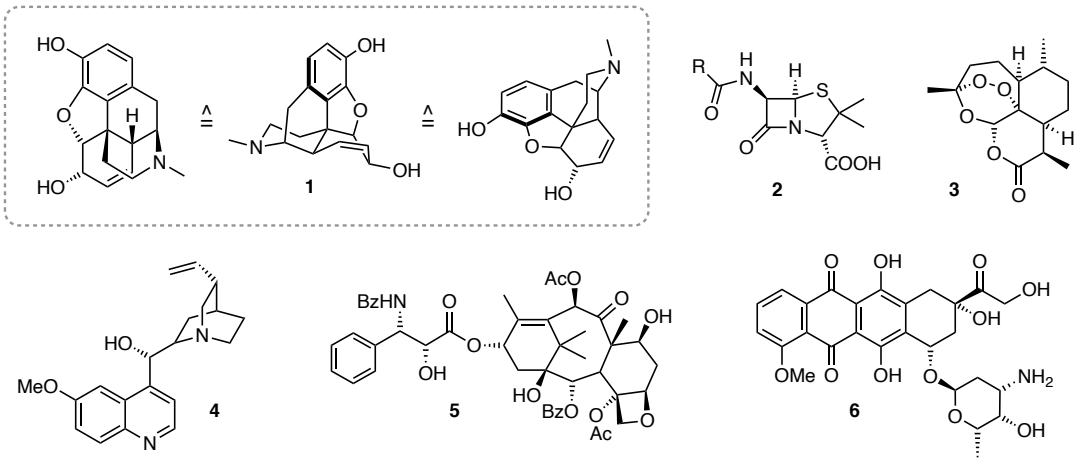

***Figure 1**: Chemical structures of historically important therapeutic drugs **1-6**.* Me = methyl, Bz = benzoyl, Ac = acetyl

By the mid-twentieth century the evaluation of secondary metabolites for medicinal purposes has become an established protocol for small molecule drug development.[5-10] The discovery of penicillin (**2**)[11] initiated an intensive screening of microorganisms for new antimicrobial pharmacores and the golden age of antibiotics provided many of today's most commonly used drugs (Figure 1). Human medicine was revolutionized and for the first time ever, effective treatment of severe infectious diseases became a reality. Besides the unprecedented advances in antibacterial drug design, many other natural products were soon identified as essential medications. Antimalarial drugs such as artemisinin (**3**)[12-14] and quinine (**4**)[15-17] were discovered, whereas paclitaxel (**5**)[18] and doxorubicin (**6**)[19] have found application in anticancer therapy. Owing to the efficiency of these drugs, the life expectancy of human beings was significantly increased by several decades. In addition to their importance to prevail against severe diseases, all of these compounds share another remarkable feature: an intriguing chemical architecture, which poses a formidable challenge to the imagination and creativity of synthetic chemists.[20]

Along these lines, it is indeed a fascinating scenario how nature assembles complex molecules from simple, prochiral starting materials.[21] A prominent example illustrating the extraordinary selectivity in biochemical transformations is the biosynthesis of paclitaxel (**5**) (Scheme 1).[22] In this process, baccatin III (**7**) and 10-deacetylbaccatin III (**8**) are advanced intermediates, which in turn stem from the highly oxygenated compound **9**. The perhaps most interesting feature of this biosynthesis is a series of highly selective hydroxylation reactions promoted by a variety of monooxygenases.[23] Of note, the carbon skeleton is not altered during these steps, conclusively tracing back to taxadiene (**10**) derived from a stereoselective cyclization of the linear precursor geranylgeranyl pyrophosphate (**11**).[24-25]

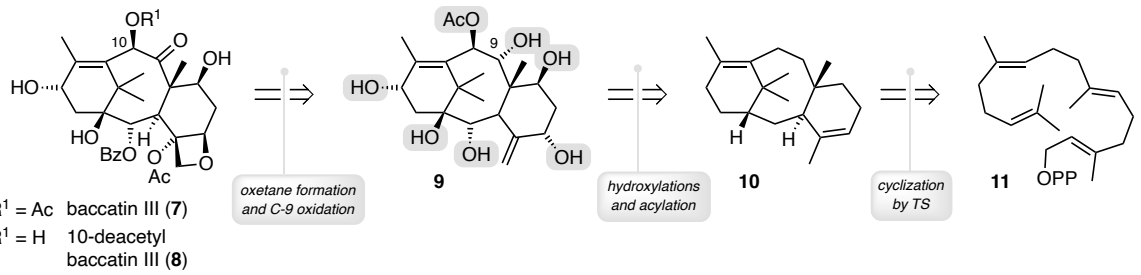

***Scheme 1**: Retrosynthetic analysis of the biosynthesis of paclitaxel (**5**). PP = diphosphate, TS = taxadiene synthase*

Although from a synthetic perspective the efficiency in which paclitaxel is constructed remains admirable, only neglectable amounts of the coveted anticancer drug are produced. Specifically, the bark of 12 trees of the pacific yew *taxus brevifolia* is required in order to provide 1 gram of paclitaxel.[26-27] This shortage can be circumvented by a semi-synthetic derivatization of its closely related congeners **7** and **8** to ultimately yield paclitaxel.[28-29] Previous efforts on the total synthesis of paclitaxel have impressively shown the high demand of modern organic synthesis,[30-35] but unfortunately have contributed little to meet the distribution needs of the world.

It is therefore proposed that the development of new selective transformations is essential to be able to reach out to the complexity of nature's secondary metabolites. Within this context, selective hydroxylation reactions remain one of the key synthetic challenges.[36-37] The scope of the presented work is to discuss recent advances in oxygenation reactions catalyzed by small molecule model systems and outline their limitations for site- and enantioselective organic synthesis. Moreover, it serves to comprehensively elaborate how the utility of non-covalent interactions can provide a relief to override intrinsic reactivity patterns and eventually help to solve the quest for stereoselective synthesis.

Oxygenation Reactions Catalyzed by Cytochrome P450

Among the plethora of natural enzymes engaged in biosynthetic processes the cytochrome P450 family arguably belongs to the most intriguing class of biocatalysts.[38] Their most recognized feature is its unique ability to activate atmospheric oxygen to facilitate highly selective oxygen insertions into unactivated carbon hydrogen (C–H) bonds under mild physiological conditions.[39]

The active site of these heme proteins contains an iron protoporphyrin IX center coordinated by a cysteine thiolate (Scheme 2). Formally operating as an oxidoreductase, dioxygen (O_2) is cleaved, whereupon one oxygen atom is reduced to form water (**A** → **B**) and the other oxygen atom is incorporated into a variety of biomolecules (**B** → **C**). With an additional oxidizing equivalent delocalized over the porphyrin macrocycle, its catalytically active species is postulated to be an iron(IV) radical intermediate (**B**).[40-45]

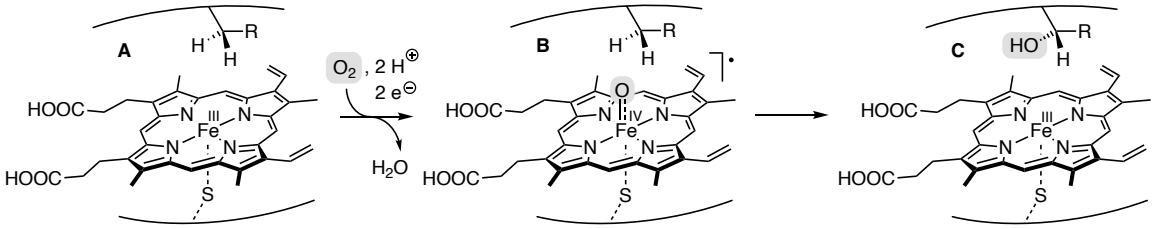

***Scheme 2**: Oxidation of the iron complex **A** to **B** via oxygen activation and subsequent hydroxylation to **C**.*

The exact mechanism of oxygenation reactions catalyzed by cytochrome P450 and related model systems has been extensively studied over the past decades (Scheme 3).[38-39, 46-52] In its initial state, the resting iron(III) species is likely coordinated by two axial ligands, a cysteine thiolate and a water molecule. Coordination of a suitable substrate (**A**) is accompanied by a spin-state change of the iron center, whereupon an NADPH dependent single electron reduction is initiated to furnish the transient iron(II) species (**D**). Molecular oxygen coordinates rapidly to the metal center and the ferric superoxo (O_2^{-}) complex (**E**) undergoes a consecutive reduction-protonation step. At this stage, the oxygen molecule (O_2) has experienced a two-electron reduction arriving at the hydroperoxo (O_2^{2-}) complex (**F**). Another protonation initiates the crucial O–O bond cleavage to produce water and eventually generate the previously illustrated highly reactive iron(IV) radical intermediate (**B**). The final step involves the stereoselective hydroxylation of an unactivated C–H bond (**B** → **C**), whereupon the product is released to close the catalytic cycle.

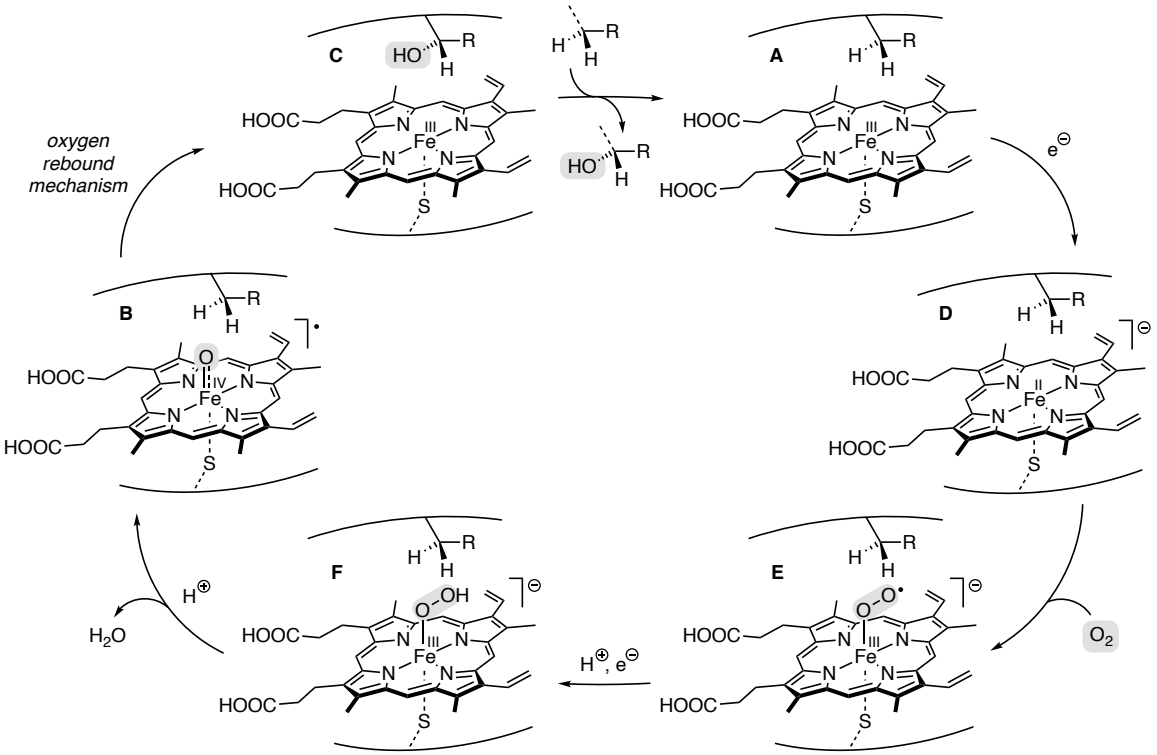

***Scheme 3**: Catalytic cycle of the oxygen activation and transfer by cytochrome P450.*

The key feature of this multistep reaction sequence is the C–H oxygenation step (**B** → **C**), which has been further reviewed in great detail.[51, 53] Pioneering work was reported by the group of *Groves* in the late 1970s, who proposed an oxygen rebound mechanism.[54-55] More specifically, they envisioned that the highly reactive iron porphyrin radical (**B**) abstracts a hydrogen atom from a suitable substrate to furnish the hydroxido iron(IV) complex (**G**) and a transient alkyl radical (Scheme 4). Based on detailed kinetic studies with large kinetic isotope effects,[56-57] it was suggested that the initial C–H abstraction is rate-limiting, ensued by rapid recombination of the hydroxido ligand with the incipient methylene group. In the following years several mechanistic studies, such as position scrambling during the allylic hydroxylation of olefins and deletion of the stereocenter at the oxygenated carbon atom, eventually provided strong evidence for a radical mechanism commencing by scission of the C–H bond.[58-60]

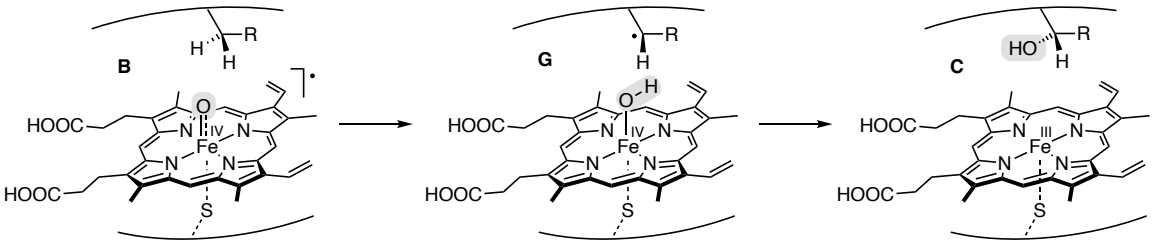

***Scheme 4**: Oxygen rebound mechanism of the cytochrome P450 catalyzed hydroxylation.*

The group of *Groves* quickly recognized the exceptional potential of cytochrome P450 enzymes for preparative organic chemistry and accordingly developed a small molecule model system. In their seminal work on hydroxylation reactions, 5,10,15,20-tetraphenylporphyrin (TPP) iron(III) chloride (**14**) was used as the catalyst to oxidize cyclohexane (**12**) to cyclohexanol (**13**) at ambient temperature (Scheme 5).[61] While synthetically highly interesting, their systems clearly displayed a lack of utility, given that the even low yield of 8% was based on the stochiometric oxidant iodosobenzene (PhIO) and the substrate was used in large excess (>30 equivalents) relative to the oxidant. Nevertheless, it is often considered a landmark study keeping in mind the inert nature of cyclohexane (**12**) towards conventional organic transformations.

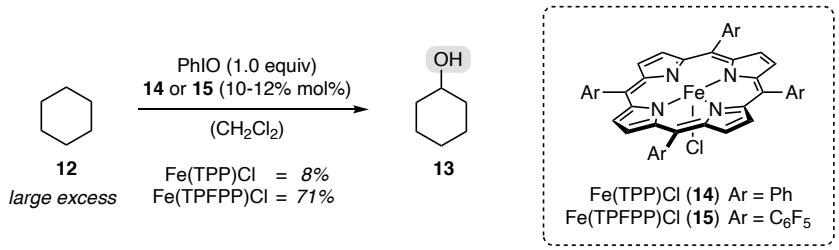

***Scheme 5**: Hydroxylation of cyclohexane (**12**) to cyclohexanol (**13**) by **14** and **15**.[61-62] Ar = aryl, Ph = phenyl*

Besides the high activation barrier of aliphatic C–H bonds, another reason for the low efficiency of this process was rationalized by oxidative degradation of catalyst **14**. Specifically, the group of *Chang* at Michigan State University identified the problem to be an irreversible oxidation of the porphyrin ring resulting in inactivity of the catalyst.[62] It was therefore envisioned, that an electron-deficient porphyrin ligand can not only increase the electrophilicity of the reactive oxo iron(V) species, but might also prolong the lifetime of the catalyst thus providing an enhanced reactivity.[63] Indeed when promoted by the fluorinated catalyst 5,10,15,20-tetrakis(pentafluorophenyl)porphyrin (TPFPP) iron (III) chloride (**15**), the yield of the oxygenated product (**13**) increased drastically to 71%.[64] The presented examples are key studies in the field of cytochrome P450 model systems and accordingly have laid the groundwork of many future studies on site and enantioselective hydroxylation reactions.

Enantioselective Oxygenation Reactions in Organic Synthesis

Over the past greater decade, the direct functionalization of unactivated C–H bonds has evolved into a compelling tool to provide precious building blocks and versatile intermediates in organic chemistry.[65-75] The perhaps most fundamental challenge lies in providing sufficient selectivity emanated by the ubiquitous number of hydrocarbons in organic molecules.[36, 76-79] With regard to sp^3 C–H activation this enigma becomes even more complicated due to the formation of enantio- or diastereoisomers.[80-83] Given that the vast majority of important organic molecules exhibit stereogenic centers, the development of chiral catalysts is essential in order to facilitate an enantioselective reaction.

In stark contrast to the previously illustrated oxygen rebound mechanism (*cf.* Scheme 4), conventional transition-metal-catalyzed C–H activation strategies are typically engaged in an inner-sphere mechanism (Scheme 6, left). In these systems, the chirality is transferred by a chiral ligand directly coordinating to the organometallic intermediate **16** or through close proximity during the concerted metallonitrene or -carbene insertion **17**.[80-81, 84-85]

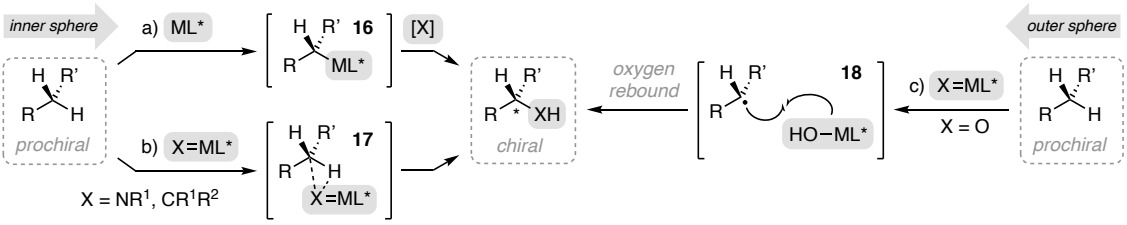

***Scheme 6**: General scheme of transition-metal-catalyzed C–H activation strategies. M = metal, L* = chiral ligand*

The situation significantly aggravates in the event of an outer sphere mechanism (Scheme 6, right). The hydroxylation *via* an oxygen rebound mechanism does not involve a C–H insertion step, but instead the reactive oxo metallo species initiates a hydrogen atom transfer (HAT) from the substrate to the catalyst. Even in the case of an enantioselective HAT, one has to consider the lifetime of the transient radical **18**, as radical epimerization is a fast process. Moreover, it can be envisioned that the rebound step has a substantial effect on the overall selectivity of the hydroxylation, comprehensively demonstrating a less constrained contact between the catalyst and the substrate compared to the inner sphere approach. Even once the hydroxyl entity is successfully installed in an enantioselective fashion, an additional notable issue arises, given that the newly generated stereocenter can be deleted by a consecutive oxidation step. Taking into account that carbon centered radicals adjacent to heteroatoms are well stabilized, hydroxylation reactions are intuitively accompanied by significant ketone formation, which unfortunately does not necessarily have to be a favorable kinetic resolution.

It becomes evident from these considerations, that the development of enantioselective hydroxylation reactions belongs to the most challenging transformations within the field of enantioselective C–H functionalization. Nevertheless, there have been numerous efforts to develop bioinspired chiral oxygenation catalysts.[86] One popular approach to benefit from the apparent problem of overoxidation is realized by an oxidative kinetic resolution (OKR) (Scheme 7a). Although there have been several reports on the OKR of racemic alcohols into highly enantiomerically enriched material,[87-93] it should be noted that the yield is inherently limited to a maximum of 50%, while the other half is transformed into an undesired side product. In other words, it represents the separation of two enantiomers executed by a transition metal catalyzed organic transformation. Most importantly, the kinetic resolution of a racemic alcohol does not by all means have to involve a C–H activation step, but can also be achieved by conventional oxidation strategies in connection with a chiral ligand,[94-95] stereoselective hydrogenation of allylic alcohols[96-97] or through enantioselective acylation of one of the two alcohols.[98-101] As part of this work aiming to highlight advances in C–H oxygenation chemistry, OKRs are not reviewed in more detail.

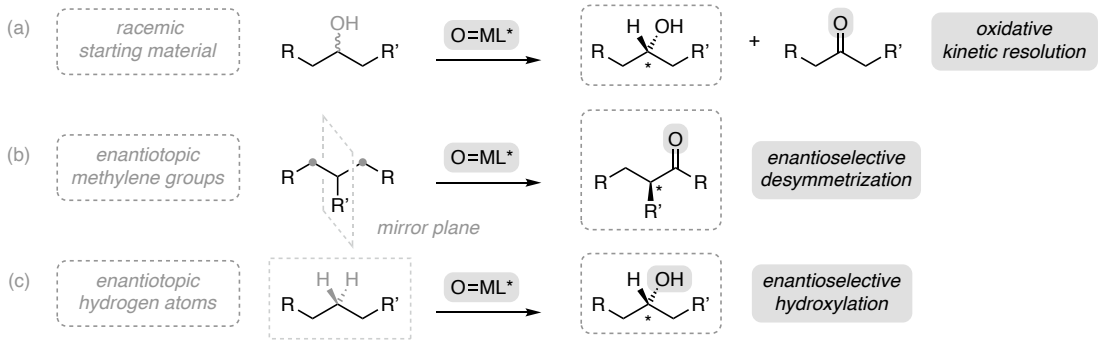

***Scheme 7**: General scheme of an OKR, as well as an enantioselective desymmetrization and hydroxylation reaction.*

The more elegant strategy to embed the overoxidation dilemma is pursued *via* a desymmetrization approach. In this process, the substrate exhibits an additional prostereogenic carbon center[102] that is not affected by the oxygenation event. More specifically, the assignment is to distinguish between enantiotopic methylene groups to furnish a chiral ketone (Scheme 7b), instead of differentiation between enantiotopic hydrogen atoms to generate a chiral secondary alcohol (Scheme 7c).

Along these lines, the most common chiral oxygenation catalysts engaged in enantioselective reactions are depicted in Figure 2. Inspired by their biological origin in natural enzymes, porphyrin catalysts **19** are popular catalysts for C–H functionalization reactions.[103-105] Due to their conjugated planar carboskeleton, a straightforward way to introduce chirality can be accomplished by functionalization of its *meso*-substituents.

Retrosynthetically, porphyrins are often derived from a condensation reaction between an aldehyde and pyrrole, but cross coupling reactions from the corresponding porphyrin bromides are also conceivable.[106-108] Chiral manganese salen complexes **20** have been involved in a variety of oxygenation reactions owing to their well-studied properties in enantioselective epoxidations and sulfoxidations.[109-114]

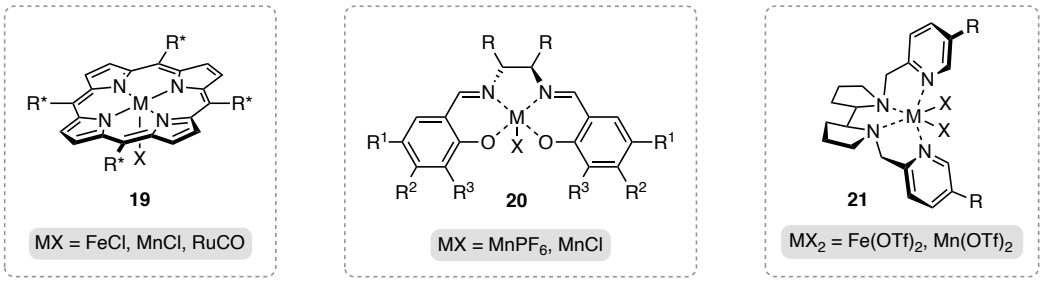

***Figure 2**: Chemical structure of common chiral oxygenation catalysts. R* = chiral entity, Tf = trifluoromethanesulfonyl*

Recently, aminopyridine ligands **21** have received significant attention not only in enantioselective, but also site-selective oxygenation reactions.[115-117] Of note, the 2,2'-bipyrrolidine scaffold is sometimes replaced by a 1,2-diaminocyclohexane entity and derivatization of the pyridine functionalities to other nitrogen containing heterocycles has been reported.

Chiral Porphyrin Complexes

Encouraged by their seminal studies on oxygenation reactions with Fe(TPP)Cl (*cf.* Scheme 5), *Groves* and co-workers reported the first enantioselective hydroxylation protocol (Scheme 8). Promoted by the D_2-symmetric binol derived porphyrin **19a** the oxygenation of prochiral benzylic methylene groups was investigated.[118] The best result was obtained with tetrahydronaphthalene (**22**) whereupon the enantiomerically enriched (73% *ee*) alcohol **23** was isolated in 47% yield based on one equivalent of the oxidant PhIO.

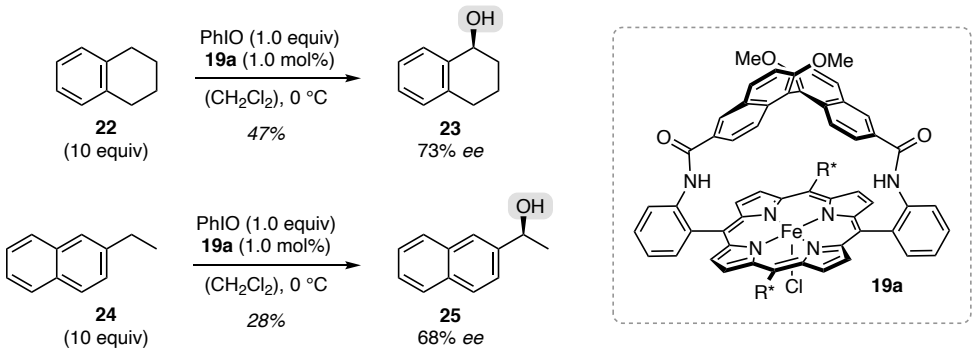

***Scheme 8**: Enantioselective hydroxylation of **22** and **24** to alcohol **23** and **25** catalyzed by the iron complex **19a**.[118]*

When acyclic substrates such as 2-ethylnaphthalene (**24**) were probed under identical conditions, the yield (19-40%) as well as the enantioselectivity (40-68% *ee*) of the corresponding alcohol **25** deteriorated notably.

An important contribution to the design and synthesis of chiral porphyrin ligands was made by the group of *Halterman*.[119] The chiral entity was introduced *via* the well-established *Diels-Alder* reaction of cyclopentadiene and benzoquinone.[120] Hydrogenation of the olefin, reduction of the two ketone moieties and a final dehydration step furnished the aromatic dinorbonyl carboskeleton R* as a racemic mixture (Scheme 9).[121] The prerequisite aldehyde for the pyrrole condensation was introduced by a *Friedel-Crafts* formylation[122] and consecutively converted into a mixture of diastereomeric ketals[123] thus inviting chiral resolution to obtain enantiomerically pure material.

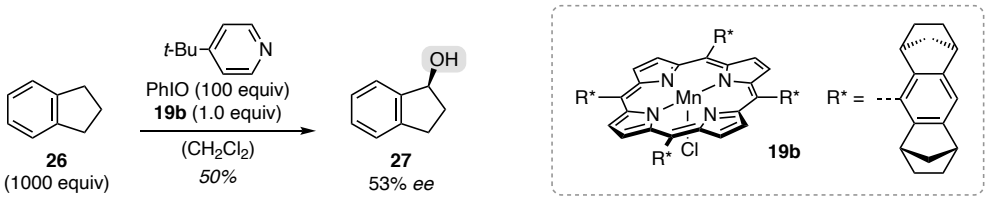

***Scheme 9**: Enantioselective hydroxylation of indane (**26**) to indanol (**27**) by the porphyrin catalyst **19b**.[124] Bu = butyl*

With the D_4-symmetric manganese porphyrin complex **19b** in hand, the catalyst was explored in enantioselective hydroxylation reactions.[124] In a stochiometric experiment, indane (**26**) was converted to 1-indanol (**27**) in a moderate yield and 53% *ee*. 4-*tert*-Butylpyridine was added as an additional axial ligand, which drastically shortened the reaction time (*e.g.* from 47 h to 16 h). Although run as a non-catalytic experiment, it was reported that the catalyst **19b** can be recovered at the completion of each reaction.

The excellent potential of this particular porphyrin ligand for stereoselective synthesis was further reviewed by the group of *Che*.[103] The ruthenium porphyrin analogue **19c** was employed in the catalytic enantioselective hydroxylation of *para*-substituted ethylbenzene derivatives (Scheme 10), whereupon 4-ethylanisole (**28**) was converted into the enantiomerically enriched alcohol **29** (70% yield based on 20% conversion, 76% *ee*).[125-126]

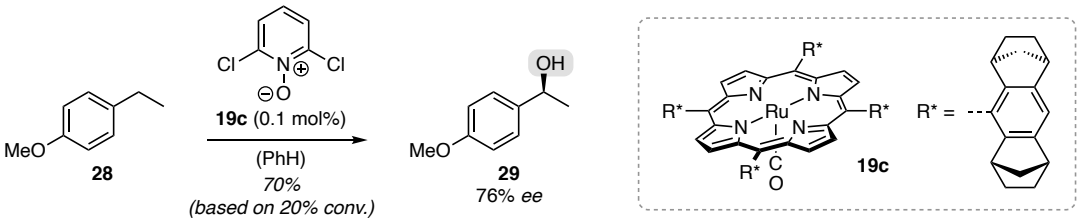

***Scheme 10**. Enantioselective hydroxylation of 4-ethylanisole (**28**) to alcohol **29** by the Ru-porphyrin complex **19c**.[125]*

Although they developed a moderately enantioselective process (62-75% *ee*) and the catalyst loading was remarkably low (0.1 mol%), it must not go unnoticed that the reported yields refer to reisolated starting material, of which in all cases less than one quarter was converted (28-72% yield based on 10-23% conversion).

More than a decade later the *Halterman* ligand was readopted by the group of *Simonneaux*, who further derivatized the chiral norbornyl unit with a sodium sulfonate entity (Scheme 11). Now operating in an aqueous media, the hydroxylation of *para*-bromoethylbenzene (**30**) was catalyzed by the iron porphyrin complex **19d** (1.0 mol%) and 10 mol% of imidazole (Im) as a co-ligand to yield alcohol **31** in good enantiomeric excess (76% *ee*). The yield for this transformation seemed reasonable (47%), but it referred to one equivalent of the oxidant iodobenzene diacetate and excess of the substrate **30** (10 equivalents).[127]

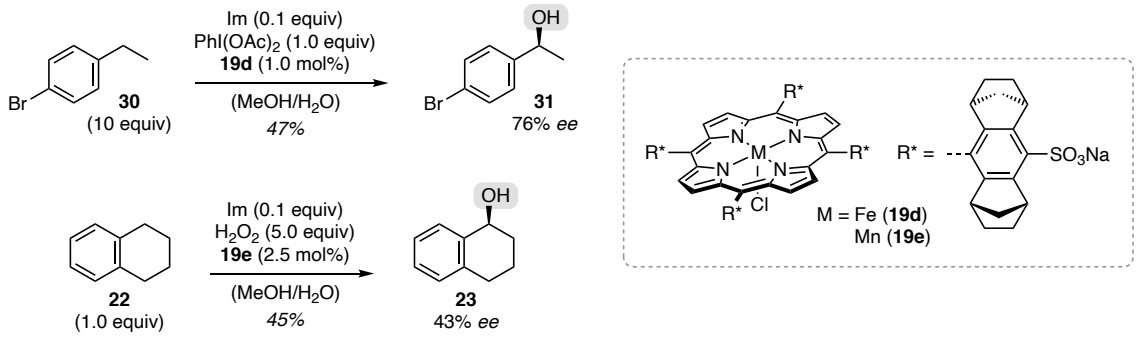

***Scheme 11**: Enantioselective hydroxylation of **30** and **22** to alcohol **31** and **23** by porphyrin catalyst **19d** and **19e**.*[127-128]

Interestingly, it was also feasible to use the related manganese porphyrin complex **19e**, to promote the hydroxylation of tetrahydronaphthalene (**22**). In a catalytic experiment (2.5 mol%) and the substrate as the limiting reagent (5.0 equivalents of the oxidant hydrogen peroxide), 1,2,3,4,-tetrahydro-1-naphthol (**23**) was obtained in a similar yield (45%), but reduced enantioselectivity (43% *ee*).[128]

Chiral Salen Complexes

As previously discussed, the oxidative desymmetrization of enantiotopic methylene groups is a powerful tool to access optically enriched ketones (Scheme 7b). Within this context, the group of *Katsuki* developed a series of interesting oxygenation protocols utilizing chiral manganese salen complexes **20**. One of the first examples involved the enantioselective hydroxylation of tetrahydrofuran **32** to obtain the hemiacetal **33** in a satisfactory yield and very high enantioselectivity (91% *ee*) (Scheme 12).[129] Further oxidation using pyridinium chlorochromate (py = pyridine) provided lactone **34**. Along these lines, the *N*-protected

pyrrolidine **35** (Bn = benzyl) was also compatible using pentafluoroiodosobenzene as the stochiometric oxidant, however the corresponding hemiaminal **36** was not isolated. Instead, a consecutive oxidation step using the *Jones* reagent[130] (H_2SO_4 and CrO_3) furnished lactam **37** in a moderate yield over two steps and high enantiomeric excess (84% *ee*).[131-132]

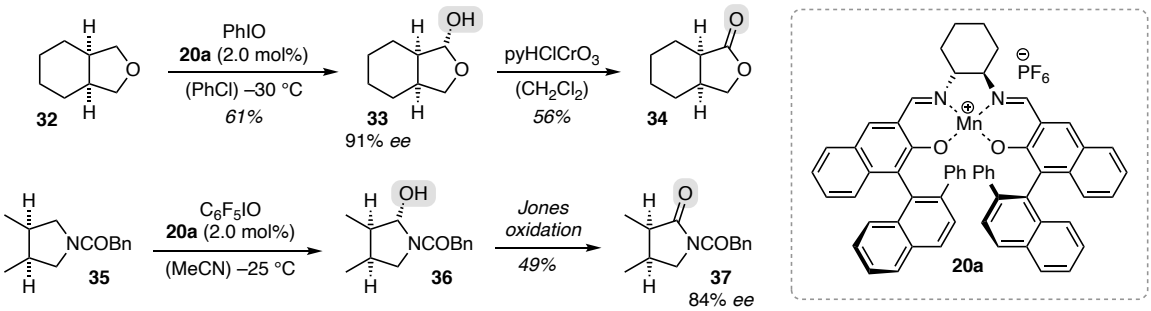

***Scheme 12**: Seminal studies on oxidative desymmetrizations catalyzed by manganese salen complex **20a**.*[129, 131-132]

A related approach was pursued by the group of *Murahashi*, who studied the desymmetrization of indanols and tetrahydronaphthalenes. The manganese salen complex **20b** was employed in the enantioselective oxygenation of the *tert*-butyldimethylsilyl (TBS) protected 2-indanol (**38**) to furnish ketone **40** in reasonable enantiomeric excess (70% *ee*), albeit in a very low yield of 13% (Scheme 13).[133] 4-Phenylpyridine-*N*-oxide (**39**) was added as a substoichiometric additive (0.5 equivalents), which was previously reported by the *Jacobsen* group to increase the conversion as well as the reaction rate in epoxidation reactions catalyzed by manganese-salen complexes.[134] Interestingly, after desilylation of **40** the ketone entity can be further functionalized into a 1,2-*cis*-aminoalcohol,[135] which in turn is a key intermediate in the synthesis of indinavir, a potent inhibitor of the protease of the human immunodeficiency virus (HIV).[136-137] Further studies were devoted to explore the desymmetrization of disilylether **41**. In a catalytic oxidative desymmetrization by the same complex **20b**, ketone **42** was obtained in very high enantioselectivity (93% *ee*), but the reaction again suffered from a very low conversion (15%).[138]

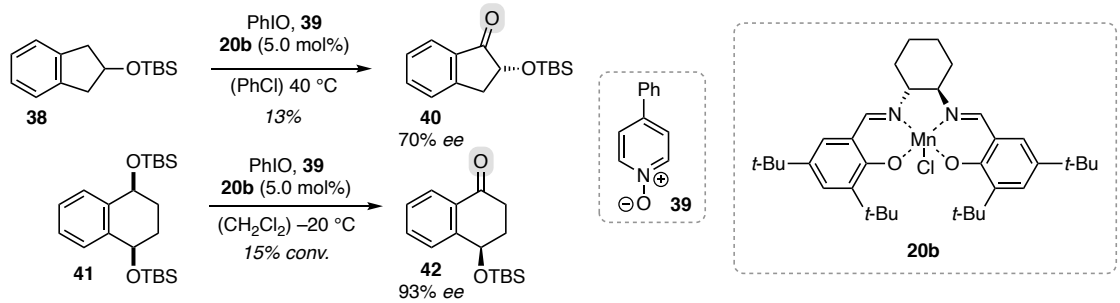

***Scheme 13**: Oxidative desymmetrization of silylether **38** and disilylether **41** to ketone **40** and **42** catalyzed by **20b**.*[133, 138]

Besides their efforts to examine desymmetrization reactions, *Katsuki* and co-workers explored the direct hydroxylation of benzylic methylene groups by employing the bulky manganese salen catalysts **20c** and **20d** (TBDPS = *tert*-butyldiphenylsilyl, Mes = mesityl = 2,4,6-trimethylphenyl). A highly enantioselective reaction was observed when 1,1-dimethylindane (**43**) was converted into **44** (90% *ee*), but as often the case for hydroxylation reactions, it turned out to be low yielding (Scheme 14). Nevertheless, hydroxylation of a less constrained substrate was likewise feasible, as 4-ethylanisole (**28**) was successfully hydroxylated to furnish **29** in high enantioselectivity (87% *ee*).

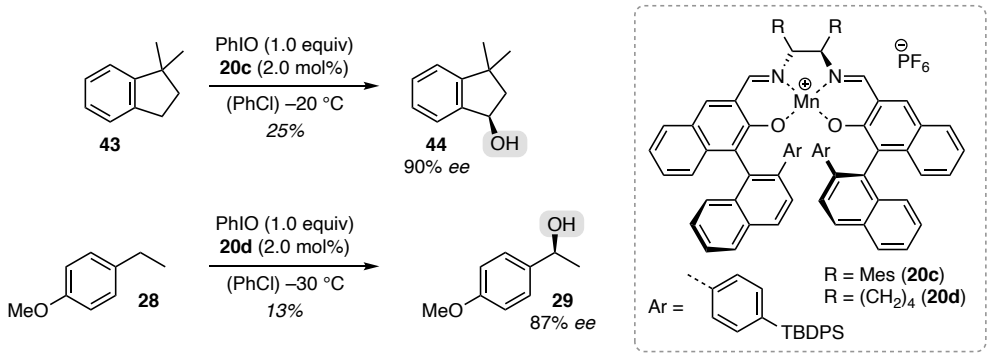

***Scheme 14**: Enantioselective hydroxylation of **43** and **28** to alcohol **44** and **29** by the Mn-salen complex **20c** and **20d**.*[139]

Chiral Aminopyridine Complexes

Unlike porphyrin and salen ligands, aminopyridine complexes **21** and its closely related congeners, have only recently started to attract attention for oxygenation reactions.[140] Particularly, the *White* group has excessively used these catalysts for site-selective oxygenation reactions and the late-stage functionalization of biologically active molecules.[141-145] While it was beyond the scope of these studies to facilitate an enantioselective reaction, *Wei Sun* and co-workers have among others[116] investigated enantioselective epoxidations by iron aminopyridine complexes.[115, 146-151] Encouraged by their previous studies on the OKR of racemic alcohols[92] and most likely inspired by pioneering work of our own group on enantioselective oxygenation reactions (*cf.* Scheme 32),[152] they recently reported the highly enantioselective desymmetrization of spirocyclic hydrocarbons. Interestingly, the reaction runs at a very low catalyst loading (0.5 mol%) and utilizes hydrogen peroxide as an environmentally benign oxidant.[153] Along these lines, the oxygenation of indanone **45** to diketone **47** catalyzed by the modified aminobenzimidazole complex **46** proceeded in exceptionally high enantioselectivity (98% *ee*) and good yield using 2,2-dimethylbutyric acid (DMBA) as an additive (Scheme 15).

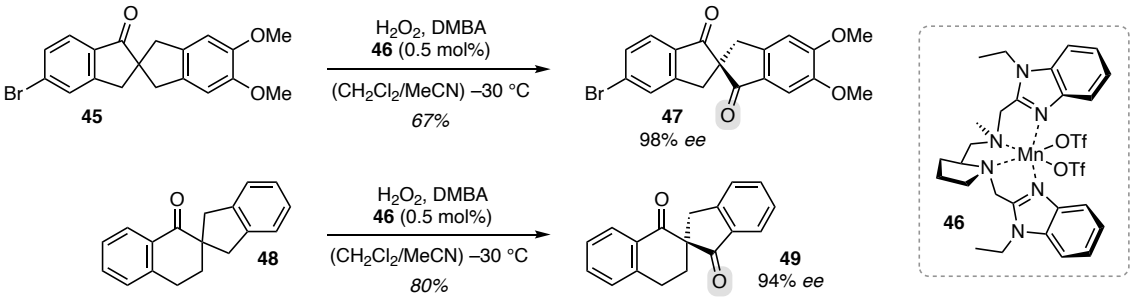

***Scheme 15**: Spirocyclic oxygenation of **45** and **48** to diketone **47** and **49** catalyzed by manganese complex **46**.[153]*

Within this context, it was previously reported that the corresponding carboxylic acid additive has a substantial effect on the oxygenation reaction, probably due to formation of a metal peroxy acid complex.[154-158] While the reaction turned out to tolerate a variety of simple functional groups (11 examples, 51-94% yield, 68-98% *ee*), the scope was eventually expanded to the oxygenation of tetralone derivatives (9 examples, 57-80% yield, 77-94% *ee*). In this case, the best result was obtained when tetralone **48** was converted to diketone **49** in outstanding enantioselectivity (94% *ee*) and high yield.

A closely related study was reported by the same group on the oxygenation of *N-tert*-butyloxycarbonyl (Boc) protected oxindoles (12 examples, 42-67% yield, 55-91% *ee*) and the hydroxylation of 4-quinolones (9 examples, 22-41% yield, 41-63% conversion, 70-99% *ee*) (Scheme 16).[159] A representative example illustrates the oxygenation of an unsubstituted oxindole **50** to yield ketone **51** in very high enantiomeric excess (91% *ee*). The same complex **46** was applied to perform an enantioselective hydroxylation of 4-quinolone **52** providing the secondary alcohol **53** in remarkable enantioselectivity (98% *ee*). Although the yield for the oxygenation of 4-quinolones was lower, the fact that an enantioselective hydroxylation was feasible is by itself an interesting observation. By contrast, previous efforts on enantioselective hydroxylation reactions catalyzed by aminopyridine ligands by the group of *Bryliakov* did not lead to any substantial advances compared to the previously described studies involving porphyrin and salen ligands.[160]

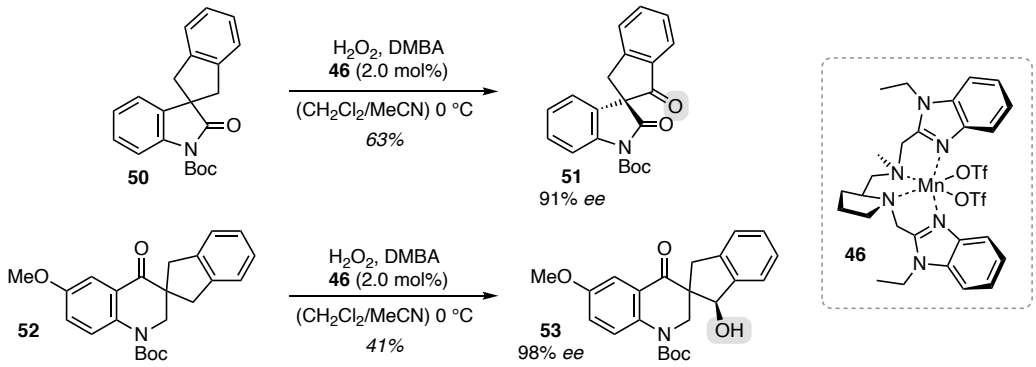

***Scheme 16**: Spirocyclic oxygenation of oxindole **50** and 4-quinolone **52** to ketone **51** and alcohol **53** catalyzed by **46**.[159]*

Although there have been numerous well executed studies on enantioselective C–H oxygenation reactions, all of the above described examples exhibit a slightly activating group adjacent to the oxygenation site. Particularly, an aromatic substituent or a heteroatom appear to be inevitable to stabilize the transient carbon centered radical and provide sufficient reactivity. To fill this gap, the group of *Costas* reported the first highly enantioselective non-enzymatic oxidation of non-activated methylene sites.

The substrates engaged in this process are bulky cyclohexyl amides, whereupon a highly site- and enantioselective oxygenation at the C-3 position of the cyclohexyl carboskeleton was realized (12 examples, 8-85% yield, 62-96% *ee*) (Scheme 17). Along these lines, **54** (R = 2-methylbut-2-yl) can be converted into the almost enantiomerically pure (94% *ee*) ketone **56** in high yield.[161] Closely related to their initial findings, the same group recently discovered that the enantioselective oxygenation of 4-*trans*-subtituted *N*-cyclohexyl amides is feasible using the same catalyst **55** (TIPS = triisopropylsilyl), however using acetic acid instead of cyclopropane-carboxylic acid (CPCA).[162]

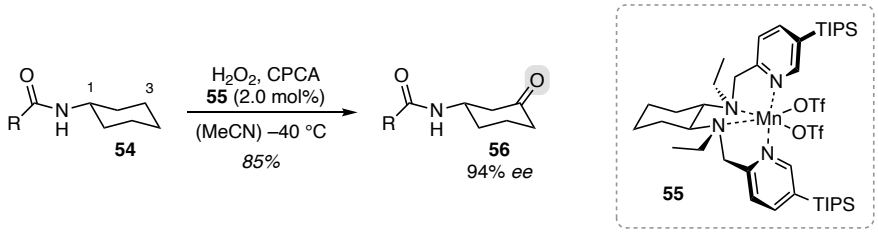

***Scheme 17**: Oxygenation of lactam **54** to ketone **56** catalyzed by the manganese complex **55**.[161]*

In the light of aliphatic oxygenations, *Costas* and co-workers very recently disclosed an intriguing enantioselective lactonization reaction. Specifically, adamantylacetic acid (**57**) was found to undergo a site-selective reaction to yield highly enantiomerically enriched lactons **58-60** (Scheme 18, TFE = trifluoroethanol).[163] The transformation turned out to be highly dependent on the choice of the aminopyridine complex and the substituent at the C-3' position of the adamantyl carboskeleton. Substrates containing an oxygen, nitrogen or chloro substituent (such as **57a**, R = NHCO*t*-Bu) underwent lactonization to the proximal position (**58a** = 96% *ee*) when catalyzed by the bulky complex **21a** (TIBS = triisobutylsilyl) (6 examples, 28-57% yield, 88-99% *ee*). In stark contrast, when the less rigid catalyst **21b** was employed for the same series of substrate, the strained lacton **59a** (94% *ee*) was formed as the major product (6 examples, 23-39% yield, 88-94% *ee*). As soon as alkyl or aryl substituents were introduced (**57b**, R = Ph), the reactive site relocated to furnish lacton **60b** (95% *ee*), preferably by using manganese complex **21b** [10 examples, 46-73% yield, 95-99% ee, *r.r.* = regioisomeric ratio defined as **60**/(**58**+**59**) ranging from 47/53 to 82/18].

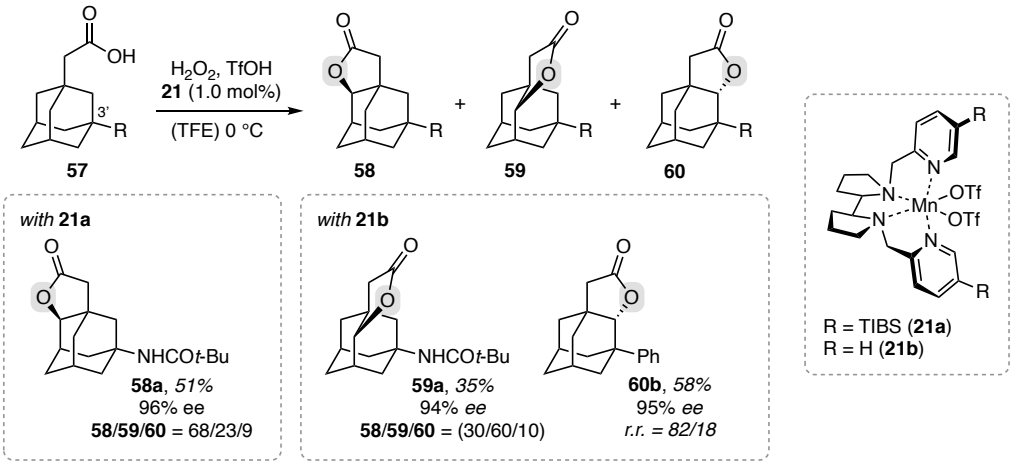

***Scheme 18**: Enantioselective lactonization of adamantylacetic acid (**57**) to lactons **58-60** catalyzed by **21a** and **21b**.*[163]

The lesson learnt from this chapter is that the catalytic oxidative desymmetrization as well as enantioselective hydroxylation reactions are generally feasible to yield optically enriched material. For this purpose, a variety of different porphyrin, salen and aminopyridine derivatives have been employed. Regarding the former transformation, the perhaps most efficient methodology was developed by the group of *Wei Sun*, who was able to provide dense, highly enantiomerically enriched spirocycles.[115, 153, 159] Furthermore, *Costas* has provided an enantioselective protocol for the synthesis of cyclohexanones carrying a bulky amide at the C-3 position.[161] As for the hydroxylation of benzylic methylene sites, it becomes evident that an enantioselective reaction comes with severe limitations. Since initial reports by the group of *Groves*,[118] primarily the work of *Katsuki* as well as *Murahashi* has shown potential for highly enantioselective approaches,[129, 131-132, 138-139] but the major drawback is typically the very low conversion barely exceeding 25%. In addition, it appears to be a general problem that with an increasing concentration of the alcohol the formation of the ketone becomes predominant.[164] Therefore, a high substrate turnover is sometimes not even desirable given that re-isolation of unreacted starting material is commonly preferred over formation of an overoxidized side product. To circumvent overoxidation, adding excess of the substrate and using one equivalent of the oxidant turned out to be a reliable strategy. Stated another way, the reaction is terminated due to the lack of oxidant before larger amounts of ketone can be formed.

Site-selective Oxygenation Reactions Directed by Molecular Recognition

Although the outstanding enantioselectivity belongs to the most admired features of enzymatic reactions, it is often the site-selectivity that turns out to be the most useful catalytic property. Even if a chemical reaction is not highly enantioselective, there are often opportunities to increase the enantiomeric excess of the desired product *a posteriori* (Scheme 19a).[165] Common techniques involve co-crystallization with a chiral additive, chiral resolution (either kinetically or induced *via* chemical derivatization) or simply preparative column chromatography on a chiral stationary phase. The differentiation between reactive sites, however, appears to determine the general utility of a chemical transformation. Specifically, if the reaction does not proceed at the desired position, the undesired constitutional isomer is often useless due to its significantly altered physical or chemical properties (Scheme 19b). Furthermore, possibilities to convert the side product into the desired compound will involve - if at all feasible - additional synthetic steps.

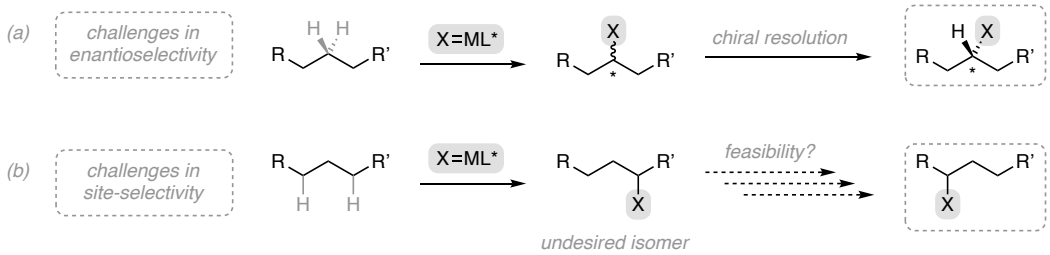

***Scheme 19**: Challenges and opportunities in enantioselective (a) and site-selective (b) C–H functionalization.*

Within this context, natural enzymes possess the unique ability to elegantly overcome site-selectivity problems by precoordination of a given substrate. Such a scenario constitutes the precise exposure of a single C–H bond towards its catalytically active site, while an undesired oxidation is prevented by spatial distance.[38, 166-168] The structural complexity of these biocatalysts introduces a series of attractive and repulsive non-covalent interactions of weak nature, therefore allowing catalytic turnovers *via* a reversible association. The major caveat, however, is manifested by a typically very narrow substrate scope, sometimes limited to a single compound providing the required shape to squeeze into the catalytic cleft of a particular enzyme.

As previously stated, establishing high site-selectivity in C–H activation chemistry remains a fundamental challenge.[76-77, 169] In order to be able to direct or even predict site-selectivity in non-enzymatic reactions, the key question that needs to be pointed out carefully is: What are the main objectives that drive selectivity in an organic transformation?[36, 78-79, 170]

The arguably most commonly used and perhaps even most intuitive aspect is the influence of sterics (Scheme 20). Similar to conventional organic transformations, if a potential electrophilic site exhibits a sterically demanding chemical environment, it will become exceedingly difficult for any appropriate nucleophile to attack. The same holds true for C–H oxygenation chemistry and as a result, particularly in the case of bulky transition metal complexes, the most accessible C–H bond will be functionalized (FG = bulky, electronically innocent substituent).[143, 171-172] Secondly, electronic factors play a crucial role, especially in C–H oxygenation reactions.[173-174] As part of the *Curtin-Hammett* principle the outcome of a chemical reaction is not obligatorily driven by the stability of reactive conformations assuming they interconvert rapidly.[175] Instead, the generated product is a reflection of the rate-limiting transition state, which exhibits the lowest energy and is therefore most accessible. In the case of oxygenation reactions, several experimental studies have provided evidence for a rate-limiting initial hydrogen abstraction.[51, 53, 56-60] Therefore, the most-stabilized carbon centered radical will determine the reactive site due to its lowest bond dissociation energy (BDE) (FG = heteroatom or aryl substituent).

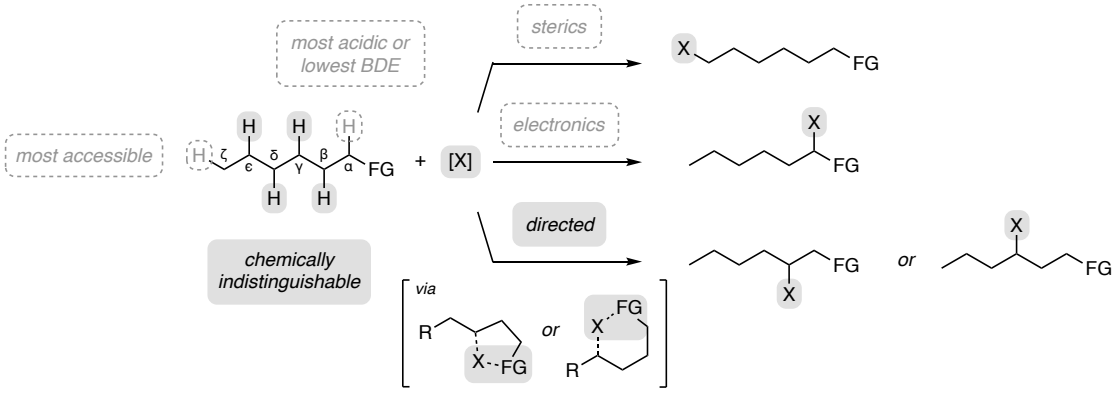

***Scheme 20**: Selectivity aspects in the functionalization of unactivated C–H bonds. FG = functional group*

More recently, numerous efforts were devoted to developing C–H activation strategies that utilize a directing group eventually overriding these intrinsic reactivity pattern.[66, 176-178] In transition-metal-catalyzed reactions, those moieties are often covalently linked coordinating groups, which stabilize the adjacent metal insertion intermediate in a 5- or 6-membered transition state (FG = directing functional group).[65, 83, 179] Within this context, interesting new protocols for the remote functionalization of unactivated C–H bonds were developed in the field of photoredox chemistry, where a 1,5-HAT generates a highly reactive carbon centered radical thus introducing interesting possibilities to access 1,4-functionalized products.[180-182] With regard to oxygenation reactions, similar directing strategies have been engaged for the synthesis of 1,3-diols.[183-185]

Although many of the directed oxygenation approaches have demonstrated a remarkable synthetic potential,[186] their applications are limited to a 1,3-functionalization. In order to imitate biological systems more appropriately, the utility of non-covalent interactions provides an attractive opportunity to selectively functionalize C–H bonds.[187-191] Despite the fact that many of these interactions have been extensively studied for enantioselective catalysis,[192] *e.g.* chiral Brønsted or Lewis acids,[193-195] hydrogen bonding[196-200] or ion pairing,[201-204] examples remain scarce where regio- and site-selectivity issues were sufficiently addressed.[188] While it is beyond the scope of this work to review all the numerous well-executed efforts, this thesis aims to highlight milestones in oxygenation reactions directed by supramolecular recognition.[205]

The general prerequisite for supramolecular communication is a preinstalled recognition group at a given substrate **61** to invite an attractive interaction (Scheme 21). Regardless of the nature of this interaction, the counterpart can either be attached to a stoichiometric complexing reagent or covalently linked to the catalyst. In the former case, the substrate-catalyst complex **62** establishes steric shielding of a designated area whereupon a chemical reaction is prevented. However, in order to ensure complete deactivation, it will most likely be necessary to add a superstoichiometric amount.

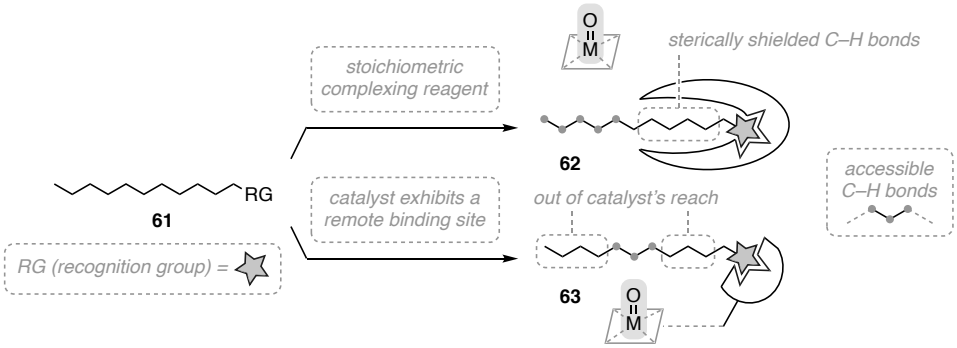

***Scheme 21**: Site-selective C–H functionalization directed by supramolecular recognition.*

The more elegant operation is realized by a bifunctional metal complex exhibiting a catalytically active center, as well as a remote molecular recognition device. Along these lines, a suitable substrate will be anchored *via* non-covalent interactions forming complex **63**, whereupon the substrate is aligned in a position, where only a very limited number of C–H bonds are exposed towards the catalytically active metal center. The major caveat, however, often lies in the complex synthesis of these catalysts.

Hydrophobic Interactions

Preliminary studies involving non-covalent interactions for site-selective hydroxylation reactions were disclosed by the group of *Groves*. A manganese porphyrin complex was decorated with four linear cholic amides and subsequently incorporated into a lipid bilayer.[206-207] Due to the high organization of hydrophilic and lipophilic residues in aqueous solution, the hydroxylation of cholesterol proceeded exclusively at the hydrophobic terminal alkyl chain pointing directly to the catalytically active center. Unfortunately, owing to the very strong binding affinity of the substrate-catalyst-complex, dissociation of the product was inhibited and therefore prevented a catalytic turnover. Along these lines, *Grieco* and co-workers investigated the site-selective hydroxylation of steroids that were covalently linked to a porphyrin catalyst. Although the selectivity during this transformation was remarkable, it resembles an intramolecular reaction and accordingly failed to provide a catalytic approach.[208-210]

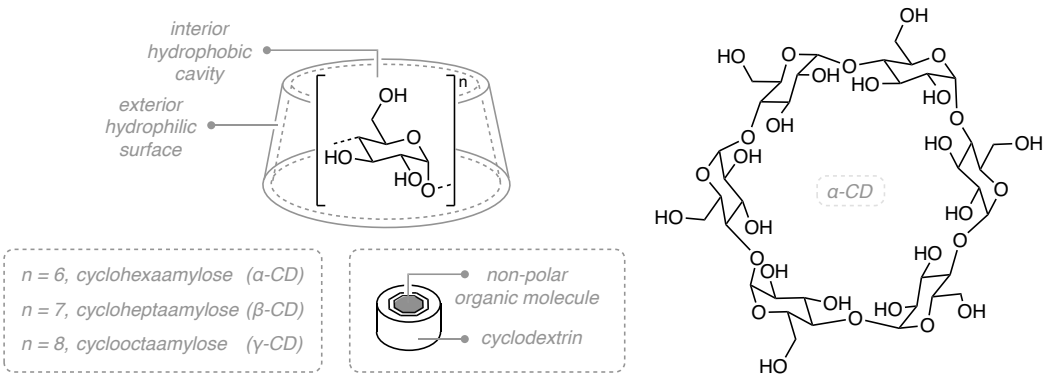

***Figure 3**: General model structure of cyclodextrin and chemical structure of cyclohexaamylose (α-CD).*

The arguably most-commonly pursued strategy to introduce non-covalent interactions in supramolecular catalysis involves the use of cyclodextrins. Their wide-spread availability as well as well-established procedures for further derivatization have made them a powerful tool for biomimetic catalysis.[211-215] Cyclodextrins are a class of cyclic oligosaccharides composed of glucose monomers, which exhibit a hydrophobic cavity surrounded by polar hydroxyl groups (Figure 3). In aqueous solution the hydroxyl groups are orientated to the outside and can either react with an eligible substrate or be used to attach catalytic functional groups. Interestingly, the hydrophobic cleft in the inside of the cyclodextrin provides a high amplification affinity to non-polar organic molecules.[216] The most commonly used isomers consist of 6 (α-CD), 7 (β-CD) or 8 (γ-CD) glucose subunits and vary in size thus offering different binding properties depending on the geometry of the substrate.

As an undisputable pioneer within the field of biomimetic catalysis *Breslow* and co-workers extensively studied the catalytic properties of porphyrin complexes attached to cyclodextrins.[215, 217] In their seminal report on selective epoxidation reactions,[218] geometrical effects of the substrate-catalyst-complex were carefully examined, which comprehensively illuminated the unique binding mode. Specifically, the oxidation rate of the *trans*-stilbene derivative **64a** relative to its closely related congener **64b** was studied, whereas the only difference between these substrates lays in the *para*-nitrophenyl substituent of **64a** (Figure 4). The porphyrin catalysts engaged in these reactions were flanked by aryl substituents, which are covalently linked to a β-cyclodextrin moiety. In particular, a tetra-substituted porphyrin **65**, as well as the di-*trans*-substituted and the di-*cis*-substituted porphyrins **66** and **67** were probed.

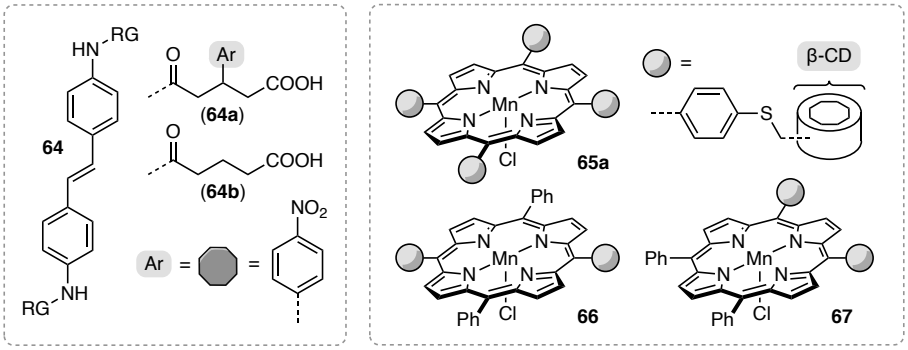

***Figure 4**: Structure of the stilbene derivative **64** engaged in selective epoxidation catalyzed by **65a**, **66** and **67**.[218]*

Remarkably, the *para*-nitrophenyl group revealed an exceptional binding affinity towards β-cyclodextrin. A relative rate of $k_{64a}/k_{64b} = 50$ was observed for the epoxidation catalyzed by complex **65a** exhibiting a simple 1,4-phenyl linker between the porphyrin scaffold and the cyclodextrin. Addition of 2.5 equivalents of adamantyl carboxylic acid was found to be essential to ensure selectivity, probably due to coordination to the axial position of the reactive oxo manganese(V) species, which in turn prevents an unselective epoxidation.[219] Interestingly, when the di-*trans*-substituted porphyrin **66** was employed, the relative rate remained unaffected. However, as soon as the di-*cis*-substituted complex **67** was subjected under otherwise identical conditions, the relative rate decreased by a factor of four clearly suggesting that the substrate is preferably aligned in a linear shape.

Encouraged by these results, *Breslow* and co-workers started to investigate the site-selective hydroxylation of the andostrane-3,17-diol carboskeleton **68** (Scheme 22). The two hydroxyl groups were functionalized with a linear ester carrying a *tert*-butylphenyl recognition group, which was envisioned to fit into the hydrophobic cavity of β-CD, as well as a sulfonate chain to warrant solubility in water.

In their initial studies, the prefunctionalized substrate **68a** was subjected to a hydroxylation reaction catalyzed by **65a** (10 mol%) and the products were carefully examined after a subsequent hydrolysis step.[220-221] In this context, it was an intriguing observation, that the C-6 oxygenated triol **69** was identified as the only product in a total yield of 40% along with 60% of recovered starting material **68b**. If one of the two recognition groups was omitted (R = H) or the geometry was altered (*i.e.* elongation *via* incorporation of additional methylene groups), the selectivity of this transformation deteriorated dramatically to yield a complex mixture of several oxygenated products.

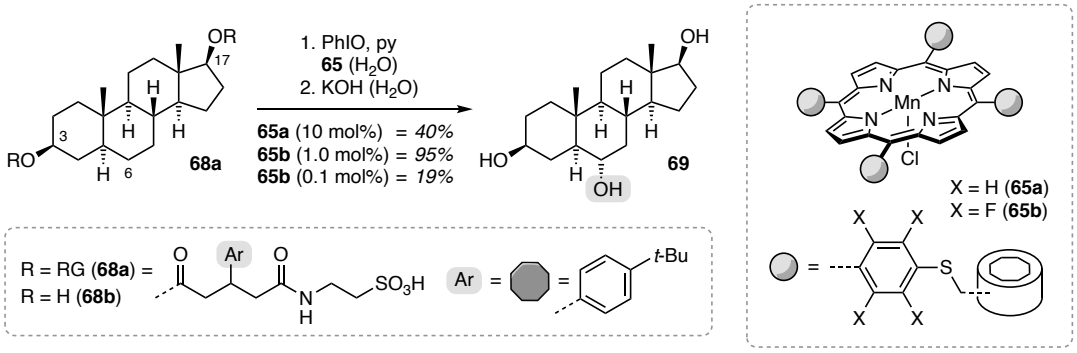

***Scheme 22**: C-6 site-selective hydroxylation of andostrane-3,17-diol **68a** catalyzed by complexes **65a** and **65b**.*[220-222]

The relatively low activity of only four catalytic turnovers was attributed to an oxidative degradation of the catalyst and accordingly, the group of *Breslow* sought for possibilities to increase the stability of the catalyst. Along these lines, the perfluorinated porphyrin complex **65b** turned out to be substantially more robust[63] and with only 1.0 mol% under otherwise identical conditions, the corresponding triol **69** was isolated in 95% yield.[222] Of note, the turn over number (TON) could be further increased to up to 187 by lowering the catalyst loading to 0.1 mol%, albeit at only 19% conversion. The significant effect of the aryl linker at the porphyrin catalyst **65** was later further investigated by introducing an *ortho*-nitrophenyl substituent as well as an intramolecularly coordinating pyridine group, whereupon TONs of up to 3000 were achieved.[223] Changing to a covalently linked thiolate ligand introduced the possibility to use environmentally benign oxidants such as sodium hypochlorite or hydrogen peroxide with TONs of up to 15.[224]

The molecular picture that evolves from these data is depicted in Figure 5. The two-fold bound substrate **68a** spanning the porphyrin **65a** directs the steroid ring B in close proximity to the catalytically active metal center. Moreover, it appears as if the geometry constrains of this complex allows for no other than the 6α-hydrogen atom to be attacked by the reactive oxo manganese species thus explaining the exclusive formation of **69**. Without the ester groups, there is no conversion of the substrate **68b**, probably due to its

poor solubility in water. Either way, the lack of reactivity of the unbound substrate **68b** is crucial in order to eliminate any background reactions that would lead to a diminished selectivity. Most importantly, the oxidation of steroidal alcohols with high concentration of related metalloporphyrins results in predominant formation of the corresponding ketone. Indeed, the reaction proceeds without any notable ketone formation, suggesting that the axial 6β-hydrogen atom points away from the active center, whereupon a consecutive hydrogen abstraction becomes unlikely.

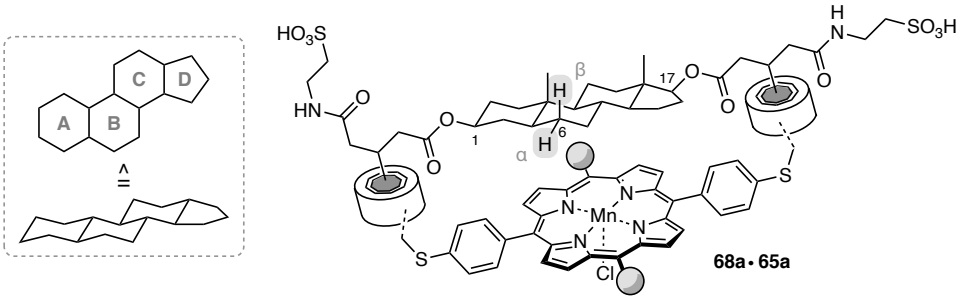

***Figure 5**: Proposed transition state for the site-selective hydroxylation of **68a** catalyzed by **65a**.*

While the high selectivity observed in this transformation is impressive, the hydroxylation at the C-6 carbon center was of no substantial synthetic value. Based on molecular modeling, it seemed possible to relocate the hydroxylation to the C-9 carbon center. This would be highly interesting, given that the dehydrated 9,11-unsaturaed steroid is a key precursor for the synthesis of 9-fluorocorticosteroids,[225-228] however the at this point only method to access the C-9 carbon center was *via* biological fermentation.[229-230]

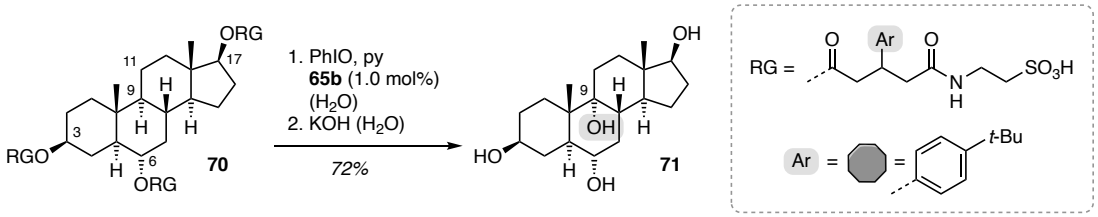

***Scheme 23**: Site-selective hydroxylation of triester **70** to tetraol **71** catalyzed by the perfluorinated catalyst **65b**.[231]*

In a remarkable follow-up approach, the consecutive hydroxylation of triol **69** was investigated.[232] As soon as **69** was tagged with a third recognition group, the corresponding triester **70** was selectively converted into tetraol **71** if 1.0 mol% of the perfluorinated catalyst **65b** were employed (Scheme 23).[231] As opposed to previous studies, it was envisioned that rotation of the linear bound complex **68a·65a** was now prevented as soon as a third anchor was installed. Along these lines, the axial 9β-hydrogen atom is perfectly exposed towards the catalytically active center.

The observed highly selective consecutive reaction raised the question, whether a selective 9β-hydroxylation is feasible by changing the geometry of the binding mode. It was anticipated that by omitting the C-17 ester, 3,6-functionalization of 6-hydroxyandrosterone (**72b**) will induce an angular binding mode that prevents any rotation. Preliminary experiments with substrate **72a** and **65b** as the catalyst exhibiting the established 1,4-tetrafluorophenyl linker indeed delivered triol **73**, however, with almost equal amounts of the C-15 hydroxylated product.[233] The authors suggested a notable change in geometry was necessary in order to bring the catalytically active metal center closer to ring B of the steroid scaffold. The first effort involved the *meta*-functionalized porphyrin complex **65c** (1,3-phenyl linker), whereupon **73** was obtained as an exclusive regioisomer, albeit with less than 3 turnovers, before the catalyst was destroyed (Scheme 24). Having in mind that electron withdrawing aryl substituents can significantly increase catalytic turnovers, the modified, electron-poor catalyst **65d** was probed under otherwise identical conditions, eventually increasing the TON to up to 90.

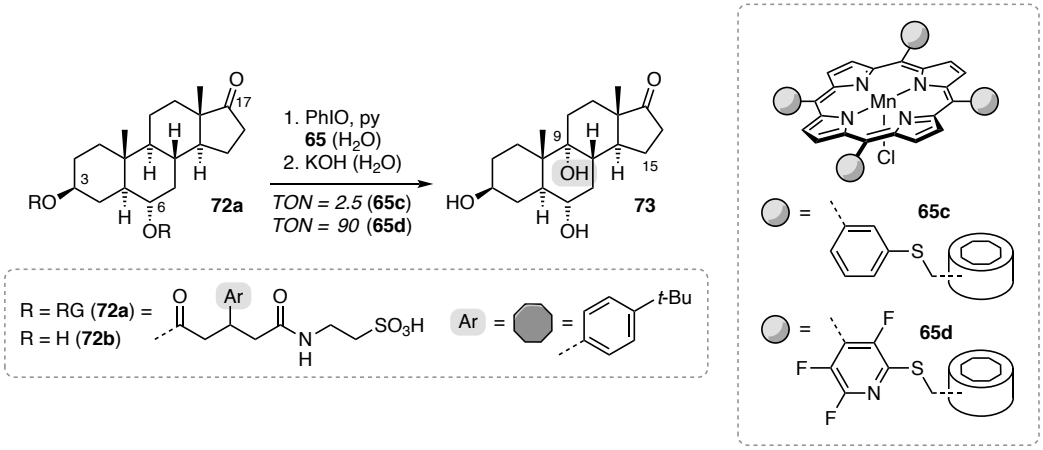

***Scheme 24**: Selective hydroxylation of the 6-hydroxyandrosterone **72a** to triol **73** catalyzed by **65c** and **65d**.[233]*

In a final report by the group of *Breslow,* further experiments were devoted to study the geometrical influence of the aromatic binding groups to direct the hydroxylation to other positions within the steroidal carboskeleton. The initial idea was to truncate the *tert*-butyl phenyl group of the C-3 ester to a simple *tert*-butyl moiety (R^1 = *t*-Bu), while concomitantly inserting an additional phenyl linker at the C-17 ester (Figure 6).[231] When substrate **74a** was subjected to the established oxygenation protocol using catalyst **65b**, the major product was the 7β-alcohol **75** accompanied by minor amounts of the previously obtained triol **69** as well as the 15α-hydroxylated product **76** (**69/75/76** = 20/60/20). The lack of selectivity was rationalized by a too flexible diphenyl group, potentially rotating while binding to β-cyclodextrin. Accordingly, a 1,4-xylyl linker was incorporated into substrate **74b**. Indeed, the outcome changed drastically, as formation of **75** was entirely suppressed instead a 1 to

1 mixture of **69** and **76** was obtained. A final attempt to increase the selectivity was pursued by changing the *tert*-butyl group to a bulkier adamantyl group (R^1 = Ad), as they are known to bind more than 60 times stronger to β-cyclodextrin. Anticipating that a tighter binding might improve selectivity, **74c** was probed in the hydroxylation reaction whereupon a preferred hydroxylation at C-15 was observed (**69**/**75**/**76** = 33/-/67).

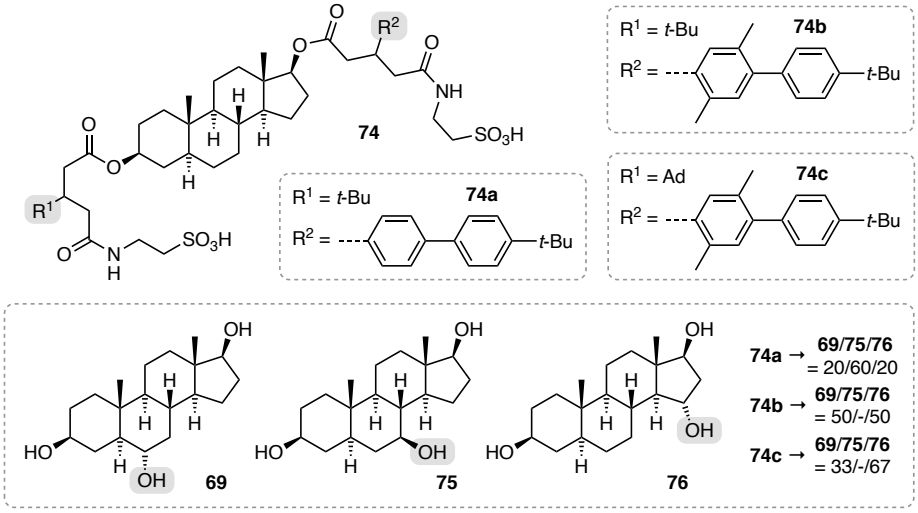

***Figure 6**: Selective hydroxylation of triester **74** depending on the hydrophobic binding groups R^1 and R^2.*

In summary, *Breslow's* studies serve as a compelling demonstration on how supramolecular catalysts can gain control over site-selectivity in the C–H hydroxylation of complex steroids. The highly selective 6α- and 9α-hydroxylation was accomplished by carefully adjusting the geometry of the substrate-catalyst-complex, as well as by increasing the rigidity of the proposed binding mode. The price to pay are elaborate and super-sized catalysts as well as sophisticated recognition groups. Moreover, some transformations provide vivid examples on how marginal changes can dramatically affect the binding mode in a sometimes unpredictable manner.

Chelating and Complexing Interactions

Apart from cyclodextrins, the group of *Breslow* explored the possibility to utilize metal coordination as a recognition element. In their seminal work on epoxidation reactions, the manganese salen complex **77** was prepared, which is decorated with two bipyridine moieties hence enabling the complexation of copper(II) ions (Figure 7).[234-235] Along these lines, an olefin equipped with a suitable recognition group was preferentially oxidized over a non-binding substrate.[236] As proposed by the authors, the fast ligand exchange of first-row metal coordination complexes provided a high catalytic turnover.

Encouraged by these results and keeping in mind the outstanding selectivity that was accomplished with supramolecular porphyrin complexes exhibiting cyclodextrin recognition elements, the manganese porphyrin complex **78** as well as the fluorinated congener **79** were prepared.[237-238]

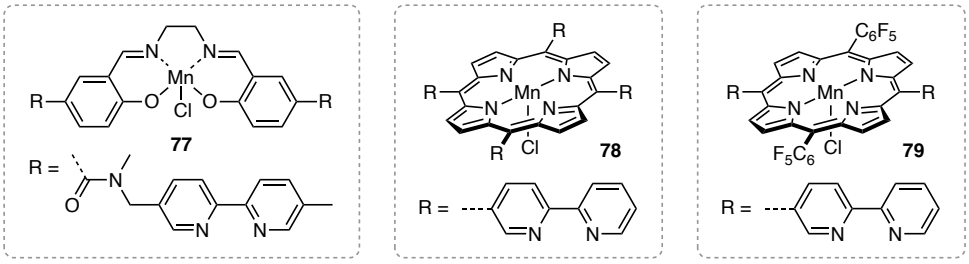

***Figure** 7: Structure of the manganese salen complex **77** and the two manganese porphyrin catalysts **78** and **79**.*

The search of an appropriate recognition group to be attached to the steroid scaffold led to a 2,2'-bipyridinyl-5-carboxylate, given that other metal coordinating groups such as picolinate, nicotinates as well as pyridinylhydrazones and hydroxyquinoline were not stable under the oxidizing conditions. When the C-17 ester **80a** was probed in a first hydroxylation experiment, a geometrically controlled hydroxylation lead to the formation of the secondary alcohol **81a**, the corresponding overoxidized ketone and the regioisomer **82a** in a 50/35/15 ratio (Scheme 25).[237] Although the observed site-selectivity was relatively high, as much as 50 mol% of **78** were necessary to convert 20% of the substrate. A control experiment was performed, in which the bipyridinylcarboxylate **80a** was replaced by benzoate **80b**. Interestingly, without any possibility of metal coordination, the reactive site relocated from ring D to the C-5 and C-6 carbon center at ring B. It is therefore suggested that complexation of the copper ions by both the substrate and the catalyst, directs the oxygenation to a position in close proximity to the C-17 recognition ester.

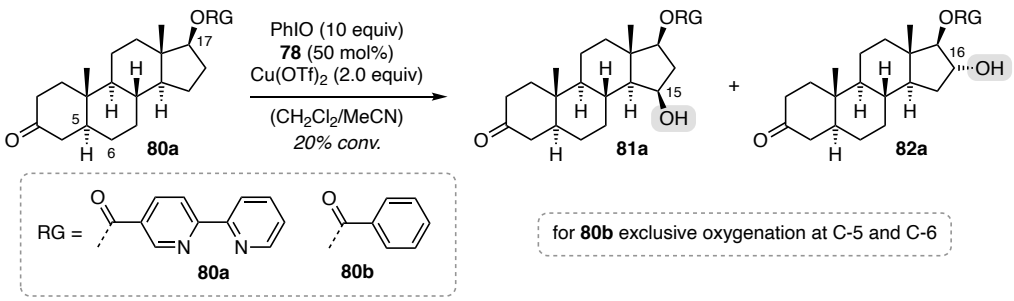

***Scheme 25**: Site-selective oxygenation of 2,2,-bipyridinyl-5-carboxylate **80a** to alcohol **81a** and **82a**.[237]*

A different approach was conceived when the respective C-3 ester was employed in a slightly more concentrated reaction mixture. Substrate **83a** appeared to be less reactive, whereupon the oxidant was added in six portions (10 equivalents every hour) until the conversion of **83a** has entirely ceased.

Under these conditions, a site-selective transformation to the 6α-alcohol **84a** was observed, albeit with significant amount of the ketone **85a**, the product of over-oxidation (**84a**/**85a** = 37/63) (Scheme 26). Once again, a control experiment in which the corresponding C-3 benzoate **83b** was employed under otherwise identical conditions, led to an unselective oxygenation at C-6, C-7, C-12 and C-14 at 27% conversion.

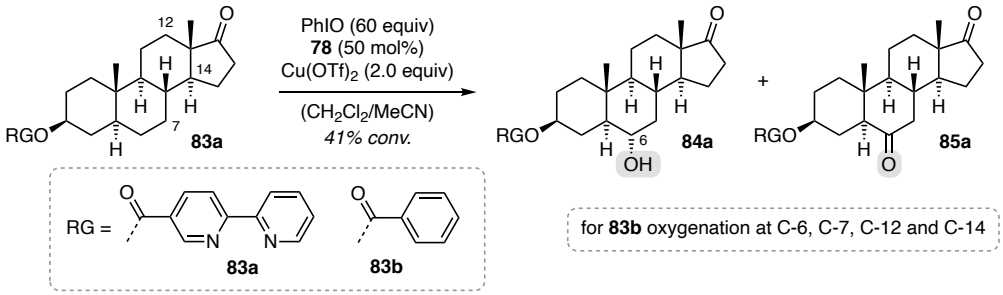

***Scheme 26**: Site-selective oxygenation of 2,2,-bipyridinyl-5-carboxylate **83a** to alcohol **84a** and ketone **85a**.*[237]

The relatively poor catalytic performance in this biomimetic study was attributed to two major restrains. On one hand, the nitrogen atoms of the 2,2'-bipyridinyl-5-carboxylates **80a** and **83a** as well as those at catalyst **78** are easily oxidizable. Once the corresponding *N*-oxides are formed there will be a retarded coordination to the metal center, which will likely result in an unselective reaction. On the other hand, it seems safe to assume that the lack of catalytic turnovers is closely related to the general lability of catalyst **78**, given that previous studies involving cyclodextrin recognition group revealed that incorporation of aryl fluorides can significantly increase the robustness of the catalyst.[63-64, 222]

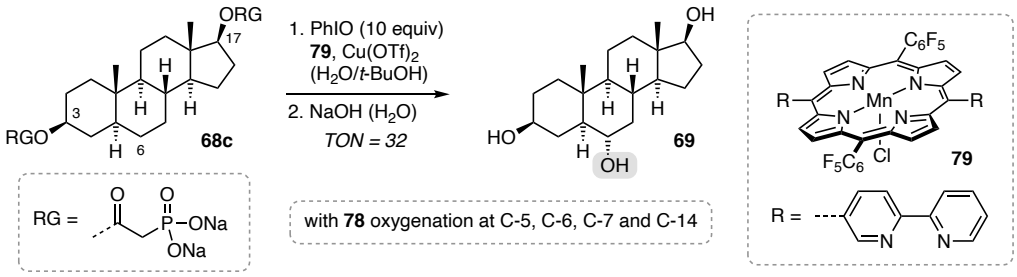

***Scheme 27**: Site-selective hydroxylation of diphosphate **68c** by manganese porphyrin complex **79**.*[238]

With this in mind, both aspects were successfully tackled in a follow-up approach by the same group.[238] Andostrane-3,17-diol **68** was functionalized with two α-phosphonoacetyl recognition groups and subjected to a modified oxygenation procedure using the fluorinated manganese porphyrin **79** (Scheme 27). Besides the improved stability, it was envisioned that the two *trans* recognition groups in **68c** can help to provide a more constrained linear binding mode, as opposed to four recognition groups potentially allowing angular binding *via* two *cis* bipyridine groups

Indeed, **79** catalyzed the hydroxylation of the steroidal carboskeleton **68c** at a specific side. Similar to the cyclodextrin studies, triol **69** was isolated as the major product after a subsequent hydrolysis step in a relative selectivity of 90% over other, unidentified oxidized products. The TON increased to 32, which supported the hypothesis of **79** being a more robust catalyst. Nevertheless, both the selectivity as well as the catalytic activity were not quite as efficient as in the case of the cyclodextrin directed approach and accordingly no further efforts were made to improve the metal coordination directed strategy.

As previously alluded to, the group of *Costas* is primarily interested in the oxygenation of unactivated C-H bonds.[239] Their most commonly employed catalysts involve manganese aminopyridine complexes **21** which often carry a bulky substituent at the C-5 position of the pyridinyl moiety (Figure 8). As a recent supplement to this type of catalysts, the elaborate complex **21d** was synthesized, carrying an 18-benzocrown-6 ether recognition device. The authors anticipated, that non-covalent binding to primary ammonium ions can induce a geometrically controlled oxygenation at a distinct remote position.[77, 172, 240-241]

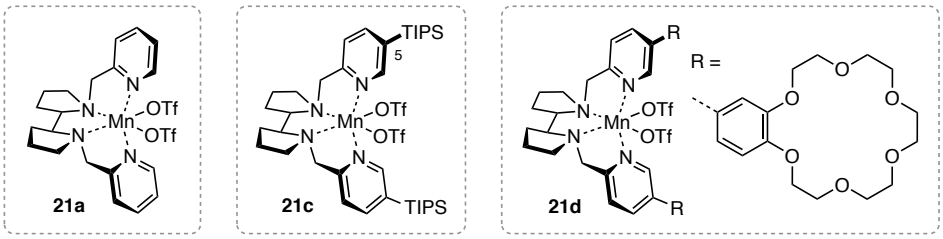

***Figure 8**: Structure of aminopyridine complexes **21**. **21d** carries a 18-benzocrown-6 ether recognition element.[242]*

At the outset, decylammonium tetrafluoroborate (**86**) was envisioned to be a suitable substrate for this approach. The non-directed oxygenation catalyzed by the simple manganese aminopyridine complex **21a** (1.0 mol%) delivered a mixture of oxygenated products in 34% yield (C-3 to C-9 ketone). The carbon centers located close to the protonated amine turned out to be less reactive (<15% selectivity for the C-3, C-4 and C-5 ketones), while the terminal, easier accessible carbon centers produced favorably the C-8 ketone **87** and the C-9 ketone **88** (53% selectivity for **87** and **88**) (Scheme 28). Introducing a bulky TIPS moiety at the catalyst **21c** had no notable effect on the product distribution.

When the crown ether **21d** was employed under otherwise identical conditions, the selectivity for the distal ketones **87** and **88** increased (81% selectivity), suggesting that supramolecular recognition is responsible for the preferred oxygenation at the remote position. In order to examine this hypothesis more carefully, a set of control experiments were performed.

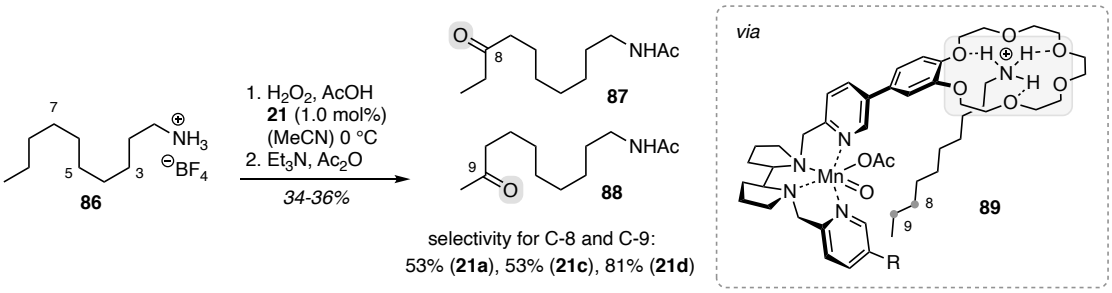

***Scheme 28**: Site-selective oxygenation of decylammonium ion (**86**) directed by molecular recognition.*[242] Et = ethyl

Addition of dibenzo-18-crown-6 ether to the undirected reaction did not alter the selectivity, clearly suggesting that a simple binding of the substrate to the crown ether does not relocate reactive site. However, addition of $Ba(ClO_4)_2$ to the directed approach suppressed any selectivity effects due to saturation of the receptor binding group. Along a similar line, introducing *N*-methyl groups to the substrate prevented amplification to the catalyst **21d** and resulted in a deteriorated selectivity. Finally, when prolonging the linear carbon chain of the substrate, the selectivity for the C-8 and C-9 position was maintained as long as **21d** was utilized, while the oxygenation promoted by catalyst **21a** continued to deliver the most accessible terminal ketones. Conclusively, it seems very likely that the protonated decylamine **86** is anchored by the remote crown ether of **21d** whereupon carbon C-8 and C-9 are directly exposed towards the catalytically active metal center **89**. A preferential oxidation of one of the two carbon centers was not observed, probably owing to the high flexibility of the linear catalyst substrate complex. Inspired by *Breslow's* competing experiments,[236] a follow up approach by the same group revealed that a very high substrate selectivity can be achieved. For example, menthyl acetate is preferentially oxidized by catalyst **21a** (the ratio of the corresponding products was 80/20). In stark contrast, when **21d** was employed the outcome changed dramatically and a reversed selectivity was observed (product ratio = 2/98).[243]

Hydrogen bonding

Although hydrogen bonding has found numerous applications in catalytic reactions, they were predominantly implemented to control enantioselectivity.[187, 197-199] For instance, our own group has a rich history in enantioselective photochemical reactions,[244] which are controlled by two-point hydrogen bonding.[200] Particularly, chiral lactams derived from *Kemp's* triacid[245] were extensively studied,[246-251] which in turn were inspired by *Rebek's* seminal molecular recognition studies.[252-256] Following these pioneering studies, the group of *Crabtree* sought for a possibility to induce a site-selective oxygenation reaction

controlled by a structurally related non-covalent interaction. The respective carboxylate obtained from the same carbon scaffold was utilized as a hydrogen bonding motif,[257-260] and was eventually tethered to a catalytically active metal center. In this context, it was previously reported, that the di-μ-oxo dimanganese complex **90a** features outstanding catalytic properties to oxidize C–H bonds using *Oxone* (peroxomonosulfate) as a stoichiometric oxidant (Figure 9).[261-262]

The *Rebek* type imide **91** was eventually functionalized with a terpyridine ligand, spatially divided by a 1,4-phenyl linker. Metal insertion was performed by using manganese(II) chloride while a subsequent oxidation with *Oxone* furnished the active catalyst (**91**)Mn(μ-O)$_2$Mn(**91**) (**90c**).[263] As opposed to **90b** (R = Ph) being incapable of any supramolecular communication, it was envisioned that the carboxylate **90c** (R = molecular recognition element derived from **91**) can dock a suitable substrate *via* hydrogen bonding thus introducing a site-selective oxygenation at the di-μ-oxo dimanganese center.

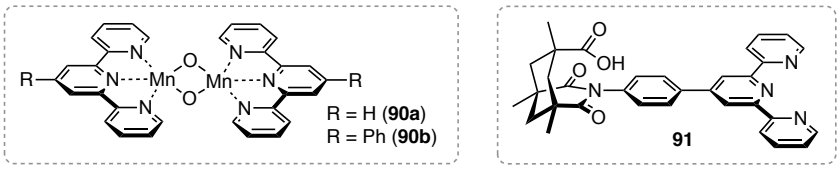

***Figure 9**: Structure of the highly oxidizing di-μ-oxo dimanganese complex **90** and the bifunctional ligand **91**.*

Ibuprofen (**92**) was anticipated to be a promising substrate, given it is decorated with an eligible recognition group and exhibits two benzylic methylene sites. The undirected oxygenation catalyzed by complex **90b** and tetrabutylammonium *Oxone* (TBAO) furnished ketone **93** in an already relatively selective transformation (**93/94** = 78/22) at 54% conversion (Scheme 29). The corresponding regioisomer was proposed to be **94**, as hydroxylation adjacent to the carboxylate induced a spontaneous decarboxylation. When **90c** was employed, the observed selectivity increased drastically and virtually exclusive formation of **93** was observed (**93/94** = 99/1, at 53% conversion).

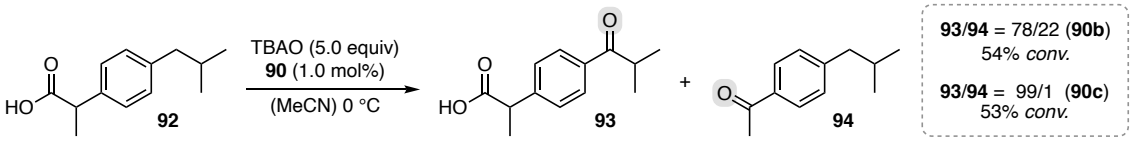

***Scheme 29**: Site-selective oxygenation of ibuprofen (**92**) by the di-μ-oxo dimanganese catalysts **90b** and **90c**.[263]*

In order to confirm whether indeed simple hydrogen bonding is responsible for the enhanced reactivity, further mechanistic studies were conducted involving acetic acid as a superstoichiometric additive (4.0 equivalents). Interestingly, protonation of the carboxylate prevented any hydrogen bonding, whereupon the selectivity was lost (**93/94** = 75/25, 58%

conversion at 20 °C when catalyzed by **90c**), clearly indicating that the carboxylate directs the oxygenation to a designated site. In this context, molecular modeling using the X-ray parameters derived from **91** were in line with the proposed transition state **95** (Figure 10), where indeed the isobutyl moiety is directly exposed to the active metal center.[264] As a final remark, the TON of complex **90c** can substantially be increased to up to 710 turnovers by lowering the catalyst loading (0.1 mol%) to circumvent any oxidative degradation as well as using deuterated acetonitrile as the solvent to prevail hydrogen abstraction of the solvent.

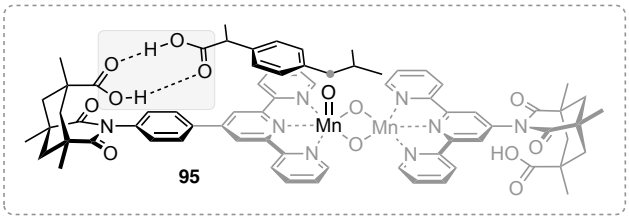

***Figure 10**: Proposed transition state **95** for the hydrogen-bond-mediated oxygenation of ibuprofen (**92**).*

Encouraged by the remarkable selectivity in the oxygenation of ibuprofen (**92**) the authors studied the hydroxylation of (4-methylcyclohexyl)acetic acid (**96**). In a competing experiment, the 1,4-*trans*-isomer **96** and the 1,4-*cis*-isomer **96'** were subjected to a non-directed oxygenation catalyzed by **90b**. None of the two diastereoisomers seemed to show a higher reactivity towards the hydroxylation and equal amounts of **97** and **97'** were formed at 19% conversion (Scheme 30). As soon as a molecular recognition group was introduced by using catalyst **90c**, the observed reactivity was significantly altered and the corresponding axial alcohol **97** was obtained almost exclusively (**97**/**97'** = 99/1, 18% conversion).

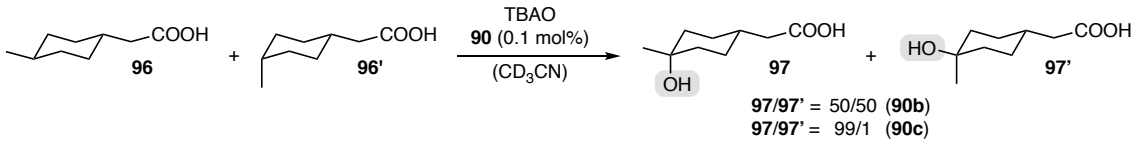

***Scheme 30**: Hydroxylation of cyclohexyl acetic acid **96** and its diasterisomer **96'** to secondary alcohols **97** and **97'**.*

Inspired by the work of *Breslow*[236, 238] and *Costas*,[242] the group of *Higuchi* very recently disclosed the preparation of the ruthenium porphyrin catalyst **98** (Figure 11). While equipped with two electron withdrawing pentafluorophenyl substituents to sustain oxidative degradation, two additional pyridinyl-2,6-diamide groups were installed in **98b** to invite three-point hydrogen bonding.[265]

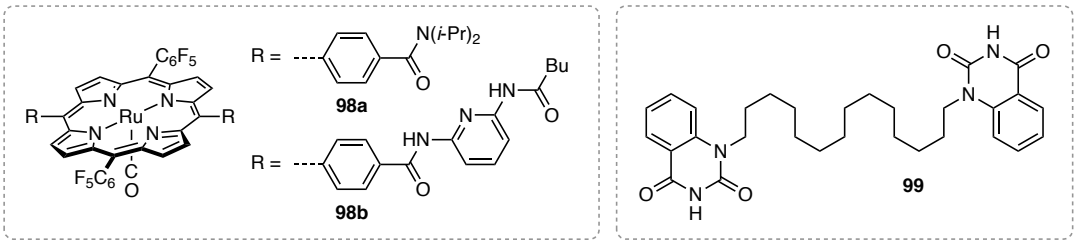

***Figure 11**: Structure of ruthenium porphyrin catalyst **98** and linear substrate **99**.[265] i-Pr = isopropyl*

A suitable counterpart for their concept was envisioned to be the linear tetradecyl substrate **99**, which carries a molecular recognition group on each of its terminal ends. The major products in the directed oxygenation of **99** catalyzed by the ruthenium complex **98b** (1.0 mol%) and 2,6-dichloropyridine-*N*-oxide, were identified as the corresponding C-5, C-6 and C-7 ketones in an overall yield of 55% (Scheme 31). Favorably, the C-7 ketone **100** was formed in a relative selectivity of 74% over the C-5 and C-6 ketone (*r.r.* = 74/26).

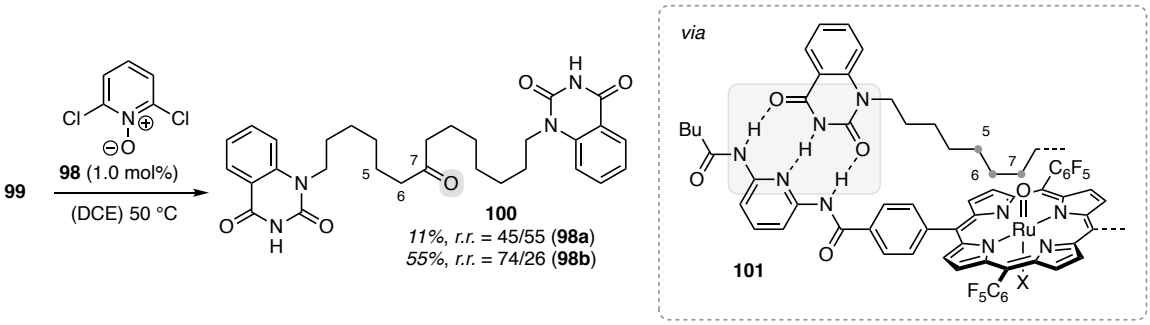

***Scheme 31**: Site-selective C-7 oxygenation of **99** catalyzed by ruthenium porphyrin **98**.[265] DCE = 1,2-dichloroethane*

The undirected oxygenation with **98a** as the catalyst lead to a sluggish reaction (11% yield) and failed to provide a notable selectivity as almost equal amounts of the three products were formed (*r.r.* = 45/55). It becomes apparent that hydrogen bonding not only influences selectivity, but also appears to have a rate acceleration effect. More specifically, the actual yield of **100** is 8-fold higher as soon as non-covalent interactions are involved to guide the reaction to a specific site (5% with **98a** vs. 41% with **98b**). The dramatic effect on the yield can be rationalized by a tightly bound quinozaline-2,4-dione to the pyridine diamide spanning the linear carbon chain over the ruthenium porphyrin, whereupon the C-7 carbon atom is precisely exposed towards the oxo ruthenium species[266] (Figure 12). In line with the proposed model **101**, detailed kinetic experiments revealed that the initial rate for a reaction catalyzed by **98b** is more than 3-fold higher than for the undirected approach (3.9 vs. 1.2×10^{-3} mmol L^{-1} min^{-1}).

As previously stated, our group has been involved in hydrogen-bond directed catalysis for more than two decades.[200] Primarily focusing on photochemical reactions, the concept of supramolecular recognition commenced with the synthesis of the lactam **102**.[267] In these

systems, the chiral hydrogen bonding site was installed at the incipient imide group, while the carboxylate, later used by the group of *Crabtree*,[263-264] was derivatized into a sterically demanding tetrahydronaphthalene unit (Figure 12). Along these lines, lactam **102** is a textbook example for a chiral complexing agent (*cf.* Scheme 21). Coordination to a suitable substrate, typically planar, prochiral amides, provides notable enantioface differentiation due to steric shielding by the rigid heteroaromatic tricycle.[268-273] Specifically, the [2+2]-photocycloaddition of 4-methoxyquinolone (**103**) and an appropriate olefin **104** proceeds almost exclusively at the more accessible *re* face (relative to carbon C-3).[269] The intuitive drawback, however, correlates to the fact that significant amounts of **102** had to be added to the reaction mixture (typically around 2.5 equivalents), in order to achieve high enantioselectivity (>90% *ee*).

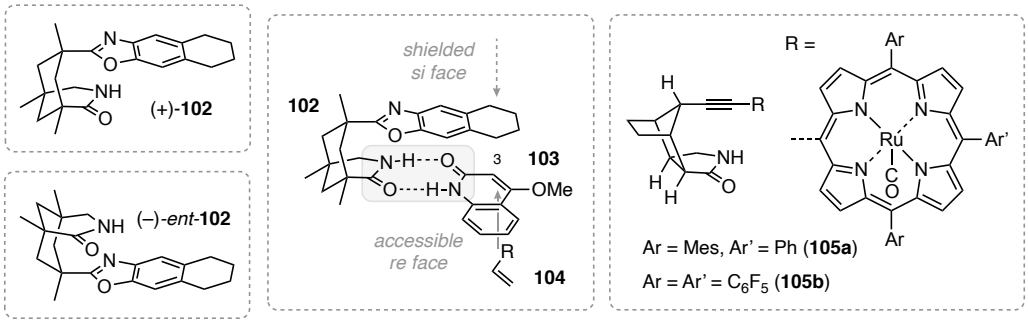

***Figure 12**: Structure of the chiral lactam **102** coordinating to quinolone **103** and the Ru-porphyrin complex **105**.*

Encouraged by our seminal work on enantioselective photocatalysis, we focused our attention on the development of chiral transition metal catalysts equipped with a comparable binding site. Similarly to the work of *Rebek*, the group of *Deslongchamp* explored elaborate imines in molecular recognition studies.[274-276] The anticipated advantage of the slightly altered octahydro-1*H*-4,7-methanoisoindol-1-one skeleton **105** was a less rigid structure compared to the previously used 1,5,7-trimethyl-3-azabicyclo[3.3.1]nonan-2-one scaffold **102**, which indeed has failed to provide a high enantioselectivity in preliminary sulfoxidation experiments.[277] As opposed to the chiral complexing agent, where a constrained binding mode of the substrate is favorable, a catalytically active metal center demanded more spatial flexibility for a functional group to be transferred. The chiral ruthenium porphyrin complex **105a** emerged from these ideas and conclusively demonstrated its remarkable potential for enantioselective catalysis in the epoxidation of 3-vinylquinolones.[278-279]

Our initial discoveries, as well as related studies using a chiral rhodium catalyst with the same binding motif,[280-281] prompted us to further investigate the direct oxygenation of methylene groups. In order to provide a more robust catalyst, the porphyrin substituents

were exchanged by pentafluorophenyl groups.[63] Spirocyclic oxindoles **106** appeared to be a valid starting point for the envisioned oxygenation, because of its structural similarities to the previously employed quinolones. Closely related to the later reported study by the group of *Sun,*[159] we aimed for a desymmetrization *via* direct C–H oxygenation to ketone **107**.

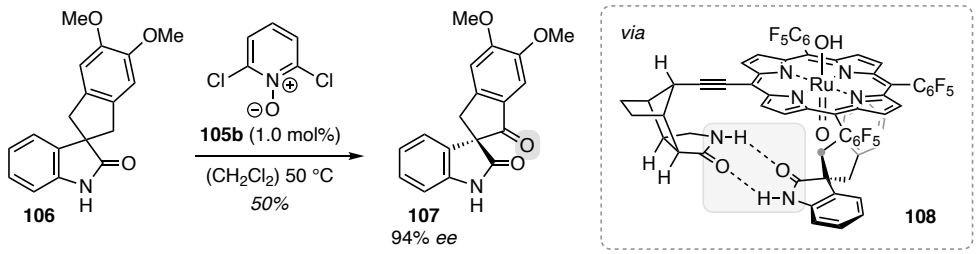

***Scheme 32**: Enantioselective oxygenation of spirocyclic oxindoles **106** by the ruthenium prophyrin catalyst **105b**.*[152]

As anticipated, the oxygenation of **106** using the modified catalyst **105b** and 2,6-pyridine-*N*-oxide as the oxidant furnished the desired product **107** in exceptional enantioselectivity (94% *ee*) and a reasonable yield of 50% (Scheme 32).[152] In some cases, overoxidation to the corresponding ketone was realized by a consecutive oxidation step using pyridinium chlorochromate[282-283] or *Swern* conditions[284-285] (9 examples, 48-70% yield, 38-94% *ee*). The proposed catalytic cycle for the enantioselective oxygenation is depicted in Figure 13.

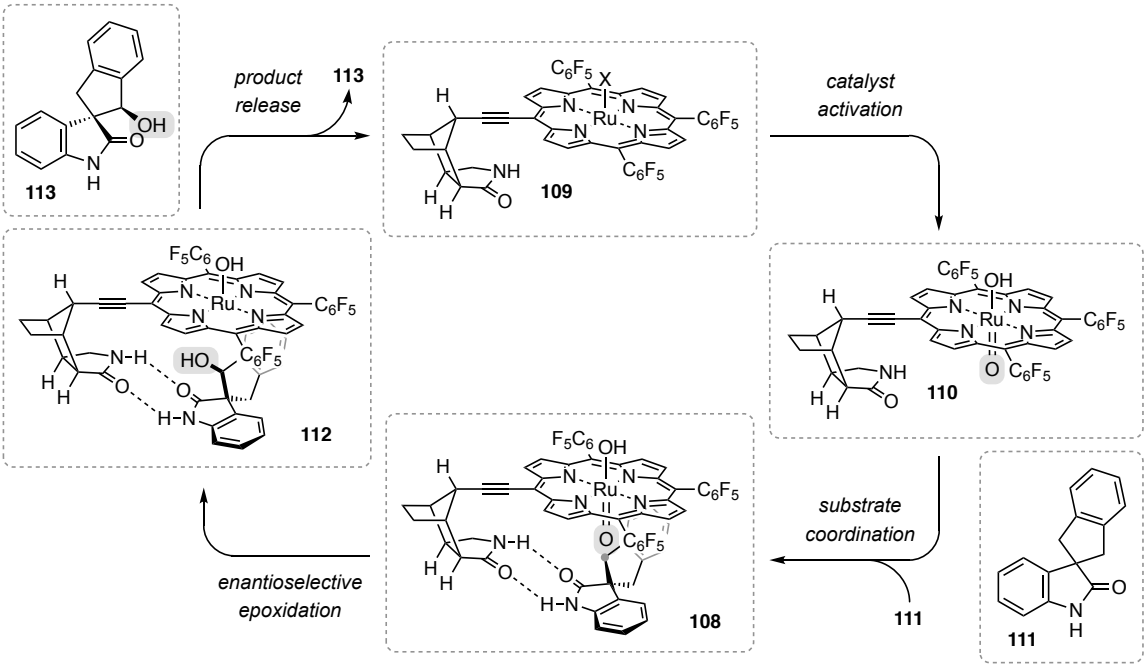

***Figure 13**: Proposed catalytic cycle for the enantioselective oxygenation of **111** catalyzed by **105b**.*

It is generally accepted that the ruthenium carbonyl complex **105b** is a valid precatalyst, which is subsequently oxidized by 2,6-dichloropyridine-*N*-oxide to the oxo ruthenium complex **110**.[286] Upon coordination of oxindole **111** to the active catalyst **110** *via* two-point

hydrogen bonding, the substrate is located at a position, where one of the two methylene sites in **108** is directly exposed to the active center thus inviting the initial hydrogen abstraction. At this stage, an experimentally derived kinetic isotope effect of 6.1 supported the hypothesis of a rate-limiting C–H scission. A consecutive rapid rebound mechanism is anticipated to eventually furnish the hydroxylated product **112**, which is finally released to close the catalytic cycle. Mechanistically, it seems likely that the catalytic cycle is mediated by highly active ruthenium(III) **109** and oxo ruthenium(V) **110** species, instead of *trans* dioxo ruthenium(VI) and oxo ruthenium (IV) porphyrin complexes.[266] Of note, **113** is not the final product and can undergo a second catalytic cycle to ultimately deliver the desired ketone. Although an enantiomerically enriched product **113** is a possible intermediate as later shown by our group on a geometrically very similar substrate,[287] it was envisioned that **113** can undergo a retro-aldol cleavage whereupon the stereoinformation would be lost.[288]

The presented overview aims to illustrate how the precise orientation of a distinct substrate towards the oxidizing species can dictate the selective oxygenation in an enzyme-like fashion. A constrained binding-mode gives the opportunity to override intrinsic reactivity pattern thus opening up new avenues for sophisticated reaction sequences. Especially seminal studies by the group of *Breslow* have provided intriguing compounds inaccessible by conventional methods, which in fact minimized unselective background reactions. As for most accomplishments in organic synthesis, prosperity comes with limitations that are yet to overcome. For instance, the development of simple, ubiquitous binding groups would be a major achievement to improve the general utility of supramolecular catalysis. Nevertheless, the potential of using attractive interactions to lower transition states and provide enhanced reactivity or even facilitate an enantioselective reaction should not be overlooked as opposed to increasing the rigidity and steric bulk of a given transition metal complex.

Site- and Enantioselective C–H Oxygenation Catalyzed by a Chiral Manganese Porphyrin Complex with a Remote Binding Site

Title: "Site- and Enantioselective C–H Oxygenation Catalyzed by a Chiral Manganese Porphyrin Complex with a Remote Binding Site"

Status: Communication, published online December 22, 2017

Journal: *Angewandte Chemie International Edition* **2018**, *57*, 2953-2957.

Publisher: John Wiley and Sons

DOI: 10.1002/anie.201712340

Authors: Finn Burg, Maxime Gicquel, Stefan Breitenlechner, Alexander Pöthig, Thorsten Bach

Content: The direct transformation of prochiral methylene groups into its corresponding enantiomerically enriched secondary alcohols unambiguously belongs to the most intriguing and challenging chemical reactions in organic synthesis. Inspired by the natural enzyme cytochrome P450, there have been numerous efforts to develop chiral oxygenation catalysts, but the quest to achieve significant selectivity (>90% ee) at reasonable turnover (>50% conversion) had remained unsolved. In the presented work, selectivity and moreover reactivity issues were successfully overcome by a chiral manganese porphyrin complex equipped with a remote hydrogen bonding site. Along these lines, the hydroxylation of quinolone analogues proceeded in outstanding site- and enantioselectivity (up to 99% ee and 97% conversion), while strictly controlled by communication *via* two-point hydrogen bonding to a chiral lactam entity. Further kinetic studies where devoted to shine light on the mode of action of the catalyst.

F. Burg and M. Gicquel planned and executed all experiments (approximately 50% each). F. Burg and T. Bach wrote the manuscript. S. Breitenlechner helped with the kinetic studies and proof reading of the manuscript. A. Pöthig conducted all SC XRD-measurements and managed the processing of the respective data. All work was performed under the supervision of T. Bach.

Oxygenation

International Edition: DOI: 10.1002/anie.201712340
German Edition: DOI: 10.1002/ange.201712340

Site- and Enantioselective C–H Oxygenation Catalyzed by a Chiral Manganese Porphyrin Complex with a Remote Binding Site

*Finn Burg[+], Maxime Gicquel[+], Stefan Breitenlechner, Alexander Pöthig, and Thorsten Bach**

Abstract: *A chiral manganese porphyrin complex with a two-point hydrogen-bonding site was prepared and probed in catalytic C–H oxygenation reactions of 3,4-dihydroquinolones. The desired oxygenation occurred with perfect site selectivity at the C4 methylene group and with high enantioselectivity in favor of the respective 4S-configured secondary alcohols (12 examples, 29–97 % conversion, 19–68 % yield, 87–99 % ee). Mechanistic studies support the hypothesis that the reaction proceeds through a rate- and selectivity-determining attack of the reactive manganese oxo complex at the hydrogen-bound substrate and an oxygen transfer by a rebound mechanism.*

The direct oxygenation of methylene compounds to secondary alcohols[1] poses a significant challenge to the imagination and creativity of synthetic organic chemists. Several selectivity issues need to be addressed: Further oxidation of the alcohol should be avoided (chemoselectivity), the reaction should occur at a specific site (site selectivity), and most importantly, a single enantiomer should be formed (enantioselectivity). Along these lines, there have been numerous efforts to develop enantioselective oxygenation methods in which a transition-metal catalyst mediates the oxygenation of prochiral methylene compounds with a stoichiometric oxidant. Common transition metals employed in these catalysts include ruthenium,[2,3] iron,[4,5] and manganese,[6,7] and the chirality is typically provided by a chiral ligand. Some prominent examples for benzylic oxygenation reactions include the use of a chiral ruthenium porphyrin complex (up to 76 % *ee* at 36 % conversion), a chiral iron porphyrin complex (up to 72 % *ee* at 47 % yield based on oxidant), and a chiral manganese salen complex (up to 87 % *ee* at 13 % yield). It is evident from these data that there is a need for new methods to process prochiral methylene compounds in a more selective fashion.

A potential way to achieve this goal is the development of catalysts that exhibit a distinct binding mode for a given substrate[8,9] and thus display superior site and enantioselectivity in the oxygenation protocol. In previous work, we developed chiral ruthenium porphyrin complexes displaying a chiral hydrogen-bonding entity, which proved to be efficient catalysts for enantioselective epoxidation and enantiotopos-selective oxygenation reactions.[10] However, their propensity to promote the further oxidation of secondary alcohols to ketones and their limited availability due to loss of material in the ruthenium incorporation step made us consider other metal complexes for selective oxygenation reactions.

Inspired by the work of Groves and co-workers on C–H activation reactions by manganese porphyrin complexes,[11] we strived for the synthesis of a porphyrin complex[12] that would be attached to an octahydro-1*H*-4,7-methanoisoindol-1-one hydrogen-bonding motif. Gratifyingly, we found that the Sonogashira cross-coupling reaction of alkyne **1**[10a] with zinc porphyrin complex **2** proceeded smoothly and without extensive hydrodebromination (Scheme 1). Upon acidic

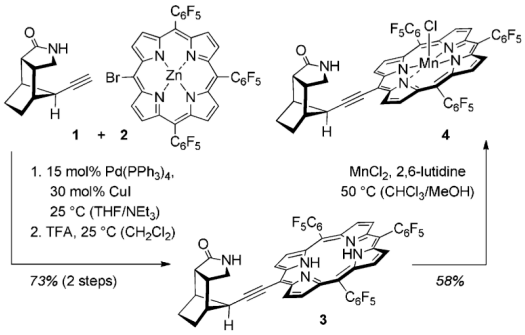

Scheme 1. Preparation of Mn^{III} catalyst **4** by a Sonogashira cross-coupling of Zn^{II} porphyrin **2** and subsequent metal–metal exchange.

(TFA = trifluoroacetic acid) removal[13] of the zinc atom, the enantiomerically pure porphyrin **3** was obtained and fully characterized. The insertion of manganese into the porphyrin core was performed as previously described,[14] and compound **4** showed spectroscopic and analytical properties that matched the data of known manganese porphyrin complexes.[15]

Oxygenation reactions were attempted with 3,3-disubstituted 3,4-dihydroquinolones, which represent a class of heterocyclic compounds with significant biological activity.[16] We envisioned that a late-stage modification of this compound class would lead to secondary alcohols that have not yet become available in enantiomerically pure form.[17] Iodosobenzene was used as the stoichiometric oxidant in dichloromethane solution (Table 1). Substrate **5a**[16b] reacted

[*] M. Sc. F. Burg,[+] Dr. M. Gicquel,[+] Dr. S. Breitenlechner, Dr. A. Pöthig, Prof. Dr. T. Bach
Department Chemie and Catalysis Research Center (CRC)
Technische Universität München
Lichtenbergstraße 4, 85747 Garching (Germany)
E-mail: thorsten.bach@ch.tum.de
Homepage: http://www.oc1.ch.tum.de/home_en/
[+] These authors contributed equally to this work.
Supporting information and the ORCID identification number(s) for the author(s) of this article can be found under: https://doi.org/10.1002/anie.201712340.

Table 1: Optimization of the manganese-catalyzed enantioselective oxygenation of substrate **5a**.

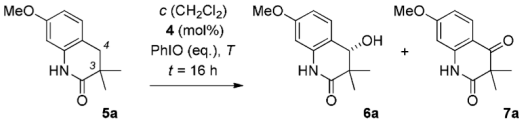

Entry	c[a] [mM]	**4** [mol%]	PhIO[b] [equiv]	T [°C]	**5a** [%]	**6a** [%]	**7a** [%]	*ee*[c] [%]
1	20	2	2.0	25	32	52	11	97
2	20	2	2.0	0	6	59	15	98
3	20	2	2.0	−20	9	44	19	99
4	20	1	2.0	0	5	52	21	99
5	20	2	3.0	0	–	33	31	99
6	20	2	1.5	0	19	60	13	98
7	20	2	1.2	0	36	53	7	97
8	40	2	2.0	0	6	60	13	97
9	10	2	2.0	0	8	68	19	99
10	5	2	2.0	0	19	38	21	92

[a] The reactions were performed under the indicated conditions and were initiated by addition of the catalyst to the pre-cooled reaction mixture. All yields refer to isolated material. [b] Amount of oxidant (PhIO) in equivalents relative to **5a**. [c] Enantiomeric excess (*ee*) of secondary alcohol **6a** as determined by HPLC analysis on a chiral stationary phase.

Table 2: Influence of the substituents X and R on the catalytic enantioselective oxygenation of 3,4-dihydroquinolones **5**.[a]

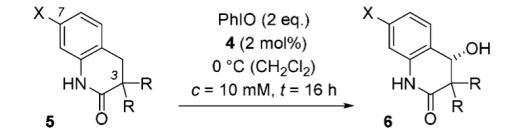

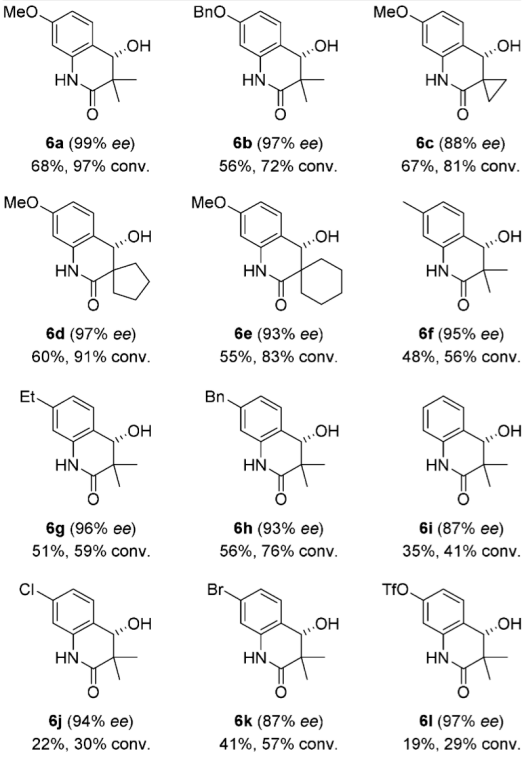

with remarkable enantioselectivity even at ambient temperature (entry 1). A temperature decrease led to an improved enantioselectivity for product **6a** but simultaneously induced the formation of ketone **7a** (entries 2 and 3). A good compromise in terms of reactivity versus selectivity was found at a temperature of 0 °C, at which the ratio of oxidant and catalyst was varied (entries 4–7). While there was little improvement in yield, an experiment with slightly super-stoichiometric quantities of oxidant (entry 7) revealed that the enantioselectivity remained high, even at low ketone formation. A substrate concentration of 10 mM (entry 9) was identified as optimal within the probed concentration range (entries 8–10).

Under the optimized reaction conditions (Table 1, entry 9), product **6a** was isolated in 68 % yield and readily separated from starting material **5a** and ketone **7a**. For better comparability, the reactions of all other substrates **5** were performed under identical conditions, and they were all terminated after a reaction time of 16 hours (Table 2). Yields refer to isolated material, and the conversion (conv.) was determined by re-isolation of the starting material. The main parameter to be studied was the influence of the substitution pattern in positions C3 and C7 on the yield and the enantioselectivity.

Benzyl ether **5b** reacted similarly to methyl ether **5a** and delivered product **6b** with 97 % *ee*. Modification of the geminal disubstitution at position C3[18] did not reduce the reactivity of the three substrates **5c**–**5e** (> 80 % conversion). The *ee* values of products **6c**–**6e** remained high but turned out to be slightly more variable (88–97 % *ee*). Alkyl substitution in position C7 slightly lowered the reactivity of the substrates (56–76 % conversion) but the enantioselectivity remained very high (93–96 % *ee*). Neither the benzylic methyl group in substrate **5f** nor the benzylic methylene group in substrate **5g** displayed any reactivity towards C–H oxygenation. Most remarkably, the potentially reactive, doubly aryl-substituted methylene group in substrate **5h** was not touched by the oxygenation reagent, which illustrates the exquisite site selectivity of the reaction. The parent compound **5i** and 3,4-dihydroquinolones with an electron-withdrawing group in position C7 (**5j**–**5l**) exhibited reduced reactivity, and the conversions were lower (29–57 %) than for the more electron-rich substrates. Even for less reactive substrates, the fidelity of the catalyst remained high. Compounds **5i** and **5k** turned out to be processed with comparably low enantioselectivity (87 % *ee*) while the 7-chloro- and the 7-trifluoromethylsulfonyloxy-substituted quinolones **5j** and **5l** gave the respective products with 94 % and 97 % *ee*, respectively.

Control experiments were performed to shed some light on the mode of action of the catalyst (Scheme 2). In the first experiment, racemic alcohol *rac*-**6a** was subjected to the reaction conditions of the oxygenation reaction. Oxidation to

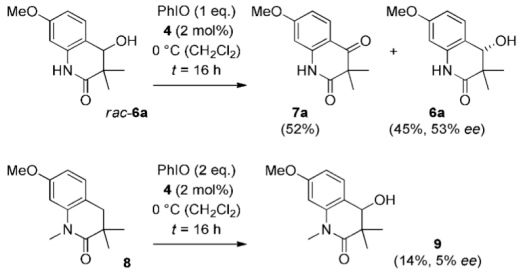

Scheme 2. Control experiments performed with the racemic alcohol *rac*-**6a** and with the N-methylated dihydroquinolone **8**.

ketone **7a** was observed but the kinetic resolution was not extensive. At a conversion of 55 %, an enantiomeric excess of 53 % *ee* was recorded in favor of the *S*-configured (see below) alcohol **6a**. The relative rate of the two enantiomers (*s* factor) can be calculated from these values to be $k_R/k_S = 4.2$.[19] In a second control experiment, the influence of the hydrogen-bond-donating NH group was probed. The N-methylated substrate **8**, which lacks this hydrogen-bonding site, reacted poorly under the standard oxygenation conditions. Alcohol **9** was obtained in almost racemic form (5 % *ee*) and in only 14 % yield.

Although the low *s* factor obtained in the kinetic resolution experiment (Scheme 2) indicated that the prime reason for the observed enantioselectivity was the differentiation of the two enantiotopic hydrogen atoms in the oxygenation event, the enantiomeric excess was monitored over time (Figure 1). It was found that for the transformation of **5a** into

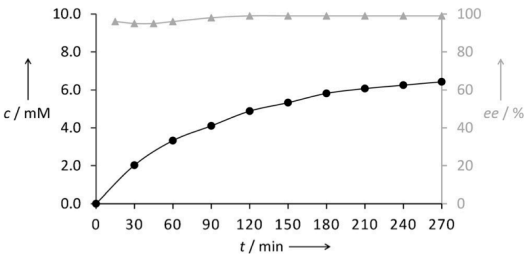

Figure 1. Rate and *ee* profile for the enantioselective oxygenation of substrate **5a** to product **6a** under the standard reaction conditions (see Table 2).

6a, the enantioselectivity was already high (> 95 % *ee*) at low substrate conversion (< 20 %), clearly supporting the hypothesis that the oxygenation reagent is guided to a specific substrate position by the hydrogen-bonding interaction. Detailed kinetic studies with an internal standard (see the Supporting Information for details) revealed that the reaction was first order in substrate (concentration range $c = 2.5$–15 mM) and first order in catalyst ($c = 0.1$–0.3 mM). The oxidant loading was found to be inconsequential for the rate law (zero order).

The mechanistic picture that evolves from the experimental data includes a reactive Mn^V oxo species whose active site is directed to a specific C–H bond by hydrogen bonding (Figure 2). The absolute configuration determined for prod-

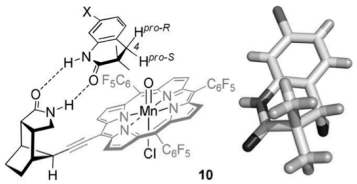

Figure 2. Complex **10** of substrates **5** with the active Mn^V catalyst enables enantioselective oxygenation to the respective 4*S*-configured alcohol, as confirmed by the crystal structure of product **6j** (X = Cl).

uct **6j** by anomalous X-ray diffraction is in line with preferred attack at the pro-*S* hydrogen atom attached to carbon atom C4. The geometric constraints allow for no other hydrogen atom to be attacked by the oxygenation reagent. In line with the rate law, the rate-determining step is the oxygenation event, which is likely to occur by a rebound mechanism,[20] that is, by hydrogen atom abstraction and subsequent delivery of the hydroxyl group from the manganese atom.

In our specific case, the reaction of substrate **5c** provided evidence for an oxygen rebound mechanism. The transient cyclopropyl-substituted radical **11** (Figure 3) in the above-

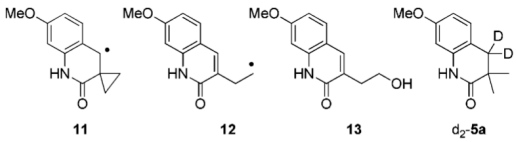

Figure 3. Structures of radicals **11** and **12** and quinolones **13** and d_2-**5a**.

mentioned mechanistic scenario would be an intermediate that is expected to open to the homobenzylic radical **12**. Rate constants for cyclopropyl methyl/but-3-enyl radical clocks[21] are on the order of $10^8\ s^{-1}$, and the ring opening should therefore compete with the hydroxyl transfer from the manganese atom. The homobenzylic alcohol **13** was expected as a side product, and was indeed isolated in 5 % yield from the reaction of **5c** to give **6c** (Table 2). This finding supports the intermediacy of a transient radical in the oxygenation reaction. The hypothesis that the cleavage of the C–H bond was rate-determining was corroborated by kinetic isotope effect (KIE) studies. Experiments were performed with substrates d_2-**5a** and **5a** ($c = 10$ mM, 2 mol % **4**), and the individual reactions were followed by GLC analysis (with an internal standard). The KIE obtained from the individual reaction rate constants is $k_H/k_D = 3.0 \pm 0.2$, which matches values previously recorded for oxygenation reactions catalyzed by manganese porphyrin complexes.[22]

A bent transition state has been suggested to account for the relatively low KIEs obtained for oxygenation reactions catalyzed by manganese porphyrin complexes.[22a] Preliminary DFT calculations[23] support a reaction proceeding via a Mn^{V} oxo triplet intermediate and a bent transition state but a complete active space (CAS) analysis seems warranted to obtain a more reliable picture.

In summary, we have shown that a hydrogen-bonding ligand serves as a key element in controlling the selectivity of a manganese porphyrin catalyzed C–H oxygenation reaction. 3,3-Disubstituted 3,4-dihydroquinolones reacted exclusively and with high enantioselectivity at the C4 position of the heterocyclic skeleton. Evidence was collected that the reaction proceeds via oxygen transfer from a manganese oxo complex in a rebound mechanism. It appears that the hydrogen-bonding event lowers the activation barrier for attack at a specific C–H bond, and it is likely that this mode of action will apply also to related reactions. More importantly, it seems to be possible to address distinct C–H positions in a given substrate by spatially adjusting the position of the catalytic entity relative to the hydrogen-bonding substrate.

Acknowledgements

Financial support by the Deutsche Forschungsgemeinschaft (grant Ba 1372-17) is gratefully acknowledged. O. Ackermann and J. Kudermann are acknowledged for their help with HPLC and GLC analysis and Prof. S. Huber (Bochum) for preliminary DFT calculations.

Conflict of interest

The authors declare no conflict of interest.

Keywords: enantioselectivity · hydrogen bonds · manganese · oxygenation · porphyrinoids

How to cite: *Angew. Chem. Int. Ed.* **2018**, *57*, 2953–2957
Angew. Chem. **2018**, *130*, 3003–3007

[1] For reviews on C–H oxygenation reactions, see: a) G. B. Shul'pin, *Catalysts* **2016**, *6*, 50; b) "C–O Bond Formation by C–H Activation": R. Irie in *Comprehensive Chirality, Vol. 5* (Eds.: E. M. Carreira, H. Yamamoto), Elsevier, Amsterdam, **2012**, pp. 36–68; c) M. Costas, *Coord. Chem. Rev.* **2011**, *255*, 2912–2932; d) T. Newhouse, P. S. Baran, *Angew. Chem. Int. Ed.* **2011**, *50*, 3362–3374; *Angew. Chem.* **2011**, *123*, 3422–3435; *Angew. Chem. Int. Ed.* **2011**, *50*, 3422–3435; e) C.-M. Che, V. K.-Y. Lo, C.-Y. Zhou, J.-S. Huang, *Chem. Soc. Rev.* **2011**, *40*, 1950–1975; f) H. Lu, P. Zhang, *Chem. Soc. Rev.* **2011**, *40*, 1899–1909.

[2] a) R. Zhang, W.-Y. Yu, T.-S. Lai, C.-M. Che, *Chem. Commun.* **1999**, 1791–1792; b) Z. Gross, S. Ini, *Org. Lett.* **1999**, *1*, 2077–2080; c) R. Zhang, W.-Y. Yu, C.-M. Che, *Tetrahedron: Asymmetry* **2005**, *16*, 3520–3526.

[3] For a recent review on ruthenium oxo complexes, see: T. Ishizuka, H. Kotani, T. Kojima, *Dalton Trans.* **2016**, *45*, 16727–16750.

[4] a) J. T. Groves, P. Viski, *J. Am. Chem. Soc.* **1989**, *111*, 8537–8538; b) J. T. Groves, P. Viski, *J. Org. Chem.* **1990**, *55*, 3628–3634.

[5] For a recent review on iron-catalyzed oxygenation reactions, see: A. C. Lindhorst, S. Haslinger, F. E. Kühn, *Chem. Commun.* **2015**, *51*, 17193–17212.

[6] a) K. Hamachi, R. Irie, T. Katsuki, *Tetrahedron Lett.* **1996**, *37*, 4979–4982; b) L. Halterman, S.-T. Jan, H. L. Nimmons, D. J. Standlee, M. A. Khan, *Tetrahedron* **1997**, *53*, 11257–11276; c) N. Komiya, S. Noji, S.-I. Murahashi, *Tetrahedron Lett.* **1998**, *39*, 7921–7924; d) T. Hamada, R. Irie, J. Mihara, K. Hamachi, T. Katsuki, *Tetrahedron* **1998**, *54*, 10017–10028; e) S.-I. Murahashi, S. Noji, N. Komiya, *Adv. Synth. Catal.* **2004**, *346*, 195–198; f) H. Srour, P. Le Maux, G. Simonneaux, *Inorg. Chem.* **2012**, *51*, 5850–5856; g) P. Le Maux, H. Srour, G. Simonneaux, *Tetrahedron* **2012**, *68*, 5824–5828; h) M. Milan, M. Bietti, M. Costas, *ACS Cent. Sci.* **2017**, *3*, 196–204.

[7] For recent reviews on manganese-catalyzed oxidation and oxygenation reactions, see: a) M. M. Najafpour, G. Renger, M. Holynska, A. N. Moghaddam, E.-M. Aro, R. Carpentier, H. Nishihara, J. J. Eaton-Rye, J.-R. Shen, S. I. Allakhverdiev, *Chem. Rev.* **2016**, *116*, 2886–2936; b) R. V. Ottenbacher, E. P. Talsi, K. P. Bryliakov, *Molecules* **2016**, *21*, 1454.

[8] For recent reviews, see: a) H. J. Davis, R. J. Phipps, *Chem. Sci.* **2017**, *8*, 864–877; b) P. Dydio, J. N. H. Reek, *Chem. Sci.* **2014**, *5*, 2135–2145; c) M. Raynal, P. Ballester, A. Videl-Ferran, P. W. N. M. Van Leeuwen, *Chem. Soc. Rev.* **2014**, *43*, 1660–1733; d) S. Carboni, C. Gennari, L. Pignatoro, U. Piarulli, *Dalton Trans.* **2011**, *40*, 4355–4373.

[9] For previous studies on site-selective oxygenation reactions mediated by catalysts with a remote binding site, see: a) R. Breslow, X. Zhang, Y. Huang, *J. Am. Chem. Soc.* **1997**, *119*, 4535–4536; b) J. Yang, R. Breslow, *Angew. Chem. Int. Ed.* **2000**, *39*, 2692–2694; *Angew. Chem.* **2000**, *112*, 2804–2806; c) B. Schönecker, T. Zheldakova, Y. Liu, M. Kötteritzsch, W. Günther, H. Görls, *Angew. Chem. Int. Ed.* **2003**, *42*, 3240–3244; *Angew. Chem.* **2003**, *115*, 3361–3365; d) S. Das, C. D. Incarvito, R. H. Crabtree, G. W. Brudvig, *Science* **2006**, *312*, 1941–1943; e) D. Font, M. Canta, M. Milan, O. Cussó, X. Ribas, R. J. M. Klein Gebbink, M. Costas, *Angew. Chem. Int. Ed.* **2016**, *55*, 5776–5779; *Angew. Chem.* **2016**, *128*, 5870–5873; for a recently reported highly enantiotopos-selective manganese-catalyzed oxygenation reaction of methylene compounds to ketones, see Ref. [6h].

[10] a) P. Fackler, C. Berthold, F. Voss, T. Bach, *J. Am. Chem. Soc.* **2010**, *132*, 15911–15913; b) P. Fackler, S. M. Huber, T. Bach, *J. Am. Chem. Soc.* **2012**, *134*, 12869–12878; c) J. R. Frost, S. M. Huber, S. Breitenlechner, C. Bannwarth, T. Bach, *Angew. Chem. Int. Ed.* **2015**, *54*, 691–695; *Angew. Chem.* **2015**, *127*, 701–705.

[11] a) J. T. Groves, W. J. Kruper, R. C. Haushalter, *J. Am. Chem. Soc.* **1980**, *102*, 6375–6377; b) J. T. Groves, J. B. Lee, S. S. Marla, *J. Am. Chem. Soc.* **1997**, *119*, 6269–6273; c) N. Jin, M. Ibrahim, T. Spiro, J. T. Groves, *J. Am. Chem. Soc.* **2007**, *129*, 12416–12417.

[12] For reviews on functionalized and chiral porphyrins, see: a) S. Hiroto, Y. Miyake, H. Shinokubo, *Chem. Rev.* **2017**, *117*, 2910–3043; b) K. Rybicka-Jasińska, W. Ciszewski, D. T. Gryko, D. Gryko, *J. Porphyrins Phthalocyanines* **2016**, *20*, 76–95; c) M. O. Senge, *Chem. Commun.* **2011**, *47*, 1943–1960.

[13] G. Sargsyan, B. M. Leonhard, J. Kubelka, M. Balaz, *Chem. Eur. J.* **2014**, *20*, 1878–1892.

[14] D. Lahaye, K. Muthukumaran, C.-H. Hung, D. Gryko, J. S. Rebouças, I. Spasojević, I. Batinić-Haberle, J. S. Lindsey, *Bioorg. Med. Chem.* **2007**, *15*, 7066–7086.

[15] a) L. J. Boucher, J. J. Katz, *J. Am. Chem. Soc.* **1967**, *89*, 1340–1345; b) B. De Poorter, B. Meunier, *J. Chem. Soc. Perkin Trans. 2* **1985**, 1735–1740.

[16] More than 100 biologically active compounds of this class are known. For two recent examples, see: a) T. Takai, T. Koike, M. Nakamura, Y. Kajita, T. Yamashita, N. Taya, T. Tsukamoto, T. Watanabe, K. Murakami, T. Igari, M. Kamata, *Bioorg. Med.*

Chem. **2016**, *24*, 3192 – 3206; b) S. Susanta, A. Chandrasekhar, S. Sanjita, H. Subramanya, *Heterocyclic Derivatives as Bromodomain Inhibitors*, WO Patent 2015/104653, **2015**.
[17] a) M. D. Ferretti, A. T. Neto, A. F. Morel, T. S. Kaufman, E. L. Larghi, *Eur. J. Med. Chem.* **2014**, *81*, 253 – 266; b) J. P. N. Papillon et al., *J. Med. Chem.* **2015**, *58*, 4749 – 4770.
[18] The parent 3,4-dihydroquinolone without substituents at C3 (R = H) and C7 (X = H) underwent the oxygenation reaction with high enantioselectivity (95 % *ee*) but the major product resulted from subsequent water elimination to quinolone.
[19] A similar *s* factor was determined in a kinetic resolution experiment with a chiral 4-methyl-substituted 3,4-dihydroquinolone (see the Supporting Information for further details).
[20] a) X. Huang, J. T. Groves, *J. Biol. Inorg. Chem.* **2017**, *22*, 185 – 207; b) W. Liu, M.-J. Cheng, R. J. Nielsen, W. A. Goddard III, J. T. Groves, *ACS Catal.* **2017**, *7*, 4182 – 4188, and references therein.
[21] D. C. Nonhebel, *Chem. Soc. Rev.* **1993**, *22*, 347 – 359.
[22] a) A. Sorokin, A. Robert, B. Meunier, *J. Am. Chem. Soc.* **1993**, *115*, 7293 – 7299; b) K. W. Kwong, T.-H. Chen, W. Luo, H. Jeddi, R. Zhang, *Inorg. Chim. Acta* **2015**, *430*, 176 – 183.
[23] Preliminary DFT calculations were performed with the M06L-D3 functional, the SDD basis set (including a pseudopotential) for Mn, and the 6-31G* basis set for all other atoms.

Manuscript received: December 1, 2017
Accepted manuscript online: December 22, 2017
Version of record online: February 9, 2018

Lactam Hydrogen Bonds as Control Elements in Enantioselective Transition-Metal-Catalyzed and Photochemical Reactions

Title: "Lactam Hydrogen Bonds as Control Elements in Enantioselective Transition-Metal-Catalyzed and Photochemical Reactions"

Status: Perspective Article, published online June 10, 2019

Journal: *The Journal of Organic Chemistry* **2019**, *84*, 8815-8836.

Publisher: ACS Publications

DOI: 10.1021/acs.joc.9b01299

Authors: Finn Burg, Thorsten Bach

Content: For more than two decades the group of Thorsten Bach has been engaged in the development of enantioselective chemical transformations, which operate under the influence of two-point hydrogen bonding. In this *perspective article*, the numerous contributions to the field of enantioselective photocatalysis and transition metal catalysis by our own group are carefully reviewed and analyzed. The first chapter involves a detailed descripted on how a chiral complexing agent was developed and has found several applications as a superstoichiometric chirality transfer reagent in a variety of photochemically induced radical reactions. Related to these chiral lactams, the progression towards chiral catalysts exhibiting appropriate chromophores for harvesting photons in the UV and visible light region is elaborated. Finally, it is summarized how our group became interested in the design and synthesis of chiral transition metal catalyst that are decorated with a very similar binding motif. Within this context, the main objective was to illuminate our latest achievements in the field of epoxidation, sulfoxidation and oxygenation reactions, as well as aziridination and C–H aminations reactions.

F. Burg and T. Bach wrote the manuscript. No experiments were conducted for this article.

JOC The Journal of Organic Chemistry
Cite This: J. Org. Chem. 2019, 84, 8815−8836
Perspective
pubs.acs.org/joc

Lactam Hydrogen Bonds as Control Elements in Enantioselective Transition-Metal-Catalyzed and Photochemical Reactions

Finn Burg and Thorsten Bach*

Department of Chemistry and Catalysis Research Center (CRC), Technical University of Munich, Lichtenbergstrasse 4, 85747 Garching, Germany

ABSTRACT: In the last two decades, hydrogen bonds have been established as useful interactions to control the selectivity of various chemical transformations. In this Perspective, the contributions by our group to this growing field of research are summarized and analyzed. In the first section, a chiral template is presented which displays a 1,5,7-trimethyl-3-azabicyclo[3.3.1]nonan-2-one skeleton with a lactam binding site and that has been used in superstoichiometric quantities in a variety of photochemical and radical reactions. Chiral catalysts with a related architecture evolved from the template by introducing a suitable chromophore for harvesting photons in the ultraviolet (benzophenone, xanthone) or visible region (thioxanthone). They act mainly by sensitization and allow for a high catalytic turnover in enantioselective [2 + 2] photocycloadditions and in deracemization reactions. Eventually, the concept of lactam hydrogen bonding was transferred to transition-metal catalysis, and catalysts have been developed which combine, in an enzyme-like fashion, a site for substrate binding and a catalytically active site. Substrate binding has been mainly achieved by a V-shaped ligand based on a tricyclic octahydro-1*H*-4,7-methanoisoindol-1-one scaffold with a lactam hydrogen-bonding site. The catalytically active metal (ruthenium, manganese, rhodium) is perfectly positioned to the substrate for a site- and enantioselective transfer of an oxygen atom (oxidation, oxygenation) or a nitrogen-based fragment (aziridination, amination).

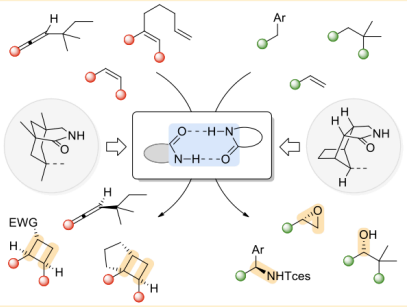

INTRODUCTION

Hydrogen bonds belong to the most important noncovalent interactions and have been extensively explored for many decades.[1] Given the vast number of studies on the topic, it is somewhat difficult to introduce the research field of this Perspective without involuntarily omitting many important contributions. This section thus serves exclusively as a personal reflection on how we became interested in the use of chiral lactams for enantioselective transformations but not as a comprehensive survey of work which has been done in the field of hydrogen-bonding catalysis.[2] Our work in the area commenced in the final years of the 20th century and was stimulated by the discovery that several secondary amides and dihydropyridones could be successfully used as olefin components in the Paternò−Büchi reaction.[3] Even sensitive olefins such as *N*-vinyl formamide turned out to be compatible with the irradiation conditions, and this finding raised the question whether hydrogen-bonding interactions might be employed to induce an enantioface differentiation at the olefinic double bond. Encouraging precedence for the fact that even a single hydrogen bond could be a control element to induce facial diastereoselectivity (dr = diastereomeric ratio) came from the early work of Masamune on the intermolecular Diels−Alder reaction of dienophile **1**[4] and from a more recent contribution by Crimmins on the intramolecular intramolecular [2 + 2] photocycloaddition of substrate *rac*-**3**.[5] In both cases, hydrogen bonds were invoked in the respective conformations **1′** and *rac*-**3′** to explain the high diastereoselectivity of the reaction toward products **2** and *rac*-**4** (Scheme 1).

Even more closely related to our olefins were the 2-pyridones which Sieburth and co-workers had employed for photochemical [4 + 4] photocycloaddition reactions.[6] There was evidence that hydrogen bonding was important to control the diastereoselectivity in the intramolecular [4 + 4] photocycloaddition of substrates such as *rac*-**5** (Scheme 2). In the nonpolar solvent benzene, the reaction was proposed to proceed via complex *rac*-**5′** to generate product *rac*-**6**.

As mentioned above, there was extensive additional work which suggested the use of hydrogen bonds as control elements in photochemical reactions. Two reviews which report on noncovalent synthesis using hydrogen bonding and which appeared at the turn of the century may serve to reflect the state of the art at this period in time.[7] The lactam binding motif with which we eventually chose to probe a potential enantioface differentiation in the Paternò−Büchi reaction of achiral olefins rested on the 1,5,7-trimethyl-3-azabicyclo[3.3.1]nonane skeleton. The precursor to ester *rac*-**7** could be readily synthesized from Kemp's triacid[8] and related imides had proven to exhibit a U-shaped three-point interaction with various substrates.[9] Still, there was no precedence that a two-point interaction would be sufficient to precoordinate a lactam to a 1,5,7-trimethyl-3-

Received: May 15, 2019
Published: June 10, 2019

DOI: 10.1021/acs.joc.9b01299
J. Org. Chem. 2019, 84, 8815−8836

Scheme 1. Seminal Work on Diastereoselective Transformations Mediated by a Single Hydrogen Bond as Control Element

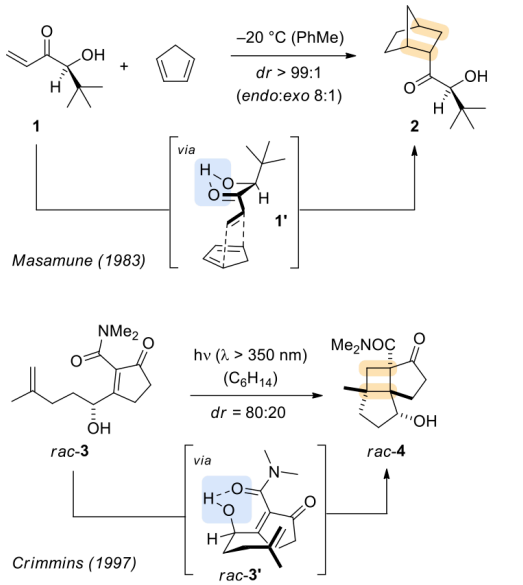

Scheme 2. Intramolecular Two-Point Hydrogen Bonding in the Diastereoselective [4 + 4] Photocycloaddition of Substrate *rac*-5

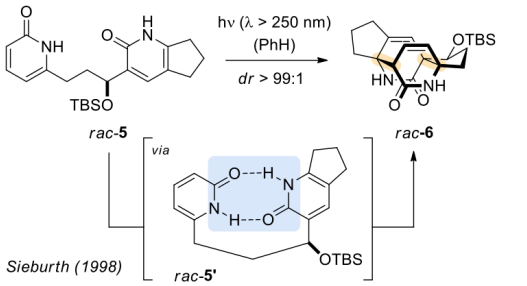

azabicyclo[3.3.1]nonan-2-one, and we were delighted to find a high diastereomeric excess for oxetane *rac*-**10** (Scheme 3) in the Paternò–Büchi reaction with dihydropyridone **8**. It was assumed that the reaction proceeds via an initial C–O bond formation which occurs almost exclusively at the formal *Re* face of dihydropyridone **8** (relative to carbon atom C-5). 1,4-Diradical intermediate *rac*-**9** gives oxetane *rac*-**10** in which the relative configuration was proven by single-crystal X-ray crystallography.[10]

Encouraged by the promising diastereoselectivity of the Paternò–Büchi reaction, we wondered whether it would be possible to employ a related chiral template (chiral complexing agent) for enantioselective reactions. Such a template would not be involved in the stoichiometry of the individual reaction but would only transfer its chirality to the reaction products by hydrogen bonding. The story of these templates, which are used in stoichiometric quantities or in excess (up to 2.6 equiv), will be told in the next section before continuing with related chiral lactams, which can be employed catalytically.

Scheme 3. Intermolecular Two-Point Hydrogen Bonding in the Diastereoselective Paternò–Büchi Reaction of Aldehyde *rac*-7 and Dihydropyridone 8

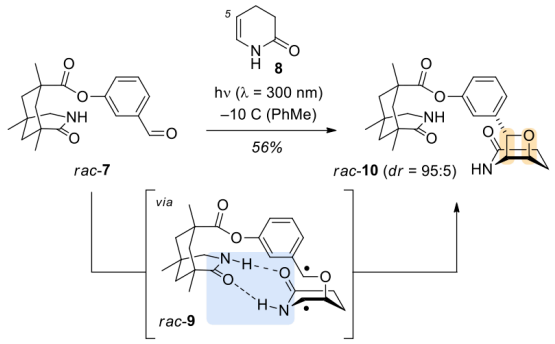

■ CHIRAL COMPLEXING AGENTS

Discovery and Initial Applications. Compound **7** served as a validated starting point to develop a chiral template.[11] The challenge, however, was not only to bind a prochiral substrate by two-point hydrogen bonding but also to provide sufficient enantioface differentiation for an intermolecular approach of a second molecule—as opposed to the intramolecular attack of the aldehyde in the Paternò–Büchi reaction (Scheme 3). It was quickly realized that the flexible ester linkage had to be replaced by a more rigid heterocyclic skeleton and that the potential enantioface differentiating entity had to be extended to a tetrahydronaphthalene unit. The two enantiomeric compounds **11** and *ent*-**11** emerged from our studies and turned out to be readily accessible[12] on large scale in enantiopure form (Figure 1). The absolute configuration of

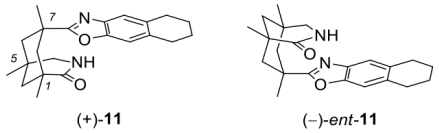

Figure 1. Structure of the dextrorotatory complexing agent **11** and of its levorotatory enantiomer *ent*-**11** with a 1,5,7-trimethyl-3-azabicyclo[3.3.1]nonan-2-one skeleton.

levorotatory compound *ent*-**11** was proven by single-crystal X-ray diffraction (anomalous dispersion), and the compounds were shown to be spectroscopically transparent at a wavelength of $\lambda \geq 300$ nm.[13]

Initial applications of the templates[13a] were performed with 4-alkenyloxyquinolones such as compound **12** which were known[14] to undergo an intramolecular [2 + 2] photocycloaddition. It was found that chiral complexing agents **11** and *ent*-**11** induced a high enantioselectivity in this process. With one equivalent of *ent*-**11**, the reaction already proceeded in 78% enantiomeric excess (ee) at −15 °C, and the enantioselectivity could be further increased at lower temperature employing a superstoichiometric amount of the complexing agent (Scheme 4). Since the recovery of the complexing agent by chromatography is straightforward and recovery yields are close to quantitative, a loading of 2–2.6 equiv has been typically applied in many other enantioselective reactions mediated by compounds **11** and *ent*-**11** (vide infra).

DOI: 10.1021/acs.joc.9b01299
J. Org. Chem. 2019, 84, 8815–8836

Scheme 4. Enantioselective Intramolecular [2 + 2] Photocycloaddition of 4-Allyloxyquinolone (12) Mediated by Complexing Agent *ent*-11

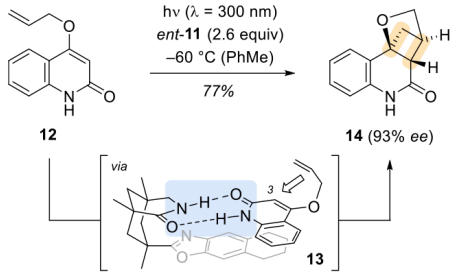

The absolute configuration of product **14** was in agreement with the assumed complexation of substrate **12** and lactam *ent*-**11** in the hydrogen-bonded complex **13**. The tetrahydronaphthalene unit avoids an intramolecular attack of the olefin from the bottom face but rather the olefin approach to the photoexcited quinolone occurs from the top face (*Si* face relative to carbon atom C-3). The regioselectivity of the reaction is determined by the facile ring closure to a five-membered ring which eventually leads to formation of crossed photocycloaddition products. Indeed, the reaction proceeds on the triplet hypersurface with initial C–C bond formation to a 1,4-diradical and subsequent ring closure.[15]

Binding Properties. The most striking feature of templates **11** and *ent*-**11** is the fact that they operate with only two hydrogen bonds. As any substrate, such as quinolone **12**, can also form two hydrogen bonds by dimerization, it appears to be counterintuitive that lactam substrates would bind exclusively to the template. A closer look at the binding properties of 1,5,7-trimethyl-3-azabicyclo[3.3.1]nonan-2-ones serves to resolve this apparent contradiction. Compound **11** does not form a 1:1 complex with another 1,5,7-trimethyl-3-azabicyclo[3.3.1]nonan-2-one **A** of the same handedness (Scheme 5). There is no dimerization of compound **11**

Scheme 5. Molecular "Handshake" between Two 1,5,7-Trimethyl-3-azabicyclo[3.3.1]nonan-2-ones of Opposite Chirality (11, *ent*-A)

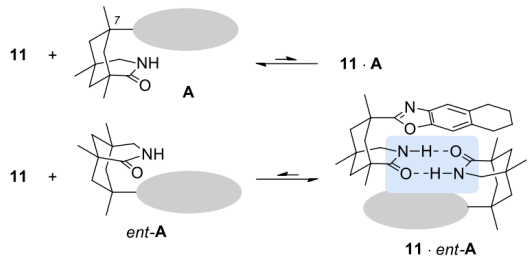

($K_{dim} \cong 0$), and a solution of homochiral template **11** is exclusively composed of the monomeric species.[16] Addition of 1,5,7-trimethyl-3-azabicyclo[3.3.1]nonan-2-ones *ent*-**A** with opposite handedness leads to smooth formation of dimers whose existence is apparent by an extensive shift of the NH lactam ^{1}H NMR signal of compounds **11** and *ent*-**A**.[17]

The heterochiral interaction can be extremely useful in assigning the absolute configuration of 7-substituted 1,5,7-trimethyl-3-azabicyclo[3.3.1]nonan-2-ones and related compounds.[18] The enantiomer that forms hydrogen bonds with template **11** exhibits an opposite handedness (*ent*-**A**), while enantiomers **A** with the same handedness will not be involved in an association. Unlike a human handshake, the molecular "handshake" of 1,5,7-trimethyl-3-azabicyclo[3.3.1]nonan-2-ones requires opposite chirality of the two components. The fact that there are homochiral and heterochiral dimers of compound **11** and its enantiomer *ent*-**11** allowed for an asymmetric amplification in reactions in which the template was not enantiopure. A positive nonlinear effect was observed, i.e., the product ee was higher than the ee of the template.[19]

It is qualitatively clear now why dimerization of lactam substrates in the presence of template **11** is not preferred and why these substrates rather bind to template **11**. The former interaction (dimerization) requires two substrate molecules to form two hydrogen bonds while the latter interaction allows for the total formation of four hydrogen bonds from two substrate molecules. This phenomenon was quantitatively accessed by studying 4-(4-iodobutyl)quinolone (**15**) and template **11** in ^{1}H NMR titration experiments.[19] The dimerization constants were determined in toluene-d_8 at 25 and 0 °C as $K_{dim} = 2001 \pm 160$ M^{-1} and $K_{dim} = 5614 \pm 706$ M^{-1}, respectively. The association constants K_a were in the same ballpark reflecting the fact that the hydrogen bonds are of similar strength. The equilibrium is shifted toward **11·15** because the equilibrium constant for the reaction $(\mathbf{15})_2$ with 2 equiv **11** to form two molecules of dimer **11·15** is $K_a^2 K_{dim}^{-1}$ and roughly equals K_a if K_a and K_{dim} are similar (Scheme 6).

Scheme 6. Representative Example for Binding of a Lactam (Quinolone 15) to Complexing Agent 11

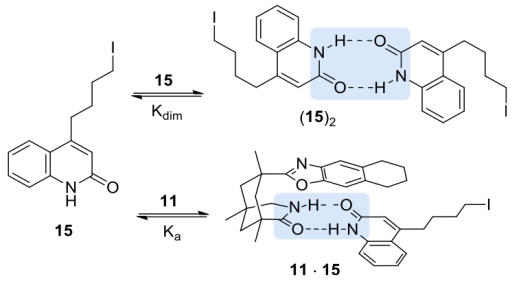

The latter expression reflects quantitatively the qualitative analysis that four hydrogen bonds are preferred over two hydrogen bonds. The data recorded for dimer **11·15** suggest at a typical substrate concentration of c = 10 mM that more than 90% of the substrate is bound to the template at 0 °C. It is conceivable that attractive noncovalent interactions (π stacking) enhance the stability of complexes such as **11·15**, but no attempts have yet been made to quantify this interaction.

Template **11** is very sensitive toward unfavorable steric interactions with its rigid tetrahydronaphthalene unit, and it was shown that enantiomers of chiral lactams (vide infra) bind differently to template **11**. The different binding properties result in different ^{1}H NMR shifts for the lactam protons of the individual enantiomers, and templates **11** and *ent*-**11** can serve as chiral shift reagents.[20]

Applications. Typically, complexing agents **11** and *ent*-**11** have been used to facilitate enantioselective photochemical and

DOI: 10.1021/acs.joc.9b01299
J. Org. Chem. 2019, 84, 8815–8836

Scheme 7. Enantioselective Photochemical and Radical Reactions Promoted by Chiral Complexing Agents 11 and *ent*-11

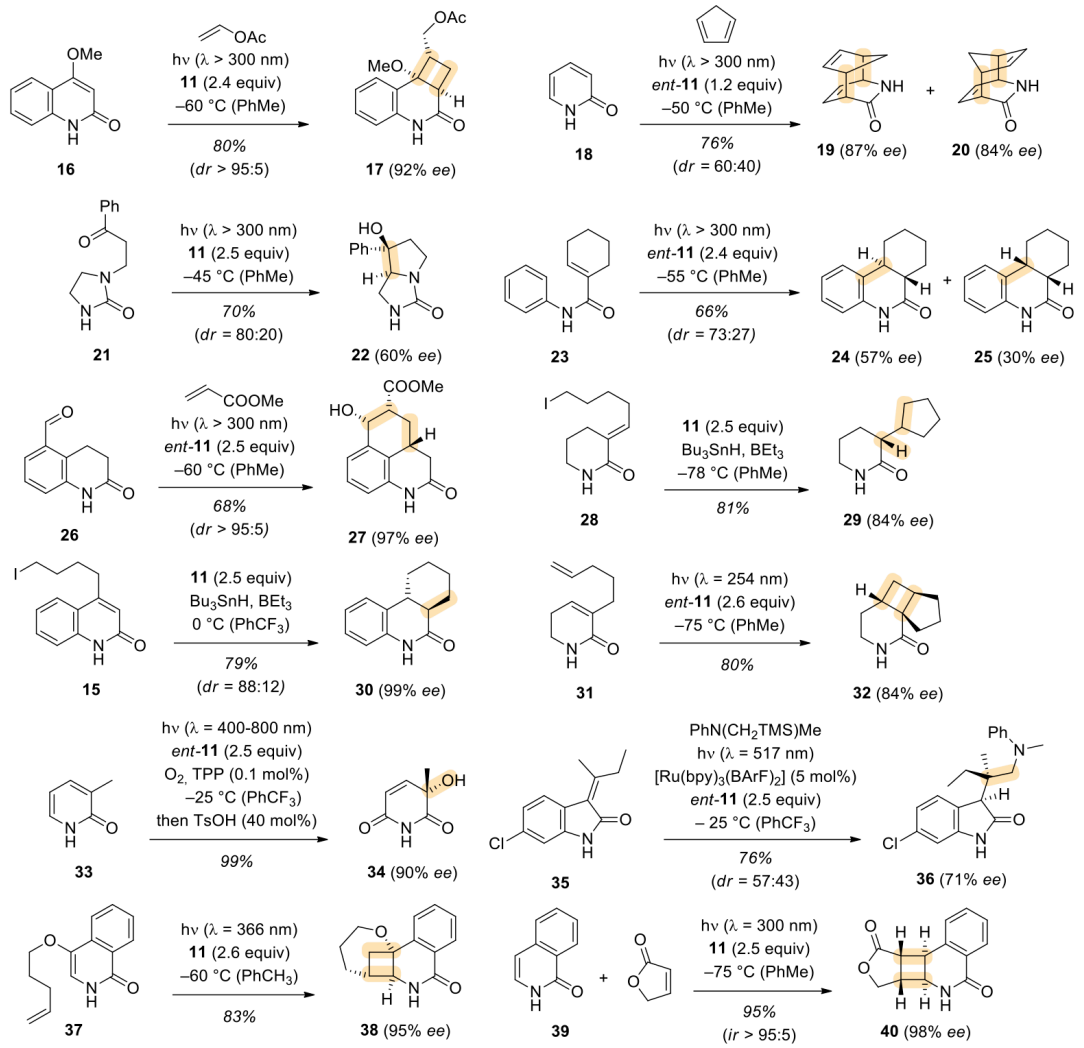

radical reactions.[21] A few representative examples for individual reactions are listed in Scheme 7. Several of the early experiments were performed with a mercury high-pressure lamp and a Duran glass filter (λ > 300 nm). More recently, light sources with a narrower emission spectrum have been used, specifically fluorescent lamps or light emitting diodes (LEDs). The [2 + 2] photocycloaddition of vinyl acetate and 4-methoxyquinolone (**16**) to product **17** demonstrates that the above-mentioned intramolecular reactions can be also performed intermolecularly.[13,22] The [4 + 4] photocycloaddition of 2-pyridone (**18**) illustrates the fact that this heterocyclic compound class is also suited for hydrogen bonding to the lactam motif of templates **11** and *ent*-**11**.[23] Even at a relative low loading (1.2 equiv) of template *ent*-**11**, products **19** and **20** were obtained with high enantioselectivity. A first indication that not only the enantiotopic faces of a double bond could be differentiated by hydrogen bonding but also the enantiotopic faces of a prostereogenic carbon radical was realized when studying the Norrish–Yang cyclization of imidazolidin-2-ones such as **21**. Excitation of the ketone carbonyl group leads via hydrogen abstraction to a 1,5-diradical which reacts enantioselectively to alcohol **22**. This study clearly showed the superior properties of templates **11** and *ent*-**11** as compared to 1,5,7-trimethyl-3-azabicyclo[3.3.1]-nonan-2-ones with an ester group in position C-7.[24]

The [6π] photocyclization of amides such as **23**[25] requires the amide bond to be *cis*-configured, which in turn should enable two-point hydrogen bonding to chiral lactam templates. Indeed, it was found that the reaction proceeds enantioselectively to provide a mixture of the two diastereomeric products **24** and **25**.[26] Compound *ent*-**11** served in this reaction not only as a passive template but acted as a chiral Brønsted acid in the protonation of the intermediate zwitterions. When photochemically excited, *ortho*-substituted aromatic aldehydes and ketones undergo an intramolecular hydrogen abstraction and the intermediate (*E*)-dienols (*o*-

DOI: 10.1021/acs.joc.9b01299
J. Org. Chem. 2019, 84, 8815–8836

quinodimethanes) are reactive components in a thermal Diels–Alder reaction.[27] This photoenolization/Diels–Alder sequence was first performed with high enantioselectivity for substrates such as aldehyde **26**. In the depicted example, methyl acrylate was employed as the dienophile and product **27** was formed.[28] Apart from photochemical reactions, radical reactions turned out to be particularly suited for an application of chiral complexing agents **11** and *ent*-**11**. Triethylborane was an ideal reagent to initiate radical reactions at low temperature and promoted the reductive cyclization of iodide **28** to product **29**.[29] In this case, the primary 5-*exo-trig* cyclization product is a carbon-centered radical, and the attack of the hydrogen atom donor, tributyltin hydride, occurs with high enantioselectivity, presumably because the radical intermediate is bound to template **11**. Templated radical reactions are also enantioselective for substrates which expose a prochiral double bond to a radical.[19,30] Here, the radical addition step is enantioselective, and in some cases, the enantioselectivity is enhanced by hydrogen atom transfer to a second stereogenic center. The radical cyclization of the above-mentioned iodide **15** represents a good example for a 2-fold enantiodifferentiation by chiral template **11**. Even at a relatively high temperature of 0 °C, the formation of *trans*-product **30** remained highly enantioselective. It turned out in the studies on radical reactions that template **11** can also be applied in catalytic amounts (10 mol %) demonstrating its potential for a chirality multiplication.[30a]

In terms of irradiation conditions, the reactions of 5,6-dihydropyridone **31** and 2-pyridone **33** represent rather extreme cases. The former reaction was performed at very short wavelength (λ = 254 nm) because α,β-unsaturated lactams display a blue-shifted absorption as compared to aromatic lactams, such as quinolones and pyridones. Despite the fact that template *ent*-**11** is not transparent for photons of this wavelength, it survived the irradiation conditions sufficiently well to induce a high enantioselectivity in product **32**.[18b] In the latter reaction, the addition of singlet oxygen to 2-pyridones was induced by irradiation at long wavelength with visible light and required a co-catalyst for singlet oxygen formation. Tetraphenylporphyrine (TPP) was used, and the in situ generated singlet oxygen[31] added enantioselectively in a [2 + 4] cycloaddition to 2-pyridones, such as **33**.[32] The primarily formed endoperoxide was not isolated. Instead, it directly underwent an acid-catalyzed Kornblum–DeLaMare rearrangement[33] to tertiary alcohol **34**. Another visible-light-induced reaction required a ruthenium catalyst to generate a radical from an α-silylated amine[34] by single-electron transfer. While the addition reactions to 3-alkylidene indolin-2-ones such as **35** were enantioselective in the presence of template *ent*-**11**, a drawback was the insufficient control of the protonation event which resulted in the formation of two diastereoisomers one of which (**36**) is depicted.[35] In general, photoredox catalytic reactions are frequently incompatible with the requirements of a hydrogen-bonding lactam template. Electron transfer occurs preferentially in polar solvents which preclude coordination of the substrate to the template. Our most recent work with templates **11** and *ent*-**11** was concerned with the intra- and intermolecular [2 + 2] photocycloaddition of isoquinolones. The intramolecular reaction of substrate **37**, for example, was found to proceed to the crossed product **38** with excellent enantioselectivity.[36] Isoquinolone itself (**39**) and some of its substituted derivatives reacted with a wide array of alkenes to afford cyclobutanes such as **40** (ir = isomeric ratio).[37]

Although the isoquinolone [2 + 2] photocycloaddition invites several applications in natural product synthesis,[38] it has not yet been successfully implemented into a complete synthetic sequence toward isoquinoline alkaloids. The enantioselective quinolone [2 + 2] photocycloaddition, however, has proven to be a useful tool in organic synthesis. It is particularly suited to access a 3,4-dihydroquinolin-2(1*H*)-one (3,4-dihydroquinolones) with a high degree of functionalization at carbon atoms C-3 and C-4. Since there are no natural products with a cyclobutane that would be 3,4-annulated to a dihydroquinolone, successive ring opening reactions need to be implemented in the synthesis plan. In the total synthesis of (+)-meloscine (**44**), quinolone **41** was enantioselectively converted into [2 + 2] photocycloaddition product **42** before a retro-benzilic acid rearrangement to **43** was applied that generated the central five-membered ring of the target molecule (Scheme 8).[39]

Scheme 8. Enantioselective [2 + 2] Photocycloaddition Reaction as a Key Step in the Total Synthesis of (+)-Meloscine

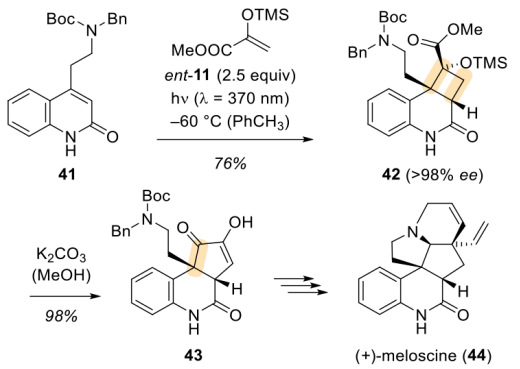

The naturally occurring 3,4-dihydroxylated 3,4-dihydroquinolone (−)-pinolinone (**49**) was approached by a combination of a [2 + 2] photocycloaddition and a Baeyer–Villiger type oxidation (Scheme 9).[40] The pivotal photochemical step commenced with quinolone **45** which was enantioselectively converted into cyclobutanes **46** (dr = 71/29). The diastereomeric mixture was *N*-methylated and the acetate was hydrolyzed under mild conditions to deliver free alcohols **47**. Oxidation to lactone **48** erased the stereogenic center at the acetal carbon atom and yielded a single product, the two stereogenic centers of which resulted directly or indirectly from the enantioselective [2 + 2] photocycloaddition step. Reduction to the lactol and a Wittig reaction concluded the total synthesis of (−)-pinolinone (**49**).

Over the years, a few variants of chiral templates **11** and *ent*-**11** have been synthesized for specific purposes. Alcohol **50** (Figure 2) was used to immobilize the lactam template by attaching it either to a Wang resin or to a methoxypolyethylene glycol (MPEG 2000). The transparent MPEG-supported template was soluble in toluene and could be recovered quantitatively by precipitation with ether. In five successive runs of the reaction *rac*-**12** → *rac*-**14** (Scheme 4), there was no deterioration in yield or enantioselectivity when using the recovered MPEG supported template.[41]

DOI: 10.1021/acs.joc.9b01299
J. Org. Chem. 2019, 84, 8815–8836

Scheme 9. Enantioselective [2 + 2] Photocycloaddition Reaction as a Key Step in the Total Synthesis of (−)-Pinolinone

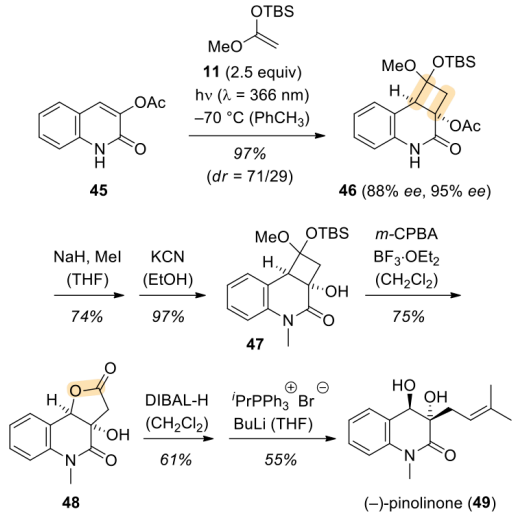

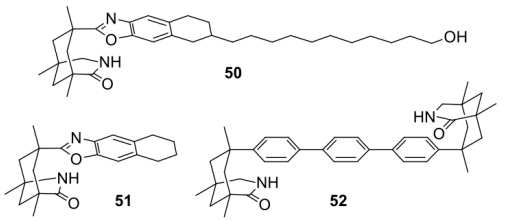

Figure 2. Structure of other complexing agents with a lactam binding site.

The nor-analogue **51** of template **11** was prepared to evaluate its binding properties toward 5,6-dihydropyridone, which in turn underwent an intramolecular [2 + 2] photocycloaddition (e.g., **31**, Scheme 7). There was an improved enantioselectivity but the effect was not very pronounced.[18b] The C_2-symmetric terphenyl template **52** was designed as a complexing agent for dicarboxylic acids. Indeed, it was successfully used to induce a moderate enantioselectivity (up to 55% ee) in the [4 + 4] photodimerization of anthracene-2,6-dicarboxylic acid.[42]

■ CHIRAL PHOTOCATALYSTS (ELECTRON TRANSFER, SENSITIZATION)

Basic Considerations. Many photochemical reactions do not proceed from the directly accessible, excited singlet state S_1 but from the triplet state T_1. Since relaxation of a molecule from the triplet hypersurface to the ground state (S_0) is spin-forbidden, the lifetime of a molecule in T_1 is long, which in turn allows to utilize its reactivity in intra- and intermolecular reactions. The majority of [2 + 2] photocycloaddition reactions are triplet processes[15] and the triplet state can be populated by intersystem crossing (ISC) from the respective S_1 state. As an example, 2-quinolone (**53a**) can be involved in an intermolecular [2 + 2] photocycloaddition reaction if excited within its typical absorption wavelength range that reaches up to $\lambda \cong 360$ nm (Scheme 10).[14a,43] Irradiation with a high-pressure mercury lamp in Pyrex glass ($\lambda > 280$ nm) promotes

Scheme 10. Reaction Pathway for the Intermolecular [2 + 2] Photocycloaddition of 2-Quinolone (53a) and an Electron-Deficient Olefin[a]

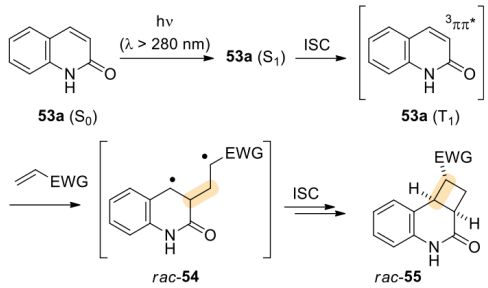

[a]EWG = electron-withdrawing group.

the molecule into its singlet state from which ISC occurs within less than 1 ns. ISC rates are governed by symmetry rules (El-Sayed rules[44]) and ISC from states of $n\pi^*$ to states of $\pi\pi^*$ character is rapid. The long-lived triplet T_1 is quenched by olefins and the initial addition step is decisive for the enantioselectivity of the reaction. In the absence of any chiral information, the intermediate 1,4-diradical is racemic (*rac*-**54**). The regioselectivity of the addition is governed by the stability of the respective 1,4-diradical. The simple diastereoselectivity of the reaction is determined by the constraints within the cyclobutane ring and by the fact that the substituent, in this case an electron-withdrawing group, will be positioned in the least hindered position of product *rac*-**55**, i.e., *trans* to the benzo group.

The relevance of the triplet state to catalytic enantioselective photochemical reactions stems from the fact that it is not only directly accessible via S_1 but also via an indirect excitation, known as triplet energy transfer or sensitization. A typical triplet sensitizer (Sens) that can catalyze a photochemical reaction exhibits a long-wavelength absorption beyond the absorption of the substrate (bathochromic). In other words, its S_1 state must be lower in energy than the S_1 state of the substrate. To be applicable to 2-quinolone (**53a**), an appropriate sensitizer should therefore exhibit a significant absorption at $\lambda > 360$ nm. The sensitizer must have a high ISC rate to populate efficiently its T_1 state, which in turn should have an energy $E(T_1)$ that allows an energy transfer as depicted in Scheme 11 (left panel). Although it is recognized that the energy transfer should be exothermic,[45] a moderately endothermic energy transfer is feasible if the T_1 state of the sensitizer is long-lived and if the T_1 state of the substrate is quickly depopulated. The tabulated triplet energy of 2-quinolone (**53a**) is 276 kJ mol^{-1}.[46] The mechanism of the triplet energy transfer bears some analogy to a single electron transfer as it is an electron exchange process[47] (Scheme 11, right panel).

The unpaired electron which resides in the former LUMO of the sensitizer populates the LUMO of the substrate, which for quinolone is its π^* orbital. Simultaneously, the indicated electron of the quinolone π orbital with antiparallel spin is transferred to the single occupied orbital (former HOMO) of the sensitizer. There is no change in the overall spin states and

DOI: 10.1021/acs.joc.9b01299
J. Org. Chem. 2019, 84, 8815−8836

Scheme 11. Important Parameters of Triplet Energy Transfer in Catalytic Photochemical Reactions

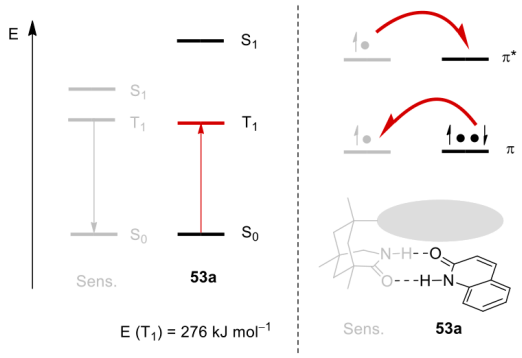

the process is rapid, provided that there is a finite orbital overlap. The latter requirement is responsible for the fact that the rate k_{ET} of energy transfer depends—like electron transfer—on the distance between the sensitizer and the substrate. If the molecules are within van der Waals contact, the rate of energy transfer is in the order of $k_0 = 10^{13}$ s^{-1}.[48] The rate falls off exponentially to an increase in distance Δr beyond van der Waals contact, and the rate of energy transfer k_{ET} can be roughly estimated as $k_{ET} = k_0\, e^{-\beta\Delta r}$, with β being typically in a range of 10^{-2} pm^{-1}.[48] The remarkable feature of the 1,5,7-trimethyl-3-azabicyclo[3.3.1]nonan-2-one skeleton is the fact that a substituent in the 7-position is spatially extremely close to a bound substrate such as 2-quinolone (**53a**). Molecular models and DFT calculations[26] gave a rough estimate for this distance as being ca. 400 pm. The van der Waals radius of a carbon atom is 170 pm, which seemed for us to indicate that the orbitals of a substrate, such as 2-quinolone (**53a**), and a potential sensitizing entity attached to position C-7 of a 1,5,7-trimethyl-3-azabicyclo[3.3.1]nonan-2-one are almost in van der Waals contact. If the energy of the sensitizing unit was properly chosen, there was an ideal scenario for efficient sensitization *and* high enantioface differentiation.

The aspect of enantioface differentiation was actually even more important than the energy-transfer criterion since all previous attempts to employ chiral triplet sensitizers for enantioselective photochemical reactions had failed to deliver a high enantioselectivity (>50% ee).[49] Initial experiments by our group to attach the sensitizer to the lactam backbone by an ester bond were equally futile as the respective catalysts did not deliver a high enantioselectivity.[50] Linkage via a rigid oxazole unit turned out to be a superior solution which in turn required that the aromatic ketones are available as *o*-aminophenols or appropriate analogues to allow for the condensation reaction with the carboxylic acid. The first compounds that succeeded in the synthesis were benzophenones **56a** and *ent*-**56a**[18a] (Figure 3) followed by xanthones **56b** and *ent*-**56b**[51] and thioxanthones **56c** and *ent*-**56c**.[52] Since all compounds **56** are preferentially used in a nonpolar solvent to enforce hydrogen bonding, we attempted to measure their triplet energy in a matrix which mimics this environment. Triplet energies were obtained from phosphorescence spectra at 77 K and were found to be (solvent matrix in brackets) 291 kJ mol^{-1} (pentane/isopentane) for **56a**,[53] 316 kJ mol^{-1} (pentane/isopentane) for **56b**,[53] and 263 kJ mol^{-1} (trifluorotoluene) for **56c**.[54]

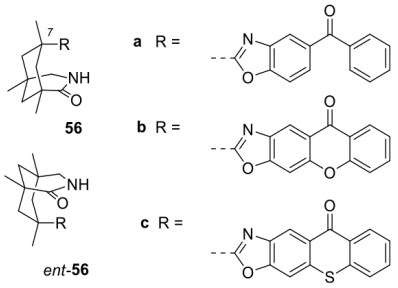

Figure 3. Structure of the chiral photocatalysts **56** and *ent*-**56** with a 1,5,7-trimethyl-3-azabicyclo[3.3.1]nonan-2-one backbone.

Applications in C–C Bond-Forming Photochemical Reactions. In preliminary [2 + 2] photocycloaddition experiments with benzophenone **56a** as the catalytic triplet sensitizer,[55] the enantioselectivity remained relatively low (39% ee).[51] An explanation for this disappointing outcome rested on an insufficient association due to the nonplanarity of benzophenones. Their aryl groups are twisted out of plane both in the ground state and in the excited state.[56] For example, a twist angle of 44° was calculated for the phenyl planes in the T_1 state of parent benzophenone.[57] It was hoped that a radical process via a ketyl radical[58] intermediate might provide improved results, and 2-quinolone **57** was synthesized which seemed amenable to single electron transfer to a photoexcited benzophenone.[59] To our delight, the respective product **59** was obtained in 70% ee, and the enantioface differentiation could be explained by addition of an intermediate α-amino radical to carbon atom C-4 of the quinolone in complex **58** (Scheme 12).[18a]

Scheme 12. Enantioselective Formation of Tetracyclic Product 59 from 2-Quinolone 57 by a Radical Cyclization

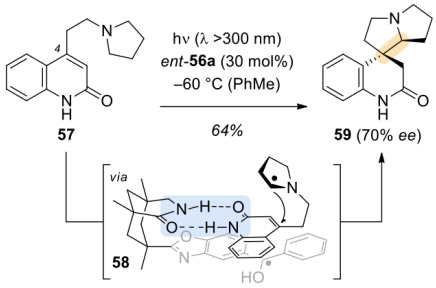

Despite this initial success, benzophenones **56a** and *ent*-**56a** did not find any additional applications and were not further used for sensitization experiments after xanthones **56b** and *ent*-**56b** became synthetically available. The only disadvantage of the xanthones was found to be their high instability in solvents which are amenable to hydrogen abstraction. The xanthone T_1 state in a nonpolar solvent has nπ* character[60] which translates into a high electrophilicity of the oxygen atom. When irradiated in toluene solution, xanthones **56b** and *ent*-**56b** decomposed instantaneously. Trifluorotoluene turned out to be a suitable nonpolar solvent in which hydrogen abstraction was minimized and which still has a low melting point of −29 °C. Intramolecular [2 + 2] photocycloaddition reactions of various 4-alkenyloxy-2-quinolones (Scheme 13) established

DOI: 10.1021/acs.joc.9b01299
J. Org. Chem. 2019, 84, 8815−8836

Scheme 13. Enantioselective Triplet-Sensitized [2 + 2] Photocycloaddition Reaction of Various 4-Alkenyloxy-2-quinolones 60 to Cyclobutanes 61[a]

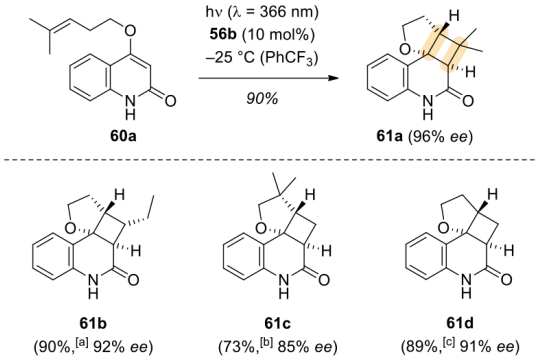

[a]Key: [a] rr = 88:12, [b] rr = 82:18, [c] rr = 77:23.

Scheme 14. Enantioselective Intermolecular [2 + 2] Photocycloaddition of 2-Pyridones 62 and Acetylenedicarboxylates to Cyclobutenes 64

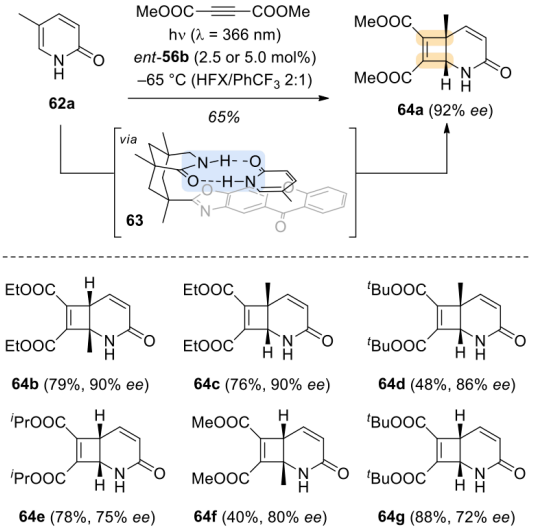

the powerful combination of energy transfer by the sensitizing xanthone unit and high enantioface differentiation due to hydrogen bonding at the lactam motif of catalyst **56b**.[61] Two observations should be mentioned in this context. (a) Xanthone **56b** remained prone to hydrogen abstraction: In addition to product **61d**, its regioisomer was detected after an irradiation time of 1 h (λ = 366 nm, T = −25 °C), and the regioisomeric ratio (rr) was found to be 78/22. After 4 h, the other regioisomer could no longer be detected, and the photocycloaddition yield decreased from 90% to 55%. Simultaneously, a significant decomposition of the xanthone was notable, which indicates that the catalyst deterioration is linked to hydrogen abstraction at the minor regioisomer. (b) The rate of C−C bond formation is important for the enantioselectivity. Although compounds such as **60a** reach their triplet state efficiently by energy transfer when bound to sensitizer **56b** the chirality transfer depends on the rate of initial C−C bond formation relative to the rate of dissociation from catalyst **56b**. The first C−C bond formation (cf. Scheme 10) leads to a 1,4-radical and establishes the first stereogenic center. If dissociation occurs prior to this step, there will be no enantioselectivity. The fact that the 4-alkenyloxy-2-quinolones with a 4-(pent-4-enyl)oxy but not a 4-(but-3-enyl)oxy substituent reacted with low enantioselectivity was ascribed to the fact that their cyclization is slower by 2 orders of magnitude.[61a] The dissociation rate constant of a photoexcited quinolone substrate from **56b** was estimated to be in the order of 10^7 s^{-1}.

Despite the kinetic limitations of an enantioselective photochemical reaction catalyzed by sensitizers **56** and *ent*-**56**, intermolecular processes were discovered which proceed with high enantioselectivity. A notable example is the [2 + 2] photocycloaddition of 2-pyridones such as **62a** with acetylenedicarboxylates, which was performed with low loadings (2.5−5.0 mol %) of catalyst *ent*-**56b** (Scheme 14).[62] The reaction was performed with an excess of the alkyne (50 equiv) in a solvent mixture of hexafluoro-*m*-xylene (HFX) and trifluorotoluene which allowed for irradiation at low temperature (T = −65 °C).[63] Products **64** represent densely functionalized precursors for further reactions at different sites.

Preferable substrates for an application of catalysts **56b** and *ent*-**56b** exhibit a planar π system with prostereogenic carbon atoms. As depicted for complex **63**, the xanthone fulfills nicely its dual task of energy transfer and subsequent enantioface differentiation. Attempts to involve a sp^3-hybridized epoxide in an enantioselective rearrangement to 3-acylindolin-2-ones were met with only limited success (16−33% ee).[64]

Given the large scientific interest in visible light-mediated transformations,[65] thioxanthones **56c** and *ent*-**56c** represent versatile analogues of xanthones **56b** and *ent*-**56b** with the added benefit that they can be excited with long-wavelength light. The absorption maximum is shifted from 350 nm (ε = 9200 M^{-1} cm^{-1}, in $PhCF_3$) for xanthone **56b** to 387 nm (ε = 4540 M^{-1} cm^{-1}, in $PhCF_3$) for thioxanthone **56c**. The thioxanthones are yellow solids and turned out to be extremely useful catalysts. Regarding [2 + 2] photocycloaddition reactions, they initially proved their potential in the reaction of the 4-alkenyl-2-quinolones **65** (Scheme 15).[52] While these substrates do not absorb visible light, they have triplet energies which make their T_1 state accessible by sensitization[66] via thioxanthone **56c**.

Upon binding of substrate **65a**, rapid energy transfer occurs in complex **67** and the intramolecular olefin approaches the prostereogenic double bond in the $\pi\pi^*$-excited quinolone from the bottom face. Products **66** were obtained in good to excellent yields with high enantioselectivity. It was probed whether the reaction can be performed also with sunlight, and an appropriate reactor was designed in which the reaction **65a** → **66a** was performed. In the absence of any cooling device or UV filter, the photocycloaddition reaction proceeded in 90% yield (4 h diffuse sunlight irradiation) and with 80% ee. The enantioselectivity improved when the UV part of the sunlight was removed by an $Fe_2(SO_4)_3$ solution (for the experimental setup, see Scheme 15) and reached 94% ee if additional cooling to −25 °C was applied (92% yield).[67] The UV filter solution serves to avoid direct excitation of substrate **65a** which leads to a racemic [2 + 2] photocycloaddition.

Thioxanthone **56c** also paved the way for the intermolecular [2 + 2] photocycloaddition of 2-quinolones **53**, including the

DOI: 10.1021/acs.joc.9b01299
J. Org. Chem. 2019, 84, 8815−8836

Scheme 15. Enantioselective Visible-Light-Mediated [2 + 2] Photocycloaddition Reaction of Various 4-Alkenyl-2-quinolones 65 to Cyclobutanes 66

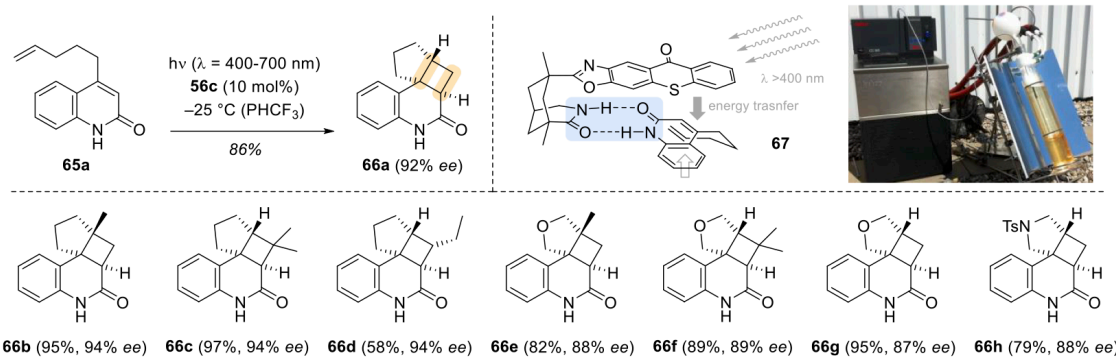

parent compound **53a** (cf. Scheme 10), with electron-deficient olefins (Scheme 16).[68]

Scheme 16. Enantioselective Intermolecular [2 + 2] Photocycloaddition of 2-Quinolones 53 and Electron-Deficient Olefins to Cyclobutenes 55

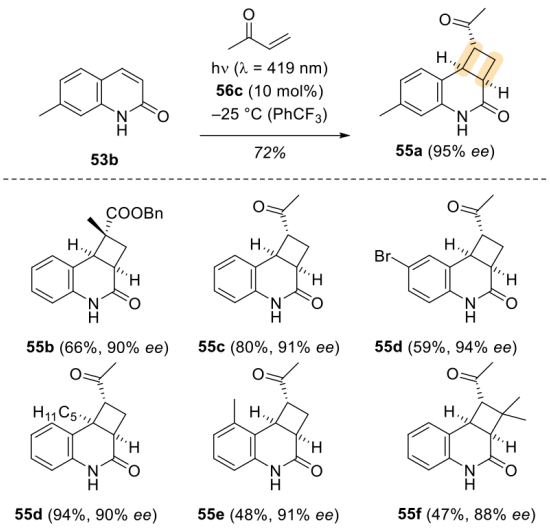

In contrast to xanthone **56b**, thioxanthone **56c** has no spectral overlap with the substrates, and a direct excitation of 2-quinolones can be avoided if the reaction is performed at λ > 360 nm. In this specific case, fluorescent lamps were used with an emission maximum at λ = 419 nm. As pointed out previously, an important requirement for intermolecular enantioselective reactions for catalysts **56** to be successful is a high rate constant for the reaction between the sensitized substrate and the intermolecular reaction partner. It was found by competition experiments for the reaction of 2-quinolones that electron-rich olefins (e.g., vinyl acetate) react roughly 1 order of magnitude slower than electron-deficient olefins. As a result, the enantioselectivities in their reaction do not reach the high values obtained with electron-deficient olefins.[68]

Deracemization Reactions. It has been a continuing theme of our research in photochemistry that we wish to access compounds which cannot be formed thermally and that we wish to ideally access them in enantiomerically pure form. In this regard, we were fascinated by an idea that had been formulated for decades but had yet been properly realized: the preparation of enantiopure compounds by a catalytic deracemization reaction with a chiral sensitizer.[49a,69] Transformations of this type would indeed be extremely useful given the fact that racemic chiral compounds are separated on a ton scale to gain access to a single enantiomer[70] and that frequently the other enantiomer is not even needed. A major requisite for this process is—apart from a switchable stereogenic element with a chiral molecule—a more rapid racemization of one enantiomer over the other. Given the previously mentioned ability of 1,5,7-trimethyl-3-azabicyclo[3.3.1]nonan-2-ones to distinguish between two enantiomers via hydrogen bonding (vide supra), it was conceivable that one enantiomer would indeed show a higher association constant and a higher reaction rate. The choice for allenes *rac*-**67** turned out to be extremely fortuitous as they underwent from the very start of our experiments an extremely selective deracemization (Scheme 17).[54] Surprisingly, the reaction not only proceeded in the nonpolar solvent trifluorotoluene but also in acetonitrile. The catalyst loading was low (2.5 mol %) and a photostationary state was established in all cases within less than 4 h. A total of 17 allenes were taken into the deracemization reaction several of which bore a functional group. Enantioselectivities were in the range of 89–97% ee, and very often the reactions proceeded in close to quantitative yields.

Although our mechanistic understanding of the deracemization has only started to emerge, it appears that both association constants and sensitization rates are important parameters. The major enantiomer **68a** binds with a lower association constant to the chiral sensitizer *ent*-**56c** than the minor enantiomer *ent*-**68a** (Scheme 18). Sensitization of allenes occurs within complexes **69** and **69′** which induces the racemization process (vide infra). DFT calculations suggest that the distance between the two chromophores in **69′** is in the range of a van der Waals contact. In stark contrast, complex **69** not only forms with a lower association constant but also displays the allene chromophore to the sensitizer at an extended distance with Δr in the range of ca. 150 pm. As a crude estimate, the energy transfer rate k_{ET} within **69** is by a factor of 0.2 ($\cong e^{-1.5}$) smaller than the rate within **69′**.

DOI: 10.1021/acs.joc.9b01299
J. Org. Chem. 2019, 84, 8815–8836

Scheme 17. Catalytic Deracemization of Allenes *rac*-67 by Visible-Light-Mediated Sensitization with Chiral Thioxanthone *ent*-56c

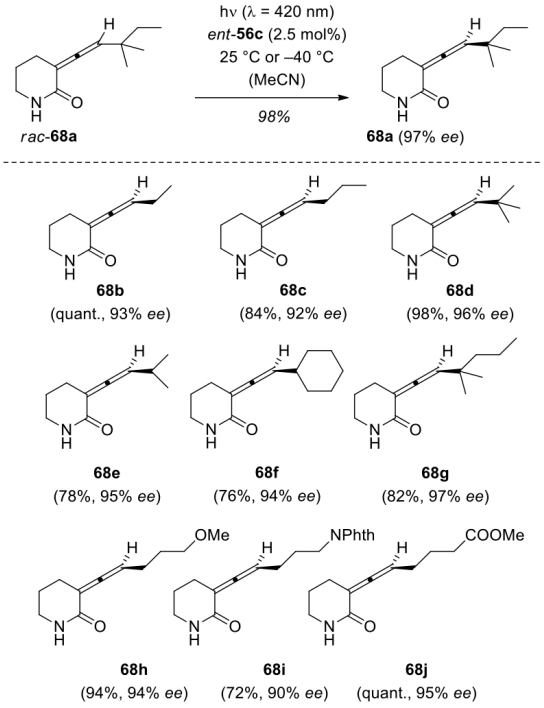

Scheme 18. Key Features of the Enantioselective Deracemization Reaction: Association and Sensitization

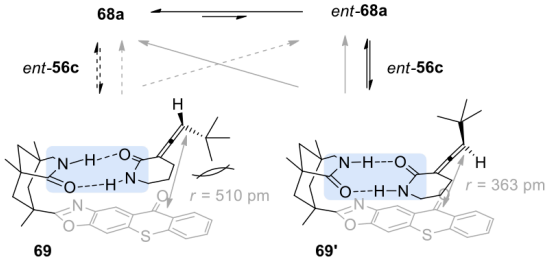

So far, the intermediate triplet allene which is responsible for the racemization has not been identified. However, based on analogy to known allene triplets[71] it is assumed to be a planar species **70** (Figure 4) which can rotate in either direction to form allenes **68** or *ent*-**68**.

Indeed, an important key element in any photochemical deracemization reaction is the intermediacy of an achiral intermediate from which the respective enantiomers are to be populated. Accidentally, we came across the putative 1,3-diradicals **71** when studying the di-π-methane rearrangement of 3-alkenyl-2-quinolones **72** (Scheme 19).[72] The substrates are related to the 4-alkenyl-2-quinolones **65**, but due to the shorter alkenyl chain, they do not undergo an intramolecular [2 + 2] photocycloaddition but rather form the respective cyclopropanes via a 1,4-diradical intermediate.

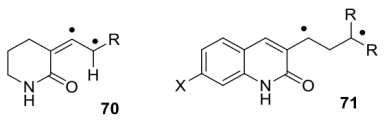

Figure 4. Intermediates **70** and **71** of photochemical deracemization reactions.

Scheme 19. Enantioselective Formation of Cyclopropanes 73 by a Sequence of the Di-π-methane Rearrangement and Deracemization

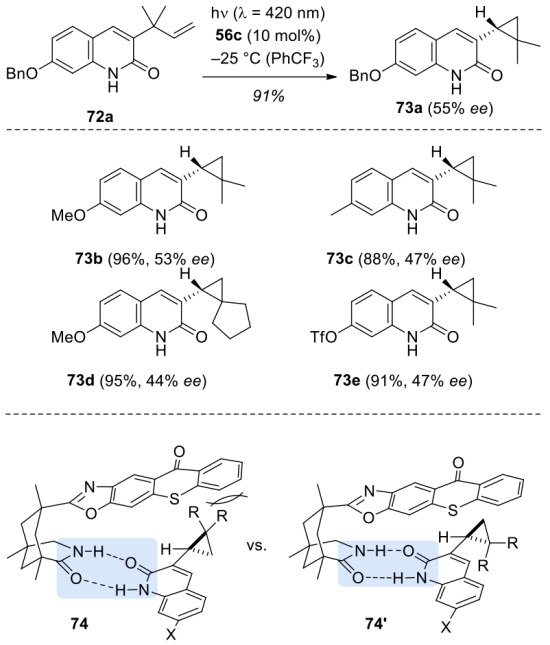

It turned out, however, that products **73** are not configurationally stable when irradiated in the presence of an appropriate triplet sensitizer. The enantioselectivity of the reaction was shown to originate from a deracemization reaction but not from a kinetically controlled enantioselective di-π-methane rearrangement. Products **73** were obtained in high yields but with only moderate enantioselectivity. In this case, the most likely intermediates are 1,3-diradicals **71** (Figure 4) which are formed by sensitization within complexes **74** and **74′**. Again, it was shown that the association constants of the two enantiomers are different and that complex **74′** (K_a = 2300 ± 130 M^{-1} in benzene-d_6 at 25 °C) displays a higher association constant than that complex **74** (K_a = 253 ± 14 M^{-1} in benzene-d_6 at 25 °C). Interestingly, preliminary DFT calculation suggest that the distance between the chromophores within **74** and **74′** is less pronounced than in complexes **69** and **69′**. In addition, the short lifetime of 1,3-diradicals **71** might lead to a ring closure within the complex to the sensitizer. Both factors would favor an increased formation of cyclopropanes *ent*-**73** which in turn might explain the lower enantioselectivity of the cyclopropane deracemization as compared to the allene deracemization.

DOI: 10.1021/acs.joc.9b01299
J. Org. Chem. 2019, 84, 8815−8836

■ TRANSITION-METAL CATALYSIS

Basic Considerations. Although initially conceived for photochemical reactions, the concept of enantioselectivity control by hydrogen bonding to a lactam binding motif appeared to be also applicable to transition-metal-catalyzed organic transformations. Again, it is beyond the scope of this Perspective to review all previous studies which demonstrated hydrogen bonding in transition-metal catalysis nor is it possible to appropriately give credit to the extensive work on directed functionalization by noncovalent interactions.[73] Two pioneering studies that preceded our own work are mentioned here as they made intentional use of molecular devices which display a two-point or single-point hydrogen-bonding site (Scheme 20).

Scheme 20. Previous Examples on Regioselective and Enantioselective Transition-Metal-Catalyzed Transformations Mediated by Hydrogen Bonding

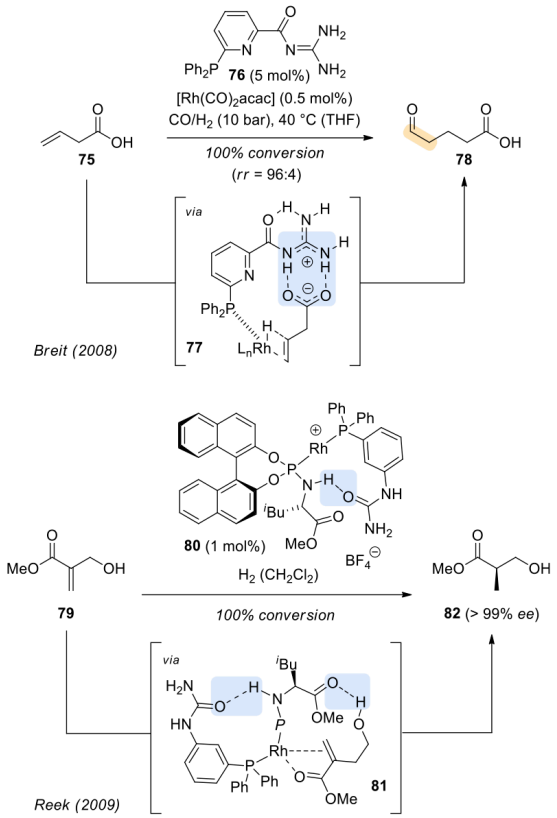

The Breit group achieved a regioselective hydroformylation of vinylacetic acid (**75**) by means of a phosphine ligand **76**, which was modified with a guanidinium-based recognition unit (acac = acetylacetonate). In this specific case, two-point hydrogen bonding between the carboxylic acid and the guanidine in rhodium complex **77** (L = ligand) aligns the olefin in a position that favors almost exclusively formation of the linear product **78**.[74,75]

Notably, if the C−P bond was omitted and a 1:1 mixture of triphenylphosphine and the respective pyridine derivative was applied, there was no considerable regioselectivity (rr = 60:40) and the conversion dropped to 20%, clearly indicating that precoordination of the substrate to the catalytic entity had a rate acceleration effect. While the former system was not designed for any enantioface differentiation, seminal work by the group of Reek[76,77] on hydrogenation reactions impressively showed how a single hydrogen bond can facilitate an enantioselective reaction. The in situ generated rhodium complex **80** (1,4-cyclooctadiene ligand omitted for clarity) was employed in the hydrogenation of alcohol **79** giving access to the enantiomerically pure Roche ester[78] **82** via a hydrogen-bonded intermediate **81** (*P* represents the phosphorus atom and its binol ligand).

Along these lines, we envisioned that the (thio)xanthone moiety from our previously used photocatalysts could be replaced by a catalytically active metal center. Based on what we had learned from catalysts **56** and *ent*-**56**, we expected that a catalyst **B**, once converted into its active form **C** by a stoichiometric reagent, could coordinate to a prochiral lactam to form complex **D**. Enantioface differentiation is now evident, and moreover, only a single reactive site should be exposed to the metal center. It was thus expected that the prefunctionalized metal center M would deliver a functional group X in an enantioselective and site-selective fashion (**E**) whereupon the chiral product would be released and lead to closure of the catalytic cycle. (Scheme 21). Catalyst **B** exhibits a substrate binding site via lactam hydrogen bonding and a reactive metal center which are linked by a U- or V-shaped skeleton.

Scheme 21. Proposed Catalytic Cycle for an Enantioselective Transition Metal-Catalyzed Functionalization Mediated by Hydrogen Bonding

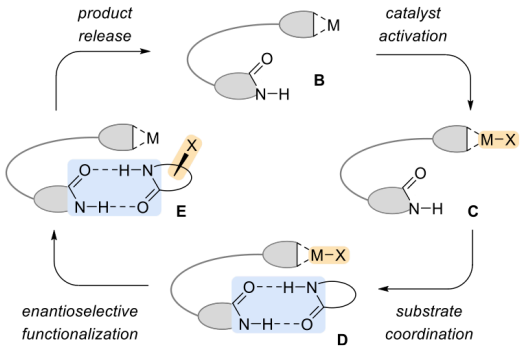

Initially, we attempted to employ the 1,5,7-trimethyl-3-azabicyclo[3.3.1]nonan-2-one scaffold with a potential metal-binding ligand to be attached to position C-7. The bis(oxazoline) ligand **83** (Figure 5) represents a typical ligand of this type which was prepared from the previously reported

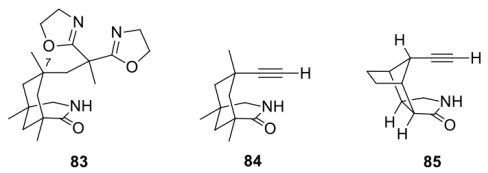

Figure 5. Structure of the bis(oxazoline) ligand **83** and of alkynes **84** and **85**.

DOI: 10.1021/acs.joc.9b01299
J. Org. Chem. 2019, 84, 8815−8836

methyl 1,5,7-trimethyl-3-azabicyclo[3.3.1]nonan-2-onyl-7-carboxylate.[79] However, it turned out that this approach was tedious and time-consuming as it required to adapt each and every synthesis protocol individually to the ligand. Although bond elongation at C-7 was possible, for example, by an aldol condensation from the corresponding C7-aldehyde or by an S_N2-type reaction from the respective C7-mesylated alcohol, further steps were required to complete the synthesis. A modular strategy seemed desirable which allowed to prepare the hydrogen bonding lactam skeleton separately and to link it—ideally in a single step—to a suitable building block with the preformed ligand. It was therefore fortunate that the previously mentioned C7-aldehyde was easily converted into the terminal alkyne **84**,[18c] whereupon a broad diversification strategy via Sonogashira cross-coupling reactions proved to be successful.

During our initial experiments with ligands derived from alkyne **84** (vide infra), there were indications that the shape of the molecular recognition unit influences the success of the desired transformation (vide infra). Unlike in our photochemical reactions, where the key for achieving high enantioface differentiation was steric shielding induced by close proximity of the substituent at C-7 to the prefunctionalized substrate, transition-metal catalysts demand more spatial flexibility for a functional group to be transferred from the metal center to the prochiral lactam. Accordingly, it appeared that the 1,5,7-trimethyl-3-azabicyclo[3.3.1]nonan-2-one scaffold might not provide sufficient space due to its tight U-shaped nature. Influenced by the work of Deslongschamps,[80] we anticipated that the octahydro-1*H*-4,7-methanoisoindol-1-one skeleton **85** would exhibit a more accessible V-shape geometry and might be the more favorable candidate. The compound was accessible from 6,6-dimethylfulvene and maleic anhydride[81] and served in most future experiments as the lactam component in the synthesis of templated chiral metal complexes.

Oxidation and Oxygenation Reactions. Natural enzymes such as cytochrome P450 possess the unique capability to catalyze highly selective oxidative transformations.[82] Although hydrogen bonds are frequently responsible for high stereocontrol in biological oxidation processes,[83] similar principles have rarely been adopted in modern organic synthesis.[84] Earlier contributions regarding selective oxidative transformations mediated by a noncovalent interplay were made among others[73] by the groups of Breslow[85] and Crabtree.[86] However, the use of hydrogen bonding as a general concept for an enantioselective approach had remained unexplored prior to our work. The well-established oxidation properties of manganese salen complexes[87] in combination with an easily feasible derivatization thereof appeared to be a reasonable starting point for preliminary experiments. The terminal alkyne **84** was linked to a 3-*tert*-butyl-salicylaldehyde via Sonogashira cross-coupling reaction and subsequently the C_2-symmetric manganese salen complex *ent*-**87** was prepared following a literature known procedure.[88] The resulting catalyst was probed in the enantioselective sulfoxidation of commercially available 2*H*-benzo[*e*][1,4]thiazin-2-one (**86**) and of other sulfides with similar structure to deliver the respective sulfoxides such as **88** (Scheme 22).[89] The enantioselectivity was remarkable (up to 71% ee) with respect to the unprecedented mode of action but remained relatively low compared to what we had expected from the results of our photocycloaddition reactions.

Scheme 22. Enantioselective Oxidation of Sulfide 86 to Sulfoxide 88 Mediated by Mn−Salen Complex *ent*-87 with a Remote Hydrogen-Bonding Motif

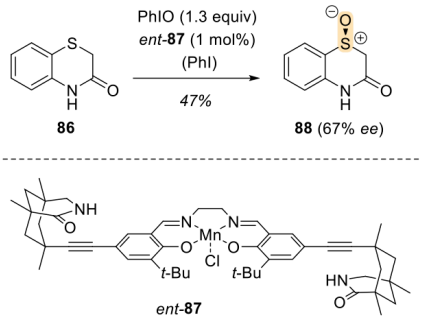

As previously alluded to, we anticipated that the initial U-shaped 7-ethynyl-1,5,7-trimethyl-3-azabicyclo[3.3.1]nonan-2-one backbone was less suited for enantioselective transition metal catalysis due to the restricted space available for the substrate at the active site. A subtle structural alteration was required. Besides varying the lactam binding site to the octahydro-1*H*-4,7-methanoisoindol-1-one skeleton , we envisioned that a different choice of the catalytic entity might also be beneficial. In this context, porphyrin ligands seemed to be an excellent choice, not only because of their frequent use in oxidation and oxygenation reactions,[90] but most importantly due to their expansive but planar geometry. At the beginning, we prepared ruthenium complex **89a**,[81b] in which the porphyrin core is flanked by two 2,4,6-trimethylphenyl (Mes) and a phenyl substituent (Figure 6). In a later version

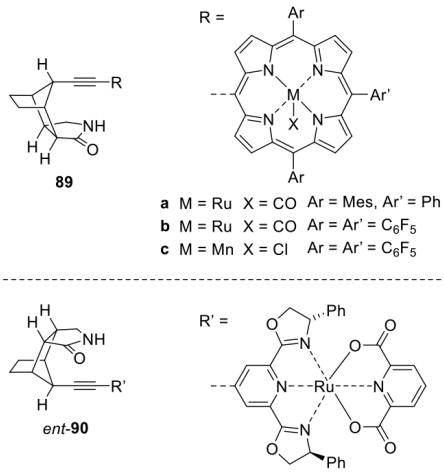

Figure 6. Structure of porphyrins **89** and of pybox complex *ent*-**90** with an octahydro-1*H*-4,7-methanoisoindol-1-one backbone.

of this catalyst (porphyrin **89b**),[91] the substituents were exchanged by three pentafluorophenyl groups with the aim to increase the electrophilicity of the reactive metal-oxo-intermediate by electron withdrawing substituents.[92] Most recently, we synthesized the manganese complex **89c**[93] with a different metal core because the ruthenium insertion step into the porphyrin led to an extensive loss of material in the

DOI: 10.1021/acs.joc.9b01299
J. Org. Chem. 2019, 84, 8815−8836

synthesis of **89a** and **89b**. Another promising candidate for the oxidation of sulfides was the pyridine-2,6-bis(oxazoline) (pybox) complex *ent*-**90** in which the ruthenium center is coordinated by an additional equivalent of 2,6-pyridinedicarboxylate.[94]

The first study related to enantioselective C–O bond formation was performed with porphyrin catalyst **89a** and concerned the enantioselective epoxidation of 3-alkenylquinolones, such as compound **91a**, with 2,6-dichloropyridine-*N*-oxide (DCPNO) as the stoichiometric oxidant (Scheme 23).[81b,95] Despite the fact that there is a free rotation around

Scheme 23. Enantioselective Epoxidation of Vinylquinolones 91 to Epoxides 93 Catalyzed by a Chiral Ruthenium Porphyrin Complex 89a with a Remote Hydrogen-Bonding Site

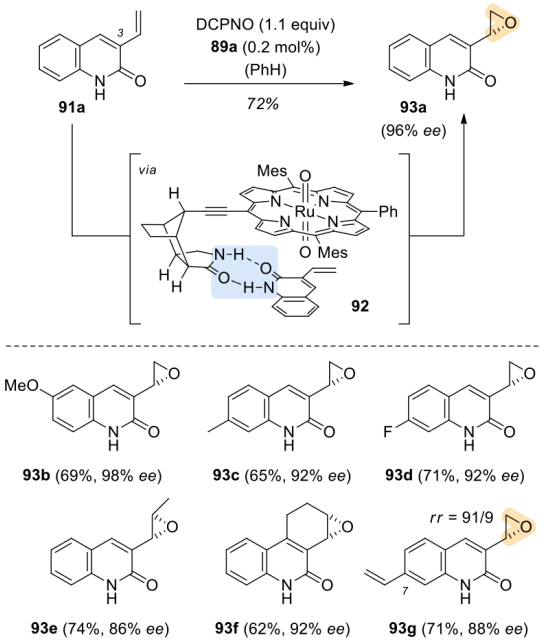

the C–C bond at quinolone carbon atom C-3, the activated ruthenium complex transfers the oxygen atom with almost perfect precision via complex **92** to a single enantiotopic face. DFT calculations support the approach shown and make it likely that a Ru^{VI} oxo complex is the active catalyst but the stereo- and regiochemical consequence would be identical with a Ru^{V} oxo complex as the reactive species. As little as 0.2 mol % of catalyst was needed to furnish the corresponding epoxides **93** in moderate to good yields and with excellent enantioselectivity. The method tolerates substitution in 6- and 7-position of the quinolone substrate (products **93b–93d**) as well as 1,2-disubstituted olefins (products **93e–93f**). Attack at the C-3 vinyl double bond was favored with high preference (rr = 91/9) over the double bond at position C-7 (product **93g**). The regioselectivity is significantly higher with chiral catalyst **89a** than with an achiral porphyrin catalyst illustrating the importance of the hydrogen bond for substrate precoordination. When the *N*-methylated derivative of substrate **91a** was taken into the reaction, the enantioselecitivity of the epoxidation was negligible (≤5% ee), and the reaction proceeded sluggishly.

The epoxidation conditions shown in Scheme 23 were also applicable to other substrates including 3-alkenylpyridones and primary alkenoic acid amides. In the former case, the epoxidation products were unstable, and the enantiomeric purity (77–87% ee) of the products had to be established after derivatization. In the latter case, the respective products were obtained with lower selectivity (70% and 45% ee) presumably because the alkyl chain lends more flexibility for the approach of the reactive catalyst to the olefinic double bond.

Preliminary attempts to apply catalyst **89a** also to oxygenation reactions at aliphatic C–H bonds were met with limited success. The catalyst seemed to be insufficiently reactive, and conversions remained low. In addition, when methylene groups were successfully oxygenated, overoxidation of the resulting chiral secondary alcohol to an achiral ketone erased the newly created stereogenic center. The reactivity issue could be overcome by attaching more strongly electron-withdrawing groups to the porphyrin ring which in turn make the metal center more electron deficient and, thus, the resulting oxo complex more electrophilic. The selectivity issue was—at least temporarily—resolved by designing C–H activation substrates that would retain a stereogenic center even if the secondary alcohol was further oxidized to a ketone. Along these lines, oxindoles **94** contain a prostereogenic spiro center which carries two enantiotopic methylene groups (Scheme 24).[91] The reaction at one of the methylene groups leads to a secondary alcohol which after further oxidation retains its chirality provided that the oxygenation reaction had selectively occurred at one of the two enantiotopic groups. Starting from

Scheme 24. Enantiotopos-Selective C–H Oxygenation of Spirocyclic Oxindoles 94 to Ketones 96 Catalyzed by the Supramolecular Ru–Porphyrin Complex 89b

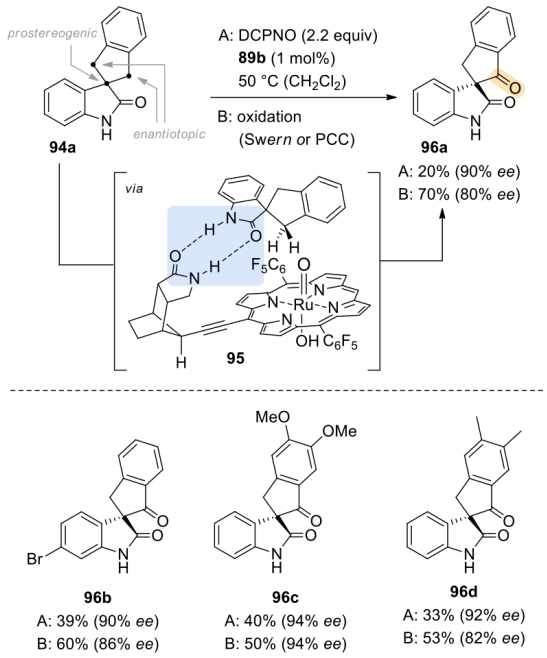

DOI: 10.1021/acs.joc.9b01299
J. Org. Chem. 2019, 84, 8815–8836

oxindole **94a** and employing DCPNO as the stoichiometric oxidant for the oxygenation reaction, the catalyzed reaction delivered 20% of ketone **96a** and significant quantities of the respective alcohol as the initial reaction product. In order to obtain exclusively a single product, the oxidation of the alcohol to the ketone was performed in a second step by the Swern protocol or with pyridinium chlorochromate (PCC).

The two-step protocol made several chiral ketones **96** accessible in high enantioselectivity. It could be shown that the templated catalyst is likely to operate via the proposed complex **95**, and DFT calculations (Figure 7) provided evidence on the selective attack of the Ru^V oxo complex at a single C−H bond. The oxygenation was suggested to proceed mechanistically by initial hydrogen abstraction and subsequent rapid rebound of the hydroxy group to the carbon radical center. The calculated primary kinetic isotope effect (k_H/k_D) for the reaction was 6.4, which parallels the experimentally determined value of 6.1. The hydrogen-abstraction step determines the enantioselectivity, and the ligand directs the active site to a specific position within substrate **94a**. The loss of enantioselectivity when comparing the enantiomeric excesses for products **96** before (A) and after alcohol oxidation (B) is likely due to a racemization via a retro-aldol reaction of the secondary alcohol. This hypothesis is in line with the fact that electron-withdrawing substituents at the oxindole showed diminished enantioselectivity.

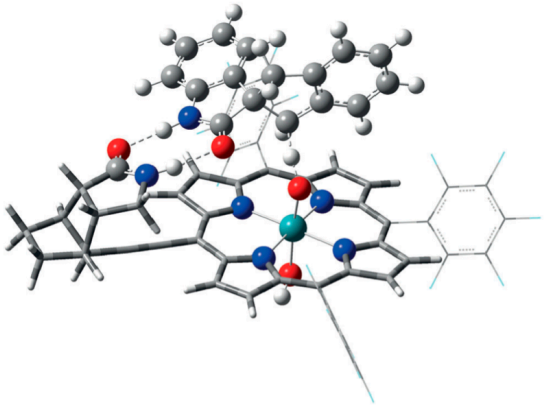

Figure 7. Proposed transition state for the reaction **94a** → **96a** as calculated by DFT methods. Reprinted with permission from ref 91. Copyright 2014 John Wiley and Sons.

Given the enormous need for enantioselective oxygenation reactions which allow for a late-stage functionalization of organic compounds, we turned toward manganese porphyrin complexes to achieve a selective oxygenation of secondary alcohols. Literature reports indicated that the propensity for overoxidation with manganese catalysts[96,97] might be lower than with the respective ruthenium porpyhrins. During the preparation of complex **89c**, it was gratifying to note that the catalytically active metal could be introduced into the preformed porpyhrin in the very last step of the synthesis. With ruthenium, all attempts to do so failed due to competitive reduction of the triple bond. 3,4-Dihydroquinolones **97** were selected as the first class of substrates to be tested in the oxygenation reaction (Scheme 25). They exhibit the required lactam binding site and were considered useful due to their known biological activity.[98] Iodosobenzene was found to be a superior oxidant and the reaction was performed with 2 mol % of catalyst **89c** at 0 °C.

Scheme 25. Enantioselective Hydroxylation of 3,3-Disubstituted 3,4-Dihydroquinolones 97 to their Corresponding Alcohols 99 Catalyzed by the Manganese Porphyrin Complex 89c

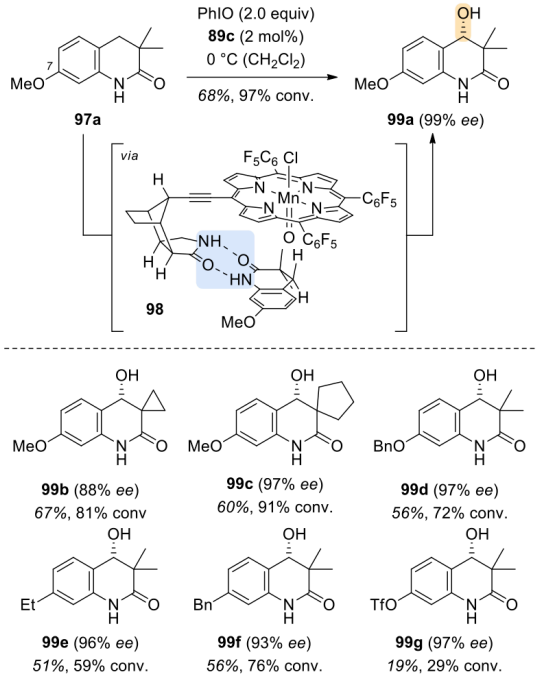

For all substrates **97**, the enantioselectivity was high but the conversion depended strongly on the electronic properties of the substrate. Electron-rich 3,4-dihydroquinolones reacted most readily and the reaction was close to completion after a reaction time of 16 h (products **99a**−**99c**). We observed that the more electron-deficient the substituent in position C-7 was, the lower was the conversion (e.g., products **99d**−**99g**). The observed selective formation of product **99a** with (*S*)-configuration correlates with a transition state **98** in which the putative Mn^V oxo complex is directed to the substrate by hydrogen bonding. The bent nature of the transition state in Mn-catalyzed oxygenation reaction had been noted earlier and was reflected for the transformation **97a** → **99a** by a relatively low kinetic isotope effect (k_H/k_D = 3.0). The oxygenation is selective for the methylene group at the C-4 site. There was no notable oxygenation at the electronically favored benzylic positions (cf. products **99d** and **99f**).

In the reactions of spiro compounds **94**[91] it was not possible to identify and characterize the secondary alcohol intermediate, but the reaction had triggered our interest in oxidation reactions which would be selective regarding one of the two enantiotopic atoms and simultaneously enantioselective at this very specific atom. Hence, it was a curiosity-driven set of experiments we performed with spirodithiolane-indoles **100**, and we tried to identify which of the four possible stereoisomeric sulfoxides was formed in an enantioselective sulfoxidation protocol.[94] Ruthenium complex *ent*-**90** which was

DOI: 10.1021/acs.joc.9b01299
J. Org. Chem. 2019, 84, 8815−8836

derived from alkyne *ent*-**85** was employed as the oxidation catalyst and cumene hydroperoxide (CHP) as the stoichiometric oxidant (Scheme 26).

Scheme 26. Enantio- and Diastereoselective Sulfoxidation of Spirodithiolane-Indoles 100 Catalyzed by Ruthenium Complex *ent*-90

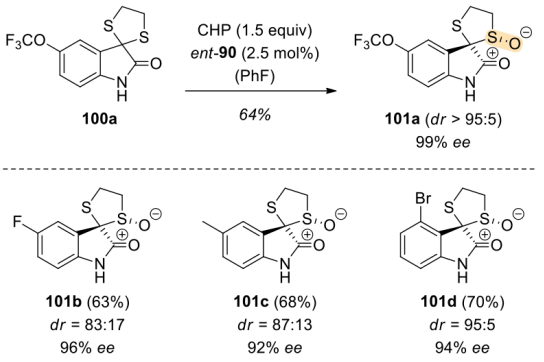

Remarkably, a single position was addressed with high preference, and products **101** were obtained with a high degree of stereoselectivity. It was found that the chirality of the pybox ligand at the ruthenium complex has an influence on the stereoselectivity and that the two elements of chirality (ligand and lactam backbone) work synergistically. The observed selectivity is in agreement with a hydrogen bonded substrate which exposes a free electron pair at a defined sulfur atom to the catalytically active ruthenium oxo complex.

Aziridination and Amination Reactions. Over the past two decades, stereoselective catalytic C−H amination reactions have gained considerable attention[99] owing to the abundant presence of nitrogen atoms in secondary metabolites[100] and nitrogen-containing heterocycles in medicinal chemistry.[101] Among others,[102] seminal studies by the group of Che[103] have shown that metal porphyrin complexes can be effective for the introduction of sulfonamides via nitrene transfer from *N*-sulfonyliminophenyliodinane precursors. Around the same time, Du Bois and co-workers have made fundamental contributions to the field when discovering rhodium-catalyzed intramolecular C−H amination reactions of carbamates and sulfamates[104] and illustrating their application to the total synthesis of complex natural products.[105] The discovery of the dicarboxylate-derived rhodium complex $Rh_2(esp)_2$ was particularly interesting as it provided superior activity in the C−H functionalized process and moreover significantly expanded the scope of this reaction type.[106] Encouraged by this work and inspired by our own interest in diastereoselective amination reactions,[107] we envisioned that a brominated version of the corresponding diethyl $\alpha,\alpha,\alpha',\alpha'$-tetramethyl-1,3-benzoldipropionate (esp ligand) would be easily accessible and thus could be tethered to our previously applied octahydro-1*H*-4,7-methanoisoindol-1-one backbone by Sonogashira cross-coupling. Indeed, the respective diethyl dicarboxylate could be obtained and was readily saponified to the free acid. Rhodium complexation furnished the desired C_2-symmetric catalyst *ent*-**102**, and its structure was unambiguously proven by X-ray crystallography (Figure 8).[108]

Comparison of this structure with the structure of ligand *ent*-**103** that was derived from ethynyl-1,5,7-trimethyl-3-

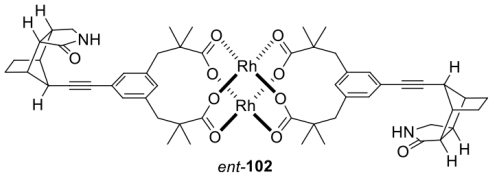

Figure 8. Structure of the C_2-symmetric Rh(II) catalyst *ent*-**102** exhibiting two remote recognition sites for hydrogen-bond-mediated coordination of prochiral quinolones.

azabicyclo[3.3.1]nonan-2-one (*ent*-**84**)[109] revealed the anticipated difference in shape (Figure 9). The angle of the ethynyl

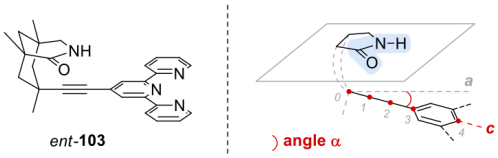

Figure 9. Structure of ligand *ent*-**103** and angle α defining the relative position of a ligand to the lactam plane.

linked substituent to the lactam can be defined as the angle α of the straight line *c* relative to the straight line *a* which in turn is parallel to the lactam plane. The angle α as determined from the mean value for the two lactam units in complex *ent*-**102** ($\alpha \cong 26°$) is significantly different from the angle for *ent*-**103** ($\alpha \cong 16°$). In both cases, the alkyne is not completely parallel to the lactam plane (U-shape) but opens up like the letter V. However, the angle is larger ($\Delta\alpha \cong 10°$) for the octahydro-1*H*-4,7-methanoisoindol-1-one skeleton, thus providing more space for a given ligated transition metal.

Based on our previous epoxidation experiments,[95] we anticipated that the new complex *ent*-**102** would likewise be capable of precoordinating quinolones and thus facilitate a comparable binding mode that would allow for enantioface differentiation. Accordingly, a methylene group in the C-3 position of the heterocyclic carbon skeleton was considered to be an ideal prochiral element, which in turn could further be activated by an electron rich aromatic substituent. We eventually chose quinolone **104** for our preliminary experiments and we were delighted to observe significant enantioselectivity (up to 72% ee) in the rhodium catalyzed amination to sulfonamide **106** (Scheme 27).[108]

The absolute configuration of product **106** was assigned by anomalous X-ray diffraction, confirming the hypothesis that hydrogen bonding is responsible for the differentiation of the two hydrogen atoms in complex **105**. It was observed that the enantioselectivity decreases significantly (30% ee) if the methylene bridge was further extended by an additional carbon atom as the amination proceeded adjacent to the 4-methoxyphenyl moiety. In order to examine whether the amination is both enantio- and site-selective, a second 4-methoxybenzyl substituent was introduced at position C-7 of the quinolone. Notably, a reversal of site-selectivity[110] was observed when *ent*-**102** (rr [C3/C7] = 63/37) was applied instead of the achiral amination catalyst $Rh_2(esp)_2$ (rr [C3/C7] = 39/61).

The application scope of Rh(II) complex *ent*-**102** was further explored regarding a potential catalysis of aziridination reactions.[111] 3-Vinylquinolone derivative **91e** was chosen as

DOI: 10.1021/acs.joc.9b01299
J. Org. Chem. 2019, 84, 8815−8836

Scheme 27. Enantioselective Amination of 3-(4-Methoxybenzyl)quinolone) 104 to Sulfonamide 106 Catalyzed by the Chiral Rh(II)-esp Catalyst *ent*-102

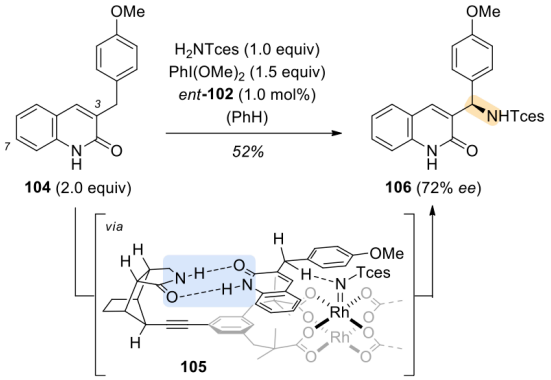

the substrate since it had provided an excellent enantioselectivity in catalytic epoxidation reactions.[81b,95] In preliminary experiments, it was observed that the racemic aziridination with $Rh_2(esp)_2$ gave a clean conversion to the corresponding aziridine *rac*-**107e** (R = H, R^1 = Me) as a single diastereoisomer. However, due to its electron-withdrawing aryloxysulfonyl substituent, the aziridine *rac*-**107e** was sufficiently electrophilic to undergo an intramolecular ring opening reaction. In a cascade reaction the *trans*-substituted heterotricycle *rac*-**108e** formed without isolation of the intermediate aziridine.[112] The asymmetric construction of 2,3-dihydrobenzo[2,3-*b*]quinolines *rac*-**108** had not been investigated prior to our work, and accordingly, we further optimized a new one-pot aziridiniation/ring opening protocol. Polar solvents such as acetonitrile accelerated the cyclization step and 1 mol % of $Rh_2(esp)_2$ was satisfactory to give rise to a large variety of 5-, 6-, and 7-substituted quinolines *rac*-**108** (12 examples, 45−78% yield).

As previously mentioned, nonpolar solvents are beneficial to establish sufficient hydrogen bonding of lactam-based catalysts to prochiral quinolone. It was hence assumed that the developed protocol had to be slightly altered for an enantioselective approach using the chiral complex *ent*-**102**. Indeed, it was found that the use of benzene instead of acetonitrile had a significant impact on the enantioselectivity. In addition, the reaction had to be run under dilute conditions to render the enantioselectivity high (up to 89% ee). At this point, other vinylquinolones **91** were examined (Scheme 28), and it was found that ethyl- or *n*-propylsubstituted olefins delivered superior enantioselectivity (**108h**−**108i**). Moreover, it was found that electron-donating groups (**108j**−**108k**) and electron-withdrawing substituents (**108l**−**108m**) were likewise tolerated in both the 6- and 7-positions of quinolone **91** and that even a benzo[*q*]quinolone delivered the respective tetracyclic ring **108n** in outstanding enantiomeric excess.

The removal of the 2,2,2-trichloroethoxysulfonyl (Tces) group was easily accomplished using zinc in a mixture of methanol and acetic acid without any racemization, and the absolute configuration was assigned by Mosher ester analysis.[113]

Scheme 28. Enantioselective Construction of 2,3-Dihydrobenzo[2,3-*b*]quinolines 108 from 3-Alkenylquinolones 91 Catalyzed by Rhodium Complex *ent*-102

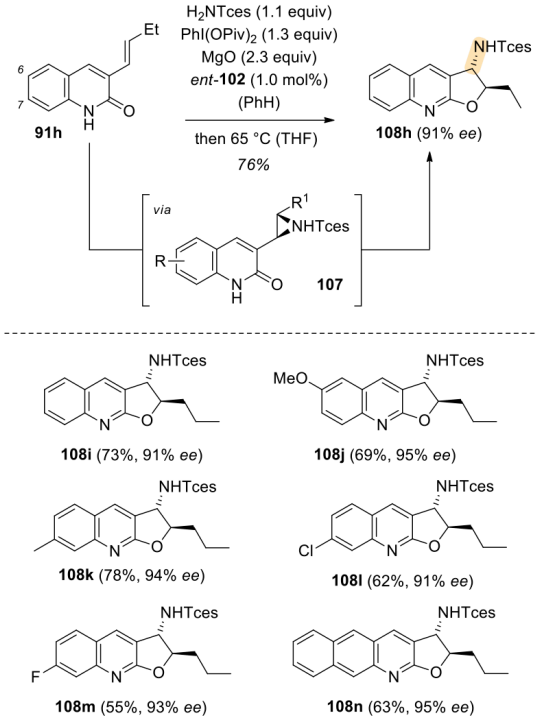

CONCLUSION

The quest for selectivity in chemical transformation can be tackled in various ways, and there is no general solution nor is there one approach which is intrinsically better than the other. A substrate precoordination by hydrogen bonds has been one of the strategies which we have chosen to entail selectivity, and this Perspective describes how different ideas have developed over the years. To this very day, it remains one of the most appealing and scientifically satisfying aspects of this approach that the use of lactam hydrogen bonds can be rationally designed and that their mode of action can be understood at a very fundamental level. It has turned out, however, that there are several complex layers of comprehension beyond the very fundamental two-point interaction which is responsible for substrate binding. As in any scientific endeavor, we learn by success and failure. To our delight, the learning curve in the current project has remained steep over several years, and we hope that this trend continues allowing us to take on even the toughest and most challenging selectivity issues which are imposed on us sometimes by curiosity and sometimes by practical needs.

AUTHOR INFORMATION

Corresponding Author
*E-mail: thorsten.bach@ch.tum.de.
ORCID
Thorsten Bach: 0000-0002-1342-0202

DOI: 10.1021/acs.joc.9b01299
J. Org. Chem. 2019, 84, 8815−8836

Notes

The authors declare no competing financial interest.

Biographies

Finn Burg studied chemistry and biochemistry at the Ludwig-Maximilians-University in Munich, where he was part of the research laboratory of D. Trauner and received his M.Sc. degree in March 2017. During his undergraduate studies he participated in a 3 month internship at Bayer HealthCare, before he conducted his master thesis with A. G. Myers at Harvard University as an Otto-Bayer Fellow. In May 2017, he started his Ph.D. studies in the group of T. Bach concerning hydrogen-bond-mediated enantioselective C−H functionalization reactions catalyzed by metal porphyrin complexes.

Thorsten Bach obtained his education at the University of Heidelberg and at the University of Southern California, where he conducted his Diplom thesis with G. A. Olah. He received his Ph.D. in 1991 from the University of Marburg with M. T. Reetz and did postdoctoral work as a NATO fellow with D. A. Evans at Harvard University. He completed his Habilitation at the University of Münster in 1996, moved to the University of Marburg as an associate professor in 1997, and was appointed to the Chair of Organic Chemistry I at the Technische Universität München (TUM) in 2000. He is an elected member of the German Academy of Sciences (Leopoldina) since 2006 and of the Bavarian Academy of Sciences since 2009.

■ ACKNOWLEDGMENTS

Our own research on this topic was generously supported by the Deutsche Forschungsgemeinschaft (DFG), the TU München, the Fonds der Chemischen Industrie, the Alexander von Humboldt foundation, the Studienstiftung des Deutschen Volkes, and the Elitenetzwerk Bayern. T.B. gratefully acknowledges all colleagues worldwide who have contributed to this project in collaborations and who have been instrumental to its success. Their names are found in the references as are the names of the co-workers who have been involved in this research such as M.Sc. students, Ph.D. students, postdoctoral fellows, and academic staff. It is due to their diligence, their dedication, and their intellectual input that this research topic has turned out to be so fruitful.

■ REFERENCES

(1) (a) *Hydrogen Bonding in Organic Synthesis*; Pikho, P. M., Ed.; Wiley-VCH: Weinheim, 2009. (b) Arunan, E.; Desiraju, G. R.; Klein, R. A.; Sadlej, J.; Scheiner, S.; Alkorta, I.; Clary, D. C.; Crabtree, R. H.; Dannenberg, J. J.; Hobza, P.; Kjaergaard, H. G.; Legon, A. C.; Mennucci, B.; Nesbitt, D. J. Defining the hydrogen bond: An account (IUPAC Technical Report). *Pure Appl. Chem.* **2011**, *83*, 1619−1636. (c) *An Introduction to Hydrogen Bonding*; Jeffrey, G. A., Ed.; Oxford University Press: Oxford, 1997. (d) *Hydrogen Bonding in Biological Structures*; Jeffrey, G. A., Saenger, W., Eds.; Springer: New York, 1991.

(2) Selected reviews: (a) Min, C.; Seidel, D. Asymmetric Brønsted acid catalysis with chiral carboxylic acids. *Chem. Soc. Rev.* **2017**, *46*, 5889−5902. (b) Akiyama, T.; Mori, K. Stronger Brønsted Acids: Recent Progress. *Chem. Rev.* **2015**, *115*, 9277−9306. (c) Yu, X.; Wang, W. Hydrogen-Bond-Mediated Asymmetric Catalysis. *Chem. - Asian J.* **2008**, *3*, 516−532. (d) Doyle, A. G.; Jacobsen, E. N. Small-Molecule H-Bond Donors in Asymmetric Catalysis. *Chem. Rev.* **2007**, *107*, 5713−5743. (e) Taylor, M. S.; Jacobsen, E. N. Asymmetric Catalysis by Chiral Hydrogen-Bond Donors. *Angew. Chem., Int. Ed.* **2006**, *45*, 1520−1543. (f) Schreiner, P. R. Metal-free organocatalysis through explicit hydrogen bonding interactions. *Chem. Soc. Rev.* **2003**, *32*, 289−296.

(3) (a) Bach, T. *N*-Acyl Enamines in the Paternò−Büchi Reaction: Stereoselective Preparation of 1,2-Amino Alcohols by C−C Bond Formation. *Angew. Chem., Int. Ed. Engl.* **1996**, *35*, 884−886. (b) Bach, T.; Bergmann, H.; Brummerhop, H.; Lewis, W.; Harms, K. The [2 + 2]-Photocycloaddition of Aromatic Aldehydes and Ketones to 3,4-Dihydro-2-pyridones: Regioselectivity, Diastereoselectivity, and Reductive Ring Opening of the Product Oxetanes. *Chem. - Eur. J.* **2001**, *7*, 4512−4521.

(4) (a) Choy, W.; Reed, L. A., III; Masamune, S. Asymmetric Diels-Alder Reaction: Design of Chiral Dienophiles. *J. Org. Chem.* **1983**, *48*, 1137−1139. (b) Masamune, S.; Reed, L. A., III; Davis, J. T.; Choy, W. Asymmetric Diels-Alder Reactions: Applications of Chiral Dienophiles. *J. Org. Chem.* **1983**, *48*, 4441−4444.

(5) Crimmins, M. T.; Choy, A. L. Solvent Effects on Diastereoselective Intramolecular Photocycloadditions: Reversal of Selectivity through Intramolecular Hydrogen Bonding. *J. Am. Chem. Soc.* **1997**, *119*, 10237−10238.

(6) Sieburth, S. McN.; McGee, K. F., Jr.; Al-Tel, T. H. Fusicoccin Ring System by [4 + 4] Cycloaddition. Control of Diastereoselectivity through Hydrogen Bonding. *J. Am. Chem. Soc.* **1998**, *120*, 587−588.

(7) (a) Prins, J. L.; Reinhoudt, D. N.; Timmerman, P. Noncovalent Synthesis Using Hydrogen Bonding. *Angew. Chem., Int. Ed.* **2001**, *40*, 2382−2426. (b) Archer, E. A.; Gong, H.; Krische, M. J. Hydrogen bonding in noncovalent synthesis: selectivity and the directed organization of molecular strands. *Tetrahedron* **2001**, *57*, 1139−1159.

(8) Kemp, D. S.; Petrakis, K. S. Synthesis and Conformational Analysis of *cis,cis*-1,3,5-Trimethylcyclohexane-1,3,5-tricarboxylic Acid. *J. Org. Chem.* **1981**, *46*, 5140−5143.

(9) (a) Rebek, J., Jr.; Askew, B.; Ballester, P.; Buhr, C.; Jones, S.; Nemeth, D.; Williams, K. Molecular Recognition: Hydrogen Bonding and Stacking Interactions Stabilize a Model of Nucleic Acid Structure. *J. Am. Chem. Soc.* **1987**, *109*, 5033−5035. (b) Rebek, J., Jr.; Williams, K.; Parris, K.; Ballester, P.; Jeong, K.-S. Molecular Recognition: Stacking Interactions Influence Watson Crick vs. Hoogsteen Base-Pairing in a Model of Adenine Receptors. *Angew. Chem., Int. Ed. Engl.* **1987**, *26*, 1244−1245. (c) Askew, B.; Ballester, P.; Buhr, C.; Jeong, K.-S.; Jones, S.; Parris, K.; Williams, K.; Rebek, J., Jr. Molecular Recognition with Convergent Functional Groups. 6. Synthetic and Structural Studies with a Model Receptor for Nucleic Acid Components. *J. Am. Chem. Soc.* **1989**, *111*, 1082−1090. (d) Williams,

DOI: 10.1021/acs.joc.9b01299
J. Org. Chem. 2019, 84, 8815−8836

K.; Askew, B.; Ballester, P.; Buhr, C.; Jeong, K.-S.; Jones, S.; Rebek, Jr. J Molecular Recognition with Convergent Functional Groups. 7. Energetics of Adenine Binding with Model Receptors. *J. Am. Chem. Soc.* **1989**, *111*, 1090−1094. (e) Mori, K.; Murai, O.; Hashimoto, S.; Nakamura, Y. Highly Regio- and Stereoselective Photocycloaddition between Coumarin and Thymine by Molecular Recognition. *Tetrahedron Lett.* **1996**, *37*, 8523−8526. (f) Castellano, R. K.; Gramlich, V.; Diederich, F. Rebek Imides and Their Adenine Complexes: Preference for Hoogsteen Binding in the Solid State and in Solution. *Chem. - Eur. J.* **2002**, *8*, 118−129. (g) Faraoni, R.; Castellano, R. K.; Gramlich, V.; Diederich, F. H-Bonded complexes of adenine with Rebek imide receptors are stabilized by cation−π interactions and destabilized by stacking with perfluoroaromatics. *Chem. Commun.* **2004**, 370−371. (h) Varshney, D. B.; Gao, X.; Friščić, T.; MacGillivray, L. R. Heteroditopic Rebek's Imide Directs the Reactivity of Homoditopic Olefins within Desolvated Quaternary Assemblies in the Solid State. *Angew. Chem., Int. Ed.* **2006**, *45*, 646−650.

(10) Bach, T.; Bergmann, H.; Harms, K. High Facial Diastereoselectivity in the Photocycloaddition of a Chiral Aromatic Aldehyde and an Enamide Induced by Intermolecular Hydrogen Bonding. *J. Am. Chem. Soc.* **1999**, *121*, 10650−10651.

(11) For reviews on templated photochemical reactions, see: (a) Ramamurthy, V.; Sivaguru, J. Supramolecular Photochemistry as a Potential Synthetic Tool: Photocycloaddition. *Chem. Rev.* **2016**, *116*, 9914−9993. (b) Bibal, B.; Mongin, C.; Bassani, D. M. Template effects and supramolecular control of photoreactions in solution. *Chem. Soc. Rev.* **2014**, *43*, 4179−4198. (c) Yang, C.; Inoue, Y. Supramolecular photochirogenesis. *Chem. Soc. Rev.* **2014**, *43*, 4123−4143.

(12) For a related chiral auxiliary, see: Jeong, K.-S.; Parris, K.; Ballester, P.; Rebek, Jr. J. New Chiral Auxiliaries for Enolate Alkylations. *Angew. Chem., Int. Ed. Engl.* **1990**, *29*, 555−556.

(13) (a) Bach, T.; Bergmann, H.; Harms, K. Enantioselective Intramolecular [2 + 2]-Photocycloaddition Reactions in Solution. *Angew. Chem., Int. Ed.* **2000**, *39*, 2302−2304. (b) Bach, T.; Bergmann, H.; Grosch, B.; Harms, K.; Herdtweck, E. Synthesis of Enantiomerically Pure 1,5,7-Trimethyl-3-azabicyclo[3.3.1]nonan-2-ones as Chiral Host Compounds for Enantioselective Photochemical Reactions in Solution. *Synthesis* **2001**, *2001*, 1395−1405.

(14) (a) Kaneko, C.; Naito, T.; Somei, M. Synthesis of Cyclobuta-[c]quinolin-3-ones. Intra- and Inter-molecular Photocycloadditions of 4-Alkoxy-2-quinolone Systems with Olefins. *J. Chem. Soc., Chem. Commun.* **1979**, 804−805. (b) Kaneko, C.; Suzuki, T.; Sato, M.; Naito, T. Cycloaddition in Syntheses. XXXII. Intramolecular Photocycloaddition of 4-(ω-Alkenyloxy)-quinolin-2-(1*H*)-one: Synthesis of 2-Substituted Cyclobuta[*c*]-quinolin-3-(4*H*)-ones. *Chem. Pharm. Bull.* **1987**, *35*, 112−123.

(15) For a review, see: Poplata, S.; Tröster, A.; Zou, Y.-Q.; Bach, T. Recent Advances in the Synthesis of Cyclobutanes by Olefin [2 + 2] Photocycloaddition Reactions. *Chem. Rev.* **2016**, *116*, 9748−9815.

(16) Bach, T.; Bergmann, H.; Grosch, B.; Harms, K. Highly Enantioselective Intra- and Intermolecular [2 + 2]-Photocycloaddition Reactions of 2-Quinolones Mediated by a Chiral Lactam Host: Host−Guest Interactions, Product Configuration, and the Origin of the Stereoselectivity in Solution. *J. Am. Chem. Soc.* **2002**, *124*, 7982−7990.

(17) Bauer, A.; Bach, T. Assignment of the absolute configuration of chiral 7-substituted 3-azabicyclo[3.1.1]nona-2-ones by NMR titration experiments. *Tetrahedron: Asymmetry* **2004**, *15*, 3799−3803.

(18) (a) Bauer, A.; Westkämper, F.; Grimme, S.; Bach, T. Catalytic enantioselective reactions driven by photoinduced electron transfer. *Nature* **2005**, *436*, 1139−1140. (b) Albrecht, D.; Vogt, F.; Bach, T. Diastereo- and Enantioselective Intramolecular [2 + 2] Photocycloaddiiton Reactions of 3-(ω'-Alkenyl)- and 3-(ω'-Alkenyloxy)-Substituted 5,6-Dihydro-1*H*-pyridin-2-ones. *Chem. - Eur. J.* **2010**, *16*, 4284−4296. (c) Voss, F.; Bach, T. An Ethynyl-Substituted 1,5,7-Trimethyl-3-azabicyclo[3.3.1]nonan-2-one as a Versatile Precursor for Chiral Templates and Chiral Photocatalysts. *Synlett* **2010**, *2010*, 1493−1496.

(19) Bakowski, A.; Dressel, M.; Bauer, A.; Bach, T. Enantioselective radical cylisation reactions of 4-substituted quinolones mediated by a chiral template. *Org. Biomol. Chem.* **2011**, *9*, 3516−3529.

(20) Bergmann, H.; Grosch, B.; Sitterberg, S.; Bach, T. An Enantiomerically Pure 1,5,7-Trimethyl-3-azabicyclo[3.3.1]nonan-2-one as ^{1}H NMR Shift Reagent for the *ee* Determination of Chiral Lactams, Quinolones, and Oxazolidinones. *J. Org. Chem.* **2004**, *69*, 970−973.

(21) For previous reviews on the topic, see: (a) Bach, T. The Paternò-Büchi Reaction of *N*-Acyl Enamines and Aldehydes − The Development of a New Synthetic Method and its Application to Total Synthesis and Molecular Recognition Studies. *Synlett* **2000**, 1699−1707. (b) Grosch, B.; Bach, T. Enantioselective Photocycloaddition Reactions in Solution. In *CRC Handbook of Organic Photochemistry and Photobiology*, 2nd ed.; Horspool, W. M., Lencik, F., Eds.; CRC press: Boca Raton, 2004; Vol. *1*, pp 61.1−14. (c) Grosch, B.; Bach, T. Template Induced Enantioselective Photochemical Reactions in Solution. In *Chiral Photochemistry*; Inoue, Y., Ramamurthy, V., Eds.; Dekker: New York, 2004; Vol. *11*, pp 315−340. (d) Bach, T. Enantioselective Photochemical Reactions. In *Asymmetric Synthesis − The Essentials*, 2nd ed.; Christmann, M., Bräse, S., Eds.; Wiley-VCH: Weinheim, 2008; pp 166−170. (e) Breitenlechner, S.; Selig, P.; Bach, T. Chiral Organocatalysts for Enantioselective Photochemical Reactions. In *Organocatalysis*; Reetz, M. T., List, B., Jaroch, S., Weinmann, H., Eds.; Springer: Berlin, 2008; Vol. *2*; pp 255−279. (f) Müller, C.; Bach, T. Chirality Control in Photochemical Reactions: Enantioselective Formation of Complex Photoproducts in Solution. *Aust. J. Chem.* **2008**, *61*, 557−564. (g) Austin, K. A. B.; Bach, T. Enantioselective Photoreactions in Solution. In *CRC Handbook of Organic Photochemistry and Photobiology*, 3rd ed.; Griesbeck, A., Oelgemöller, M., Ghetti, F., Eds.; CRC Press: Boca Raton, 2012; Vol. *1*, pp 7.1−23. (h) Brimioulle, R.; Lenhart, D.; Maturi, M. M.; Bach, T. Enantioselective Catalysis of Photochemical Reactions. *Angew. Chem., Int. Ed.* **2015**, *54*, 3872−3890. (i) Coote, S. C.; Bach, T. Enantioselective Photocatalysis. In *Visible Light Photocatalysis in Organic Chemistry*; Stephenson, C. R. J., Yoon, T. P., MacMillan, D. W. C., Eds.; Wiley-VCH: Weinheim, 2018; pp 335−362.

(22) (a) Bach, T.; Bergmann, H. Enantioselective Intermolecular [2 + 2]-Photocycloaddition Reactions of Alkenes and a 2-Quinolone in Solution. *J. Am. Chem. Soc.* **2000**, *122*, 11525−11526. (b) Brandes, S.; Selig, P.; Bach, T. Stereoselective Intra- and Intermolecular [2 + 2] Photocycloaddition Reactions of 4-(2′-Aminoethyl)quinolones. *Synlett* **2004**, *2004*, 2588−2590. (c) Selig, P.; Bach, T. Photochemistry of 4-(2'-Aminoethyl)quinolones: Enantioselective Synthesis of Tetracyclic Tetrahydro-1a*H*-pyrido[4',3':2,3]-cyclobuta[1,2-*c*] Quinoline-2,11(3*H*,8*H*)-diones by Intra- and Intermolecular [2 + 2]-Photocycloaddition Reactions in Solution. *J. Org. Chem.* **2006**, *71*, 5662−5673.

(23) Bach, T.; Bergmann, H.; Harms, K. Enantioselective Photochemical Reactions of 2-Pyridones in Solution. *Org. Lett.* **2001**, *3*, 601−603.

(24) Bach, T.; Aechtner, T.; Neumüller, B. Intermolecular hydrogen binding of a chiral host and a prochiral imidazolidinone: Enantioselective Norrish−Yang cyclisation in solution. *Chem. Commun.* **2001**, 607−608. (b) Bach, T.; Aechtner, T.; Neumüller, B. Enantioselective Norrish−Yang Cyclization Reactions of N-(ω-Oxo-ω-phenylalkyl)-Substituted Imidazolidinones in Solution and in the Solid State. *Chem. - Eur. J.* **2002**, *8*, 2464−2475.

(25) Ninomiya, I.; Yamauchi, S.; Kiguchi, T.; Shinohara, A.; Naito, T. Photocyclisation of Enamides. Part V. Photocyclisation of $\alpha\beta$-Unsaturated Anilides. *J. Chem. Soc., Perkin Trans. 1* **1974**, 1747−1751.

(26) Bach, T.; Grosch, B.; Strassner, T.; Herdtweck, E. Enantioselective [6π]-Photocyclization Reaction of an Acrylanilide Mediated by a Chiral Host. Interplay between Enantioselective Ring Closure and Enantioselective Protonation. *J. Org. Chem.* **2003**, *68*, 1107−1116.

DOI: 10.1021/acs.joc.9b01299
J. Org. Chem. 2019, 84, 8815−8836

(27) Reviews: (a) Cuadros, S.; Melchiorre, P. Organocatalytic Strategies to Stereoselectively Trap Photochemically Generated Hydroxy-*o*-quinodimethanes. *Eur. J. Org. Chem.* **2018**, *2018*, 2884−2891. (b) Segura, J. L.; Martín, N. *o*-Quinodimethanes: Efficient Intermediates in Organic Synthesis. *Chem. Rev.* **1999**, *99*, 3199−3246. (c) Sammes, P. G. Photoenolisation. *Tetrahedron* **1976**, *32*, 405−422.

(28) Grosch, B.; Orlebar, C. N.; Herdtweck, E.; Massa, W.; Bach, T. Highly Enantioselective Diels−Alder Reactions of a Photochemically Generated *o*-Quinodimethane with Olefins. *Angew. Chem., Int. Ed.* **2003**, *42*, 3693−3696. (b) Grosch, B.; Orlebar, C. N.; Herdtweck, E.; Kaneda, M.; Wada, T.; Inoue, Y.; Bach, T. Enantioselective [4 + 2]-Cycloaddition Reaction of a Photochemically Generated *o*-Quinodimethane. Mechanistic Details, Association Studies, and Pressure Effects. *Chem. - Eur. J.* **2004**, *10*, 2179−2189.

(29) (a) Aechtner, T.; Dressel, M.; Bach, T. Hydrogen Bond Mediated Enantioselectivity of Radical Reactions. *Angew. Chem., Int. Ed.* **2004**, *43*, 5849−5851. (b) Dressel, M.; Aechtner, T.; Bach, T. Enantioselectivity and Diastereoselectivity in Reductive Radical Cyclization Reactions of 3-(ω-Iodoalkylidene)-piperidin-2-ones. *Synthesis* **2006**, *2006*, 2206−2214.

(30) (a) Dressel, M.; Bach, T. Chirality Multiplication and Efficient Chirality Transfer in *exo*- and *endo*-Radical Cyclization Reactions of 4-(4′-Iodobutyl)quinolones. *Org. Lett.* **2006**, *8*, 3145−3147. (b) Kapitán, P.; Bach, T. Template-Induced Enantioselectivity in the Reductive Radical Cyclization of 3-(3-Iodopropyloxy)propenoic Acid Derivatives Depending on the Binding Motif. *Synthesis* **2008**, *2008*, 1559−1564.

(31) Reviews: (a) Ghogare, A. A.; Greer, A. Using Singlet Oxygen to Synthesize Natural Products and Drugs. *Chem. Rev.* **2016**, *116*, 9994−10034. (b) Clennan, E. L.; Pace, A. Advances in singlet oxygen chemistry. *Tetrahedron* **2005**, *61*, 6665−6691.

(32) Wiegand, C.; Herdtweck, E.; Bach, T. Enantioselectivity in visible light-induced, singlet oxygen [2 + 4] cycloaddition reactions (type II photooxygenations) of 2-pyridones. *Chem. Commun.* **2012**, *48*, 10195−10197.

(33) Kornblum, N.; DeLaMare, H. E. The Base Catalyzed Decomposition of a Dialkyl Peroxide. *J. Am. Chem. Soc.* **1951**, *73*, 880−881.

(34) Examples: Miyake, Y.; Ashida, Y.; Nakajima, K.; Nishibayashi, Y. Visible-light-mediated addition of α-aminoalkyl radicals generated from α-silylamines to α,β-unsaturated carbonyl compounds. *Chem. Commun.* **2012**, *48*, 6966−6968. (b) Lenhart, D.; Bach, T. Visible-light-induced, Ir-catalyzed reactions of *N*-methyl-*N*-((trimethylsilyl)-methyl)aniline with cyclic α,β-unsaturated carbonyl compounds. *Beilstein J. Org. Chem.* **2014**, *10*, 890−896. (c) Ruiz Espelt, L.; McPherson, I. S.; Wiensch, E. M.; Yoon, T. P. Enantioselective Conjugate Additions of α-Amino Radicals via Cooperative Photoredox and Lewis Acid Catalysis. *J. Am. Chem. Soc.* **2015**, *137*, 2452−2455.

(35) Lenhart, D.; Bauer, A.; Pöthig, A.; Bach, T. Enantioselective Visible-Light-Induced Radical-Addition Reactions to 3-Alkylidene Indolin-2-ones. *Chem. - Eur. J.* **2016**, *22*, 6519−6523.

(36) Austin, K. A. B.; Herdtweck, E.; Bach, T. Intramolecular [2 + 2] Photocycloaddition of Substituted Isoquinolones: Enantioselectivity and Kinetic Resolution Induced by a Chiral Template. *Angew. Chem., Int. Ed.* **2011**, *50*, 8416−8419.

(37) (a) Coote, S. C.; Bach, T. Enantioselective Intermolecular [2 + 2] Photocycloadditions of Isoquinolone Mediated by a Chiral Hydrogen-Bonding Template. *J. Am. Chem. Soc.* **2013**, *135*, 14948−14951. (b) Coote, S. C.; Pöthig, A.; Bach, T. Enantioselective Template-Directed [2+ 2] Photocycloadditions of Isoquinolones: Scope, Mechanism and Synthetic Applications. *Chem. - Eur. J.* **2015**, *21*, 6906−6912.

(38) (a) Rimböck, K.-H.; Pöthig, A.; Bach, T. Photocycloaddition and Rearrangement Reactions in a Putative Route to the Skeleton of Plicamine-Type Alkaloids. *Synthesis* **2015**, *47*, 2869−2884. (b) Wahl, M. H.; Jandl, C.; Bach, T. A [2 + 2] Photocycloaddition−Fragmentation Approach toward the Carbon Skeleton of *cis*-Fused Lycorine-type Alkaloids. *Org. Lett.* **2018**, *20*, 7674−7678.

(39) (a) Selig, P.; Bach, T. Enantioselective Total Synthesis of the *Melodinus* Alkaloid (+)-Meloscine. *Angew. Chem., Int. Ed.* **2008**, *47*, 5082−5084. (b) Selig, P.; Herdtweck, E.; Bach, T. Total Synthesis of Meloscine by a [2 + 2]-Photocycloaddition/Ring Expansion Route. *Chem. - Eur. J.* **2009**, *15*, 3509−3525.

(40) Mayr, F.; Wiegand, C.; Bach, T. Enantioselective, intermolecular [2 + 2] photocycloaddition reactions of 3-acetoxyquinolone: total synthesis of (−)-pinolinone. *Chem. Commun.* **2014**, *50*, 3353−3355.

(41) Breitenlechner, S.; Bach, T. A Polymer-Bound Chiral Template for Enantioselective Photochemical Reactions. *Angew. Chem., Int. Ed.* **2008**, *47*, 7957−7959.

(42) Maturi, M. M.; Fukuhara, G.; Tanaka, K.; Kawanami, Y.; Mori, T.; Inoue, Y.; Bach, T. Enantioselective [4 + 4] photodimerization of anthracene-2,6-dicarboxylic acid mediated by a C_2-symmetric chiral template. *Chem. Commun.* **2016**, *52*, 1032−1035.

(43) (a) Evanega, G. R.; Fabiny, D. L. The photocycloaddition of carbostyril to olefins. *Tetrahedron Lett.* **1968**, *9*, 2241−2246. (b) Loev, B.; Goodman, M. M.; Snader, K. M. Photochemical cycloaddition reactions involving carbostyrils. *Tetrahedron Lett.* **1968**, *9*, 5401−5404. (c) Evanega, G. R.; Fabiny, D. L. The Photocycloaddition of Carbostyril to Olefins. The Stereochemistry of the Adducts. *J. Org. Chem.* **1970**, *35*, 1757−1761. (d) Buchardt, O.; Christensen, J. J.; Harrit, N. The Photocycloaddition of Cyclohexene to Carbostyrils. *Acta Chem. Scand.* **1976**, *30*, 189−192. (e) Kaneko, C.; Naito, T. Intermolecular Photochemical Cycloaddition of 4-Methoxy-2-quinolone with Olefins: a Regioselective Synthesis of 5-Substituted Cyclobuta[*c*]-2-quinolones. *Chem. Pharm. Bull.* **1979**, *27*, 2254−2256.

(44) (a) El-Sayed, M. A. Spin-Orbit Coupling and the Radiationless Processes in Nitrogen Heterocyclics. *J. Chem. Phys.* **1963**, *38*, 2834−2838. (b) El-Sayed, M. A. Triplet state: Its Radiative and Nonradiative Properties. *Acc. Chem. Res.* **1968**, *1*, 8−16.

(45) (a) Sandros, K. Transfer of Triplet State Energy in Fluid Solutions. *Acta Chem. Scand.* **1964**, *18*, 2355−2374. (b) Strieth-Kalthoff, F.; James, M. J.; Teders, M.; Pitzer, L.; Glorius, F. Energy transfer catalysis mediated by visible light: principles, applications, directions. *Chem. Soc. Rev.* **2018**, *47*, 7190−7202.

(46) *Handbook of Photochemistry*, 2nd ed.; Murov, S. L., Carmichael, I., Hug, G. L., Eds.; Dekker: New York, 1993.

(47) (a) Dexter, D. L. A. Theory of Sensitized Luminescence in Solids. *J. Chem. Phys.* **1953**, *21*, 836−850.

(48) *Modern Molecular Photochemistry of Organic Molecules*; Turro, N. J., Ramamurthy, V., Scaiano, J., Eds.; University Science Books: Sausalito, 2010.

(49) (a) Ouannès, C.; Beugelmans, R.; Roussi, G. Asymmetric Induction During Transfer of Triplet Energy. *J. Am. Chem. Soc.* **1973**, *95*, 8472−8474. (b) Horner, L.; Klaus, J. Möglichkeiten und Grenzen photochemisch induzierter asymmetrischer Synthesen. *Liebigs Ann. Chem.* **1979**, *1979*, 1232−1257. (c) Demuth, M.; Raghavan, P. R.; Carter, C.; Nakano, K.; Schaffner, K. Photochemical High-yield Preparation of Tricyclo [3.3.0.0^{2,8}]octan-3-ones. Potential Synthons for Polycyclopentanoid Terpenes and Prostacyclin Analogs. *Helv. Chim. Acta* **1980**, *63*, 2434−2439. (d) Rau, H.; Hörmann, M. Kinetic resolution of optically active molecules and asymmetric chemistry: asymmetrically sensitized photolysis of *trans*-3,5-diphenylpyrazoline. *J. Photochem.* **1981**, *16*, 231−247. (e) Cauble, D. F.; Lynch, V.; Krische, M. J. Studies on the Enantioselective Catalysis of Photochemically Promoted Transformations: "Sensitizing Receptors" as Chiral Catalysts. *J. Org. Chem.* **2003**, *68*, 15−21.

(50) Sitterberg, S. Chirale Sensibilisatoren für enantioselektive intramolekulare [2 + 2]-Photocycloadditionen. Ph.D. Dissertation, Technische Universität München, 2003.

(51) Müller, C.; Bauer, A.; Bach, T. Light-Driven Enantioselective Organocatalysis. *Angew. Chem., Int. Ed.* **2009**, *48*, 6640−6642.

(52) Alonso, R.; Bach, T. A Chiral Thioxanthone as an Organocatalyst for Enantioselective [2 + 2] Photocycloaddition Reactions Induced by Visible Light. *Angew. Chem., Int. Ed.* **2014**, *53*, 4368−4371.

DOI: 10.1021/acs.joc.9b01299
J. Org. Chem. 2019, 84, 8815−8836

(53) Bauer, A.; Bach, T. Unpublished results, Technische Universität München, 2018.
(54) Hölzl-Hobmeier, A.; Bauer, A.; Silva, A. V.; Huber, S. M.; Bannwarth, C.; Bach, T. Catalytic deracemization of chiral allenes by sensitized excitation with visible light. *Nature* **2018**, *564*, 240−243.
(55) For related work by Wagenknecht and co-workers, see: (a) Gaß, N.; Wagenknecht, H.-A. Synthesis of Benzophenone Nucleosides and Their Photocatalytic Evaluation for [2 + 2] Cycloaddition in Aqueous Media. *Eur. J. Org. Chem.* **2015**, *2015*, 6661−6668. (b) Gaß, N.; Gebhard, J.; Wagenknecht, H.-A. Photocatalysis of a [2 + 2] Cycloaddition in Aqueous Solution Using DNA Three-Way Junctions as Chiral PhotoDNAzymes. *ChemPhotoChem.* **2017**, *1*, 48−50.
(56) (a) Hoffmann, R.; Swenson, J. R. Ground- and Excited-State Geometries of Benzophenone. *J. Phys. Chem.* **1970**, *74*, 415−420. (b) Merz, T.; Wenninger, M.; Weinberger, M.; Riedle, E.; Wagenknecht, H.-A.; Schütz, M. Conformational control of benzophenone-sensitized charge transfer in dinucleotides. *Phys. Chem. Chem. Phys.* **2013**, *15*, 18607−18619.
(57) Sergentu, D.-C.; Maurice, R.; Havenith, R. W. A.; Broer, R.; Roca-Sanjuan, D. Computational determination of the dominant triplet population mechanism in photoexcited benzophenone. *Phys. Chem. Chem. Phys.* **2014**, *16*, 25393−25403.
(58) Kawai, A.; Hirakawa, M.; Abe, T.; Obi, K.; Shibuya, K. Specific Solvent Effects on the Structure and Reaction Dynamics of Benzophenone Ketyl Radical. *J. Phys. Chem. A* **2001**, *105*, 9628−9636.
(59) Bertrand, S.; Hoffmann, N.; Pete, J.-P. Highly Efficient and Stereoselective Radical Addition of Tertiary Amines to Electron-Deficient Alkenes − Application to the Enantioselective Synthesis of Necine Bases. *Eur. J. Org. Chem.* **2000**, *2000*, 2227−2238.
(60) Cavaleri, J. J.; Prater, K.; Bowman, R. M. An investigation of the solvent dependence on the ultrafast intersystem crossing kinetics of xanthone. *Chem. Phys. Lett.* **1996**, *259*, 495−502.
(61) (a) Müller, C.; Bauer, A.; Maturi, M. M.; Cuquerella, M. C.; Miranda, M. A.; Bach, T. Enantioselective Intramolecular [2 + 2]-Photocycloaddition Reactions of 4-Substituted Quinolones Catalyzed by a Chiral Sensitizer with a Hydrogen-Bonding Motif. *J. Am. Chem. Soc.* **2011**, *133*, 16689−16697. (b) Maturi, M. M.; Wenninger, M.; Alonso, R.; Bauer, A.; Pöthig, A.; Riedle, E.; Bach, T. Intramolecular [2 + 2] Photocycloaddition of 3- and 4-(But-3-enyl)oxyquinolones: Influence of the Alkene Substitution Pattern, Photophysical Studies, and Enantioselective Catalysis by a Chiral Sensitizer. *Chem. - Eur. J.* **2013**, *19*, 7461−7472.
(62) Maturi, M. M.; Bach, T. Enantioselective Catalysis of the Intermolecular [2 + 2] Photocycloaddition between 2-Pyridones and Acetylenedicarboxylates. *Angew. Chem., Int. Ed.* **2014**, *53*, 7661−7664.
(63) A related solvent mixture was employed in a study on enantioselective [2 + 2] photocycloaddition reactions mediated by thiourea hydrogen bonds: Vallavoju, N.; Selvakumar, S.; Jockusch, S.; Sibi, M. P.; Sivaguru, J. Enantioselective Organo-Photocatalysis Mediated by Atropisomeric Thiourea Derivatives. *Angew. Chem., Int. Ed.* **2014**, *53*, 5604−5608.
(64) (a) Maturi, M. M.; Pöthig, A.; Bach, T. Enantioselective Photochemical Rearrangements of Spirooxindole Epoxides Catalyzed by a Chiral Bifunctional Xanthone. *Aust. J. Chem.* **2015**, *68*, 1682−1692. (b) Böhm, A.; Bach, T. Synthesis of Supramolecular Iridium Catalysts and Their Use in Enantioselective Visible-Light-Induced Reactions. *Synlett* **2016**, *27*, 1056−1060.
(65) Silvi, M.; Melchiorre, P. Enhancing the potential of enantioselective organocatalysis with light. *Nature* **2018**, *554*, 41−49.
(66) For a related approach, see: Skubi, K. L.; Kidd, J. B.; Jung, H.; Guzei, I. A.; Baik, M.-H.; Yoon, T. P. Enantioselective Excited-State Photoreactions Controlled By A Chiral Hydrogen-Bonding Iridium Sensitizer. *J. Am. Chem. Soc.* **2017**, *139*, 17186−17192.
(67) Alonso, R.; Bauer, A.; Bach, T. Unpublished results, Technische Universität München, 2018.
(68) Tröster, A.; Alonso, R.; Bauer, A.; Bach, T. Enantioselective Intermolecular [2 + 2] Photocycloaddition Reactions of 2(1*H*)-Quinolones Induced by Visible Light Irradiation. *J. Am. Chem. Soc.* **2016**, *138*, 7808−7811.
(69) (a) Hammond, G. S.; Cole, R. S. Asymmetric Induction During Energy Transfer. *J. Am. Chem. Soc.* **1965**, *87*, 3256−3257. (b) Drucker, C. S.; Toscano, V. G.; Weiss, R. G. A General Method for the Determination of Steric Effects during Collisional Energy Transfer. Partial Photoresolution of Penta-2,3-diene. *J. Am. Chem. Soc.* **1973**, *95*, 6482−6484. (c) Balavoine, G.; Jugé, S.; Kagan, H. B. Photoactivation optique du methyl p-tolyl sulfoxyde racemique par emploi d'un sensibilisateur chiral. *Tetrahedron Lett.* **1973**, *14*, 4159−4162.
(70) Lorenz, H.; Seidel-Morgenstern, A. Processes to Separate Enantiomers. *Angew. Chem., Int. Ed.* **2014**, *53*, 1218−1250.
(71) Bucher, G.; Mahajan, A. A.; Schmittel, M. The Photochemical C^2−C^6 Cyclization of Enyne−Allenes: Interception of the Fulvene Diradical with a Radical Clock Ring Opening. *J. Org. Chem.* **2009**, *74*, 5850−5860.
(72) Tröster, A.; Bauer, A.; Jandl, C.; Bach, T. Enantioselective Visible-Light-Mediated Formation of 3-Cyclopropylquinolones by Triplet-Sensitized Deracemization. *Angew. Chem., Int. Ed.* **2019**, *58*, 3538−3541.
(73) Reviews: (a) Mote, N. R.; Chikkali, S. H. Hydrogen-Bonding-Assisted Supramolecular Metal Catalysis. *Chem. - Asian J.* **2018**, *13*, 3623−3646. (b) Davis, H. J.; Phipps, R. J. Harnessing non-covalent interactions to exert control over regioselectivity and site-selectivity in catalytic reactions. *Chem. Sci.* **2017**, *8*, 864−877. (c) Dydio, P.; Reek, J. N. H. Supramolecular control of selectivity in transition-metal catalysis through substrate preorganization. *Chem. Sci.* **2014**, *5*, 2135−2145. (d) Raynal, M.; Ballester, P.; Vidal-Ferran, A.; Van Leeuwen, P. W. N. M. Supramolecular catalysis. Part 1: non-covalent interactions as a tool for building and modifying homogeneous catalysts. *Chem. Soc. Rev.* **2014**, *43*, 1660−1733. (e) Carboni, S.; Gennari, C.; Pignataro, L.; Piarulli, U. Supramolecular ligand−ligand and ligand−substrate interactions for highly selective transition metal catalysis. *Dalton Trans* **2011**, *40*, 4355−4373. (f) Das, S.; Brudvig, G. W.; Crabtree, R. H. Molecular recognition in homogeneous transition metal catalysis: a biomimetic strategy for high selectivity. *Chem. Commun.* **2008**, 413−424.
(74) Šmejkal, T.; Breit, B. A Supramolecular Catalyst for Regioselective Hydroformylation of Unsaturated Carboxylic Acids. *Angew. Chem., Int. Ed.* **2008**, *47*, 311−315.
(75) For additional work by Breit and co-workers on this topic: (a) Šmejkal, T.; Breit, B. A Supramolecular Catalyst for the Decarboxylative Hydroformylation of α,β-Unsaturated Carboxylic Acids. *Angew. Chem., Int. Ed.* **2008**, *47*, 3946−3949. (b) Šmejkal, T.; Gribkov, D.; Geier, J.; Keller, M.; Breit, B. Transition-State Stabilization by a Secondary Substrate−Ligand Interaction: A New Design Principle for Highly Efficient Transition-Metal Catalysis. *Chem. - Eur. J.* **2010**, *16*, 2470−2478. (c) Fang, W.; Breit, B. Tandem Regioselective Hydroformylation-Hydrogenation of Internal Alkynes Using a Supramolecular Catalyst. *Angew. Chem., Int. Ed.* **2018**, *57*, 14817−14821.
(76) Breuil, P.-A. R.; Patureau, F. W.; Reek, J. N. H. Singly Hydrogen Bonded Supramolecular Ligands for Highly Selective Rhodium-Catalyzed Hydrogenation Reactions. *Angew. Chem., Int. Ed.* **2009**, *48*, 2162−2165.
(77) For additional work by Reek and co-workers on this topic: (a) Dydio, P.; Dzik, W. I.; Lutz, M.; de Bruin, B.; Reek, J. N. H. Remote Supramolecular Control of Catalyst Selectivity in the Hydroformylation of Alkenes. *Angew. Chem., Int. Ed.* **2011**, *50*, 396−400. (b) Dydio, P.; Reek, J. N. H. Supramolecular Control of Selectivity in Hydroformylation of Vinyl Arenes: Easy Access to Valuable β-Aldehyde Intermediates. *Angew. Chem., Int. Ed.* **2013**, *52*, 3878−3882. (c) Dydio, P.; Detz, R. J.; de Bruin, B.; Reek, J. N. H. Beyond Classical Reactivity Patterns: Hydroformylation of Vinyl and Allyl Arenes to Valuable β- and γ-Aldehyde Intermediates Using Supramolecular Catalysis. *J. Am. Chem. Soc.* **2014**, *136*, 8418−8429.
(78) For two selected examples in which the Roche ester was used as a key chiral building block in total synthesis, see: (a) Shin, Y.;

DOI: 10.1021/acs.joc.9b01299
J. Org. Chem. 2019, 84, 8815−8836

Fournier, J.-H.; Fukui, Y.; Brückner, A. M.; Curran, D. P. Total Synthesis of (−)-Dictyostatin: Confirmation Of Relative and Absolute Configurations. *Angew. Chem., Int. Ed.* **2004**, *43*, 4634−4637. (b) Smith, A. B., III; Adams, C. M.; Barbosa, S. A. L.; Degnan, A. P. A unified approach to the tedanolides: Total synthesis of (+)-13-deoxytedanolide. *Proc. Natl. Acad. Sci. U. S. A.* **2004**, *101*, 12042−12047.

(79) Vogt, F. Synthese neuer Liganden und Katalysatoren für einen Wasserstoffbrücken-vermittelten Chiralitätstransfer. Ph.D. Dissertation, Technische Universität München, 2010.

(80) (a) Lonergan, D. G.; Riego, J.; Deslongchamps, G. A Convergent Hydroxyimide Module for Molecular Recognition. *Tetrahedron Lett.* **1996**, *37*, 6109−6112. (b) Lonergan, D. G.; Halse, J.; Deslongchamps, G. Comparative Probe for Stacking Interactions in Simple A:T Base Pair Mimics. *Tetrahedron Lett.* **1998**, *39*, 6865−6868. (c) Lonergan, D. G.; Deslongchamps, G. Tricyclic Scaffolds for the Rapid Assembly of Abiotic Receptors. *Tetrahedron* **1998**, *54*, 14041−14052.

(81) (a) Corwin, L. R.; McDaniel, D. M.; Bushby, R. J.; Berson, J. A. Dimerization and Cycloaddition Reactions of a Trimethylenemethane Derivative, 2-Isopropylidenecyclopenta-1,3-diyl. Mechanistic Separation of Triplet and Singlet Reactions. *J. Am. Chem. Soc.* **1980**, *102*, 276−287. (b) Fackler, P.; Berthold, C.; Voss, F.; Bach, T. Hydrogen-Bond-Mediated Enantio- and Regioselectivity in a Ru-Catalyzed Epoxidation Reaction. *J. Am. Chem. Soc.* **2010**, *132*, 15911−15913.

(82) *Cytochrome P450: Structure, Mechanism, and Biochemistry*, 3rd ed.; Ortiz de Montellano, P. R., Ed.; Kluwer: New York, 2005.

(83) (a) Fasan, R. Tuning P450 Enzymes as Oxidation Catalysts. *ACS Catal.* **2012**, *2*, 647−666. (b) Lewis, J. C.; Coelho, P. S.; Arnold, F. H. Enzymatic functionalization of carbon−hydrogen bonds. *Chem. Soc. Rev.* **2011**, *40*, 2003−2021. (c) Ortiz de Montellano, P. R. Hydrocarbon Hydroxylation by Cytochrome P450 Enzymes. *Chem. Rev.* **2010**, *110*, 932−948.

(84) For reviews on biomimetic oxygenation reactions in organic syntheses, see: (a) Vidal, D.; Olivo, G.; Costas, M. Controlling Selectivity in Aliphatic C−H Oxidation through Supramolecular Recognition. *Chem. - Eur. J.* **2018**, *24*, 5042−5054. (b) Milan, M.; Bietti, M.; Costas, M. Enantioselective aliphatic C−H bond oxidation catalyzed by bioinspired complexes. *Chem. Commun.* **2018**, *54*, 9559−9570.

(85) (a) Breslow, R.; Zhang, X.; Huang, Y. Selective Catalytic Hydroxylation of a Steroid by an Artificial Cytochrome P-450 Enzyme. *J. Am. Chem. Soc.* **1997**, *119*, 4535−4536. (b) Yang, J.; Breslow, R. Selective Hydroxylation of a Steroid at C-9 by an Artificial Cytochrom P-450. *Angew. Chem., Int. Ed.* **2000**, *39*, 2692−2694. (c) Yang, J.; Gabriele, B.; Belvedere, S.; Huang, Y.; Breslow, R. Catalytic Oxidations of Steroid Substrates by Artificial Cytochrome P-450 Enzymes. *J. Org. Chem.* **2002**, *67*, 5057−5067. (d) Fang, Z.; Breslow, R. Metal Coordination-Directed Hydroxylation of Steroids with a Novel Artificial P-450 Catalyst. *Org. Lett.* **2006**, *8*, 251−254.

(86) Das, S.; Incarvito, C. D.; Crabtree, R. H.; Brudvig, G. W. Molecular Recognition in the Selective Oxygenation of Saturated C-H bonds by a Dimanganese Catalyst. *Science* **2006**, *312*, 1941−1943. (b) Das, S.; Brudvig, G. W.; Crabtree, R. H. High Turnover Remote Catalytic Oxygenation of Alkyl Groups: How Steric Exclusion of Unbound Substrate Contributes to High Molecular Recognition Selectivity. *J. Am. Chem. Soc.* **2008**, *130*, 1628−1637. (c) Hull, J. F.; Sauer, E. L. O.; Incarvito, C. D.; Faller, J. W.; Brudvig, G. W.; Crabtree, R. H. Manganese Catalysts with Molecular Recognition Functionality for Selective Alkene Epoxidation. *Inorg. Chem.* **2009**, *48*, 488−495.

(87) (a) Gupta, K. C.; Sutar, A. K. Catalytic activities of Schiff base transition metal complexes. *Coord. Chem. Rev.* **2008**, *252*, 1420−1450. (b) McGarrigle, E. M.; Gilheany, D. G. Chromium− and Manganese−salen Promoted Epoxidation of Alkenes. *Chem. Rev.* **2005**, *105*, 1563−1602. (c) Venkataramanan, N. S.; Kuppuraj, G.; Rajagopal, S. Metal−salen complexes as efficient catalysts for the oxygenation of heteroatom containing organic compounds−synthetic and mechanistic aspects. *Coord. Chem. Rev.* **2005**, *249*, 1249−1268. (d) Katsuki, T. Catalytic asymmetric oxidations using optically active (salen)manganese(III) complexes as catalysts. *Coord. Chem. Rev.* **1995**, *140*, 189−214.

(88) (a) Larrow, J. F.; Jacobsen, E. N. (*R,R*)-*N,N'*-bis(3,5-Di-*tert*-Butylsalicylidene)-1,2-Cyclohexanediamino Manganese(III) Chloride, A Highly Enantioselective Epoxidation Catalyst. *Org. Synth.* **1998**, *75*, 1−6. (b) Park, J.; Lang, K.; Abboud, K. A.; Hong, S. Self-Assembled Dinuclear Cobalt(II)-Salen Catalyst Through Hydrogen-Bonding and Its Application to Enantioselective Nitro-Aldol (Henry) Reaction. *J. Am. Chem. Soc.* **2008**, *130*, 16484−16485.

(89) Voss, F.; Herdtweck, E.; Bach, T. Hydrogen bond induced enantioselectivity in Mn(salen)-catalysed sulfoxidaton reactions. *Chem. Commun.* **2011**, *47*, 2137−2139.

(90) Reviews: (a) Huang, X.; Groves, J. T. Oxygen Activation and Radical Transformations in Heme Proteins and Metalloporphyrins. *Chem. Rev.* **2018**, *118*, 2491−2553. (b) Baglia, R. A.; Zaragoza, J. P. T.; Goldberg, D. P. Biomimetic Reactivity of Oxygen-Derived Manganese and Iron Porphyrinoid Complexes. *Chem. Rev.* **2017**, *117*, 13320−13352. (c) Senge, M. O. Stirring the porphyrin alphabet soup − functionalization reactions of porphyrins. *Chem. Commun.* **2011**, *47*, 1943−1960. (d) Che, C.-M.; Lo, V. K.-Y.; Zhou, C.-Y.; Huang, J.-S. Selective functionalisation of saturated C−H bonds with metalloporphyrin catalysts. *Chem. Soc. Rev.* **2011**, *40*, 1950−1975. (e) Costas, M. Selective C−H oxidation catalyzed by metalloporphyrins. *Coord. Chem. Rev.* **2011**, *255*, 2912−2932.

(91) Frost, J. R.; Huber, S. M.; Breitenlechner, S.; Bannwarth, C.; Bach, T. Enantiotopos-Selective C−H Oxygenation Catalyzed by a Supramolecular Ruthenium Complex. *Angew. Chem., Int. Ed.* **2014**, *54*, 691−695.

(92) Chang, C. K.; Ebina, F. NIH Shift in Haemin−Iodosylbenzene-mediated Hydroxylations. *J. Chem. Soc., Chem. Commun.* **1981**, *15*, 778−779.

(93) Burg, F.; Gicquel, M.; Breitenlechner, S.; Pöthig, A.; Bach, T. Site- and Enantioselective C−H Oxygenation Catalyzed by a Chiral Manganese Porphyrin Complex with a Remote Binding Site. *Angew. Chem., Int. Ed.* **2018**, *57*, 2953−2957.

(94) Zhong, F.; Pöthig, A.; Bach, T. Synergistic Stereocontrol in the Enantioselective Ruthenium-Catalyzed Sulfoxidation of Spirodithiolane-Indolones. *Chem. - Eur. J.* **2015**, *21*, 10310−10313.

(95) Fackler, P.; Huber, S. M.; Bach, T. Enantio- and Regioselective Epoxidation of Olefinic Double Bonds in Quinolones, Pyridones, and Amides Catalyzed by a Ruthenium Porphyrin Catalyst with a Hydrogen Bonding Site. *J. Am. Chem. Soc.* **2012**, *134*, 12869−12878.

(96) (a) Hamada, T.; Irie, R.; Mihara, J.; Hamachi, K.; Katsuki, T. Highly Enantioselective Benzylic Hydroxylation with Concave Type of (Salen)manganese(III) Complex. *Tetrahedron* **1998**, *54*, 10017−10028. (b) Murahashi, S.-I.; Noji, S.; Komiya, N. Catalytic Enantioselective Oxidation of Alkanes and Alkenes Using (Salen) Manganese Complexes Bearing a Chiral Binaphthyl Strapping Unit. *Adv. Synth. Catal.* **2004**, *346*, 195−198. (c) Srour, H.; Le Maux, P.; Simonneaux, G. Enantioselective Manganese-Porphyrin-Catalyzed Epoxidation and C−H Hydroxylation with Hydrogen Peroxide in Water/Methanol Solutions. *Inorg. Chem.* **2012**, *51*, 5850−5856. (d) Kwong, K. W.; Chen, T.-H.; Luo, W.; Jeddi, H.; Zhang, R. A biomimetic oxidation catalyzed by manganese(III) porphyrins and iodobenzene diacetate: Synthetic and mechanistic investigations. *Inorg. Chim. Acta* **2015**, *430*, 176−183. (e) Milan, M.; Bietti, M.; Costas, M. Highly Enantioselective Oxidation of Nonactivated Aliphatic C−H Bonds with Hydrogen Peroxide Catalyzed by Manganese Complexes. *ACS Cent. Sci.* **2017**, *3*, 196−204. (f) Olivo, G.; Capocasa, G.; Lanzalunga, O.; Di Stefano, S.; Costas, M. Enzyme-like substrate-selectivity in C−H oxidation enabled by recognition. *Chem. Commun.* **2019**, *55*, 917−920.

(97) For Fe-catalyzed C−H oxygenation reactions, see: (a) Groves, J. T.; Viski, P. Asymmetric Hydroxylation by a Chiral Iron Porphyrin. *J. Am. Chem. Soc.* **1989**, *111*, 8537−8538. (b) Groves, J. T.; Viski, P. Asymmetric Hydroxylation, Epoxidation, and Sulfoxidation Catalyzed by Vaulted Binaphthyl Metalloporphyrins. *J. Org. Chem.* **1990**, *55*, 3628−3634. (c) Chen, M. S.; White, M. C. A Predictably Selective

DOI: 10.1021/acs.joc.9b01299
J. Org. Chem. 2019, 84, 8815−8836

Aliphatic C−H Oxidation Reaction for Complex Molecule Synthesis. *Science* **2007**, *318*, 783−787. (d) Gómez, L.; Garcia-Bosch, I.; Company, A.; Benet-Buchholz, J.; Polo, A.; Sala, X.; Ribas, X.; Costas, M. Stereospecific C−H Oxidation with H_2O_2 Catalyzed by a Chemically Robust Site-Isolated Iron Catalyst. *Angew. Chem., Int. Ed.* **2009**, *48*, 5720−5723. (e) Chen, M. S.; White, M. C. Combined Effects on Selectivity in Fe-Catalyzed Methylene Oxidation. *Science* **2010**, *327*, 566−571. (f) Gormisky, P. E.; White, M. C. Catalyst-Controlled Aliphatic C−H Oxidations with a Predictive Model for Site-Selectivity. *J. Am. Chem. Soc.* **2013**, *135*, 14052−14055. (g) Gómez, L.; Canta, M.; Font, D.; Prat, I.; Ribas, X.; Costas, M. Regioselective Oxidation of Nonactivated Alkyl C−H Groups Using Highly Structured Non-Heme Iron Catalysts. *J. Org. Chem.* **2013**, *78*, 1421−1433. (h) Jana, S.; Ghosh, M.; Ambule, M.; Sen Gupta, S. Iron Complex Catalyzed Selective C−H Bond Oxidation with Broad Substrate Scope. *Org. Lett.* **2017**, *19*, 746−749.

(98) (a) Takai, T.; Koike, T.; Nakamura, M.; Kajita, Y.; Yamashita, T.; Taya, N.; Tsukamoto, T.; Watanabe, T.; Murakami, K.; Igari, T.; Kamata, M. Discovery of novel 5,6,7,8-tetrahydro[1,2,4]triazolo[4,3-*a*]pyridine derivatives as γ-secretase modulators. *Bioorg. Med. Chem.* **2016**, *24*, 3192−3206. (b) Susanta, S.; Chandrasekhar, A.; Sanjita, S.; Subramanya, H. Heterocyclic Derivatives as Bromodomain Inhibitors. WO Patent WO 2015/104653, 2015.

(99) For reviews on C−H amination reactions, see: (a) Buendia, J.; Grelier, G.; Dauban, P. Dirhodium(II)-Catalyzed C(sp^3)−H Amination Using Iodine(III) Oxidants. *Adv. Organomet. Chem.* **2015**, *64*, 77−118. (b) Roizen, J. L.; Harvey, M. E.; Du Bois, J. Metal-Catalyzed Nitrogen-Atom Transfer Methods for the Oxidation of Aliphatic C−H Bonds. *Acc. Chem. Res.* **2012**, *45*, 911−922. (c) Collet, F.; Lescot, C.; Dauban, P. Catalytic C−H amination: the stereoselectivity issue. *Chem. Soc. Rev.* **2011**, *40*, 1926−1936. (d) Müller, P.; Fruit, C. Enantioselective Catalytic Aziridinations and Asymmetric Nitrene Insertion into CH bonds. *Chem. Rev.* **2003**, *103*, 2905−2919.

(100) For a comprehensive overview of different type of alkaloid natural products, see: (a) Kobayashi, J.; Kubota, T. The *Daphniphyllum* alkaloids. *Nat. Prod. Rep.* **2009**, *26*, 936−962. (b) Jessen, H. J.; Gademann, K. 4-Hydroxy-2-pyridone alkaloids: Structures and synthetic approaches. *Nat. Prod. Rep.* **2010**, *27*, 1168−1185. (c) Pilli, R. A.; Rosso, G. B.; Ferreira de Oliveira, M. C. The chemistry of *Stemona* alkaloids: An update. *Nat. Prod. Rep.* **2010**, *27*, 1908−1937. (d) Eckermann, R.; Gaich, T. The Akuammiline Alkaloids; Origin and Synthesis. *Synthesis* **2013**, *45*, 2813−2823. (e) Welch, T. R.; Williams, R. M. Epidithiodioxopiperazines. occurrence, synthesis and biogenesis. *Nat. Prod. Rep.* **2014**, *31*, 1376−1404. (f) Ishikura, M.; Abe, T.; Choshi, T.; Hibino, S. Simple indole alkaloids and those with a non-rearranged monoterpenoid unit. *Nat. Prod. Rep.* **2015**, *32*, 1389−1471. (g) Jin, Z. Muscarine, imidazole, oxazole and thiazole alkaloids. *Nat. Prod. Rep.* **2016**, *33*, 1268−1317.

(101) Vitaku, E.; Smith, D. T.; Njardarson, J. T. Analysis of the Structural Diversity, Substitution Patterns, and Frequency of Nitrogen Hetereocycles among U.S. FDA Approved Pharmaceuticals. *J. Med. Chem.* **2014**, *57*, 10257−10274.

(102) (a) Breslow, S.; Gellman, S. H. Tosylamidation of Cyclohexane by a Cytochrome P-450 Model. *J. Chem. Soc., Chem. Commun.* **1982**, 1400−1401. (b) Breslow, R.; Gellman, S. H. Intramolecular Nitrene C−H Insertions Mediated by Transition-Metal Complexes as Nitrogen Analogs of Cytochrome P-450 Reactions. *J. Am. Chem. Soc.* **1983**, *105*, 6728−6729. (c) Mahy, J. P.; Bedi, G.; Battioni, P.; Mansuy, D. Allylic amination of alkenes by tosyliminoiodobenzene: manganese porphyrins as suitable catalysts. *Tetrahedron Lett.* **1988**, *29*, 1927−1930.

(103) (a) Zhou, X.-G.; Yu, X.-Q.; Huang, J.-S.; Che, C.-M. Asymmetric amidation of saturated C−H bonds catalysed by chiral ruthenium and manganese porphyrins. *Chem. Commun.* **1999**, 2377−2378. (b) Yu, X.-Q.; Huang, J.-S.; Zhou, X.-G.; Che, C.-M. Amidation of Saturated C-H Bonds Catalyzed by Electron-Deficient Ruthenium and Mangaese Porphyrins. A Hightly Catalytic Nitrogen Atom Transfer Process. *Org. Lett.* **2000**, *2*, 2233−2236. (c) Liang, J.-L.; Huang, J.-S.; Yu, X.-Q.; Zhu, N.; Che, C.-M. Metalloporphyrin-Mediated Asymmetric Nitrogen-Atom Trasnfer to Hydrocarbons: Aziridination of Alkenes and Amidation of Saturated C-H Bonds Catalyzed by Chiral Ruthenium Manganese Porphyrins. *Chem. - Eur. J.* **2002**, *8*, 1563−1572.

(104) (a) Espino, C. G.; Du Bois, J. A Rh-Catalyzed C−H Insertion Reaction for the Oxidative Conversion of Carbamates to Oxazolidinones. *Angew. Chem., Int. Ed.* **2001**, *40*, 598−600. (b) Espino, C. G.; Wehn, P. M.; Chow, J.; Du Bois, J. Synthesis of 1,3-Difunctionalized Amine Derivatives through Selective C-H Bond Oxidation. *J. Am. Chem. Soc.* **2001**, *123*, 6935−6936. (c) Fiori, K. W.; Fleming, J. J.; Du Bois, J. Rh-Catalyzed Amination of Ethereal C^{α}−H Bonds: A Versatile Strategy for the Synthesis of Complex Amines. *Angew. Chem., Int. Ed.* **2004**, *43*, 4349−4352.

(105) (a) Wehn, P. M.; Du Bois, J. Enantioselective Synthesis of the Bromopyrrole Alkaloids Manzacidin A and C by Stereospecific C−H Bond Oxidation. *J. Am. Chem. Soc.* **2002**, *124*, 12950−12951. (b) Hinman, A.; Du Bois, J. A Stereoselective Synthesis of (−)-Tetrodotoxin. *J. Am. Chem. Soc.* **2003**, *125*, 11510−11511.

(106) (a) Roizen, J. L.; Zalatan, D. N.; Du Bois, J. Selective Intermolecular Amination of C−H Bonds at Tertiary Carbon Centers. *Angew. Chem., Int. Ed.* **2013**, *52*, 11343−11346. (b) Zalatan, D. N.; Du Bois, J. Understand the Differential Performance of $Rh_2(esp)_2$ as a Catalyst for C−H Amination. *J. Am. Chem. Soc.* **2009**, *131*, 7558−7559. (c) Fiori, K. W.; Du Bois, J. Calatytic Intermolecular Amination of C−H Bonds: Method Development and Mechanistic Insights. *J. Am. Chem. Soc.* **2007**, *129*, 562−568. (d) Espino, C. G.; Fiori, K. W.; Kim, M.; Du Bois, J. Expanding the Scope of C−H Amination through Catalyst Design. *J. Am. Chem. Soc.* **2004**, *126*, 15378−15379.

(107) Nörder, A.; Warren, S. A.; Herdtweck, E.; Huber, S. M.; Bach, T. Diastereotopos-Differentiation in the Rh-Catalyzed Amination of Benzylic Methylene Groups in α-Position to a Stereogenic Center. *J. Am. Chem. Soc.* **2012**, *134*, 13524−13531.

(108) Höke, T.; Herdtweck, E.; Bach, T. Hydrogen-bond mediated regio- and enantioselectivity in a C−H amination reaction catalysed by a supramolecular Rh(II) complex. *Chem. Commun.* **2013**, *49*, 8009−8011.

(109) Voss, F.; Vogt, F.; Herdtweck, E.; Bach, T. Synthesis of Catalytically Active Ruthenium Complexes with a Remote Chiral Lactam as Hydrogen-Bonding Motif. *Synthesis* **2011**, *2011*, 961−971.

(110) For a recent study, see: Berndt, J.-P.; Radchenko, Y.; Becker, J.; Logemann, C.; Bhandari, D. R.; Hrdina, R.; Schreiner, P. R. Site-selective nitrenoid insertions utilizing postfunctionalized bifunctional rhodium(II) catalysts. *Chem. Sci.* **2019**, *10*, 3324−3329.

(111) Guthikonda, K.; Du Bois, J. A Unique and Highly Efficient Method for Catalytic Olefin Aziridination. *J. Am. Chem. Soc.* **2002**, *124*, 13672−13673.

(112) Zhong, F.; Bach, T. Enantioselective Construction of 2,3-Dihydrofuro[2,3-*b*]quinolines through Supramolecular Hydrogen Bonding Interactions. *Chem. - Eur. J.* **2014**, *20*, 13522−13526.

(113) (a) Dale, J. A.; Mosher, H. S. Nuclear Magnetic Resonance Enantiomer Reagents. Configurational Correlations *via* Nuclear Magnetic Resonance Chemical Shifts of Diastereomeric Mandelate, *O*-Methylmandelarate and α-Methoxy-α-trifluoromethylphenylacetate (MTPA) Esters. *J. Am. Chem. Soc.* **1973**, *95*, 512−519. (b) Hoye, T. R.; Jeffrey, C. S.; Shao, F. Mosher ester analysis for the determination of absolute configuration of stereogenic (chiral) carbinol carbons. *Nat. Protoc.* **2007**, *2*, 2451−2458.

DOI: 10.1021/acs.joc.9b01299
J. Org. Chem. 2019, 84, 8815−8836

Enantioselective oxygenation of exocyclic methylene groups by a manganese porphyrin catalyst with a chiral recognition site

Title: "Enantioselective oxygenation of exocyclic methylene groups by a manganese porphyrin catalyst with a chiral recognition site"

Status: Edge Article, published online January 14, 2020

Journal: *Chemical Science* **2020**, *11*, 2121-2129.

Publisher: Royal Society of Chemistry

DOI: 10.1039/C9SC06089H

Authors: Finn Burg, Stefan Breitenlechner, Christian Jandl and Thorsten Bach

Content: The main objective of the underlying study involved a follow-up approach on our seminal work on enantioselective hydroxylation reactions. Despite the previous, unprecedented advances in enantioselectivity, the major drawback was its limited utility, which was connected to the designated structure of the engaged substrates. Accordingly, it was sought to expand the scope to a series of more flexible substrates, without suffering from reduced enantioselectivity. Besides its general utility (27 examples, up to 99% ee), it was demonstrated how hydrogen bonding can be used as a compelling tool to guide the reactive site to a position, which is most likely inaccessible by commonly employed oxygenation catalysts.

F. Burg planned and executed all experiments and wrote the manuscript together with T. Bach. S. Breitenlechner helped with the kinetic studies and proof reading of the manuscript. C. Jandl conducted all SC XRD-measurements and managed the processing of the respective data. All work was performed under the supervision of T. Bach.

Chemical Science

ROYAL SOCIETY OF CHEMISTRY

EDGE ARTICLE

View Article Online
View Journal | View Issue

Check for updates

Cite this: *Chem. Sci.*, 2020, **11**, 2121

All publication charges for this article have been paid for by the Royal Society of Chemistry

Received 2nd December 2019
Accepted 13th January 2020

DOI: 10.1039/c9sc06089h

rsc.li/chemical-science

Enantioselective oxygenation of exocyclic methylene groups by a manganese porphyrin catalyst with a chiral recognition site†

Finn Burg, Stefan Breitenlechner, Christian Jandl and Thorsten Bach *

The natural enzyme cytochrome P450 is widely recognised for its unique ability to catalyse highly selective oxygen insertion reactions into unactivated C–H bonds under mild conditions. Its exceptional potential for organic synthesis served as an inspiration for the presented biomimetic hydroxylation approach. *Via* a remote hydrogen bonding motif a high enantioselectivity in the manganese-catalysed oxygenation of quinolone analogues (27 examples, 18–64% yield, 80–99% ee) was achieved. The site-selectivity was completely altered in favour of a less reactive but more accessible position.

Introduction

The direct functionalisation of carbon hydrogen (C–H) bonds unambiguously belongs to the most coveted transformations in modern organic synthesis.[1] The C–H bond activation of sp^3 carbon centres presents a significant challenge due to the inert nature of hydrocarbons and due to the desired distinction between the various aliphatic C–H bonds embodied in organic molecules.[2] In this context, the hydroxylation of prochiral methylene compounds poses an additional conundrum, as the corresponding secondary alcohol should ideally be formed as a single enantiomer without subjecting the newly generated stereogenic centre to an additional oxidation step.[3,4] Inspired by the remarkable efficiency of enzymatic oxygenations catalysed by cytochrome P450,[5] there are numerous examples of transition metal complexes, containing salen,[6,7] porphyrin,[8,9] and aminopyridine ligands[10,11] which have been employed in the oxygenation of C–H bonds. Since in many cases the chirality is transferred by a bulky ligand, it is perhaps not surprising that such a sterically demanding environment can be repulsive thus resulting in an insufficient conversion. Unlike its natural occurring congeners, these systems lack a favourable substrate–catalyst orientation which in turn facilitates an enantioselective approach to the substrate while maintaining a high turnover.

In recent years, it has been realised that the quest for enantio- and site-selective oxygenation reactions at remote positions (remote functionalisation) can be successfully tackled by catalysts with a non-covalent recognition element.[12] After seminal work by Breslow and co-workers on selective oxidation and oxygenation reactions,[13] notable contributions have been made among others by the groups of Groves,[14] Crabtree,[15] and Costas.[16] An early example that demonstrated how recognition elements can control selectivity in epoxidation reactions was reported by the group of Breslow (Fig. 1a).[13b] They used a manganese salen complex, that was functionalised by a chelating dipyridine moiety inviting coordination of other metals. In a competing experiment of a nicotinyl- and a benzoyl-substituted olefin, a very high selectivity (>20 : 1) was achieved

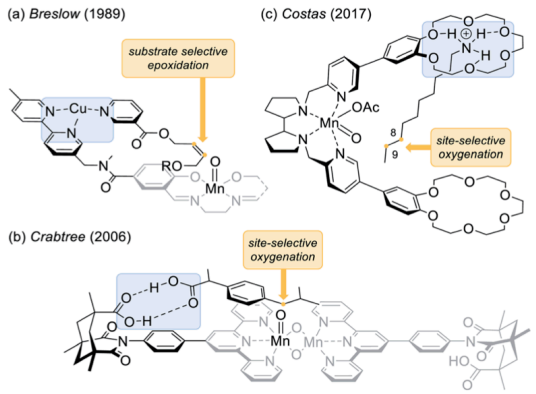

Fig. 1 Controlling selectivity in oxidation and oxygenation reactions *via* supramolecular recognition. (a) Substrate selective epoxidation of nicotinic acid derivatives controlled by complexation of copper ions. (b) Site-selective oxygenation of ibuprofen mediated by two-point hydrogen bonding between two carboxylic acids. (c) Site-selective oxygenation of ^{n}decylamine directed by a 18-crown-6 functional group.

Department Chemie, Catalysis Research Center (CRC), Technische Universität München, 85747 Garching, Germany. E-mail: thorsten.bach@ch.tum.de; Fax: +49 89 28913315; Tel: +49 89 28913330

† Electronic supplementary information (ESI) available: Synthetic procedures and full characterisation for all starting materials and products (**2–10**), spectroscopic data, NMR spectra, kinetic studies, *etc.* CCDC 1967795. For ESI and crystallographic data in CIF or other electronic format see DOI: 10.1039/c9sc06089h

for the epoxidation of the former derivative in the presence of Cu^{2+} ions indicating that pre-coordination *via* complexation of the pyridine residues enhanced the reaction.

A contribution by Crabtree[15a] and co-workers (Fig. 1b) made intentional use of hydrogen bonds as an operative tool to control selectivity in oxygenation reactions. In this specific case, a di-μ-oxo dimanganese centre is flanked by two terpyridine ligands, which in turn are connected to a molecular recognition unit derived from Kemp's triacid.[17,18] The presented site-selective oxygenation of ibuprofen can thus be rationalised by a two-point hydrogen bonding between the two carboxylic acids. In a more recent example, the group of Costas employed a manganese aminopyridine ligand that was functionalised with two 18-crown-6 ether units (Fig. 1c).[16b] The remote crown ether effectively anchors the ^{n}decylamine at the terminal ammonium ion whereupon a selective oxygenation at carbon atoms C-8 and C-9 is induced.

Although it was beyond the intended scope of the above-mentioned catalysts to differentiate between enantiotopic hydrogen atoms, there have been several reports in which hydrogen bonding was invoked as the key element to induce enantioselectivity in catalysis.[19,20] However, examples remain scarce in which both the site- and the enantioselectivity of oxygenation reactions were successfully addressed.[21] In recent years, our group has designed and synthesised bifunctional ligands with which a catalytically active metal centre is tailored to a chiral lactam[22] recognition unit. Originally conceived for applications in photochemistry the concept of two-point hydrogen bonding[23] has successfully been applied to enantioselective olefin addition[24] and C–H functionalisation[25] reactions. As a recent supplement to this type of catalysts we prepared the chiral manganese porphyrin complex **1**[25c] for an application to enantioselective oxygenation reactions (Fig. 2, left).

In the present study we report a general bioinspired approach towards the site- and enantioselective oxygenation of a vast array of 3-benzyl and 3-alkyl substituted quinolones displaying an exocyclic methylene group (Fig. 2, right). Despite the free rotation around the quinolone–methylene bond C–H oxygenations occurred with high enantioselectivities (up to 99% ee). Some of the quinolone substrates were also probed in a racemic oxygenation reaction using manganese(III)-5,10,15,20-tetrakis(pentafluorophenyl)porphyrin chloride (Mn[TPFPP]Cl), whereupon the conversion decreased drastically, suggesting that the non-covalent hydrogen bonding interactions have also a rate accelerating effect. Most importantly, in the case of a second reactive benzylic position, the site-selectivity of the racemic reaction was reverted compared to the hydrogen bond-mediated system. This observation indicates that hydrogen bonds direct the oxygenation event to a previously inaccessible carbon centre, while the intrinsically more reactive position remains intact.

Results and discussion

Our work commenced with an investigation into the enantioselective oxygenation of the literature-known 3-(4′-methylbenzyl)quinolone (**2a**)[25a] under our previously optimised reaction conditions (Scheme 1, $t = 16$ h).[25c] We were delighted to observe that the enantiomeric excess in the exocyclic oxygenation was exceptionally high (95% ee) when employing 2.0 mol% of porphyrin **1** and iodosobenzene as a stoichiometric oxidant. The reaction delivered the desired alcohol **3a**, which was accompanied by ketone **4a**, the product of over-oxidation. It was quickly realised, though, that the catalytic activity decreased significantly before even less than half of the starting material **2a** was consumed. The alcohol to ketone ratio (**3a**/**4a** = 70/30) after 4 h was relatively low compared to the ratio we had observed in related studies and accordingly we sought for ways to improve the mass balance while concomitantly increasing the catalytic turnover.

One promising approach that caught our attention was to use an excess of the lactam **2a** relative to the oxidant. In this instance, an even lower catalyst loading of 1.0 mol% was sufficient to generate a significantly higher alcohol concentration (Fig. 3), and simultaneously the alcohol to ketone ratio improved notably (**3a**/**4a** = 80/20).

We continued with our optimisation using the oxidant iodosobenzene as the limiting reagent in a dichloromethane solution and varied the amount of quinolone **2a** applied (Table 1, entries 1 and 2). With 2.0 equivalents, the alcohol to ketone ratio deteriorated (**3a**/**4a** = 76/24) and it seemed warranted to keep the concentration of the substrate – which was readily available on gram scale – high. An increase or decrease of the substrate concentration c led to a lower enantioselectivity (entries 3 and 4), while a higher catalyst loading turned out to be

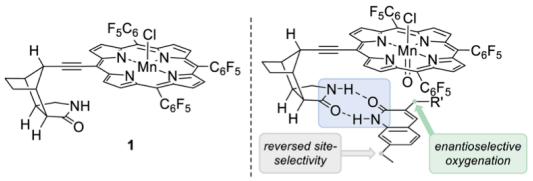

Fig. 2 Structure of the manganese porphyrin complex **1** exhibiting a chiral lactam recognition unit (left). Proposed transition state for the oxygenation of exocyclic methylene groups in quinolone analogues where hydrogen bonding effectively induces enantioface differentiation (right).

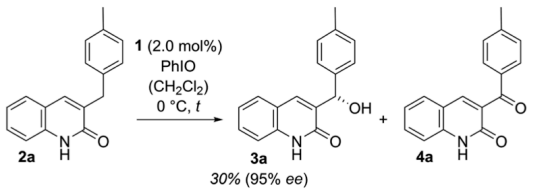

Scheme 1 Enantioselective oxygenation of 3-(4′-methylbenzyl)quinolone (**2a**) to alcohol **3a** and ketone **4a** catalysed by the chiral manganese porphyrin **1** under previously reported conditions (initial experiment, see also Fig. 3 and the narrative).[25c]

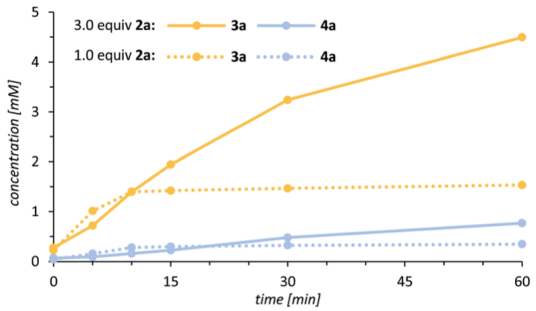

Fig. 3 Rate profile for the oxygenation of 3-(4′-methylbenzyl)quinolone (**2a**) to alcohol **3a** (yellow) and ketone **4a** (blue) catalysed by 1.0 mol% of the chiral manganese porphyrin complex **1** [0 °C, CH_2Cl_2, solid line = 3.0 equiv. of **2a**, 1.0 equiv. PhIO (c = 10 mM); dashed line = 1.0 equiv. of **2a** (c = 10 mM), 2.0 equiv. PhIO].

Table 1 Optimisation of the enantioselective oxygenation of 3-(4′-methylbenzyl)-quinolone (**2a**) catalysed by the chiral manganese porphyrin complex **1** (DCE = 1,2-dichloroethane)

Entry[a]	c[b] [mM]	**1** [mol%]	Solvent	**3a**[c] [%]	% ee[d]	**4a**[c] [%]
1	30	1.0	CH_2Cl_2	48	91	11
2[e]	20	1.0	CH_2Cl_2	42	93	13
3	20	1.0	CH_2Cl_2	39	86	11
4	60	1.0	CH_2Cl_2	50	87	12
5	30	2.0	CH_2Cl_2	48	91	10
6[f]	30	1.0	PhH	30	85	3
7	30	1.0	DCE	42	88	12
8[g]	30	1.0	CH_2Cl_2	45	85	12
9[h]	30	1.0	CH_2Cl_2	52	93	17
10[h]	30	0.5	CH_2Cl_2	37	—[i]	10
11[h]	30	1.5	CH_2Cl_2	56	95	18

[a] All reactions were run with 3.0 equiv. of **2a** (180 μmol) under the indicated conditions (0 °C, t = 4 h) and were initiated by addition of the oxidant PhIO (1.0 equiv.) to a pre-cooled solution of **2a** and **1** in the given solvent. [b] Concentration of quinolone **2a** in the solution. [c] All yields were determined by GLC-FID analysis using ^{n}dodecane as a stoichiometric internal standard. [d] Enantiomeric excess (% ee) as determined by HPLC analysis on a chiral stationary phase. [e] 2.0 equiv. of **2a** were employed. [f] The reaction was performed at 23 °C. [g] The reaction time was 16 h. [h] PhIO was added in three portions. [i] Not determined.

almost inconsequential for the outcome of the reaction (entry 5). Neither a solvent variation (entries 6 and 7) nor prolonged reaction times (entry 8) were found to be beneficial to conversion and enantioselectivity. A slightly higher yield of alcohol **3a** was achieved by a portion-wise addition of the oxidant (entry 9). Under these conditions a final variation of the catalyst loading (entries 10 and 11) was performed from which eventually a catalyst loading of 1.5 mol% turned out to be ideal (entry 11).

Under optimised conditions the enantiomerically enriched alcohol **3a** was isolated in 60% yield and with an enantiomeric excess of 96% ee (Table 2). Since a clean separation from both the starting material **2a** and the ketone **4a** was feasible the yield based on recovered starting material **2a** could be readily

Table 2 Scope of the enantioselective oxygenation of 3-benzylquinolone derivatives **2** catalysed by the chiral manganese porphyrin catalyst **1**

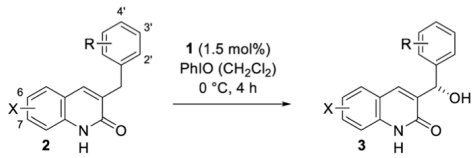

Entry[a]	**2**	X	R	**3**[b] [%]	% ee[c]
1	**2a**	H	4′-Me	60 (80)	96
2	**2b**	H	3′-Me	58 (82)	99
3	**2c**	H	2′-Me	64 (92)	97
4	**2d**	H	3′,4′-Me_2	59 (68)	92
5	**2e**	H	H	61 (84)	95
6	**2f**	H	4′-OMe	53 (74)	93
7	**2g**	H	4′-F	53 (60)	91
8	**2h**	H	4′-Cl	18 (62)	98
9	**2i**	H	3′-CF_3	26 (54)	92
10	**2j**	6-Me	4′-Me	60 (71)	98
11	**2k**	7-Me	4′-Me	53 (65)	96

[a] All reactions were conducted at a iodosobenzene concentration of 10 mM in dichloromethane employing 1.0 equiv. of PhIO (60 μmol), 3.0 equiv. of **2** (180 μmol) and 1.5 mol% of **1** (0.9 μmol). [b] All yields refer to isolated material. Yields in brackets are based on reisolated starting material **2**. [c] Enantiomeric excess (% ee) as determined by HPLC analysis on a chiral stationary phase.

determined (80%). We were interested in studying the electronic and steric effects of the benzyl substituent and accordingly prepared a series of various 3-benzylquinolones **2** which were consequentially subjected to the enantioselective oxygenation protocol. The yields in Table 2 refer to isolated material but are based on the oxidant as the limiting reagent. The yields based on substrate conversion were determined by clean reisolation of the starting material **2** and are given in brackets.

Altering the position of the methyl group to a *meta*- or *ortho*-substitution gave similar results in terms of yield (58% **3b**, 64% **3c**) and the enantiomeric excess for the corresponding alcohols **3b** and **3c** remained exceptionally high (99% ee and 97% ee). The 3′,4′-dimethylbenzyl substituted quinolone **2d** reacted almost analogously (59%), but the enantiomeric excess decreased slightly to 92% ee. The transformation of unsubstituted 3-benzylquinolone (**2e**) delivered the oxygenated product **3e** in a yield of 61% with 95% ee. An electron donating substituent (MeO) in the *para* position of the aromatic ring (**3f**, 53% yield, 93% ee) was tolerated as was an inductively electron withdrawing substituent (**3g**, 53% yield, 91% ee). Indeed, the outcome of the oxygenation seemed consistent upon variation of functional groups on the benzyl ring. A deviation was observed when 3-(4′-chlorobenzyl)quinolone (**2h**) was taken into the reaction and resulted in a low yield of only 18% (62% based on recovered starting material). While the enantioselectivity remained outstanding (98% ee), the lower conversion was attributed to the poor solubility of substrate **2h** in dichloromethane. Substrate **2i** with the strongly electron withdrawing *m*-

(trifluoromethyl)aryl substituent gave rise to the corresponding alcohol **3i** in a yield of 26% (54% based on recovered starting material) and an enantiomeric excess of 92% ee. Finally, substituents on the quinolone core were introduced into the substrates and the 6- and 7-methyl-substituted quinolones **2j** and **2k** were probed in the oxygenation event. Both substrates gave a clean conversion to the corresponding alcohols **3j** and **3k** in satisfactory yields (60% and 53%) and with remarkable enantioselectivity (98% ee and 96% ee).

In order to establish the absolute configuration of the oxygenated products, the enantiomerically enriched alcohol **3h** was subjected to a chemoselective *N*-methylation using potassium carbonate and methyl iodide in *N*,*N*-dimethylformamide (DMF) whereupon compound **5** was obtained in almost quantitative yield (Scheme 2). Colorless crystals were obtained by slow evaporation from dichloromethane which were suited for X-ray crystallographic analysis and the absolute configuration as determined by anomalous diffraction was in agreement with the proposed transition state (Fig. 2, right).

Apart from the high enantioselectivity, a most notable feature of the oxygenation reaction was its exquisite site-selectivity. When promoted by achiral Mn(TPFPP)Cl as the catalyst (2.0 mol%), substrates exhibiting a methylene group in 4′-position of the benzyl substituent [R = 4′-ethyl (**2l**); 4′-isopropyl (**2m**)] underwent a sluggish but site-selective (r.r. = regioisomeric ratio) oxygenation (Scheme 3) to the remote alcohols *rac*-**2n** (27%) and **2o** (20%). In stark contrast, catalyst **1** (1.5 mol%) guided the oxygenation reaction almost exclusively to the benzylic carbon atom adjacent to the quinolone core whereupon the oxygenated products **3l** (57%) and **3m** (50%) were obtained with excellent enantioselectivity (93% ee and 91% ee). The reversal of site-selectivity supports a pre-coordination of quinolone substrates **2** to the catalyst which in turn leads to a defined exposure of a single C–H towards the active oxomanganese[26] complex. Accordingly, non-covalent hydrogen bonding completely alters the site of the oxygenation reaction to a position that seems inaccessible by conventional oxygenation methods.

The scope of the reaction was substantially expanded by varying the size and nature of the quinolone substituent in position C-3. A brief screening of reaction conditions based on the previously developed protocol indicated that even simple 3-alkylsubstituted quinolones underwent the desired transformation (Table 3) and that an aryl group was not necessary to

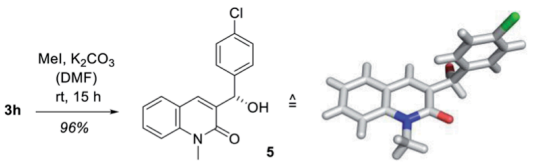

Scheme 2 Synthesis of the *N*-methylated alcohol **5** derived from 3-(4′-chlorobenzyl)-quinolone (**3h**) by chemoselective methylation and its crystal structure. The absolute configuration was determined by anomalous X-ray diffraction.

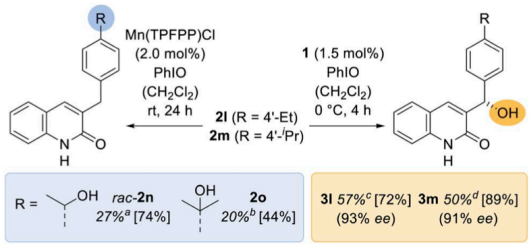

Scheme 3 Enantioselective and racemic oxygenation of quinolones **2l** and **2m** bearing an additional reactive methylene site. The racemic reaction was promoted by Mn(TPFPP)Cl (left) and the enantioselective reaction by the chiral manganese porphyrin complex **1** (right). Yields in square brackets are based on recovered starting material **2** ([a]r.r. = 93/7, [b]r.r. = 82/18, [c]r.r. = 94/6, [d]r.r. = 97/3).

activate the prostereogenic methylene group. A slightly higher catalyst loading of 2.0 mol% was required to transform 3-ethylquinolone (**6a**) into its oxygenated analogue **7a** in 56% yield and with an outstanding enantiomeric excess of 95% ee. The specific rotation of product **7a** was compared with literature data,[24a] allowing an assignment of its absolute configuration. It was interesting to see, that the formation of the corresponding ketone **8a** was less prominent (**7a**/**8a** = 88/12) than for the benzylic substrate **2a**, resulting in a high yield of 90% based on recovered starting material. Encouraged by these results, a more extensive set of 3-alkylsubstituted quinolones was prepared and

Table 3 Scope of the enantioselective oxygenation of 3-alkylquinolones **6** to alcohol **7** and ketone **8** catalysed by the chiral manganese porphyrin catalyst **1**

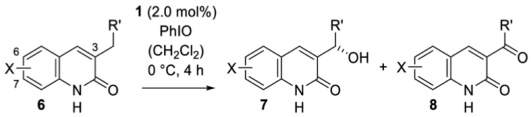

Entry[a]	6	X	R′	7[b] [%]	% ee[c]
1	**6a**	H	Me	56 (90)	95
2	**6b**	H	Et	53 (84)	88
3	**6c**	H	^{n}Pr	50 (68)	86
4	**6d**	H	^{i}Bu	48 (96)	88
5	**6e**	H	^{i}Pr	48 (89)	80
6	**6f**	6-Me	Me	51 (93)	94
7	**6g**	7-Me	Me	58 (94)	96
8	**6h**	6,7-Me$_2$	Me	51 (94)	95
9	**6i**	6-OMe	Me	21 (38)	96
10	**6j**	7-OMe	Me	62 (73)	95
11	**6k**	7-Cl	Me	34 (95)	95
12	**6l**	7-F	Me	42 (84)	96

[a] All reactions were conducted at a iodosobenzene concentration of 10 mM in dichloromethane employing 1.0 equiv. of PhIO (60 μmol), 3.0 equiv. of **6** (180 μmol) and 2.0 mol% of **1** (1.2 μmol). [b] All yields refer to isolated material. Yields in brackets are based on reisolated starting material **6**. [c] Enantiomeric excess (% ee) as determined by HPLC analysis on a chiral stationary phase.

the effect of quinolone substitution (variation of X) was examined. Upon elongation of the alkyl chain the yield remained constant [R′ = Et (53%), ^{n}Pr (50%), ^{i}Bu (48%)], but a minor decrease in enantioselectivity was observed [**7b** (88% ee), **7c** (86% ee) **7d** (88% ee)]. This effect became even more evident when a tertiary carbon atom was installed adjacent to the oxygenation site (entry 5). The oxygenated product **7e**, derived from 3-isobutylquinolone (**6e**), was obtained in 48% yield, but only with 80% ee.

When simple methyl substituents were implemented into the aromatic quinolone core the yield of isolated product remained constant for both the C-6 and the C-7 position [X = 6-Me (51%), 7-Me (58%), 6,7-Me_2 (51%)] and the enantiomeric excess was continuously high [**7f** (94% ee), **7g** (96% ee) **7h** (95% ee)]. An electron donating methoxy substituent at the C-6 carbon atom led to a diminished yield (21%), but high enantioselectivity (96% ee) possibly due to oxidative degradation of the electron rich aryl core. The same functional group was less disruptive at the deconjugated 7-position and alcohol **7j** was obtained in 62% yield and with an enantiomeric excess of 95% ee. Electron deficient quinolones seem to be slightly less reactive [X = 7-Cl (34%), 7-F (42%)]. Nevertheless, both substrates gave rise to the desired alcohols **7k** and **7l** in again exceptional enantiomeric excess (95% ee and 96% ee).

Given the high conformational flexibility of a simple 3-ethylquinolone (**6a**), it might be surprising that hydrogen bonding can provide sufficient enantioface differentiation between the two pro-stereogenic hydrogen atoms. Rotation around the indicated single bond (Scheme 4) leads to a change of topicity even if an approach of the oxygenation reagent was guided by hydrogen bonding to occur from the back face of the quinolone. It appears as if the active manganese species behaves like a catalytically active cleft similar to the active site of a natural enzyme. It reserves only a very limited reactive domain around the oxomanganese porphyrin in which an oxygenation can occur by a rebound mechanism.[27] As previously established for the epoxidation of 3-alkenylquinolone by a chiral ruthenium complex,[24b] the trajectory of the active site to the substrate requires a perfect adjustment of the rotatable single bond. In our specific case, only the *pro*-(*S*) hydrogen atom is properly positioned to engage in oxygenation while potential transition states for the *pro*-(*R*) hydrogen atom are too high in energy to be significantly populated. Based on the proposed model (Fig. 2, right), 3-ethylquinolone in its s-*trans* conformation is aligned in a way that the oxygenation event proceeds with high selectivity at the *pro*-(*S*) hydrogen atom.

Although their outstanding stereoselectivity belongs to the most admired features of enzymatic reactions, the site-selectivity is often considered as its most useful catalytic property. As previously alluded to, molecular recognition devices cannot only help to induce enantioselectivity, but also provide a powerful tool to differentiate between two potentially reactive sites in a remote functionalization approach. This aspect was further exemplified when 3,7-diethylquinolone (**6m**) and (3′-phenylpropyl)quinolone (**6o**) were subjected to the oxygenation protocol (Scheme 5). The racemic oxygenation proceeded exclusively adjacent to the phenyl ring whereupon *rac*-**6n** (20%) and *rac*-**6p** (21%) were obtained as single regioisomers. The oxygenation site was however relocated, when the manganese porphyrin complex **1** was employed. The oxygenated product **7m** was isolated in 60% yield with almost perfect enantioselectivity (98% ee). The presented site-selective oxygenation even withstands a proximal more reactive benzylic position. (3′-Phenylpropyl)quinolone (**6o**) was converted into the corresponding alcohol **7o** with reverted site-selectivity but with a slightly reduced enantioselectivity (84% ee).

To support the hypothesis that hydrogen bonding is responsible for both the chirality transfer and for the enhanced reactivity a control experiment was performed. One hydrogen bonding site of substrate **6a** was blocked by *N*-methylation to provide quinolone **9**. When compound **9** was probed in the catalytic reaction (Scheme 6) under otherwise identical conditions its oxygenated product **10** was obtained in racemic form and a notably lower yield of 22%.

Further mechanistic work was devoted to study the over-oxidation of the enantiomerically enriched alcohol to its corresponding ketone and to elucidate the fate of the catalyst in the course of the reaction. Although a relatively high alcohol to ketone ratio clearly indicated that the enantioselectivity arises from a C–H activation step, we envisioned that detailed kinetic

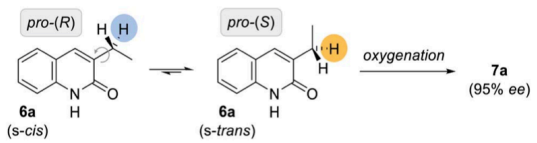

Scheme 4 Rotation around the C–C bond between the exocyclic methylene group and the quinolone carbon skeleton. Based on the proposed model, the s-*trans* isomer is favoured in the coordinated transition state whereupon the (*S*)-configured alcohol **7a** is delivered in high enantiomeric excess.

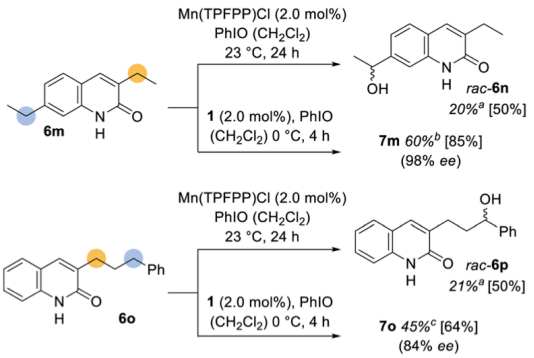

Scheme 5 Enantioselective and racemic oxygenation of 3,7-diethylquinolone (**6m**) and 3-(3′-phenylpropyl)quinolone (**6o**) using the chiral manganese porphyrin complex **1** and Mn(TPFPP)Cl, respectively. Yields in square brackets are based on recovered starting material **6** (^{a}single regioisomer, ^{b}r.r. = 88/12, ^{c}r.r. = 72/28).

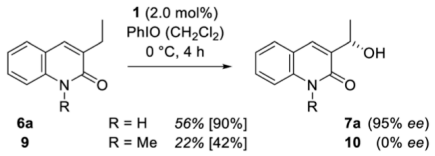

Scheme 6 Oxygenation of **6a** and the *N*-methylated congener **9** to alcohol **7a** and **10** catalysed by manganese porphyrin **1**.

studies will provide a more comprehensive mechanistic picture of the over-oxidation step. The racemic alcohol *rac*-**3a** was subjected to the oxygenation reaction (1.0 mol% **1**, 1.0 equiv. PhIO) and the formation of the ketone **4a** as well as the enantiomeric excess of the remaining starting material **3a** were closely monitored over time (Scheme 7). The rate profile derived from the experimental data indicated that after a conversion of 59% the remaining starting material **3a** was enantiomerically enriched by 71% ee (Fig. 4).

The *s*-factor[28] k_R/k_S = 6.1 calculated from these data confirmed that a kinetic resolution *via* an over-oxidation step does not contribute significantly to the enantiomeric excess.[29] Under optimised standard conditions (Table 1, entry 11) only 18% of ketone **4a** were formed but 56% of alcohol **3a** (95% ee). It is interesting to note, though, that the residual alcohol has the same absolute configuration as the alcohol derived from the C–H oxygenation step. Indeed, upon coordination of *ent*-**3a** to catalyst **1**, the remaining hydrogen atom at the former methylene group is directly exposed towards the catalytically active metal centre thus favouring an additional oxidation step *via* hydrogen abstraction.

Although all experimental data were coherent, it remained uncertain what exactly caused the rapid decrease of the catalytic activity if the quinolone substrate was used as a limiting reagent (Fig. 3). Based on detailed rate profiles, we assumed that the catalytic activity might be affected by one of the oxygenation products. To verify this hypothesis, a kinetic inhibition experiment was performed, which at the same time was supposed to shine light on the robustness of the catalyst. Quinolone **2a** was subjected towards the enantioselective oxygenation employing 1.0 mol% of the chiral catalyst **1** with 2.0 equivalents of the oxidant PhIO and the documented rate profile was used as a reference for further experiments. After 30 min 22% of the starting material **2a** had been converted into 16% of the alcohol

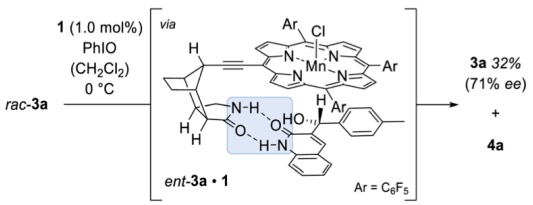

Scheme 7 Kinetic resolution of *rac*-**3a** catalysed by the chiral manganese porphyrin **1**.

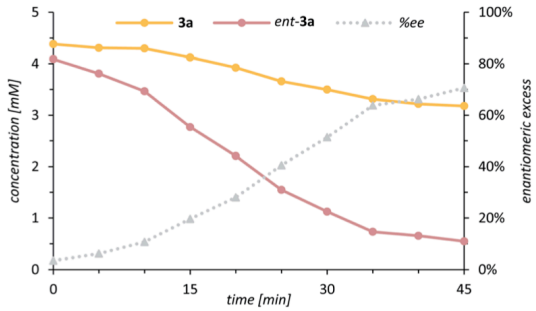

Fig. 4 Rate profile of the two enantiomers **3a** (yellow) and *ent*-**3a** (pink) in the kinetic resolution of *rac*-**3a** to ketone **4a** and enantiomeric excess (grey, dashed line) of the remaining enantiomer **3a**.

3a and 5% of the ketone **4a** (Fig. 5, solid lines). Within the next 90 min the concentration of all reactants remained almost constant (<5% conversion) clearly indicating that the catalytic activity had decreased drastically. A second oxygenation experiment was set up, in which the concentration of all reactants strictly followed the "same excess" approach.[30] Specifically, a reaction mixture containing the exact stoichiometry of all reactants **2a**, **3a** and **4a** after 60 min of the previous experiment was treated with 1.0 mol% of catalyst **1** and eventually the oxidant PhIO was added to the pre-cooled reaction mixture. The oxygenation reaction was expected to remain idle and no further conversion of the starting material **2a** should occur if the catalytic system was inhibited either by alcohol **3a** or by ketone **4a**. Upon addition of the oxidant to the premixed reaction solution, however, the oxygenation was initiated and 15% of **2a** were converted into 10% of alcohol **3a** and 7% of ketone **4a** within the next hour (Fig. 5, dashed lines).

In fact, the experiment demonstrated, that there is no inhibition by neither of the products **3a** or **4a** suggesting that after 30 min the catalyst is eventually modified resulting in a significantly diminished activity. This observation was further

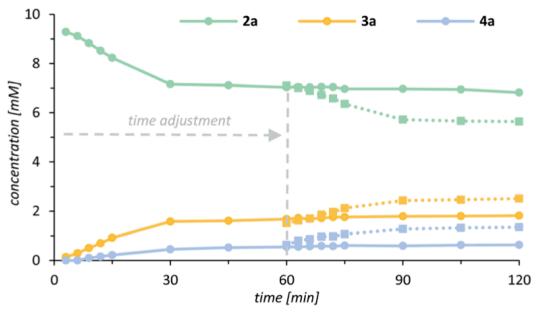

Fig. 5 Rate profile for the enantioselective oxygenation of **2a** (green) to alcohol **3a** (yellow) and ketone **4a** (blue) catalysed by the chiral manganese porphyrin complex **1** (solid lines). Overlay of the rate profile for the kinetic inhibition experiment following the "same excess" protocol[30] with a time adjustment of 60 min (dashed lines).

corroborated by a third experiment, which was set up as usual with 1.0 equivalent of the quinolone substrate and 1.0 mol% of the catalyst **1**. The reaction was initiated by addition of the oxidant (2.0 equiv.) and – as expected – ceased after 30 min at a conversion of 24%. Upon addition of a second portion of the catalyst **1** (1.0 mol% after 60 min) the reaction was resumed and another 19% of **2a** were converted into 11% of the alcohol **3a** and 8% of the ketone **4a** conclusively matching the rate profile of the "same excess" experiment. It should be noted that the reaction was only relaunched by addition of catalyst, while addition of another portion iodosobenzene turned out to be inconsequential.

With respect to all rate profiles (see the ESI† for a complete set of data), it is conspicuous that the rapid decrease in catalytic activity correlated to the iodosobenzene concentration. At high concentration, with the quinolone as the limiting reagent, the manganese catalyst quickly lost its activity resulting in retarded conversion of the substrate to the alcohol **2a** → **3a** and of the alcohol to the ketone **3a** → **4a** (Fig. 3). In other words, the reaction slowed down but continued to show the typical rate profile of a consecutive reaction in which the alcohol is an intermediate *en route* to the ketone. The alcohol to ketone ratio **3a**/**4a** decreased over time, irrespective of catalyst and oxidant concentration. For example, after prolonged reaction times the ratio **3a**/**4a** after 1 h under the conditions of Scheme 1 (2.0 mol% **1**, 1.0 equiv. of **2a**, 2.0 equiv. PhIO) was 76/24 while it decreased to 38/62 after 24 h. In stark contrast, at a low iodosobenzene concentration with an excess of quinolone, the activity of the catalyst remained high until almost the entire iodosobenzene was consumed. The reaction is terminated due to the lack of oxidant before larger amounts of ketone can be formed. Along these lines, it is inevitable to keep the concentration of the quinolone substrate **2a** high, if elevated turnover numbers (TONs) and reasonable yields for alcohol **3a** are prioritized over the amount of **2a** applied. Reducing the concentration of the oxidant to a minimum by portion-wise addition prevents catalyst degradation and can increase the lifetime of the catalyst. Under optimized reaction conditions, high TONs and excellent yields based on recovered starting material (up to 96%) were observed, while the enantioselectivity was maintained (up to 99% ee).

Conclusion

In summary, we have established that a manganese porphyrin complex linked to a chiral recognition site effectively catalyses a highly selective oxygen insertion into a variety of aliphatic and benzylic exocyclic methylene groups. A lactam recognition motif was employed which limits the scope of substrates to compounds with a matching hydrogen bonding site. In the present study, a comprehensive set of 3-substituted quinolones (27 examples, up to 64% yield) was successfully oxygenated adjacent to the 3-position of the heterocyclic carbon skeleton with outstanding site- and enantioselectivity (up to 99% ee). Catalyst **1** operates under the influence of two-point hydrogen bonding, whereupon the substrate is precisely oriented in a way that allows for no other than the *pro*-(*S*) hydrogen atom to be attacked. Kinetic experiments revealed that employing the oxidant as the limiting reagent can significantly increase the number of catalytic turnovers and improve the alcohol to ketone ratio thus providing excellent yields based on recovered starting material.

Conflicts of interest

There are no conflicts to declare.

Acknowledgements

Financial support by the Deutsche Forschungsgemeinschaft (grant Ba 1372-17) is gratefully acknowledged. O. Ackermann and J. Kudermann are acknowledged for their help with HPLC and GLC analysis. We thank M. Stierle for synthetic assistance.

Notes and references

1 For reviews on C–H activation, see: (*a*) P. Gandeepan, T. Müller, D. Zell, G. Cera, S. Warratz and L. Ackermann, *Chem. Rev.*, 2019, **119**, 2192–2452; (*b*) C. G. Newton, S.-G. Wang, C. C. Oliveira and N. Cramer, *Chem. Rev.*, 2017, **117**, 8908–8976; (*c*) J. F. Hartwig and M. A. Larsen, *ACS Cent. Sci.*, 2016, **2**, 281–292; (*d*) H. M. L. Davies and D. Morton, *J. Org. Chem.*, 2016, **81**, 343–350; (*e*) J. Wencel-Delord, T. Dröge, F. Liu and F. Glorius, *Chem. Soc. Rev.*, 2011, **40**, 4740–4761; (*f*) L. McMurray, F. O'Hara and M. J. Gaunt, *Chem. Soc. Rev.*, 2011, **40**, 1885–1898; (*g*) K. Godula and D. Sames, *Science*, 2006, **312**, 67–72; (*h*) G. Dyker, *Handbook of C–H transformations: applications in organic synthesis*, Wiley-VCH, 2005; (*i*) J. A. Labinger and J. E. Bercaw, *Nature*, 2002, **417**, 507–514.

2 For reviews on site-selective C–H functionalization, see: (*a*) F. D. Toste, M. S. Sigman and S. J. Miller, *Acc. Chem. Res.*, 2017, **50**, 609–615; (*b*) L. Ping, D. S. Chung, J. Bouffard and S.-g. Lee, *Chem. Soc. Rev.*, 2017, **46**, 4299–4328; (*c*) S. R. Neufeldt and M. S. Sanford, *Acc. Chem. Res.*, 2012, **45**, 936–946; (*d*) T. Brückl, R. D. Baxter, Y. Ishihara and P. S. Baran, *Acc. Chem. Res.*, 2012, **45**, 826–839; (*e*) W. R. Gutekunst and P. S. Baran, *Chem. Soc. Rev.*, 2011, **40**, 1976–1991.

3 For reviews on the C–H oxygenation reactions, see: (*a*) G. B. Shul'pin, *Catalysts*, 2016, **6**, 50; (*b*) E. P. Talsi and K. P. Bryliakov, *Coord. Chem. Rev.*, 2012, **256**, 1418–1434; (*c*) T. Newhouse and P. S. Baran, *Angew. Chem., Int. Ed.*, 2011, **50**, 3362–3374; (*d*) R. Curci, L. D'Accolti and C. Fusco, *Acc. Chem. Res.*, 2006, **39**, 1–9; (*e*) L. Que and W. B. Tolman, *Nature*, 2008, **455**, 333–340; (*f*) M. Costas, M. P. Mehn, M. P. Jensen and L. Que, *Chem. Rev.*, 2004, **104**, 939–986.

4 For a recent example on a selective benzylic mono-oxygenation, see: L. Tanwar, J. Börgel and T. Ritter, *J. Am. Chem. Soc.*, 2019, **141**, 17983–17988.

5 For reviews on cytochrome P450 and bioengineered congeners, see: (*a*) T. L. Poulos, *Chem. Rev.*, 2014, **114**, 3919–3962; (*b*) R. Fasan, *ACS Catal.*, 2012, **2**, 647–666; (*c*) J. C. Lewis, P. S. Coelho and F. H. Arnold, *Chem. Soc. Rev.*,

2011, **40**, 2003–2021; (*d*) P. R. Ortiz de Montellano, *Chem. Rev.*, 2010, **110**, 932–948; (*e*) P. R. Ortiz de Montellano, *Cytochrome P450: structure, mechanism, and biochemistry*, Springer Science & Business Media, 2005.

6 For reviews on metal–salen complexes, see: (*a*) K. C. Gupta and A. K. Sutar, *Coord. Chem. Rev.*, 2008, **252**, 1420–1450; (*b*) N. S. Venkataramanan, G. Kuppuraj and S. Rajagopal, *Coord. Chem. Rev.*, 2005, **249**, 1249–1268; (*c*) T. Katsuki, *Coord. Chem. Rev.*, 1995, **140**, 189–214.

7 Selected examples: (*a*) K. Hamachi, R. Irie and T. Katsuki, *Tetrahedron Lett.*, 1996, **37**, 4979–4982; (*b*) T. Hamada, R. Irie, J. Mihara, K. Hamachi and T. Katsuki, *Tetrahedron*, 1998, **54**, 10017–10028; (*c*) S.-I. Murahashi, S. Noji and N. Komiya, *Adv. Synth. Catal.*, 2004, **346**, 195–198.

8 For reviews on metalloporphyrins, see: (*a*) H. Lu and X. P. Zhang, *Chem. Soc. Rev.*, 2011, **40**, 1899–1909; (*b*) M. Costas, *Coord. Chem. Rev.*, 2011, **255**, 2912–2932; (*c*) C.-M. Che, V. K.-Y. Lo, C.-Y. Zhou and J.-S. Huang, *Chem. Soc. Rev.*, 2011, **40**, 1950–1975; (*d*) M. Senge, *Chem. Commun.*, 2011, **47**, 1943–1960.

9 Selected examples: (*a*) J. T. Groves and P. Viski, *J. Am. Chem. Soc.*, 1989, **111**, 8537–8538; (*b*) J. T. Groves and P. Viski, *J. Org. Chem.*, 1990, **55**, 3628–3634; (*c*) R. Zhang, W.-Y. Yu, T.-S. Lai and C.-M. Che, *Chem. Commun.*, 1999, 1791–1792; (*d*) Z. Gross and S. Ini, *Org. Lett.*, 1999, **1**, 2077–2080; (*e*) R. Zhang, W.-Y. Yu and C.-M. Che, *Tetrahedron: Asymmetry*, 2005, **16**, 3520–3526; (*f*) H. Srour, P. L. Maux and G. Simonneaux, *Inorg. Chem.*, 2012, **51**, 5850–5856.

10 For a recent overview of iron aminopyridine complexes, see: G. Olivo, O. Cussó and M. Costas, *Chem.–Asian J.*, 2016, **11**, 3148–3158.

11 Selected examples: (*a*) M. S. Chen and M. C. White, *Science*, 2007, **318**, 783–787; (*b*) P. E. Gormisky and M. C. White, *J. Am. Chem. Soc.*, 2013, **135**, 14052–14055; (*c*) M. Milan, M. Bietti and M. Costas, *ACS Cent. Sci.*, 2017, **3**, 196–204; (*d*) B. Qiu, D. Xu, Q. Sun, C. Miao, Y.-M. Lee, X.-X. Li, W. Nam and W. Sun, *ACS Catal.*, 2018, **8**, 2479–2487; (*e*) M. C. White and J. Zhao, *J. Am. Chem. Soc.*, 2018, **140**, 13988–14009; (*f*) R. V. Ottenbacher, E. P. Talsi, T. V. Rybalova and K. P. Bryliakov, *ChemCatChem*, 2018, **10**, 5323–5330; (*g*) J. Zhao, T. Nanjo, E. C. de Lucca and M. C. White, *Nat. Chem.*, 2019, **11**, 213–221; (*h*) B. Qiu, D. Xu, Q. Sun, J. Lin and W. Sun, *Org. Lett.*, 2019, **21**, 618–622.

12 For reviews on catalysis based on non-covalent interactions, see: (*a*) H. J. Davis and R. J. Phipps, *Chem. Sci.*, 2017, **8**, 864–877; (*b*) A. J. Neel, M. J. Hilton, M. S. Sigman and F. D. Toste, *Nature*, 2017, **543**, 637–646; (*c*) M. Raynal, P. Ballester, A. Vidal-Ferran and P. W. N. M. van Leeuwen, *Chem. Soc. Rev.*, 2014, **43**, 1660–1733; (*d*) P. Dydio and J. N. H. Reek, *Chem. Sci.*, 2014, **5**, 2135–2145; (*e*) S. Carboni, C. Gennari, L. Pignataro and U. Piarulli, *Dalton Trans.*, 2011, **40**, 4355–4373; (*f*) E. Lindbäck, S. Dawaigher and K. Wärnmark, *Chem.–Eur. J.*, 2014, **20**, 13432–13481; (*g*) S. Das, G. W. Brudvig and R. H. Crabtree, *Chem. Commun.*, 2008, 413–424.

13 (*a*) R. Breslow, *Acc. Chem. Res.*, 1980, **13**, 170–177; (*b*) R. Breslow, A. B. Brown, R. D. McCullough and P. W. White, *J. Am. Chem. Soc.*, 1989, **111**, 4517–4518; (*c*) R. Breslow, X. Zhang, R. Xu, M. Maletic and R. Merger, *J. Am. Chem. Soc.*, 1996, **118**, 11678–11679.

14 (*a*) J. T. Groves and R. Neumann, *J. Am. Chem. Soc.*, 1987, **109**, 5045–5047; (*b*) J. T. Groves and R. Neumann, *J. Org. Chem.*, 1988, **53**, 3891–3893; (*c*) J. T. Groves and R. Neumann, *J. Am. Chem. Soc.*, 1989, **111**, 2900–2909.

15 (*a*) S. Das, C. D. Incarvito, R. H. Crabtree and G. W. Brudvig, *Science*, 2006, **312**, 1941–1943; (*b*) S. Das, G. W. Brudvig and R. H. Crabtree, *J. Am. Chem. Soc.*, 2008, **130**, 1628–1637.

16 (*a*) D. Font, M. Canta, M. Milan, O. Cussó, X. Ribas, R. J. M. Klein Gebbink and M. Costas, *Angew. Chem., Int. Ed.*, 2016, **55**, 5776–5779; (*b*) G. Olivo, G. Farinelli, A. Barbieri, O. Lanzalunga, S. Di Stefano and M. Costas, *Angew. Chem., Int. Ed.*, 2017, **56**, 16347–16351; (*c*) G. Olivo, G. Capocasa, O. Lanzalunga, S. Di Stefano and M. Costas, *Chem. Commun.*, 2019, **55**, 917–920.

17 D. S. Kemp and K. S. Petrakis, *J. Org. Chem.*, 1981, **46**, 5140–5143.

18 Selected examples on hydrogen bond-mediated molecular recognition induced by a similar structural motif: (*a*) J. Rebek, K. Williams, K. Parris, P. Ballester and K. S. Jeong, *Angew. Chem., Int. Ed.*, 1987, **26**, 1244–1245; (*b*) J. Rebek, B. Askew, P. Ballester, C. Buhr, S. Jones, D. Nemeth and K. Williams, *J. Am. Chem. Soc.*, 1987, **109**, 5033–5035; (*c*) K. Williams, B. Askew, P. Ballester, C. Buhr, K. S. Jeong, S. Jones and J. Rebek, *J. Am. Chem. Soc.*, 1989, **111**, 1090–1094; (*d*) R. K. Castellano, V. Gramlich and F. Diederich, *Chem.–Eur. J.*, 2002, **8**, 118–129; (*e*) R. Faraoni, R. K. Castellano, V. Gramlich and F. Diederich, *Chem. Commun.*, 2004, 370–371; (*f*) D. B. Varshney, X. Gao, T. Friščić and L. R. MacGillivray, *Angew. Chem., Int. Ed.*, 2006, **45**, 646–650.

19 For reviews on hydrogen bond-mediated catalysis, see: (*a*) N. R. Mote and S. H. Chikkali, *Chem.–Asian J.*, 2018, **13**, 3623–3646; (*b*) X. Fang and C.-J. Wang, *Chem. Commun.*, 2015, **51**, 1185–1197; (*c*) X. Yu and W. Wang, *Chem.–Asian J.*, 2008, **3**, 516–532; (*d*) A. G. Doyle and E. N. Jacobsen, *Chem. Rev.*, 2007, **107**, 5713–5743; (*e*) M. S. Taylor and E. N. Jacobsen, *Angew. Chem., Int. Ed.*, 2006, **45**, 1520–1543; (*f*) P. R. Schreiner, *Chem. Soc. Rev.*, 2003, **32**, 289–296.

20 For recent examples, see: (*a*) Y. Park and S. Chang, *Nat. Catal.*, 2019, **2**, 219–227; (*b*) J.-P. Berndt, Y. Radchenko, J. Becker, C. Logemann, D. R. Bhandari, R. Hrdina and P. R. Schreiner, *Chem. Sci.*, 2019, **10**, 3324–3329; (*c*) X. Lu, Y. Yoshigoe, H. Ida, M. Nishi, M. Kanai and Y. Kuninobu, *ACS Catal.*, 2019, **9**, 1705–1709; (*d*) S.-T. Bai, V. Sinha, A. M. Kluwer, P. R. Linnebank, Z. Abiri, P. Dydio, M. Lutz, B. de Bruin and J. N. H. Reek, *Chem. Sci.*, 2019, **10**, 7389–7398; (*e*) S. T. Bai, C. B. Bheeter and J. N. H. Reek, *Angew. Chem., Int. Ed.*, 2019, **58**, 13039–13043; (*f*) W. Fang and B. Breit, *Angew. Chem., Int. Ed.*, 2018, **57**, 14817–14821; (*g*) X. Li, C. You, Y. Yang, Y. Yang, P. Li, G. Gu, L. W. Chung, H. Lv and X. Zhang, *Chem. Sci.*, 2018, **9**, 1919–1924; (*h*) H. J. Davis, G. R. Genov and R. J. Phipps, *Angew. Chem.,*

Int. Ed., 2017, **56**, 13351–13355; (*i*) Z. Han, P. Li, Z. Zhang, C. Chen, Q. Wang, X.-Q. Dong and X. Zhang, *ACS Catal.*, 2016, **6**, 6214–6218.

21 For reviews on bioinspired oxygenation, see: (*a*) D. Vidal, G. Olivo and M. Costas, *Chem.–Eur. J.*, 2018, **24**, 5042–5054; (*b*) M. Milan, M. Bietti and M. Costas, *Chem. Commun.*, 2018, **54**, 9559–9570.

22 For seminal work on hydrogen bond-mediated molecular recognition utilizing a related lactam, see: (*a*) D. G. Lonergan, J. Riego and G. Deslongchamps, *Tetrahedron Lett.*, 1996, **37**, 6109–6112; (*b*) D. G. Lonergan, J. Halse and G. Deslongchamps, *Tetrahedron Lett.*, 1998, **39**, 6865–6868; (*c*) D. G. Lonergan and G. Deslongchamps, *Tetrahedron*, 1998, **54**, 14041–14052.

23 For a recent perspective, see: F. Burg and T. Bach, *J. Org. Chem.*, 2019, **84**, 8815–8836.

24 (*a*) P. Fackler, C. Berthold, F. Voss and T. Bach, *J. Am. Chem. Soc.*, 2010, **132**, 15911–15913; (*b*) P. Fackler, S. M. Huber and T. Bach, *J. Am. Chem. Soc.*, 2012, **134**, 12869–12878; (*c*) F. Zhong and T. Bach, *Chem.–Eur. J.*, 2014, **20**, 13522–13526.

25 (*a*) T. Höke, E. Herdtweck and T. Bach, *Chem. Commun.*, 2013, **49**, 8009–8011; (*b*) J. R. Frost, S. M. Huber, S. Breitenlechner, C. Bannwarth and T. Bach, *Angew. Chem., Int. Ed.*, 2015, **54**, 691–695; (*c*) F. Burg, M. Gicquel, S. Breitenlechner, A. Pöthig and T. Bach, *Angew. Chem., Int. Ed.*, 2018, **57**, 2953–2957.

26 For mechanistic studies on the Mn-oxo species, see: (*a*) F. De Angelis, N. Jin, R. Car and J. T. Groves, *Inorg. Chem.*, 2006, **45**, 4268–4276; (*b*) W. J. Song, M. S. Seo, S. DeBeer George, T. Ohta, R. Song, M.-J. Kang, T. Tosha, T. Kitagawa, E. I. Solomon and W. Nam, *J. Am. Chem. Soc.*, 2007, **129**, 1268–1277; (*c*) N. Jin, M. Ibrahim, T. G. Spiro and J. T. Groves, *J. Am. Chem. Soc.*, 2007, **129**, 12416–12417; (*d*) S. Fukuzumi, N. Fujioka, H. Kotani, K. Ohkubo, Y.-M. Lee and W. Nam, *J. Am. Chem. Soc.*, 2009, **131**, 17127–17134; (*e*) X. Wu, M. S. Seo, K. M. Davis, Y.-M. Lee, J. Chen, K.-B. Cho, Y. N. Pushkar and W. Nam, *J. Am. Chem. Soc.*, 2011, **133**, 20088–20091; (*f*) D. F. Leto, R. Ingram, V. W. Day and T. A. Jackson, *Chem. Commun.*, 2013, **49**, 5378–5380; (*g*) M. Guo, M. S. Seo, Y.-M. Lee, S. Fukuzumi and W. Nam, *J. Am. Chem. Soc.*, 2019, **141**, 12187–12191.

27 (*a*) M. Guo, T. Corona, K. Ray and W. Nam, *ACS Cent. Sci.*, 2019, **5**, 13–28; (*b*) X. Huang and J. T. Groves, *Chem. Rev.*, 2018, **118**, 2491–2553; (*c*) X. Huang and J. T. Groves, *J. Biol. Inorg Chem.*, 2017, **22**, 185–207; (*d*) W. Liu, M.-J. Cheng, R. J. Nielsen, W. A. Goddard and J. T. Groves, *ACS Catal.*, 2017, **7**, 4182–4188; (*e*) C. Arunkumar, Y.-M. Lee, J. Y. Lee, S. Fukuzumi and W. Nam, *Chem.–Eur. J.*, 2009, **15**, 11482–11489; (*f*) B. Meunier, S. P. de Visser and S. Shaik, *Chem. Rev.*, 2004, **104**, 3947–3980; (*g*) J. T. Groves and M. Van der Puy, *J. Am. Chem. Soc.*, 1976, **98**, 5290–5297; (*h*) J. T. Groves and G. A. McClusky, *J. Am. Chem. Soc.*, 1976, **98**, 859–861.

28 (*a*) H. Kagan and J. Fiaud, *Topics in Stereochemistry*, John Wiley and Sons, Inc., New York, 1988; (*b*) J. M. Keith, J. F. Larrow and E. N. Jacobsen, *Adv. Synth. Catal.*, 2001, **343**, 5–26.

29 For non-enzymatic examples and reviews on the kinetic resolution of racemic alcohols with high *s*-factors, see: (*a*) B. Tao, J. C. Ruble, D. A. Hoic and G. C. Fu, *J. Am. Chem. Soc.*, 1999, **121**, 5091–5092; (*b*) S. Hashiguchi, A. Fujii, J. Takehara, T. Ikariya and R. Noyori, *J. Am. Chem. Soc.*, 1995, **117**, 7562–7563; (*c*) S. Hashiguchi, A. Fujii, K. J. Haack, K. Matsumura, T. Ikariya and R. Noyori, *Angew. Chem., Int. Ed.*, 1997, **36**, 288–290; (*d*) S. Y. Lee, J. M. Murphy, A. Ukai and G. C. Fu, *J. Am. Chem. Soc.*, 2012, **134**, 15149–15153; (*e*) H. Pellissier, *Adv. Synth. Catal.*, 2011, **353**, 1613–1666; (*f*) C. E. Müller and P. R. Schreiner, *Angew. Chem., Int. Ed.*, 2011, **50**, 6012–6042.

30 (*a*) D. G. Blackmond, *Angew. Chem., Int. Ed.*, 2005, **44**, 4302–4320; (*b*) J. S. Mathew, M. Klussmann, H. Iwamura, F. Valera, A. Futran, E. A. C. Emanuelsson and D. G. Blackmond, *J. Org. Chem.*, 2006, **71**, 4711–4722; (*c*) D. G. Blackmond, *J. Am. Chem. Soc.*, 2015, **137**, 10852–10866.

Summary of the Experimental Work and Reference to Previous Studies

The direct functionalization of prochiral methylene groups to its corresponding enantiomerically enriched secondary alcohols is a fundamental quest in organic synthesis. Inspired by the remarkable potential of the natural enzyme cytochrome P450 to catalyze selective oxygen insertions under mild conditions, numerous efforts were devoted to develop chiral oxygenation catalyst.[86] Although in some hydroxylation reactions a very high enantioselectivity was accomplished (primarily by *Katsuki* and *Murahashi*),[129, 131-132, 138-139] very low substrate turnover or retarded chemoselectivity (*i.e.* predominant overoxidation to the ketone) appeared to be inevitable barriers. Encouraged by our seminal work on hydrogen-bond-mediated photocatalysis,[200] our group started to explore metalloporphyrin complexes for the application in transition-metal-catalyzed reactions.[152, 278-279] The presented Ph.D. work commenced with the synthesis of a chiral manganese porphyrin complex that was decorated with the established chiral hydrogen bonding site. Along these lines, it enables precise orientation of quinolone substrates thus overriding the intrinsic reactivity patterns aswell as inviting excellent enantioface differentiation (Figure 14).

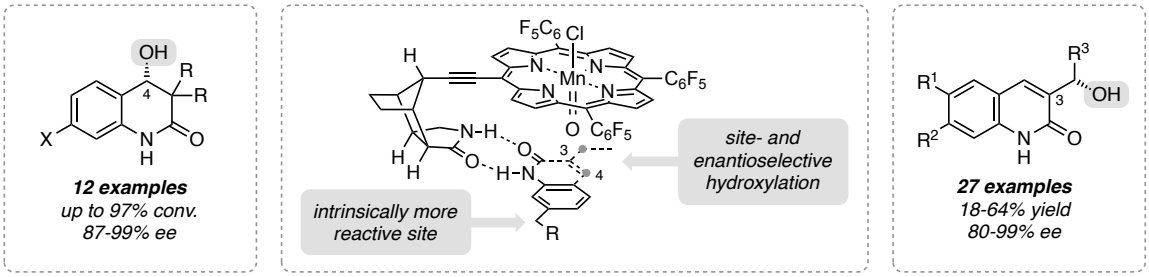

***Figure 14**: Site- and enantioselective hydroxylation of quinolone analogs directed by molecular recognition.*

It should be noted that prior to our first study involving 3,3-disubstituted-dihdyroquinolones (12 examples, 29-97% conversion, 19-68% yield, 87-99% *ee*),[289] there have been no reports on enantioselective hydroxylation reactions (>90% *ee*) that exceed a substrate conversion of 25%. Especially porphyrin complexes have failed to provide satisfactory enantioselectivity (>76% *ee*), as shown in previous studies by *Groves,*[118] *Che*[125] and *Simonneaux*.[127-128] As a final remark, several mechanistic experiments were conducted to support the hypothesis of a classical oxygen rebound mechanism[51] initiated by a C–H abstraction at the incipient methylene site.

Despite the fact that the progress concerning enantioselective hydroxylation reactions was remarkable, the major drawback was that the substrates engaged in this chemistry were limited to a cyclic oxygenation of what appeared to be tailor-made substrates. With this in mind, it seemed desirable to expand the scope to a series of compounds, which represent a higher degree of flexibility. In an elaborate follow-up approach, we investigated the exocyclic hydroxylation of simple 3-substituted quinolones.[290] To our delight, the hydroxylation continued to proceed in outstanding enantioselectivity (27 examples, 18-64% yield, 80-99% *ee*), even for a small ethyl substituent at the C-3 position of the quinolone (R^3 = Me). Unfortunately, the major caveat was that the substrate had to be added in excess relative to the oxidant (3.0 equivalents), in order to provide a high TON. Nevertheless, the unreacted starting material was re-isolated in an almost quantitative mass balance and only minor amounts of the overoxidized ketone were generated.

Apart from the high enantioselectivity, the perhaps most fascinating feature of the performed hydroxylation was its extraordinary site-selectivity. Some quinolone substrates exhibit a second benzylic methylene group, which exposes an additional reactive site (such as R^2 = Et, R^3 = 4-ethylphenyl or R^3 = $–CH_2CH_2Ph$). Similar to the observations made within *Breslow's* cyclodextrin studies,[218, 220-221, 232] when a non-directing fluorinated porphyrin complex was used for racemic reactions, a sluggish but site-selective reaction at the other reactive site occurred. The chiral manganese porphyrin complex, however, was able to guide the hydroxylation to its initial site while maintaining high enantioselectivity. In stark contrast, complementary work by *Crabtree,*[263] *Costas*[242] and *Higuchi*,[265] already showed a preferred selectivity in the non-directed reaction, which was merely further improved. Remarkably, the presented work serves a compelling demonstration how hydrogen bonds direct the oxygenation event from an intrinsically more reactive site to a previously inactive site, which to the best of our knowledges has not been reported previously.

Zusammenfassung und Eingliederung in den Literaturkontext

Die direkte Funktionalisierung von prochiralen Methylengruppen zu den entsprechenden enantiomerenangereicherten sekundären Alkoholen ist eine fundamentale Aufgabe der organischen Synthese. Inspiriert durch das bemerkenswerte Potenzial des in der Natur vorkommenden Enzyms Cytochrom P450 selektive Sauerstoffinsertionen unter milden Bedingungen zu katalysieren, wurden zahlreiche Versuche unternommen, um chirale Oxygenierungskatalysatoren zu entwickeln.[86] Obwohl in einigen Hydroxylierungsreaktionen eine hohe Enantioselektivität erreicht werden konnte (primär von *Katsuki* und *Murahashi*),[129, 131-132, 138-139] schien es, als wären der sehr niedrige Substratumsatz sowie die gestörte Chemoselektivität (d.h. dominierende Überoxidation zum Keton), unüberwindbare Barrieren. Ermutigt durch unsere bahnbrechenden Ergebnisse in Wasserstoffbrückenvermittelter Photokatalyse,[200] begann unsere Gruppe Metalloporphyrinkomplexe für die Anwendung in übergangsmetallkatalysierten Reaktionen zu erforschen.[152, 278-279] Die vorliegende Doktorarbeit begann mit der Synthese eines chiralen Manganporphyrinkomplexes, welcher mit dem etablierten chiralen Wasserstoffbrückenbindungsmotiv verziert wurde. In diesem Sinne ermöglichte er die präzise Orientierung von Chinolonanaloga, wodurch intrinsische Reaktionsmuster überwunden und eine exzellente Unterscheidung enantiotoper Halbräume ermöglicht wurde (Abbildung 14).

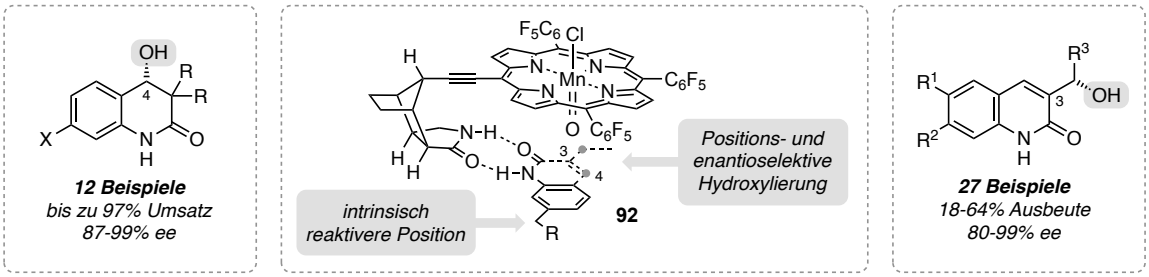

***Abbildung 15**: Positions- und enantioselektive Hydroxylierung von Chinolonanaloga durch molekulare Erkennung.*

Es sollte bemerkt werden, dass vor unserer ersten Studie, in der 3,3-disubstiuierten Dihydrochinolone involviert waren (12 Beispiele, 19-97% Umsatz, 19-68% Ausbeute, 87-99% *ee*),[289] keine Berichte zu enantioselektiven Hydroxylierungsreaktionen vorlagen, die einen Substratumsatz von 25% überstiegen. Insbesondere Porphyrinkomplexe scheiterten eine hohe Enantioselektivität zu überliefern (>76% *ee*), wie in vorherigen Studien von *Groves,*[118] *Che*[125] und *Simonneaux* gezeigt wurde.[127-128] Zuletzt wurden mehrere mechanistische Experimente durchgeführt, die die Hypothese eines klassischen *oxygen rebound* Mechanismus[51] unterstützen, welcher durch eine C–H Abstraktion an der vorherigen Methylposition initiiert wird.

Obgleich der Fortschritt bezüglich enantioselektiver Hydroxylierungsreaktionen beachtlich war, war es ein entscheidender Nachteil, dass die Substratklasse, die in diese Chemie verwickelt war, auf eine zyklische Oxygenierung an maßgeschneiderten Substraten limitiert zu sein schien. In Anbetracht dessen schien es wünschenswert, die Substratbreite zu einer Reihe von Verbindungen zu erweitern, die eine höhere Flexibilität aufweisen. In einem aufwändigen Nachfolgeansatz haben wir die exozyklische Hydroxylierung einfacher 3-substituierter Chinolone untersucht.[290] Die Hydroxylierung verlief weiterhin in herausragender Enantioselektivität (27 Beispiele, 18-64% Ausbeute, 80-99% *ee*), sogar für einen kleinen Ethylsubstituenten an der C-3 Position des Chinolons (R^3 = Me). Leider war der große Nachteil, dass die Substrate im Überschuss relativ zum Oxidationsmittel zugesetzt werden mussten (3.0 Äquivalente), um eine hohe Umsatzzahl (TON) zu erreichen. Nichtsdestotrotz konnte das Edukt in fast quantitativer Massenbilanz reisoliert werden und es wurden nur kleine Mengen des überoxidierten Ketons generiert.

Abgesehen von der hohen Enantioselektivität, war das möglicherweise faszinierendste Merkmal der durchgeführten Hydroxylierung die außergewöhnliche Positionsselektivität. Einige Chiniolonsubstrate besitzen eine zusätzliche benzylische Methyleneinheit, die eine weitere reaktive Position darlegt (z.B. R^2 = Et, R^3 = 4-Ethylphenyl oder R^3 = $–CH_2CH_2Ph$). Ähnlich zu den Beobachtungen die bei *Breslows* Cyclodextrin Studien gemacht wurden,[218, 220-221, 232] wenn ein nicht-dirigierender fluorierter Porphyrinkomplex für racemische Reaktionen verwendet wurde, fand eine träge, aber positions-selektive Reaktion an der zweiten Position statt. Der chirale Porphyrinkomplex war allerdings in der Lage die Hydroxylierung zu ihrer ursprünglichen Position zurückzuführen und gleichzeitig die hohe Enantioselektivität aufrechtzuerhalten. Im Gegensatz zu den ergänzenden Arbeiten von *Crabtree,*[263]*Costas*[242] und *Higuchi*,[265] zeigte sich dort bereits eine bevorzugte Selektivität im nicht dirigierten Ansatz, welche lediglich weiter verbessert wurde. Erstaunlicherweise dient die präsentierte Arbeit als eine überzeugende Demonstration, wie Wasserstoffbrückenbindungen das Oxygenierungsereignis von einer intrinsisch reaktiveren Stelle zu einer zuvor inaktiven Position führen, worüber nach unserem besten Wissen vorher noch nicht berichtet wurde.

Abbreviations

Ac	acetyl
Ar	aryl
Bn	benzyl
Boc	tert-butyloxycarbonyl
Bu	butyl
Bz	benzoyl
CD	cyclodextrin
cf.	*confer/conferatur* (compare)
conv.	conversion
CPCA	cyclopropanecarboxylic acid
DCE	dichloroethane
DMBA	2,2-dimethylbutyric acid
e.g.	*exampli gratia* (for example)
ee	enantiomeric excess
equiv.	equivalents
Et	ethyl
FG	functional group
HAT	hydrogen atom transfer
i.e.	*id est* (that is)
Im	imidazole
i	iso
L	ligand
M	metal
Me	methyl
Mes	mesityl (2,4,6-trimethylphenyl)
NADPH	nicotinamide adenine dinucleotide phosphate
OKR	oxidative kinetic resolution
Ph	phenyl
PP	diphosphate
Pr	propyl
py	pyridine
R	residue (typically further clarified in a given scheme)
RG	recognition group
r.r.	regioisomeric ratio
t	tert
TBAO	tetrabutylammonium oxone
Tf	trifluoromethanesulfonyl
TFE	trifluoroethanol
TBDPS	*tert*-butyldiphenylsilyl
TIBS	triisobutyl

TIPS	triisopropyl
TON	turn over number
TPP	tetraphenylporphine
TPFPP	tetrakis(pentafluorophenyl)-porphyrin
TS	taxadiene synthase

Licences

JOHN WILEY AND SONS LICENSE
TERMS AND CONDITIONS

May 03, 2020

This Agreement between Kurfürstenplatz 1a ("You") and John Wiley and Sons ("John Wiley and Sons") consists of your license details and the terms and conditions provided by John Wiley and Sons and Copyright Clearance Center.

License Number	4821380461391
License date	May 03, 2020
Licensed Content Publisher	John Wiley and Sons
Licensed Content Publication	Angewandte Chemie International Edition
Licensed Content Title	Site− and Enantioselective C−H Oxygenation Catalyzed by a Chiral Manganese Porphyrin Complex with a Remote Binding Site
Licensed Content Author	Thorsten Bach, Alexander Pöthig, Stefan Breitenlechner, et al
Licensed Content Date	Feb 9, 2018
Licensed Content Volume	57
Licensed Content Issue	11
Licensed Content Pages	5

Type of use	Dissertation/Thesis
Requestor type	Author of this Wiley article
Format	Print and electronic
Portion	Full article
Will you be translating?	No
Title	Bioinspired Site- and Enantioselective Hydroxylation Reactions Enabled by Molecular Recognition
Institution name	Technical University Munich
Expected presentation date	Jul 2020
Requestor Location	Kurfürstenplatz 1a Kurfuerstenplatz 1a Munich, 80796 Germany Attn: Kurfürstenplatz 1a
Publisher Tax ID	EU826007151
Total	0.00 EUR
Terms and Conditions	

TERMS AND CONDITIONS

This copyrighted material is owned by or exclusively licensed to John Wiley & Sons, Inc. or one of its group companies (each a"Wiley Company") or handled on behalf of a society with which a Wiley Company has exclusive publishing rights in relation to a particular work (collectively "WILEY"). By clicking "accept" in connection with completing this licensing transaction, you agree that the following terms and conditions apply to this transaction

shall not assert any such right, license or interest with respect thereto

- NEITHER WILEY NOR ITS LICENSORS MAKES ANY WARRANTY OR REPRESENTATION OF ANY KIND TO YOU OR ANY THIRD PARTY, EXPRESS, IMPLIED OR STATUTORY, WITH RESPECT TO THE MATERIALS OR THE ACCURACY OF ANY INFORMATION CONTAINED IN THE MATERIALS, INCLUDING, WITHOUT LIMITATION, ANY IMPLIED WARRANTY OF MERCHANTABILITY, ACCURACY, SATISFACTORY QUALITY, FITNESS FOR A PARTICULAR PURPOSE, USABILITY, INTEGRATION OR NON-INFRINGEMENT AND ALL SUCH WARRANTIES ARE HEREBY EXCLUDED BY WILEY AND ITS LICENSORS AND WAIVED BY YOU.

- WILEY shall have the right to terminate this Agreement immediately upon breach of this Agreement by you.

- You shall indemnify, defend and hold harmless WILEY, its Licensors and their respective directors, officers, agents and employees, from and against any actual or threatened claims, demands, causes of action or proceedings arising from any breach of this Agreement by you.

- IN NO EVENT SHALL WILEY OR ITS LICENSORS BE LIABLE TO YOU OR ANY OTHER PARTY OR ANY OTHER PERSON OR ENTITY FOR ANY SPECIAL, CONSEQUENTIAL, INCIDENTAL, INDIRECT, EXEMPLARY OR PUNITIVE DAMAGES, HOWEVER CAUSED, ARISING OUT OF OR IN CONNECTION WITH THE DOWNLOADING, PROVISIONING, VIEWING OR USE OF THE MATERIALS REGARDLESS OF THE FORM OF ACTION, WHETHER FOR BREACH OF CONTRACT, BREACH OF WARRANTY, TORT, NEGLIGENCE, INFRINGEMENT OR OTHERWISE (INCLUDING, WITHOUT LIMITATION, DAMAGES BASED ON LOSS OF PROFITS, DATA, FILES, USE, BUSINESS OPPORTUNITY OR CLAIMS OF THIRD PARTIES), AND WHETHER OR NOT THE PARTY HAS BEEN ADVISED OF THE POSSIBILITY OF SUCH DAMAGES. THIS LIMITATION SHALL APPLY NOTWITHSTANDING ANY FAILURE OF ESSENTIAL PURPOSE OF ANY LIMITED REMEDY PROVIDED HEREIN.

- Should any provision of this Agreement be held by a court of competent jurisdiction to be illegal, invalid, or unenforceable, that provision shall be deemed amended to achieve as nearly as possible the same economic effect as the original provision, and the legality, validity and enforceability of the remaining provisions of this Agreement shall not be affected or impaired thereby.

- The failure of either party to enforce any term or condition of this Agreement shall not constitute a waiver of either party's right to enforce each and every term and condition of this Agreement. No breach under this agreement shall be deemed waived or excused by either party unless such waiver or consent is in writing signed by the party granting such waiver or consent. The waiver by or consent of a party to a breach of any provision of this Agreement shall not operate or be construed as a waiver of or consent to any other or subsequent breach by such other party.

- This Agreement may not be assigned (including by operation of law or otherwise) by

References

1. F. W. A. Sertürner, *Trommsdorff's Journal der Pharmazie* **1806**, *14*, 47-93.

2. W. E. Gerabek, B. D. Haage, G. Keil, W. Wegner, *Enzyklopädie Medizingeschichte*, 1st ed., de Gruyter: Berlin, 2007.

3. J. M. Gulland, R. Robinson, *Mem. Proc. Manchester Lit. Phil. Soc.* **1925**, *69*, 79-86.

4. M. Gates, G. Tschudi, *J. Am. Chem. Soc.* **1956**, *78*, 1380-1393.

5. K. C. Nicolaou, T. Montagnon, *Molecules that Changed the World*, 1st ed., Wiley-VCH: Weinheim, 2008.

6. E. J. Corey, B. Czakó, L. Kürti, *Molecules and Medicine*, 1st ed., John Wiley & Sons: New York, 2007.

7. D. J. Newman, G. M. Cragg, *J. Nat. Prod.* **2012**, *75*, 311-335.

8. S. Danishefsky, *Nat. Prod. Rep.* **2010**, *27*, 1114-1116.

9. F. E. Koehn, G. T. Carter, *Nat. Rev. Drug. Discov.* **2005**, *4*, 206-220.

10. G. M. Cragg, D. J. Newman, K. M. Snader, *J. Nat. Prod.* **1997**, *60*, 52-60.

11. A. Fleming, *Brit. J. Exp. Pathol.* **1929**, *10*, 226.

12. J.-M. Liu, N. Mu-Yun, Y.-F. Fan , Y.-Y. Tu, Z.-H. Wu, Y.-L. Wu, W.-S. Chou, *Acta Chim. Sinica.* **1979**, *37*, 129-143.

13. L. J. Bruce-Chwatt, *Brit. Med. J.* **1982**, *284*, 767.

14. D. L. Klayman, A. J. Lin, N. Acton, J. P. Scovill, J. M. Hoch, W. K. Milhous, A. D. Theoharides, A. S. Dobek, *J. Nat. Prod.* **1984**, *47*, 715-717.

15. P. Rabe, *Ber. Dtsch. Chem. Ges.* **1908**, *41*, 62-70.

16. R. B. Woodward, W. E. Doering, *J. Am. Chem. Soc.* **1945**, *67*, 860-874.

17. M. R. Uskokovic, J. Gutzwiller, T. Henderson, *J. Am. Chem. Soc.* **1970**, *92*, 203-204.

18. M. C. Wani, H. L. Taylor, M. E. Wall, P. Coggon, A. T. McPhail, *J. Am. Chem. Soc.* **1971**, *93*, 2325-2327.

19. C. Tan, H. Tasaka, K. P. Yu, M. L. Murphy, D. A. Karnofsky, *Cancer* **1967**, *20*, 333-353.

20. E. J. Sorensen, K. C. Nicolauo, *Classics in Total Synthesis: Targets, Strategies, Methods*, 1st ed., Wiley-VCH: Weinheim, 1996.

21. P. M. Dewick, *Medicinal Natural Products: A Biosynthetic Approach*, 3rd ed., John Wiley & Sons: New York, 2002.

22. R. Croteau, R. E. Ketchum, R. M. Long, R. Kaspera, M. R. Wildung, *Phytochem. Rev.* **2006**, *5*, 75-97.

23. W. Eisenreich, B. Menhard, M. S. Lee, M. H. Zenk, A. Bacher, *J. Am. Chem. Soc.* **1998**, *120*, 9694-9695.

24. W. Eisenreich, B. Menhard, P. J. Hylands, M. H. Zenk, A. Bacher, *Proc. Natl. Acad. Sci. USA* **1996**, *93*, 6431-6436.

25. M. Hezari, N. G. Lewis, R. Croteau, *Arch. Biochem. Biophys.* **1995**, *322*, 437-444.

26. X. Zhou, Z. Wang, K. Jiang, Y. Wei, J. Lin, X. Sun, K. Tang, *Appl. Biochem. Microbiol.* **2007**, *43*, 439-443.

27. B. Ganem, R. R. Franke, *J. Org. Chem.* **2007**, *72*, 3981-3987.

28. J. N. Denis, A. E. Greene, D. Guenard, F. Gueritte-Voegelein, L. Mangatal, P. Potier, *J. Am. Chem. Soc.* **1988**, *110*, 5917-5919.

29. I. Ojima, X. Wang, Y. Jing, C. Wang, *J. Nat. Prod.* **2018**, *81*, 703-721.

30. R. A. Holton, C. Somoza, H. B. Kim, F. Liang, R. J. Biediger, P. D. Boatman, M. Shindo, C. C. Smith, S. Kim, *J. Am. Chem. Soc.* **1994**, *116*, 1597-1598.

31. R. A. Holton, H. B. Kim, C. Somoza, F. Liang, R. J. Biediger, P. D. Boatman, M. Shindo, C. C. Smith, S. Kim, *J. Am. Chem. Soc.* **1994**, *116*, 1599-1600.

32. K. C. Nicolaou, Z. Yang, J. J. Liu, H. Ueno, P. G. Nantermet, R. K. Guy, C. F. Claiborne, J. Renaud, E. A. Couladouros, K. Paulvannan, E. J. Sorensen, *Nature* **1994**, *367*, 630-634.

33. S. J. Danishefsky, J. J. Masters, W. B. Young, J. T. Link, L. B. Snyder, T. V. Magee, D. K. Jung, R. C. A. Isaacs, W. G. Bornmann, C. A. Alaimo, C. A. Coburn, M. J. Di Grandi, *J. Am. Chem. Soc.* **1996**, *118*, 2843-2859.

34. P. A. Wender, N. F. Badham, S. P. Conway, P. E. Floreancig, T. E. Glass, C. Gränicher, J. B. Houze, J. Jänichen, D. Lee, D. G. Marquess, P. L. McGrane, W. Meng, T. P. Mucciaro, M. Mühlebach, M. G. Natchus, H. Paulsen, D. B. Rawlins, J. Satkofsky, A. J. Shuker, J. C. Sutton, R. E. Taylor, K. Tomooka, *J. Am. Chem. Soc.* **1997**, *119*, 2755-2756.

35. P. A. Wender, N. F. Badham, S. P. Conway, P. E. Floreancig, T. E. Glass, J. B. Houze, N. E. Krauss, D. Lee, D. G. Marquess, P. L. McGrane, W. Meng, M. G. Natchus, A. J. Shuker, J. C. Sutton, R. E. Taylor, *J. Am. Chem. Soc.* **1997**, *119*, 2757-2758.

36. T. Newhouse, P. S. Baran, *Angew. Chem. Int. Ed.* **2011**, *50*, 3362-3374.

37. Y. Ishihara, P. S. Baran, *Synlett* **2010**, *2010*, 1733-1745.

38. *Cytochrome P450: Structure, Mechanism, and Biochemistry*, 3rd ed., Springer: Heidelberg, 2015.

39. B. Meunier, S. P. de Visser, S. Shaik, *Chem. Rev.* **2004**, *104*, 3947-3980.

40. B. Meunier, *Comprehensive coordination chemistry II: from biology to nanotechnology*, 3rd ed., Elsevier: New York, 2003.

41. S. Shaik, M. Filatov, D. Schröder, H. Schwarz, *Chem. Eur. J.* **1998**, *4*, 193-199.

42. I. Schlichting, J. Berendzen, K. Chu, A. M. Stock, S. A. Maves, D. E. Benson, R. M. Sweet, D. Ringe, G. A. Petsko, S. G. Sligar, *Science* **2000**, *287*, 1615.

43. R. Davydov, T. M. Makris, V. Kofman, D. E. Werst, S. G. Sligar, B. M. Hoffman, *J. Am. Chem. Soc.* **2001**, *123*, 1403-1415.

44. S. Shaik, S. P. de Visser, F. Ogliaro, H. Schwarz, D. Schröder, *Curr. Opin. Chem. Biol.* **2002**, *6*, 556-567.

45. J. Rittle, M. T. Green, *Science* **2010**, *330*, 933-937.

46. W.-D. Woggon, H.-A. Wagenknecht, C. Claude, *J. Inorg. Biochem.* **2001**, *83*, 289-300.

47. H. Fujii, *Coord. Chem. Rev.* **2002**, *226*, 51-60.

48. B. Meunier, J. Bernadou, *Top. Catal.* **2002**, *21*, 47-54.

49. S. Shaik, S. Cohen, Y. Wang, H. Chen, D. Kumar, W. Thiel, *Chem. Rev.* **2010**, *110*, 949-1017.

50. T. L. Poulos, *Chem. Rev.* **2014**, *114*, 3919-3962.

51. X. Huang, J. T. Groves, *J. Biol. Inorg. Chem.* **2017**, *22*, 185-207.

52. R. A. Baglia, J. P. T. Zaragoza, D. P. Goldberg, *Chem. Rev.* **2017**, *117*, 13320-13352.

53. X. Huang, J. T. Groves, *Chem. Rev.* **2018**, *118*, 2491-2553.

54. J. T. Groves, G. A. McClusky, *J. Am. Chem. Soc.* **1976**, *98*, 859-861.

55. J. T. Groves, M. Van der Puy, *J. Am. Chem. Soc.* **1976**, *98*, 5290-5297.

56. L. M. Hjelmeland, L. Aronow, J. R. Trudell, *Biochem. Biophys. Res. Commun.* **1977**, *76*, 541-549.

57. J. T. Groves, G. A. McClusky, R. E. White, M. J. Coon, *Biochem. Biophys. Res. Commun.* **1978**, *81*, 154-160.

58. J. T. Groves, D. V. Adhyam, *J. Am. Chem. Soc.* **1984**, *106*, 2177-2181.

59. R. E. White, J. P. Miller, L. V. Favreau, A. Bhattacharyya, *J. Am. Chem. Soc.* **1986**, *108*, 6024-6031.

60. R. H. McClanahan, A. C. Huitric, P. G. Pearson, J. C. Desper, S. D. Nelson, *J. Am. Chem. Soc.* **1988**, *110*, 1979-1981.

61. J. T. Groves, T. E. Nemo, R. S. Myers, *J. Am. Chem. Soc.* **1979**, *101*, 1032-1033.

62. C. K. Chang, M.-S. Kuo, *J. Am. Chem. Soc.* **1979**, *101*, 3413-3415.

63. P. E. Ellis, J. E. Lyons, *Coord. Chem. Rev.* **1990**, *105*, 181-193.

64. C. K. Chang, F. Ebina, *J. Chen. Soc. Chem. Commun.* **1981**, 778-779.

65. P. Gandeepan, T. Müller, D. Zell, G. Cera, S. Warratz, L. Ackermann, *Chem. Rev.* **2019**, *119*, 2192-2452.

66. J. He, M. Wasa, K. S. L. Chan, Q. Shao, J.-Q. Yu, *Chem. Rev.* **2017**, *117*, 8754-8786.

67. J. F. Hartwig, M. A. Larsen, *ACS Cent. Sci.* **2016**, *2*, 281-292.

68. H. M. L. Davies, D. Morton, *J. Org. Chem.* **2016**, *81*, 343-350.

69. J. F. Hartwig, *Acc. Chem. Res.* **2012**, *45*, 864-873.

70. J. Wencel-Delord, T. Dröge, F. Liu, F. Glorius, *Chem. Soc. Rev.* **2011**, *40*, 4740-4761.

71. I. A. I. Mkhalid, J. H. Barnard, T. B. Marder, J. M. Murphy, J. F. Hartwig, *Chem. Rev.* **2010**, *110*, 890-931.

72. R. G. Bergman, *Nature* **2007**, *446*, 391-393.

73. A. S. Goldman, R. Ghosh, *Handbook of C–H Transformations: Applications in Organic Synthesis*, 1st ed., Wiley-VCH: New York, 2005.

74. A. E. Shilov, G. B. Shul'pin, *Chem. Rev.* **1997**, *97*, 2879-2932.

75. B. A. Arndtsen, R. G. Bergman, T. A. Mobley, T. H. Peterson, *Acc. Chem. Res.* **1995**, *28*, 154-162.

76. L. Ping, D. S. Chung, J. Bouffard, S.-g. Lee, *Chem. Soc. Rev.* **2017**, *46*, 4299-4328.

77. S. R. Neufeldt, M. S. Sanford, *Acc. Chem. Res.* **2012**, *45*, 936-946.

78. T. Brückl, R. D. Baxter, Y. Ishihara, P. S. Baran, *Acc. Chem. Res.* **2012**, *45*, 826-839.

79. G. B. Shul'pin, *Org. Biomol. Chem.* **2010**, *8*, 4217-4228.

80. T. G. Saint-Denis, R.-Y. Zhu, G. Chen, Q.-F. Wu, J.-Q. Yu, *Science* **2018**, *359*, eaao4798.

81. C. G. Newton, S.-G. Wang, C. C. Oliveira, N. Cramer, *Chem. Rev.* **2017**, *117*, 8908-8976.

82. P. Herrmann, T. Bach, *Chem. Soc. Rev.* **2011**, *40*, 2022-2038.

83. R. Giri, B.-F. Shi, K. M. Engle, N. Maugel, J.-Q. Yu, *Chem. Soc. Rev.* **2009**, *38*, 3242-3272.

84. J. F. Hartwig, *Organotransition Metal Chemistry: From Bonding to Catalysis*, 1st ed., Univ Science Books: Sausalito, 2010.

85. H. M. L. Davies, K. Liao, *Nature Rev. Chem.* **2019**, *3*, 347-360.

86. M. Milan, M. Bietti, M. Costas, *Chem. Commun.* **2018**, *54*, 9559-9570.

87. W. Sun, H. Wang, C. Xia, J. Li, P. Zhao, *Angew. Chem. Int. Ed.* **2003**, *42*, 1042-1044.

88. M. K. Brown, M. M. Blewett, J. R. Colombe, E. J. Corey, *J. Am. Chem. Soc.* **2010**, *132*, 11165-11170.

89. T. Kunisu, T. Oguma, T. Katsuki, *J. Am. Chem. Soc.* **2011**, *133*, 12937-12939.

90. K. Murakami, Y. Sasano, M. Tomizawa, M. Shibuya, E. Kwon, Y. Iwabuchi, *J. Am. Chem. Soc.* **2014**, *136*, 17591-17600.

91. H. Mizoguchi, T. Uchida, T. Katsuki, *Angew. Chem. Int. Ed.* **2014**, *53*, 3178-3182.

92. C. Miao, X.-X. Li, Y.-M. Lee, C. Xia, Y. Wang, W. Nam, W. Sun, *Chem. Sci.* **2017**, *8*, 7476-7482.

93. E. P. Talsi, D. G. Samsonenko, K. P. Bryliakov, *ChemCatChem* **2017**, *9*, 2599-2607.

94. S. Hashiguchi, A. Fujii, K.-J. Haack, K. Matsumura, T. Ikariya, R. Noyori, *Angew. Chem. Int. Ed.* **1997**, *36*, 288-290.

95. Y. Nishibayashi, I. Takei, S. Uemura, M. Hidai, *Organometallics* **1999**, *18*, 2291-2293.

96. M. Kitamura, I. Kasahara, K. Manabe, R. Noyori, H. Takaya, *J. Org. Chem.* **1988**, *53*, 708-710.

97. H. Takaya, T. Ohta, N. Sayo, H. Kumobayashi, S. Akutagawa, S. Inoue, I. Kasahara, R. Noyori, *J. Am. Chem. Soc.* **1987**, *109*, 1596-1597.

98. M. Rachwalski, N. Vermue, F. P. J. T. Rutjes, *Chem. Soc. Rev.* **2013**, *42*, 9268-9282.

99. G. C. Fu, *Acc. Chem. Res.* **2000**, *33*, 412-420.

100. J. C. Ruble, H. A. Latham, G. C. Fu, *J. Am. Chem. Soc.* **1997**, *119*, 1492-1493.

101. A. Ghanem, H. Y. Aboul-Enein, *Chirality* **2005**, *17*, 1-15.

102. A. Werner, *Lehrbuch der Stereochemie*, 1st ed., G. Fischer: Jena, 1904.

103. C.-M. Che, V. K.-Y. Lo, C.-Y. Zhou, J.-S. Huang, *Chem. Soc. Rev.* **2011**, *40*, 1950-1975.

104. M. Costas, *Coord. Chem. Rev.* **2011**, *255*, 2912-2932.

105. H. Lu, X. P. Zhang, *Chem. Soc. Rev.* **2011**, *40*, 1899-1909.

106. J. K. Laha, S. Dhanalekshmi, M. Taniguchi, A. Ambroise, J. S. Lindsey, *Org. Process Res. Dev.* **2003**, *7*, 799-812.

107. M. O. Senge, Y. M. Shaker, M. Pintea, C. Ryppa, S. S. Hatscher, A. Ryan, Y. Sergeeva, *Eur. J. Org. Chem.* **2010**, *2010*, 237-258.

108. M. O. Senge, *Chem. Commun.* **2011**, *47*, 1943-1960.

109. K. C. Gupta, A. K. Sutar, *Coord. Chem. Rev.* **2008**, *252*, 1420-1450.

110. T. Katsuki, *Coord. Chem. Rev.* **1995**, *140*, 189-214.

111. W. Zhang, J. L. Loebach, S. R. Wilson, E. N. Jacobsen, *J. Am. Chem. Soc.* **1990**, *112*, 2801-2803.

112. E. N. Jacobsen, W. Zhang, A. R. Muci, J. R. Ecker, L. Deng, *J. Am. Chem. Soc.* **1991**, *113*, 7063-7064.

113. R. Irie, K. Noda, Y. Ito, N. Matsumoto, T. Katsuki, *Tetrahedron: Asymmetry* **1991**, *2*, 481-494.

114. N. S. Venkataramanan, G. Kuppuraj, S. Rajagopal, *Coord. Chem. Rev.* **2005**, *249*, 1249-1268.

115. W. Sun, Q. Sun, *Acc. Chem. Res.* **2019**, *52*, 2370-2381.

116. G. Olivo, O. Cussó, M. Costas, *Chem. Asian J.* **2016**, *11*, 3148-3158.

117. E. P. Talsi, K. P. Bryliakov, *Coord. Chem. Rev.* **2012**, *256*, 1418-1434.

118. J. T. Groves, P. Viski, *J. Org. Chem.* **1990**, *55*, 3628-3634.

119. R. L. Halterman, S. T. Jan, *J. Org. Chem.* **1991**, *56*, 5253-5254.

120. K. Alder, G. Stein, *Liebigs Ann. Chem.* **1933**, *501*, 247-294.

121. W. M. Dehn, K. E. Jackson, *J. Am. Chem. Soc.* **1933**, *55*, 4284-4287.

122. A. Rieche, H. Gross, E. Höft, *Chem. Ber.* **1960**, *93*, 88-94.

123. E. A. Mash, D. S. Torok, *J. Org. Chem.* **1989**, *54*, 250-253.

124. R. L. Halterman, S.-T. Jan, H. L. Nimmons, D. J. Standlee, M. A. Khan, *Tetrahedron* **1997**, *53*, 11257-11276.

125. R. Zhang, W.-Y. Yu, T.-S. Lai, C.-M. Che, *Chem. Commun.* **1999**, 1791-1792.

126. R. Zhang, W.-Y. Yu, C.-M. Che, *Tetrahedron: Asymmetry* **2005**, *16*, 3520-3526.

127. P. L. Maux, H. F. Srour, G. Simonneaux, *Tetrahedron* **2012**, *68*, 5824-5828.

128. H. Srour, P. L. Maux, G. Simonneaux, *Inorg. Chem.* **2012**, *51*, 5850-5856.

129. A. Miyafuji, T. Katsuki, *Tetrahedron* **1998**, *54*, 10339-10348.

130. K. Bowden, I. M. Heilbron, E. R. H. Jones, B. C. L. Weedon, *J. Chem. Soc.* **1946**, 39-45.

131. T. Punniyamurthy, A. Miyafuji, T. Katsuki, *Tetrahedron Lett.* **1998**, *39*, 8295-8298.

132. T. Punniyamurthy, T. Katsuki, *Tetrahedron* **1999**, *55*, 9439-9454.

133. N. Komiya, S. Noji, S.-I. Murahashi, *Tetrahedron Lett.* **1998**, *39*, 7921-7924.

134. N. S. Finney, P. J. Pospisil, S. Chang, M. Palucki, R. G. Konsler, K. B. Hansen, E. N. Jacobsen, *Angew. Chem. Int. Ed.* **1997**, *36*, 1720-1723.

135. H. Kajiro, S.-i. Mitamura, A. Mori, T. Hiyama, *Synlett* **1998**, *1998*, 51-52.

136. J. P. Vacca, B. D. Dorsey, W. A. Schleif, R. B. Levin, S. L. McDaniel, P. L. Darke, J. Zugay, J. C. Quintero, O. M. Blahy, E. Roth, *Proc. Natl. Acad. Sci. USA* **1994**, *91*, 4096-4100.

137. B. D. Dorsey, R. B. Levin, S. L. McDaniel, J. P. Vacca, J. P. Guare, P. L. Darke, J. A. Zugay, E. A. Emini, W. A. Schleif, *J. Med. Chem.* **1994**, *37*, 3443-3451.

138. S.-I. Murahashi, S. Noji, T. Hirabayashi, N. Komiya, *Tetrahedron: Asymmetry* **2005**, *16*, 3527-3535.

139. T. Hamada, R. Irie, J. Mihara, K. Hamachi, T. Katsuki, *Tetrahedron* **1998**, *54*, 10017-10028.

140. K. Nehru, S. J. Kim, I. Y. Kim, M. S. Seo, Y. Kim, S.-J. Kim, J. Kim, W. Nam, *Chem. Commun.* **2007**, 4623-4625.

141. M. S. Chen, M. C. White, *Science* **2007**, *318*, 783-787.

142. M. S. Chen, M. C. White, *Science* **2010**, *327*, 566-571.

143. P. E. Gormisky, M. C. White, *J. Am. Chem. Soc.* **2013**, *135*, 14052-14055.

144. M. C. White, J. Zhao, *J. Am. Chem. Soc.* **2018**, *140*, 13988-14009.

145. J. Zhao, T. Nanjo, E. C. de Lucca, M. C. White, *Nat. Chem.* **2019**, *11*, 213-221.

146. M. Wu, B. Wang, S. Wang, C. Xia, W. Sun, *Org. Lett.* **2009**, *11*, 3622-3625.

147. M. Wu, C.-X. Miao, S. Wang, X. Hu, C. Xia, F. E. Kühn, W. Sun, *Adv. Synth. Catal.* **2011**, *353*, 3014-3022.

148. B. Wang, S. Wang, C. Xia, W. Sun, *Chem. Eur. J.* **2012**, *18*, 7332-7335.

149. B. Wang, C. Miao, S. Wang, C. Xia, W. Sun, *Chem. Eur. J.* **2012**, *18*, 6750-6753.

150. X. Wang, C. Miao, S. Wang, C. Xia, W. Sun, *ChemCatChem* **2013**, *5*, 2489-2494.

151. C. Miao, B. Wang, Y. Wang, C. Xia, Y.-M. Lee, W. Nam, W. Sun, *J. Am. Chem. Soc.* **2016**, *138*, 936-943.

152. J. R. Frost, S. M. Huber, S. Breitenlechner, C. Bannwarth, T. Bach, *Angew. Chem. Int. Ed.* **2015**, *54*, 691-695.

153. B. Qiu, D. Xu, Q. Sun, C. Miao, Y.-M. Lee, X.-X. Li, W. Nam, W. Sun, *ACS Catal.* **2018**, *8*, 2479-2487.

154. R. Mas-Ballesté, L. Que, *J. Am. Chem. Soc.* **2007**, *129*, 15964-15972.

155. O. Cussó, I. Garcia-Bosch, X. Ribas, J. Lloret-Fillol, M. Costas, *J. Am. Chem. Soc.* **2013**, *135*, 14871-14878.

156. Y. Wang, D. Janardanan, D. Usharani, K. Han, L. Que, S. Shaik, *ACS Catal.* **2013**, *3*, 1334-1341.

157. R. V. Ottenbacher, D. G. Samsonenko, E. P. Talsi, K. P. Bryliakov, *ACS Catal.* **2016**, *6*, 979-988.

158. A. M. Zima, O. Y. Lyakin, R. V. Ottenbacher, K. P. Bryliakov, E. P. Talsi, *ACS Catal.* **2016**, *6*, 5399-5404.

159. B. Qiu, D. Xu, Q. Sun, J. Lin, W. Sun, *Org. Lett.* **2019**, *21*, 618-622.

160. E. P. Talsi, D. G. Samsonenko, R. V. Ottenbacher, K. P. Bryliakov, *ChemCatChem* **2017**, *9*, 4580-4586.

161. M. Milan, M. Bietti, M. Costas, *ACS Cent. Sci.* **2017**, *3*, 196-204.

162. M. Milan, M. Bietti, M. Costas, *Org. Lett.* **2018**, *20*, 2720-2723.

163. M. Cianfanelli, G. Olivo, M. Milan, R. J. M. Klein Gebbink, X. Ribas, M. Bietti, M. Costas, *J. Am. Chem. Soc.* **2020**, *142*, 1584-1593.

164. V. Dantignana, M. Milan, O. Cussó, A. Company, M. Bietti, M. Costas, *ACS Cent. Sci.* **2017**, *3*, 1350-1358.

165. H. Lorenz, A. Seidel-Morgenstern, *Angew. Chem. Int. Ed.* **2014**, *53*, 1218-1250.

166. P. R. Ortiz de Montellano, *Chem. Rev.* **2010**, *110*, 932-948.

167. J. C. Lewis, P. S. Coelho, F. H. Arnold, *Chem. Soc. Rev.* **2011**, *40*, 2003-2021.

168. R. Fasan, *ACS Catal.* **2012**, *2*, 647-666.

169. F. D. Toste, M. S. Sigman, S. J. Miller, *Acc. Chem. Res.* **2017**, *50*, 609-615.

170. W. R. Gutekunst, P. S. Baran, *Chem. Soc. Rev.* **2011**, *40*, 1976-1991.

171. D. Font, M. Canta, M. Milan, O. Cussó, X. Ribas, R. J. M. Klein Gebbink, M. Costas, *Angew. Chem. Int. Ed.* **2016**, *55*, 5776-5779.

172. M. Lee, M. S. Sanford, *J. Am. Chem. Soc.* **2015**, *137*, 12796-12799.

173. M. Canta, D. Font, L. Gómez, X. Ribas, M. Costas, *Adv. Synth. Catal.* **2014**, *356*, 818-830.

174. Y. Kawamata, M. Yan, Z. Liu, D.-H. Bao, J. Chen, J. T. Starr, P. S. Baran, *J. Am. Chem. Soc.* **2017**, *139*, 7448-7451.

175. F. A. Carey, R. J. Sundberg, *Advanced Organic Chemistry: Part A: Structure and Mechanisms*, 5th ed., Springer: New York, 2007.

176. J. C. K. Chu, T. Rovis, *Angew. Chem. Int. Ed.* **2018**, *57*, 62-101.

177. T. W. Lyons, M. S. Sanford, *Chem. Rev.* **2010**, *110*, 1147-1169.

178. Q. Shao, K. Wu, Z. Zhuang, S. Qian, J.-Q. Yu, *Acc. Chem. Res.* **2020**, *53*, 833-851.

179. K. M. Engle, T.-S. Mei, M. Wasa, J.-Q. Yu, *Acc. Chem. Res.* **2012**, *45*, 788-802.

180. J. C. K. Chu, T. Rovis, *Nature* **2016**, *539*, 272-275.

181. G. J. Choi, Q. Zhu, D. C. Miller, C. J. Gu, R. R. Knowles, *Nature* **2016**, *539*, 268-271.

182. L. M. Stateman, K. M. Nakafuku, D. A. Nagib, *Synthesis* **2018**, *50*, 1569-1586.

183. K. Chen, J. M. Richter, P. S. Baran, *J. Am. Chem. Soc.* **2008**, *130*, 7247-7249.

184. E. M. Simmons, J. F. Hartwig, *Nature* **2012**, *483*, 70-73.

185. B. Li, M. Driess, J. F. Hartwig, *J. Am. Chem. Soc.* **2014**, *136*, 6586-6589.

186. K. Chen, P. S. Baran, *Nature* **2009**, *459*, 824-828.

187. N. R. Mote, S. H. Chikkali, *Chem. Asian J.* **2018**, *13*, 3623-3646.

188. H. J. Davis, R. J. Phipps, *Chem. Sci.* **2017**, *8*, 864-877.

189. P. Dydio, J. N. H. Reek, *Chem. Sci.* **2014**, *5*, 2135-2145.

190. M. Raynal, P. Ballester, A. Vidal-Ferran, P. W. N. M. van Leeuwen, *Chem. Soc. Rev.* **2014**, *43*, 1660-1733.

191. S. Carboni, C. Gennari, L. Pignataro, U. Piarulli, *Dalton Trans.* **2011**, *40*, 4355-4373.

192. P. I. Dalko, *Comprehensive Enantioselective Organocatalysis: Catalysts, Reactions, and Applications*, 1st ed., John Wiley & Sons: New York, 2013.

193. T. Akiyama, K. Mori, *Chem. Rev.* **2015**, *115*, 9277-9306.

194. C. Min, D. Seidel, *Chem. Soc. Rev.* **2017**, *46*, 5889-5902.

195. J. Mlynarski, *Chiral Lewis Acids in Organic Synthesis*, 1st ed., Wiley-VCH: Weinheim, 2017.

196. X. Yu, W. Wang, *Chem. Asian J.* **2008**, *3*, 516-532.

197. P. R. Schreiner, *Chem. Soc. Rev.* **2003**, *32*, 289-296.

198. M. S. Taylor, E. N. Jacobsen, *Angew. Chem. Int. Ed.* **2006**, *45*, 1520-1543.

199. P. M. Pihko, *Hydrogen Bonding in Organic Synthesis*, 1st ed., Wiley-VCH: Weinheim, 2009.

200. F. Burg, T. Bach, *J. Org. Chem.* **2019**, *84*, 8815-8836.

201. R. J. Phipps, G. L. Hamilton, F. D. Toste, *Nat. Chem.* **2012**, *4*, 603-614.

202. M. Mahlau, B. List, *Angew. Chem. Int. Ed.* **2013**, *52*, 518-533.

203. K. Brak, E. N. Jacobsen, *Angew. Chem. Int. Ed.* **2013**, *52*, 534-561.

204. S. Shirakawa, K. Maruoka, *Angew. Chem. Int. Ed.* **2013**, *52*, 4312-4348.

205. D. Vidal, G. Olivo, M. Costas, *Chem. Eur. J.* **2018**, *24*, 5042-5054.

206. J. T. Groves, R. Neumann, *J. Am. Chem. Soc.* **1987**, *109*, 5045-5047.

207. J. T. Groves, R. Neumann, *J. Am. Chem. Soc.* **1989**, *111*, 2900-2909.

208. P. A. Grieco, T. L. Stuk, *J. Am. Chem. Soc.* **1990**, *112*, 7799-7801.

209. T. L. Stuk, P. A. Grieco, M. M. Marsh, *J. Org. Chem.* **1991**, *56*, 2957-2959.

210. M. D. Kaufman, P. A. Grieco, D. W. Bougie, *J. Am. Chem. Soc.* **1993**, *115*, 11648-11649.

211. L. Marchetti, M. Levine, *ACS Catal.* **2011**, *1*, 1090-1118.

212. L. Marinescu, M. Bols, *Curr. Org. Chem.* **2010**, *14*, 1380-1398.

213. J. Bjerre, C. Rousseau, L. Marinescu, M. Bols, *Appl. Microbiol. Biotechnol.* **2008**, *81*, 1-11.

214. V. T. D'Souza, *Supramol. Chem.* **2003**, *15*, 221-229.

215. R. Breslow, S. D. Dong, *Chem. Rev.* **1998**, *98*, 1997-2012.

216. F. Cramer, *Einschlussverbindungen*, 1st ed., Springer: Berlin, 1954.

217. R. Breslow, *Acc. Chem. Res.* **1980**, *13*, 170-177.

218. R. Breslow, X. Zhang, R. Xu, M. Maletic, R. Merger, *J. Am. Chem. Soc.* **1996**, *118*, 11678-11679.

219. P. L. Anelli, S. Banfi, F. Montanari, S. Quici, *J. Chem. Soc., Chem. Commun.* **1989**, 779-780.

220. R. Breslow, X. Zhang, Y. Huang, *J. Am. Chem. Soc.* **1997**, *119*, 4535-4536.

221. R. Breslow, Y. Huang, X. Zhang, J. Yang, *Proc. Natl. Acad. Sci. USA* **1997**, *94*, 11156-11158.

222. R. Breslow, B. Gabriele, J. Yang, *Tetrahedron Lett.* **1998**, *39*, 2887-2890.

223. R. Breslow, J. Yang, J. Yan, *Tetrahedron* **2002**, *58*, 653-659.

224. Z. Fang, R. Breslow, *Bioorg. Med. Chem. Lett.* **2005**, *15*, 5463-5466.

225. J. Fried, E. F. Sabo, *J. Am. Chem. Soc.* **1954**, *76*, 1455-1456.

226. J. Fried, E. F. Sabo, *J. Am. Chem. Soc.* **1957**, *79*, 1130-1141.

227. C. G. Bergstrom, R. T. Nicholson, R. M. Dodson, *J. Org. Chem.* **1963**, *28*, 2633-2640.

228. R. F. Hirschmann, R. Miller, J. Wood, R. E. Jones, *J. Am. Chem. Soc.* **1956**, *78*, 4956-4959.

229. R. M. Dodson, R. D. Muir, *J. Am. Chem. Soc.* **1958**, *80*, 6148-6148.

230. R. M. Dodson, R. D. Muir, *J. Am. Chem. Soc.* **1961**, *83*, 4631-4635.

231. J. Yang, B. Gabriele, S. Belvedere, Y. Huang, R. Breslow, *J. Org. Chem.* **2002**, *67*, 5057-5067.

232. J. Yang, R. Breslow, *Angew. Chem. Int. Ed.* **2000**, *39*, 2692-2695.

233. R. Breslow, J. Yan, S. Belvedere, *Tetrahedron Lett.* **2002**, *43*, 363-365.

234. R. J. Fereday, P. Hodgson, S. Tyagi, B. J. Hathaway, *J. Chem. Soc., Dalton Trans.* **1981**, 2070-2077.

235. J. Foley, S. Tyagi, B. J. Hathaway, *J. Chem. Soc., Dalton Trans.* **1984**, 1-5.

236. R. Breslow, A. B. Brown, R. D. McCullough, P. W. White, *J. Am. Chem. Soc.* **1989**, *111*, 4517-4518.

237. S. Belvedere, R. Breslow, *Bioorg. Chem.* **2001**, *29*, 321-331.

238. Z. Fang, R. Breslow, *Org. Lett.* **2006**, *8*, 251-254.

239. M. Milan, M. Salamone, M. Costas, M. Bietti, *Acc. Chem. Res.* **2018**, *51*, 1984-1995.

240. C. T. Mbofana, E. Chong, J. Lawniczak, M. S. Sanford, *Org. Lett.* **2016**, *18*, 4258-4261.

241. M. Lee, M. S. Sanford, *Org. Lett.* **2017**, *19*, 572-575.

242. G. Olivo, G. Farinelli, A. Barbieri, O. Lanzalunga, S. Di Stefano, M. Costas, *Angew. Chem. Int. Ed.* **2017**, *56*, 16347-16351.

243. G. Olivo, G. Capocasa, O. Lanzalunga, S. Di Stefano, M. Costas, *Chem. Commun.* **2019**, *55*, 917-920.

244. R. Brimioulle, D. Lenhart, M. M. Maturi, T. Bach, *Angew. Chem. Int. Ed.* **2015**, *54*, 3872-3890.

245. D. S. Kemp, K. S. Petrakis, *J. Org. Chem.* **1981**, *46*, 5140-5143.

246. T. Bach, H. Bergmann, B. Grosch, K. Harms, *J. Am. Chem. Soc.* **2002**, *124*, 7982-7990.

247. A. Bauer, F. Westkämper, S. Grimme, T. Bach, *Nature* **2005**, *436*, 1139-1140.

248. C. Müller, A. Bauer, M. M. Maturi, M. C. Cuquerella, M. A. Miranda, T. Bach, *J. Am. Chem. Soc.* **2011**, *133*, 16689-16697.

249. R. Alonso, T. Bach, *Angew. Chem. Int. Ed.* **2014**, *53*, 4368-4371.

250. A. Tröster, R. Alonso, A. Bauer, T. Bach, *J. Am. Chem. Soc.* **2016**, *138*, 7808-7811.

251. A. Hölzl-Hobmeier, A. Bauer, A. V. Silva, S. M. Huber, C. Bannwarth, T. Bach, *Nature* **2018**, *564*, 240-243.

252. J. Rebek, B. Askew, P. Ballester, C. Buhr, S. Jones, D. Nemeth, K. Williams, *J. Am. Chem. Soc.* **1987**, *109*, 5033-5035.

253. B. Askew, P. Ballester, C. Buhr, K. S. Jeong, S. Jones, K. Parris, K. Williams, J. Rebek, *J. Am. Chem. Soc.* **1989**, *111*, 1082-1090.

254. K. Williams, B. Askew, P. Ballester, C. Buhr, K. S. Jeong, S. Jones, J. Rebek, *J. Am. Chem. Soc.* **1989**, *111*, 1090-1094.

255. R. K. Castellano, V. Gramlich, F. Diederich, *Chem. Eur. J.* **2002**, *8*, 118-129.

256. R. Faraoni, R. K. Castellano, V. Gramlich, F. Diederich, *Chem. Commun.* **2004**, 370-371.

257. J. Rebek, *Science* **1987**, *235*, 1478-1484.

258. J. Rebek, B. Askew, M. Killoran, D. Nemeth, F. T. Lin, *J. Am. Chem. Soc.* **1987**, *109*, 2426-2431.

259. W. L. Jorgensen, S. Boudon, T. B. Nguyen, *J. Am. Chem. Soc.* **1989**, *111*, 755-757.

260. J. Rebek, *Acc. Chem. Res.* **1990**, *23*, 399-404.

261. J. Limburg, J. S. Vrettos, L. M. Liable-Sands, A. L. Rheingold, R. H. Crabtree, G. W. Brudvig, *Science* **1999**, *283*, 1524-1527.

262. J. Limburg, J. S. Vrettos, H. Chen, J. C. de Paula, R. H. Crabtree, G. W. Brudvig, *J. Am. Chem. Soc.* **2001**, *123*, 423-430.

263. S. Das, C. D. Incarvito, R. H. Crabtree, G. W. Brudvig, *Science* **2006**, *312*, 1941-1943.

264. S. Das, G. W. Brudvig, R. H. Crabtree, *J. Am. Chem. Soc.* **2008**, *130*, 1628-1637.

265. S. Teramae, A. Kito, T. Shingaki, Y. Hamaguchi, Y. Yano, T. Nakayama, Y. Kobayashi, N. Kato, N. Umezawa, Y. Hisamatsu, T. Nagano, T. Higuchi, *Chem. Commun.* **2019**, *55*, 8378-8381.

266. C. Wang, K. V. Shalyaev, M. Bonchio, T. Carofiglio, J. T. Groves, *Inorg. Chem.* **2006**, *45*, 4769-4782.

267. T. Bach, H. Bergmann, B. Grosch, K. Harms, E. Herdtweck, *Synthesis* **2001**, *2001*, 1395-1405.

268. T. Bach, H. Bergmann, K. Harms, *Angew. Chem. Int. Ed.* **2000**, *39*, 2302-2304.

269. T. Bach, H. Bergmann, *J. Am. Chem. Soc.* **2000**, *122*, 11525-11526.

270. B. Grosch, C. N. Orlebar, E. Herdtweck, W. Massa, T. Bach, *Angew. Chem. Int. Ed.* **2003**, *42*, 3693-3696.

271. T. Aechtner, M. Dressel, T. Bach, *Angew. Chem. Int. Ed.* **2004**, *43*, 5849-5851.

272. M. Dressel, T. Bach, *Org. Lett.* **2006**, *8*, 3145-3147.

273. S. C. Coote, T. Bach, *J. Am. Chem. Soc.* **2013**, *135*, 14948-14951.

274. D. G. Lonergan, J. Riego, G. Deslongchamps, *Tetrahedron Lett.* **1996**, *37*, 6109-6112.

275. D. G. Lonergan, J. Halse, G. Deslongchamps, *Tetrahedron Lett.* **1998**, *39*, 6865-6868.

276. D. G. Lonergan, G. Deslongchamps, *Tetrahedron* **1998**, *54*, 14041-14052.

277. F. Voss, E. Herdtweck, T. Bach, *Chem. Commun.* **2011**, *47*, 2137-2139.

278. P. Fackler, C. Berthold, F. Voss, T. Bach, *J. Am. Chem. Soc.* **2010**, *132*, 15911-15913.

279. P. Fackler, S. M. Huber, T. Bach, *J. Am. Chem. Soc.* **2012**, *134*, 12869-12878.

280. T. Höke, E. Herdtweck, T. Bach, *Chem. Commun.* **2013**, *49*, 8009-8011.

281. F. Zhong, T. Bach, *Chem. Eur. J.* **2014**, *20*, 13522-13526.

282. E. J. Corey, W. Suggs, *Tetrahedron Lett.* **1975**, *16*, 1647-2650.

283. S. Agarwal, H. P. Tiwari, J. P. Sharma, *Tetrahedron* **1990**, *46*, 4417-4420.

284. K. Omura, D. Swern, *Tetrahedron* **1978**, *34*, 1651-1660.

285. A. J. Mancuso, D. Swern, *Synthesis* **1981**, *1981*, 165-185.

286. W. P. Griffith, *Chem. Soc. Rev.* **1992**, *21*, 179-185.

287. F. Zhong, A. Pöthig, T. Bach, *Chem. Eur. J.* **2015**, *21*, 10310-10313.

288. K. Yoshida, J. Goto, Y. Ban, *Chem. Pharm. Bull.* **1987**, *35*, 4700-4704.

289. F. Burg, M. Gicquel, S. Breitenlechner, A. Pöthig, T. Bach, *Angew. Chem. Int. Ed.* **2018**, *57*, 2953-2957.

290. F. Burg, S. Breitenlechner, C. Jandl, T. Bach, *Chem. Sci.* **2020**, *11*, 2121-2129.